

**Université de Lille 1**

Ecole Doctorale «Sciences de la Matière, du Rayonnement et de l'Environnement»

**Laboratoire «Geosystèmes» UMR 8217 CNRS – LILLE 1**

Thèse présentée pour obtenir le titre de Docteur de l'Université de Lille 1

Spécialité: Géosciences

Par

**José MARGOTTA**

**Stratigraphic architecture and sedimentary evolution of the Holocene deposits  
in the French Flemish coastal plain, Northern France**

Soutenue le 24 mars 2014 à Villeneuve d'Ascq (59)

Devant le jury composé de :

**Bernadette TESSIER**, Directrice de recherche CNRS; Université de Caen Basse Normandie; Rapporteur

**Robert LAFITE**, Professeur; Université de Rouen; Rapporteur

**Cecile BAETEMAN**, Chercheur principal; Service Géologique de Belgique ; Examinatrice

**Fabien PAQUET**, Chercheur; BRGM; Examineur

**Jean-Yves REYNAUD**, Professeur, Université Lille 1; Examineur

**Nicolas TRIBOVILLARD**, Professeur, Université Lille 1; Examineur

**Alain TRENTESAUX**, Professeur, Université Lille 1; directeur de thèse



## Acknowledgements

Firstly I would like to thank my supervisor, Alain Trentesaux, and the Director of Doctoral Studies, Nicolas Tribovillard, for giving me the opportunity of this PhD project and to explore the Holocene deposits of French Flemish Coastal Plain. I have lucky to join a great team with commitment and expertise who supported me throughout this study.

Alain Trentesaux is thanked by his friendly guidance, contributions, time and effort to the success of this research. His advice, patient and enriching discussions helped me to gain the tools to propose a regional model in spite the complexity of this study area.

I want to acknowledge Fundayacucho and CampusFrance for providing me the scholarship to carry out this research. I would also like to thank the Renard Centre of Marine Geology, particularly Wim Versteeg and Koen de Rycker, University Caen Basse-Normandie, especially Bernadette Tessier, and the International Association of Sedimentologists (IAS) to collaborate with this project.

I wish to thank people of Bierne and Les Attaques communities to give us the opportunity to take our cores and samples in their properties. Likewise, thanks to the *Bureau de Recherches Géologiques et Minières* (BRGM) to provide us a large subsurface database and *Voies navigables de France* (VNF) for the permits to use the waterways to achieve our seismic survey.

I am deeply grateful with Virginie Vergne and Eric Armynot du Châtelet for their time, support, encouragement and specialized vision to perform the results and interpretations of the micropaleontological data. I also thank Jean-Yves Reynaud for our interesting discussions about stratigraphy and his helpful advice. Similarly, I give many thanks to Cecile Baeteman and Jean Sommé for their interest in the subject, information and the opportunity to share their wisdom about the evolution of the study area.

My sincere gratitude to the entire technical staff of Geosystemes, for their time and assistance, always ready to help me. Especially thanks to Romain Abraham, a key player in our team. Likewise, I would also like to thank the researchers; academic and administrative staff of the *bâtiment SN5* the very best for all of you.

I must give thanks to all the members of my thesis committee. Their interest, comments, questions, and discussions have enriched this study and are greatly appreciated.

On the way, I found a great Venezuelan team: Melesio, Brenda, Joselyn, Roberto and their families, you will be always members of my family. On this way, I also found unforgettable colleagues and friends; I would like to thank them for their genuine friendship.

Finally, I want to give great thanks to my family, who encouraged and pushed me, always looking forward with honesty. My deepest gratitude is to my wife Fanny for her patient, sacrifice, love and support during this experience.

A Lille, Francia...la llevo en el corazón...Gracias totales!

## Résumé

Cette thèse a pour objectif la reconstitution des étapes ayant conduit au remplissage sédimentaire de la plaine maritime flamande française au cours de l'Holocène. L'approche utilisée a consisté en l'utilisation conjointe de bases de données de forages, de sondages et d'observations réalisées au cours de cette étude et, pour la première fois de données issues d'une campagne de sismique à très haute résolution dans les voies navigables de la plaine côtière. La relecture des données lithologiques au regard de nos propres observations permet de définir précisément les faciès de remplissage de la plaine. Les données lithologiques, minéralogiques (argiles) et micropaléontologiques (foraminifères et pollens) sont à la base de la reconnaissance de 5 faciès sédimentaires représentatifs du remplissage. Ces faciès ont été interprétés en assemblages de faciès de dépôt. Ceux-ci ont été regroupés en 3 unités caractérisant l'évolution verticale des conditions de dépôt. A la base une plaine alluviale, puis une série estuarienne dominée par la marée et une série d'estran tidal. La première unité correspond à des dépôts tardi-pléistocènes, tandis que les deux autres représentent les dépôts holocènes remplissant la majorité de l'espace d'accommodation disponible. Une série de 10 profils au travers de la plaine maritime permet de comprendre la distribution et la géométrie de ces unités ainsi que l'organisation des faciès sédimentaires. L'arrangement stratigraphique met en évidence les interactions entre le taux de remontée du niveau marin et les conditions hydrodynamiques caractérisées par un régime macrotidal et influencées localement par la houle. Notre étude permet de mieux comprendre le fonctionnement de ce type de zone basse et ouvre des perspectives de modélisation de scénarios futurs d'évolution.

## Abstract

The aim of this study is to reconstruct the evolution of the Holocene deposits along the French Flemish Coastal Plain. This approach is achieved combining available and newly dataset from boreholes, cores descriptions and, for the first time in this plain, the interpretation of VHR seismic profiles on the coastal plain waterways. The study of lithology, micropaleontological assemblages (foraminifera and pollen analyses) and clay mineralogy provides the basis to recognize five sedimentary facies as representative of the Holocene infill. These sedimentary facies were interpreted as depositional facies assemblages in accordance to their depositional features. Depositional facies were grouped in three sedimentary units that better define the depositional environment. From base to top, the units are: alluvial plain, tide-dominated estuary and tidal flats. The alluvial plain consist of late Pleistocene deposits while estuarine and tidal flats units represent the Holocene deposits covering almost the whole available accommodation space. Distribution and geometry of these sedimentary units and their internal architecture of depositional facies were observed from ten cross-sections that cover most of the coastal plain. Stratigraphic arrangement shows the interaction of the Holocene sea-level rise and the coastal hydrodynamic conditions, dominated by the macrotidal regime and influenced by waves action, as the main factors that ruled the sedimentation of the area. This study opens new possibilities to better understand the coastal processes that acted in this lowland, as well as serves as a basis for future studies or modelling possible future scenario



## Table of contents

Acknowledgements .....	3
Résumé .....	5
Abstract .....	5
Table of contents .....	7
List of figures .....	9
List of tables .....	14
Chapter 1. General introduction .....	15
1.1 Introduction .....	15
1.2 Thesis aims.....	20
1.3 Thesis outlined.....	21
Chapter 2. French Flemish Coastal Plain: Regional Background .....	23
2.1 Introduction .....	23
2.2 Geographic context.....	23
2.3 Hydrodynamic context .....	32
2.4 Geologic context .....	36
2.5 Development of the Quaternary stratigraphy .....	40
2.6 Holocene sea level rise.....	45
2.7 Comments about the literature review and vision of this research .....	48
Chapter 3. Sedimentary facies analysis and depositional system of the French Flemish coastal plain .....	49
3.1 Introduction .....	49
3.2 Methods .....	50
3.2.1 Subsurface facies analysis.....	50
3.2.2 Foraminifera .....	56
3.2.3 Pollen analysis .....	57
3.2.4 Clay mineralogy .....	58
3.2.5 Radiocarbon dating .....	58
3.3 Sedimentary facies – Results .....	59
3.3.1 Pleistocene deposits .....	60
3.3.2 Holocene deposits.....	63
3.4 Sedimentary facies - interpretation .....	81
3.4.1 Pleistocene deposits .....	81
3.4.2 Holocene deposits.....	83
3.5 - Conclusions .....	92

Chapter 4. Very High-resolution seismic: Looking to the subsurface features of the Holocene infill of the French Flemish coastal plain. ....	93
4.2 Material and methods .....	95
4.2.1 Seismic data acquisition.....	95
4.2.2 Seismic data processing .....	97
4.2.3 Seismic data interpretation.....	98
4.3 Results.....	102
4.3.1 Seismic Stratigraphy .....	102
4.3.2 Pre-Holocene unconformity.....	102
4.3.3 Seismic units .....	106
4.4 Seismic approach to the Holocene sedimentary arrangement .....	112
4.5 Conclusions .....	114
Chapter 5. Stratigraphy architecture of the Holocene deposits of the French Flemish Coastal Plain .....	117
5.1 Introduction .....	117
5.2 Stratigraphic framework.....	118
5.2.1 N-S oriented profiles .....	119
5.2.2 E-W oriented profiles.....	125
5.3 Discussion .....	128
5.3.1 Stratigraphic architecture depositional history of FFCP .....	128
5.3.2 Depositional history of French Flemish Coastal Plain.....	131
5.4 Conclusions .....	145
Chapter 6. General conclusions and further research.....	147
References .....	151
APPENDIX A.....	173
APPENDIX B.....	183
APPENDIX C.....	188
APPENDIX D.....	190
APPENDIX E.....	192
APPENDIX F.....	194



## List of figures

- Figure 1.1. Sedimentation controls in depositional environments from Catuneanu (2006). The diagram shows the allogenic processes and their relationship to environmental energy flux, sediment supply, accommodation and depositional trends. The interplay of allogenic processes and autigenic dynamics determines the distribution of depositional elements within a depositional system.....16
- Figure 1.2. Coastal classification from Boyd *et al.* (1992). Left: organization of all major clastic coastal environments in prograding (below) and transgressive conditions (above). The influence of tides relative to wave power increases from right to left. Right: triangular coastal classification using the process parameters of rivers, waves and tides, together with the provenance of sediment supply.....17
- Figure 1.3. Influence and interactions between the different factors into the coastal changes. Modified from Reed *et al.*, (2009).....18
- Figure 1.4. Chronostratigraphical subdivision table for the last 27ka. Ages for the Global Holocene subdivision from Walker *et al* (2012). European pollen analysis based on Iversen (1954) in Hodson and West (1972). Ages for Pleistocene subdivision from Rasmussen *et al.* (2006) and Huijzer and Vandenberghe (1998).....19
- Figure 2.1. Map of the Southern North Sea region highlighting the position of the north-western Europe coastal plain.....24
- Figure 2.2. Map of the French Flemish coastal plain, showing the position of the major physiographic areas surrounding the plain, drainage system (blue lines), cities (●) and towns (.). Bathymetric map from BRGM. Surface digital elevation model (DEM) and French-Belgium border from IGN.....25
- Figure 2.3. Photography of the Boulonnais zone. Jurassic rocks outcropping between Cap de la Crèche and Wimereux.....25
- Figure 2.4. Photography of the Artois hills. A) Visual from the coastal plain around Audruicq. B) View of the Escalles village showing the undulating appearance and the small runoff valleys that affected the surface.....26
- Figure 2.5. Photography of Sangatte area on direction to the French Flemish coastal plain. A) Sangatte cliff with the Pleistocene outcrops bordering the coastal plain. B) Artois foothills and the French Flemish Coastal Plain in the background.....27
- Figure 2.6. Eastern part of the French Flemish Coastal Plain from the Dunkerque – Watten canal. Inner Flanders relief in the background.....28
- Figure 2.7. Bathymetric DEM of the zone offshore Calais. Shallow waters with sand banks are visible in light colours, while darker colours make visible a part of an ancient drainage that could be the trace of a paleo-Aa river toward the Dover Strait. Notice that this trace is just offshore Oye, while the present-day Aa outflow is 5 km East at the city of Gravelines. Map established with SHOM data delivered to the University Lille 1 under the 205/2010 contract.....29
- Figure 2.8. Coastal dunes system at the east of Dunkerque. Easternmost part of the French Flemish coastal plain.....30

Figure 2.9. Two photographs of the Ghyvelde dunes systems. A) A general vision of the current aspect of the inland dunes. B) An approach detailed the aspect of the upper part of the dunes showing aeolian cross-bedding and soil development. A pen is used as scale.....	31
Figure 2.10. Diagram illustrating tidal levels and depths measured in the FFCP. MHW: Mean high water, MTL: Mean tide level, MLW: Mean low water.....	34
Figure 2.11. Tides and currents to the English Channel and the southern North Sea. From <a href="http://www.mumm.ac.be">http://www.mumm.ac.be</a> .....	35
Figure 2.12. Wind direction averages to the north-western France. Data obtained of <a href="http://www.meteofrance.com">http://www.meteofrance.com</a> from Cartier (2011).....	35
Figure 2.13. Harmonized geological map of the study area. Courtesy from Julie PICOT-2014, BRGM, Service Régional Nord- Pas de Calais. We translated the original legend from French and adapted it to the terrains outcropping in the area. Supplementary information can be found at Infoterre website: <a href="http://infoterre.brgm.fr">http://infoterre.brgm.fr</a> .....	37
Figure 2.14. Structural model for the Dover Strait breaching (From Colbeaux, 1980). Upper: Artois horst formed around the Eocene period. Middle: Formation of the graben during the Pleistocene. Lower: Graben flank erosion caused by the rivers.....	39
Figure 2.15. Paleogeographical map illustrating the river system of northwest Europe during the maximum extent of glaciations in the late Weichselian. Data originally published by Philip Gibbard in 1988 and updated to the NEESDI project 2001. Map obtained from <a href="http://www.qpg.geog.cam.ac.uk/research/projects/nweurorivers/#The_maps">http://www.qpg.geog.cam.ac.uk/research/projects/nweurorivers/#The_maps</a> .....	40
Figure 2.16. Schematic stratigraphic table of the Quaternary deposits in the French –Belgian coastal plain area.....	42
Figure 2.17. Comparative table showing the widely-used palynological Holocene subdivision and the stratigraphy of the north-western Europe according with the transgressive – regressive record. From Gosselin (2011).....	44
Figure 2.18. Relative sea-level curves in the southern North Sea. A) Sea-level curve by Behre (2007) showing changes in the late Holocene relative sea-level rise. German ordinance datum (NN) is similar to the French mean level (NGF). B) Sea-level curve by Denys and Baeteman (1995) showing a smooth late-Holocene relative sea-level rise. The Belgian datum (TAW) is 2.33 m lower than the French datum (NGF).....	47
Figure 3.1. Map of available subsurface data used in this study. BRGM boreholes ( ). Previous published studies ( ). Cores obtained during our fieldwork campaigns ( ). Cities and towns ( ). Details on the location and name of boreholes in appendix A. <i>Contour lines correspond to +5m NGF (red line), +10m NGF (yellow line) and +20m NGF (green line)</i> .....	51
Figure 3.2. Map showing the position of the newly acquired cores (black circles) during the FFCP fieldwork and archaeological site in the area of Bierne (black lines). Upper: Bierne site. Lower: Les Attaques site. Les Attaques 1 is very close (50 m) to the canal where seismic profile Nr. 8 was shot.....	53

Figure 3.3. Archaeological trenches and pits from Bierne diagnostic site. Pictures A and B show the work progress to generate the trenches and pits. Pictures A and B are courtesy of Christine Louvion from Archaeological Service of the General Council of the Nord Department. C: Example of an about 1m-deep archaeological trench. D: Disposition of parallel trenches. E: Example of the process of cleaning and description of sedimentary features in these trenches.....	54
Figure 3.4. Pictures of core acquisition campaigns. A Bierne; B Les Attaques area.....	55
Figure 3.5. Picture showing the different parts of the percussion corer used in the FFCP....	55
Figure 3.6. Core images from Bierne 3 (A) and Bierne 4 (B) showing the characteristics of the Pleistocene deposits in the subsurface of the FFCP. Scale in centimetres. A Greyish clayey silt with rust-coloured mottling (1), Holocene – Pleistocene sharp contact (2) grey sands of the basal Holocene deposits (3). B Blue-greyish mottled clays of the Pleistocene deposits (4) affected by possible ice wedge (5) and filled by grey fine sands with chalky granules (6).....	61
Figure 3.7. Borehole data used in this study showing the Pleistocene deposits of the southern part of the coastal plain. Pleistocene interval is highlighted to show the predominant lithology for this period. Lithology description from Sommé <i>et al.</i> (1994) and Gandouin (2003).....	62
Figure 3.8. Stratigraphic succession for the Holocene deposits at Les Attaques. See location of core in figure 4.2 and appendix A.....	64
Figure 3.9. Stratigraphic succession for the Holocene deposits in Bierne. 14C ages in appendix E. See location of core in figure 4.2 and appendix A.....	65
Figure 3.10. Example of typical clay mineralogy distribution along the cores of Les Attaques and Bierne sites. Clay assemblages show smectite (blue) illite (black), kaolinite (red) and chlorite (green).....	66
Figure 3.11. Borehole 385 showing the pollen diagram of Watten boring. Red square highlights the characteristic of peat layers. Interpretation was obtained from Sommé <i>et al.</i> , 1994 and modified by Vergne <i>et al.</i> , 2009. See location in Appendix A.....	67
Figure 3.12. Core photo of surface peat layer. A: Fibrous peat layer of Bierne 1 core. Note the laminated aspect and the well-preserved rest of wood into the organic material (1). B: Surface peat layer of Les Attaques 1 core. It shows the process of humification of the peat bed (2). C: Surface peat layer of Bierne 7 core. It displays an amorphous aspect caused by the total decomposition of the peat (3).....	69
Figure 3.13. Core photo of organic-rich muds. A: Organic-rich mud of core Les Attaques 1. Bioturbation shows predominant vertical burrows (1). B: Transitional contact between the underlying mud facies and the organic-rich muds (2) of core Bierne 1. Bioturbation shows a diversity of sizes and shapes, mostly rounded and cylindrical (3).....	70
Figure 3.14. Mud facies of FFCP. A: Bierne 1 core showing a structureless part of this facies with scattered plant debris (1) and slightly parallel lamination (2). B: Bierne 7 core showing the intensity of roots in the muddy deposits (2). C: Les Attaques 2 core showing the development of anthropized soils (3) in the uppermost part of this facies and the last sedimentary cover of the FFCP.....	72

Figure 3.15. Heterolithic facies of the FFCP. A: Bierne 1 core displaying the interbedded layers of sand (1) and mud (2) with parallel and wavy lamination. Relative quantity of mud is increasing upwards. B: Les Attaques 1 core showing heterolithic bedding and abundant shell fragments. Note the erosive contact (red line) with underlying mud facies.....	74
Figure 3.16. Sand facies from Les Attaques area. A: Les Attaques 1 core showing typical lower massive bluish-grey sand facies with scattered shell fragments. B: Les Attaques 3 core showing typical upper light-grey sand facies with common shell and peat fragments. Lower contact with underlying organic-rich facies is generally erosive (red line).....	75
Figure 3.17. Sand facies from Bierne area. Bierne 2 core showing the typical bluish-grey sand with thinly parallel bedding and rare mud laminae. Lower contact with Pleistocene deposits is erosive (red line).....	77
Figure 3.18. Photos of archaeological trench at Bierne location showing sand-dominated small channels detailed in B. These channels, also called creeks, exhibit an erosive lower contact with underlying organic-rich facies.....	78
Figure 3.19. Common shells observed widespread in the last sedimentary cover at Bierne area. <i>Cerastoderma edule</i> (upper) and <i>Scrobicularia plana</i> (lower).....	79
Figure 3.20. Description of borehole 174 around Calais area emphasizing (red square) the gravel facies observed in the FFCP. See location in Appendix A.....	80
Figure 3.21. Aerial picture in an area close to Bierne displaying a section of a major channel bend with connected small meandering creeks (Source <a href="http://www.geosur.info">www.geosur.info</a> ). This is part of the most recent tidal network before definitive anthropization of the plain.....	86
Figure 3.22. Schematic distribution of the depositional facies within the tidal environments of the FFCP during the Holocene. (Adapted and modified from Weimer <i>et al.</i> , 1982).....	91
Figure 4.1. Map of the French Flemish coastal plain showing the shape of the plain, the drainage system and the seismic survey differentiated by thick black colour lines .....	95
Figure 4.2. Views of Boomer profiler used in this study. It belongs to the Renard Centre of Marine Geology (RCMG) of Ghent University.....	96
Figure 4.3. A) Differential GPS. B) Real-time position record during the seismic survey.....	97
Figure 4.4. Example of spectral survey of raw seismic data (Line 8) showing the average range of frequency obtained in the FFCP.....	99
Figure 4.5. Example of seismic profile (Line 8) before and after processing. A) Pre-processed raw form. B) Result of the processing applied in the seismic line. The presence of noise is diminished in the post-processed profile.....	100
Figure 4.6. Examples of reflector relationships and termination patterns in depositional sequences. Modified from Mitchum <i>et al.</i> , 1977.....	101
Figure 4.7. Examples of reflection configuration patterns. Source: Mitchum <i>et al.</i> , 1977. Modified from Stocker <i>et al.</i> , 1997.....	101
Figure 4.8. Location of seismic lines (in red) selected as examples of Pre-Holocene/Holocene subdivision of the sedimentary succession. Profiles interpreted are in the borders of the coastal plain.....	102

Figure 4.9. VHR seismic profile and its comparison with the boreholes described in the FFCP (Core Les Attaques 1 and borehole 197) showing the Holocene sedimentary infilling. Bottom of Borehole 197 reaches the pre-Holocene deposits.....	103
Figure 4.10. This profile depicts seismic line 1 in the FFCP subsurface. Above: non-interpreted seismic line. Below: interpreted seismic line showing the seismic unit and the Pre-Holocene unconformity. Note the high-quantity of multiples (parallel reflectors) and the low contrast impedance in the profile.....	104
Figure 4.11. This profile depicts seismic line 8 described in the FFCP subsurface. Above: non-interpreted seismic line. Below: interpreted seismic line showing both seismic unit and the Pre-Holocene unconformity. Here it is also possible to observe the high-quantity of multiples (parallel reflectors) and the low impedance contrast of the profile.....	105
Figure 4.12. Pre-Holocene unconformity interpreted in seismic line 8. It is a good example to show how the Pre-Holocene substratum is incised and subsequently filled by Holocene deposits.....	106
Figure 4.13. Location of seismic lines (in red) selected as exemplars to show the seismic units features. Profiles interpreted are in axial part of the coastal plain.....	107
Figure 4.14 – Image of seismic profiles showing the non-interpreted seismic (above) and interpretation of the seismic units and seismic facies described in the Holocene deposits (below). The depth-time conversion uses a sound velocity in soft sediments of 1500 m/s. It is possible to distinguish the channel-fill that characterize the seismic facies A, and the slightly prograding clinofolds of the seismic facies B.....	108
Figure 4.15 – Seismic profile showing more characteristics of the seismic unit and Holocene seismic facies. Above: non-interpreted profile. Below: interpretation of the seismic units and seismic facies described in the Holocene deposits. Holocene deposits present clear incisions into the Pre-Holocene substrate and facies A show deeper channels compared to channels observed in figure 4.14.....	109
Figure 4.16. Seismic profile showing details of the facies A and its channel fill characteristics. Above: non-interpreted profile. Below: interpretation of the seismic units and seismic facies described in the Holocene deposits.....	111
Figure 5.1. Location map of FFCP correlation profiles. Saint-Omer – Gravelines (1), Audruicq – Oye-Plage (2), Les Attaques – Calais (3), Pitgam – Dunkerque Ferry port (4), Bierne – Dunkerque (5), Les Moères – Bray – Dunes (6); Calais – Dunkerque (7); Les Attaques – Bierne (8); Les Attaques – Looberghe (9) and Bergues – Les Moères (10). Names and location of boreholes are shown in the profiles and appendix A.....	118
Figure 5.2. Profil 1 Saint-Omer-Gravelines.....	119
Figure 5.3 Profil 2 Audruicq-Oye-Plage.....	121
Figure 5.4 Profile 3 Les Attaques – Calais.....	122
Figure 5.5 Profile 4 Pitgam – Dunkerque ferry port.....	123
Figure 5.6 Profile 5 Bierne – Dunkerque.....	124
Figure 5.7 Profile 6 Les Moères – Ghyvelde.....	124
Figure 5.8 Profile 7 Calais – Dunkerque.....	125

Figure 5.9 Profile 8 Les Attaques – Bierne .....	126
Figure 5.10 Profile 9 Les Attaques – Looberghe.....	127
Figure 5.11 Profile 10 Bergues - Les Moères.....	128
Figure 5.12. 3D blocks of idealised coastal depositional environments interpreted into the FFCP. From base (A) to top (C) the vertical succession of sedimentary units and evolution of the coastal system. (Adapted and modified after Plink-Björklund, 2005 and Dalrymple and Choi, 2007).....	129
Figure 5.13. Fence diagram giving a simplified regional picture of the 3D vertical and lateral stratigraphic relationships between Holocene sedimentary units of the FFCP. For location see figure 5.1.....	131
Figure 5.14. Pre-Holocene surface obtained from boreholes and seismic data. Contour interval 5 m relative to NGF.....	132
Figure 5.15. Early Holocene around 9000 cal BP (MSL around -17m NGF). It shows the dispersed distribution of organic-rich facies included basal peat accumulation. The position of the main Aa River and the other small coastal streams were inferred from the morphology of the Pre-Holocene surface and valleys observed in the profiles. Shoreline should be some kilometres offshore than its current location.....	134
Figure 5.16. Paleogeography around 7000 cal BP (MSL around -7m NGF) showing the development of the estuarine unit, increase of the tidal prism and the change of the Aa River mouth towards the East. Shoreline may be further inland than present-day location.....	136
Figure 5.17. Paleogeography around 5000 BP (MSL around -2m NGF). It is showing the extent of the surface peat layer, decreasing of tidal prism and the change in the position of the Aa River mouth towards the East.....	141
Figure 5.18. Paleogeography around 3000 BP (MSL around -2m NGF) showing the expansion of intertidal deposits along the FFCP. Aa River present small distributaries separated by intertidal flats.....	142

**List of tables**

Table 4.1. Seismic reflection attributes commonly used in seismic stratigraphy and their geological significance. Modified from Mitchum <i>et al.</i> (1977).....	100
---	-----

# Chapter 1. General introduction

## 1.1 Introduction

Ancient and modern coastal environments have been extensively studied by geologists through time due to their abundant natural resources and particular significance to general exploration for oil and gas, renewable energies, natural hazards, as well as the engineering and coastal management. The growing needs of the world population demands new challenges in the development of these environments on ways to build new approaches in the knowledge of the nature and evolution of these areas.

Coastal environments (including deltas, estuaries, lagoons, strand plains and tidal flats) represent extremely variable and dynamic sedimentary systems (Harris *et al.*, 2002). Many long-term geological processes (e.g., subsidence, isostasy) and short-term dynamics (e.g., tidal regime, waves) are reflected in their settings controlling the interactions between fluvial and marine systems and their influence in the evolution of the coastal zone (Syvitski *et al.*, 2005).

The stratigraphy of the coastal systems is variable and complex. Understanding the interactions and influences of the allogenic and autogenic processes that ruled their sedimentation determines the distribution of depositional elements within the sedimentary system. (Catuneanu, 2006) (Fig. 1.1). The magnitude and responses induced by their combination reflect the influences of the external forces or the autogenic behaviour in the coastal changes, suggesting important insights about the coastal evolution and predict possible future scenarios.

In coastal evolution the morphodynamics play an important role in the influence of coastal changes through time, in terms of how and why the shoreline and landforms have been altered by the processes-form interactions (Woodroffe, 2002). According to their dynamic and morphological characteristics, it is possible to give essential clues about the importance of sea-level changes, sediment supply, hydrodynamics conditions and their fingerprints on different time and spatial scales.

As any dynamic zone with multiple parameters shaping the landforms, coastal environments have been differently classified to provide some clues to understand their possible evolution. One of the most effective coastal classifications

was proposed by Boyd *et al.* (1992) based on the genetic process relationships (Fig. 1.2). It employs the variables of transgressive or regressive trends and the balance between marine processes, river input and the relative power of waves and tides. Their approach provides the basis to identify coastal clastic depositional environments and to document the major controls on their morphology.

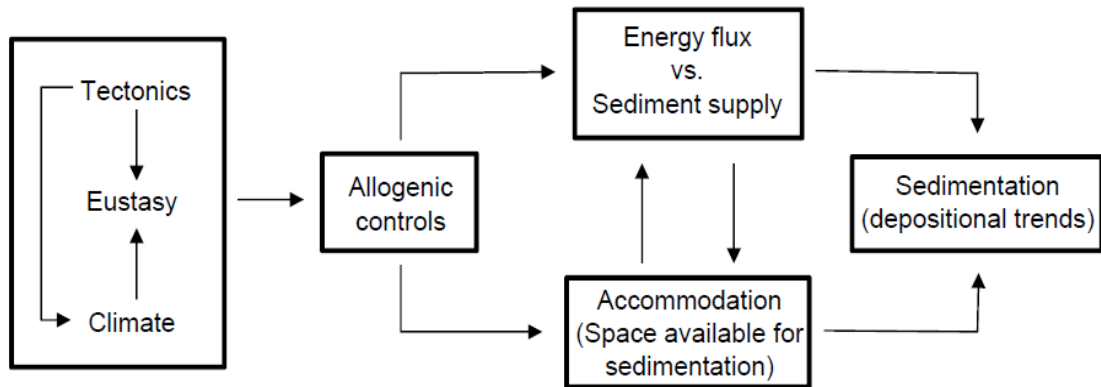


Figure 1.1. Sedimentation controls in depositional environments from Catuneanu (2006). The diagram shows the allogenic processes and their relationship to environmental energy flux, sediment supply, accommodation and depositional trends. The interplay of allogenic processes and autigenic dynamics determines the distribution of depositional elements within a depositional system.

In the coastal zones, sediment erosion, transport and deposition are closely related to the power of waves and tides (Swift and Thorne, 1991). The contribution of waves and tides are extremely important in the coastal morphology and the arrangement of available sediments (Davis and Hayes, 1984). In addition, the impact of sea-level changes influences the tendency of coastal landforms. The measurement or prediction of this variable provides input parameter to determinate the morphological changes of the coast (Fitzgerald *et al.*, 2008). In a recent history of the coastal areas, the effect of human influences should also be considered within the geomorphic changes parameters (Reed *et al.*, 2009) (Fig. 1.3).

During the Quaternary, like in most of the World (e.g., Voris, 2000), North-western Europe experienced significant changes in its coastal zones, linked to the interaction between Glacial-Interglacial cycles and their impact over these areas (Ehlers *et al.*, 2011). The sedimentary succession and the landforms recorded the



variable responses and interactions between climatic and glacio-eustatic sea-level changes.

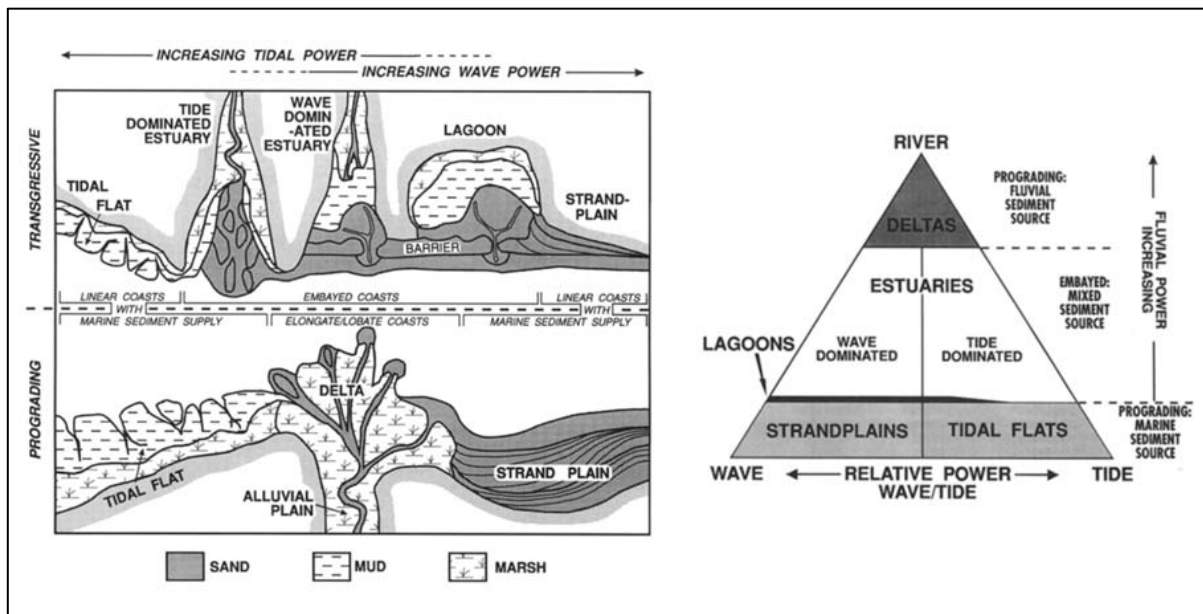


Figure 1.2. Coastal classification from Boyd *et al.* (1992). Left: organization of all major clastic coastal environments in prograding (below) and transgressive conditions (above). The influence of tides relative to wave power increases from right to left. Right: triangular coastal classification using the process parameters of rivers, waves and tides, together with the provenance of sediment supply.

Many other factors also modified the palaeoenvironment conditions such as tidal forcing, short-term glacio-hydro-isostatic adjustment and long-term background tectonics (Hijma, 2009). These North-western European examples served as comparison elements with other coastal areas of the world and have been extensively used as modern analogues to ancient depositional systems.

After the last glacial maximum (LGM), when glacial ice reached its maximum globally between 26.5 and 19 ka (Ehlers *et al.*, 2011), the climate became warmer and sea level rose worldwide with non-uniform and non-synchronic rates generating several regional curves (Pirazzoli, 1991; Lambeck, 1997). The sea-level rise became, progressively, the main control parameter for the coastal evolution, especially at the transition from late Pleistocene to early Holocene shifting the position of the coastline and gradually causing a transgression over the previous lowlands (Beets and van der Spek, 2000; Cleveringa, 2000).

The dominance was even more marked over large continental shelves, such as the Southern North Sea, due to its very gentle slope. However, during the

Holocene (Fig. 1.4) with ongoing sea-level rise, the interactions between accommodation, sediment supply and transport mechanisms started to play a major role in the sedimentation. This resulted in a complex coastal depositional system that is the product of the interplay between the eustatic changes and the dynamic of the sedimentary system.

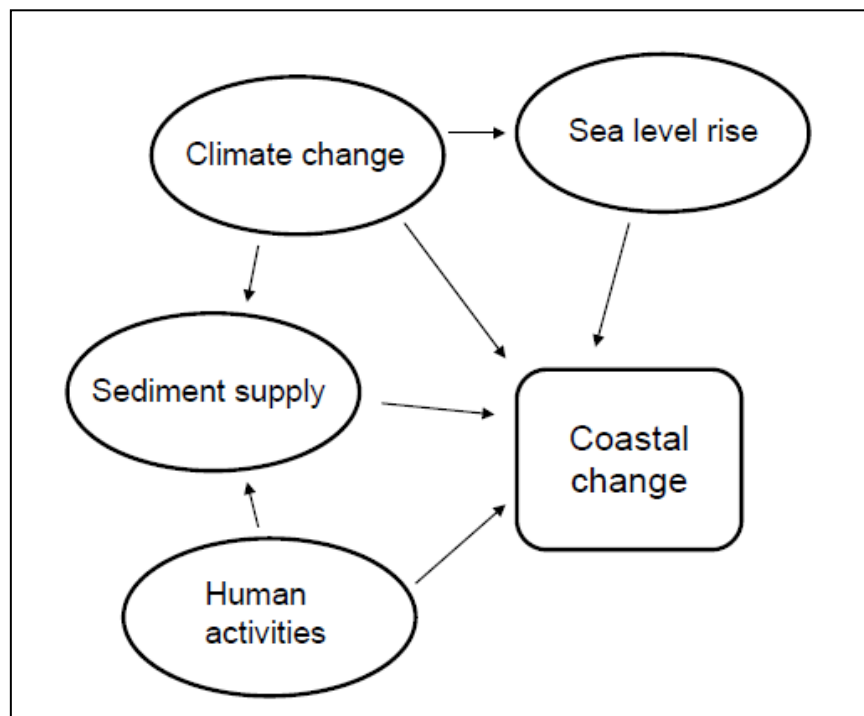


Figure 1.3. Influence and interactions between the different factors into the coastal changes. Modified from Reed et al. (2009).

The Holocene infill that is preserved in the French Flanders coastal plain represents an excellent archive to document the mechanisms acting in the sedimentation of Southern North Sea basin. It also represents an important place to explain the environmental changes and the general stratigraphic arrangement of an area that changed significantly after the last glaciation. Moreover, these areas were then intensively affected by anthropogenic changes in addition to the other natural processes that act in the coastal plain.

Although a large database has been constituted along the last two centuries involving boreholes and temporary outcrops, some key questions about the infilling processes and the paleoenvironments distribution remain open due to the large variability of the deposits and the lack of regional correlations covering the whole area. Previous studies provided an important heritage to understand the sedimentary

composition of the Holocene infill. However, the regional framework requires more research on the French side, it is necessary to move from a broad vision of the changes occurring along the 150 km long coast between Calais and the Netherlands to a more detailed description.

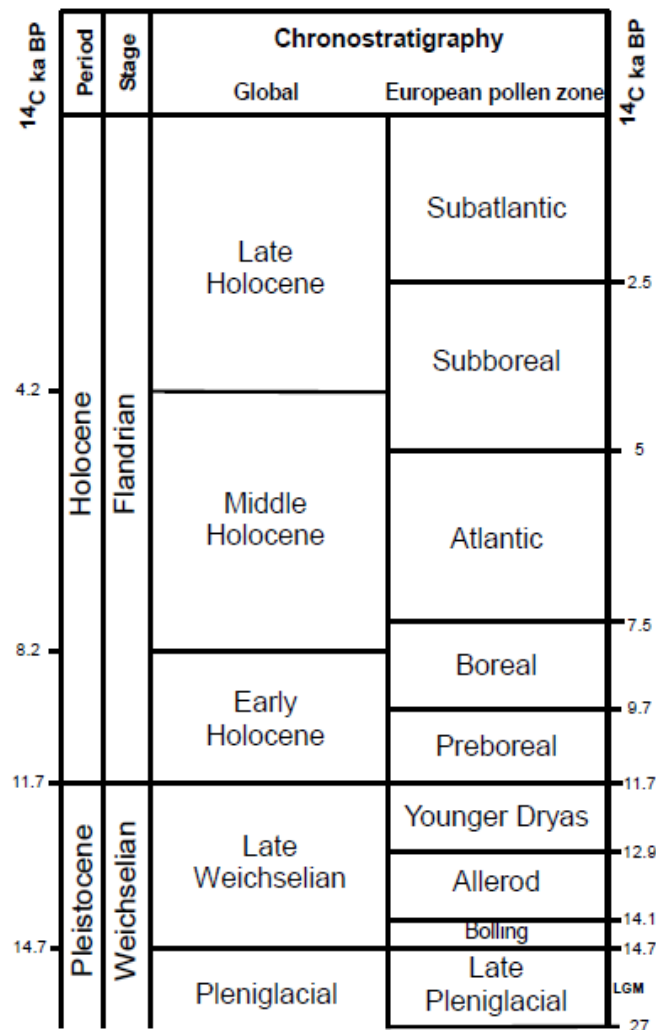


Figure 1.4. Chronostratigraphical subdivision table for the last 27ka. Ages for the Global Holocene subdivision from Walker *et al* (2012). European pollen analysis based on Iversen (1954) in Hodson and West (1972). Ages for Pleistocene subdivision from Rasmussen *et al.* (2006) and Huijzer and Vandenberghe (1998).

A good knowledge on the nature of the sediments and the geometry and distribution of the Holocene deposits is indispensable. This is especially the case if we want to determine the relative importance of the controls involved in the development of this area: sea level implications on the sedimentation,

progradation/retrogradation of the coastline, balance between sedimentary inputs and compaction effects for these lowlands.

Thus, regrouping and honouring all the available data, and integrating new techniques and results that we obtained during the thesis, the regional architectural interpretation seemed to be handy to generate a new approach of the large-scale Holocene coastal evolution. This could be mapped and linked with the coastal-evolution models developed in neighbouring countries, contributing to a better understanding of the Holocene infilling history of the Southern North Sea area.

## **1.2 Thesis aims**

The principal objective of this thesis is to provide an improved understanding of the Holocene sedimentary evolution of the French Flanders coastal plain. We aim at determining the depositional environments, elucidating its sedimentary architecture and developing a palaeogeographic reconstruction based on the integration of different sources of data. For the first time in the French waterways of this plain, we combined sedimentologic and stratigraphic information from boreholes and cores data, with a series of very high-resolution seismic profiles, defining some major sedimentary units. Radiocarbon dating from the new cores and calibrated from previous works allowed reconstructing the temporal framework of the plain

Furthermore, in view of the growing concern about the sea-level rise and coastal changes around the world, this research can provide a scientific basis to studies for coastal sensivity, as well as the development of town planning operations along the French Flemish coastal plain. Some elements related to geological settings and processes acting in the shallow subsurface of the area become useful to drive regional assessments and predict future scenarios. In addition, this study could be an input to geological or reservoir modelling. Holocene coastal systems provide interesting analogues for depositional environments of heterogeneous hydrocarbon reservoirs, presenting a more realistic portray of the spatial complexity and properties of the reservoir units.

### **1.3 Thesis outlined**

This thesis includes an extensive literature review and regional background in Chapter 2, summarizing a detailed overview of the regional geology and geography context for the Holocene of the French Flemish coastal plain. The chapter 3 presents the methods, results and facies interpretations obtained from cores, borehole data and archaeological trenches. Lithology, micropaleontology and clay mineralogy were integrated to the facies analysis in order to define the typical depositional facies. The chapter 4 consists in the acquisition, results and seismo-stratigraphic characterisation of the Holocene infill obtained from a very high-resolution seismic survey that we carried out on the navigable channels of the plain. The chapter 5 describes the distribution of depositional facies and their assemblages in sedimentary units to illustrate the sedimentary architecture of the French Flemish coastal plain. In addition, it presents the depositional evolution of the Holocene deposits explained from palaeogeographic maps. Finally, the main conclusions and some perspectives putting forward by this study are given in chapter 6.



# Chapter 2. French Flemish Coastal Plain: Regional Background

## 2.1 Introduction

This chapter consists in a concise overview of the geographic and geologic context in which the French Flemish Coastal Plain (FFCP) has developed through the Late Quaternary. The study of the coastal deposits in the area has a long and intermittent history of research, illustrating the different ways of thinking about the interpretation of the sedimentary deposits and their evolution.

The examination and analysis based on previous researches involve aspects of morphology and stratigraphy, which provides valuable considerations about the current knowledge of the events and depositional conditions that made up the Holocene sedimentary arrangement. In this regard, the historical conception and the advances documented by a range of publications are the bridge to incorporate new highlights and perspectives in the understanding of the coastal development.

## 2.2 Geographic context

The French Flemish Coastal Plain or "*Plaine maritime*" (Blanchard, 1906; Sommé, 1977, 1979) forms the southwestern extremity of the Holocene coastal area extending along the continental southern North Sea (Fig. 2.1). It is located within the region of Nord-Pas-de-Calais of northern France (Fig. 2.2) and is limited by:

Toward de west, the coastal plain is bounded by the Boulonnais (Fig. 2.3) and the Artois hills (Fig 2.4). Various authors such as Blanchard (1906), Dubois (1924) and Sommé (1977) denominated this area as "Haut Pays" due to their high relief compared with the flat coastal area. Current vision of Artois hills suggests a plateau region, with gentle slopes and various altitudes that provide a relatively homogeneous undulating appearance (Fig 2.4). At the Sangatte cliff, the plateau descends gently towards the northwest, becoming part of the subsurface of the coastal plain sediments (Fig. 2.5). Towards the Boulonnais, the landforms become more variable. Changes in the morphology are controlled by the tectonic structures and the deep and narrow small rivers activity (Sommé, 1977).

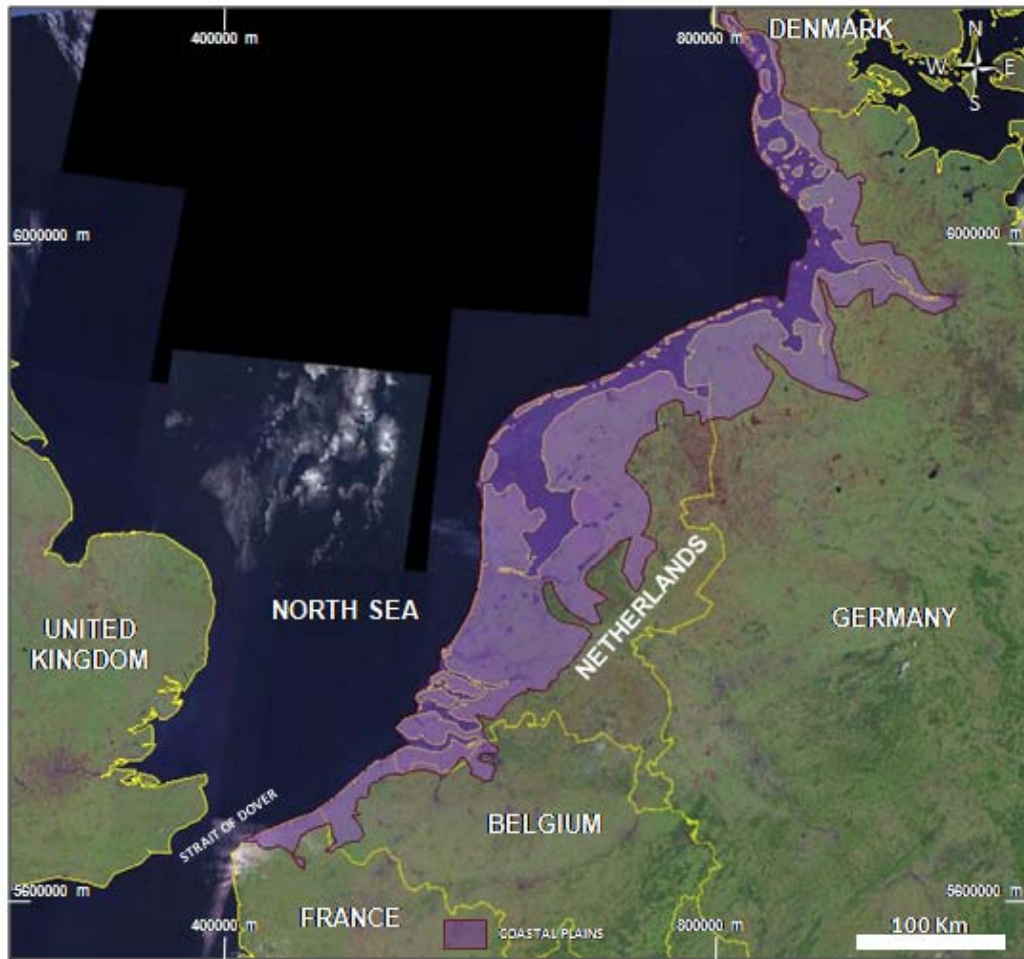


Figure 2.1. Map of the Southern North Sea region highlighting the position of the north-western Europe coastal plain.

The Artois hills represent the main source for the hydrographic network caught in the plain. Two drainage systems, the Aa and Hem rivers, flow down from the Artois hills. The Aa river rises at 122 m around the Bourthes village (Fig.2.2) and is 89 km long (SAGE du delta de L'Aa, 2005).

The characteristics of its slopes allow us dividing its course in two sections, the first interval is observed descending from the hills, with a SO-NE direction between the Bourthes and Arques towns. It is characterised by a mean slope of 2% and represents a small and rugged river with an aspect rather natural without much man-induced modification (Blanchard, 1906; Courty, 1916). Some tributaries as the Blequin and Thiembronne small rivers enter the watercourse in this interval and the total average flow discharge is  $10 \text{ m}^3\text{s}^{-1}$  (I.F.R.E.M.E.R, 1986).



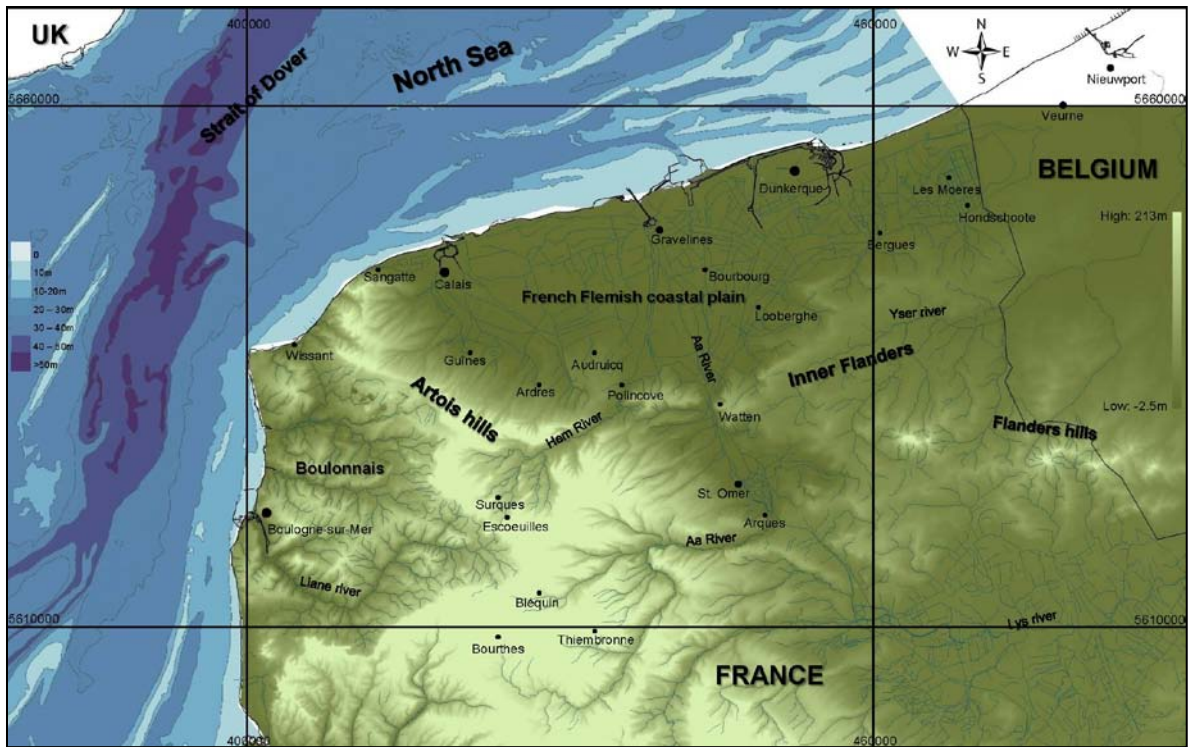


Figure 2.2. Map of the French Flemish coastal plain, showing the position of the major physiographic areas surrounding the plain, drainage system (blue lines), cities (●) and towns (·). Bathymetric map from BRGM. Surface digital elevation model (DEM) and French-Belgium border from IGN.



Figure 2.3. Photography of the Boulonnais zone. Jurassic rocks outcropping between Cap de la Crèche and Wimereux.



*Figure 2.4. Photography of the Artois hills. A) Visual from the coastal plain around Audruicq. B) View of the Escalles village showing the undulating appearance and the small runoff valleys that affected the surface.*

The Hem River springs at 115 m at Surques and Escoeuilles villages. Its length is around 25 km with SW - NE as the dominant direction. The average slope of the Hem River is 4.6% and in some areas incise deeply the bedrock. Upstream, the river collects significant input from several small tributaries. The Hem River has fluctuations in its flow regime during the year, high waters are associated to winter overflows and the low water stages during summer periods. Its average flow discharge is  $1.5 \text{ m}^3\text{s}^{-1}$ .

The inner Flanders (Houtland in Dutch or Haut Pays in French) corresponds to the series of regularly and disconnected low hills that represent the south-eastward bound of the coastal plain (Fig. 2.6). The hydrographic system

extends in the area being drained by the Yser (Ijzer in Dutch) that flows through France and descends with an average slope of 0.9% to the Belgium coastal plain where it debouches into the North Sea at Nieuwpoort (Belgium).



*Figure 2.5. Photography of Sangatte area on direction to the French Flemish coastal plain. A) Sangatte cliff with the Pleistocene outcrops bordering the coastal plain. B) Artois foothills and the French Flemish Coastal Plain in the background.*

The offshore limit of the coastal plain is the southern North Sea. This section of the North Sea is characterized by a series of large sand banks (van Veen, 1936) organised in two groups of parallel banks: the coastal banks, close and about parallel to the present-day shoreline and, further offshore, the Flemish banks (Eisma *et al.*, 1979). These mostly-sandy deposits cover an erosional surface cut over different strata (De Batist, 1989; Tessier *et al.*, 1997; Trentesaux *et al.*, 1999; Mathys, 2009). These sand banks represent a huge pile of sand that could be available for coastal construction either by providing some sand to the system (Anthony *et al.*, 2000) or by sand-bank welding to the coast (Garlan, 1990). Over this surface in places where

tidal currents are too strong to leave much mobile sediment possible ancient drainage system can be visible flowed to the centre of the Dover Strait (Fig. 2.7).



*Figure 2.6. Eastern part of the French Flemish Coastal Plain from the Dunkerque – Watten canal. Inner Flanders relief in the background.*

The French coastal plain itself is called Blooteland, Heuvelland or, in French, Bas-Pays or Plaine maritime flamande. This is the place of our study; it possesses a wedge form and a surface area of approximately 750 km<sup>2</sup>. Gosselet (1893) defined this area as the lowland area which had been totally drowned at high tides. It was identified from west to east through different towns beginning since Sangatte extending to the east towards Ardres, Audruicq, Watten and heading to the northeast towards Bergues, Hondchoote and Veurne, then, continuing to different cities in Belgium (Fig. 2.2).

J. Sommé (1977) mentioned that the domain of the French Flemish Coastal Plain (FFCP) is extended to the south towards the surrounding areas of Saint Omer because their morphological characteristics and very low altitude forming a whole depression with the wide area to the north of Watten. This entire area represents a place where the Aa drainage basin was developed and the Quaternary changes were well-recorded.

In general, different geomorphological features have been recognised in the coastal plain from maps, digital elevation models and fieldworks. Sand/dunes complex, sand and gravel bars, confined inland depressions and flat coastal lands plains represent the current surface features of the area.

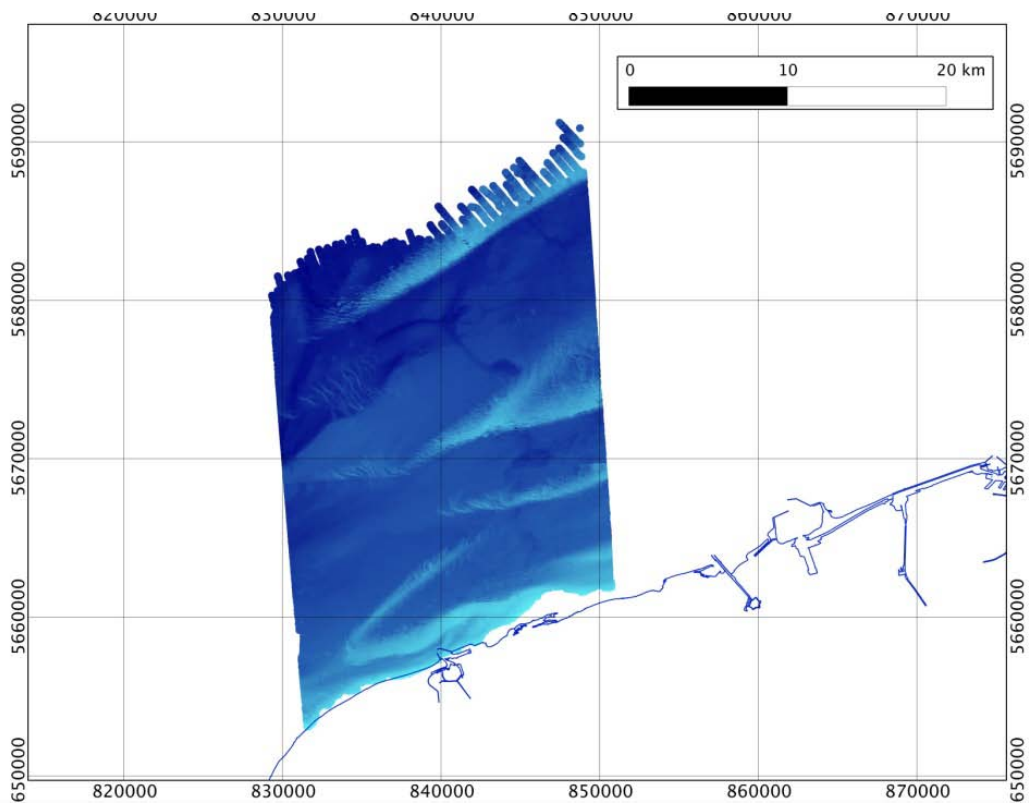


Figure 2.7. Bathymetric DEM of the zone offshore Calais. Shallow waters with sand banks are visible in light colours, while darker colours make visible a part of an ancient drainage that could be the trace of a paleo-Aa river toward the Dover Strait. Notice that this trace is just offshore Oye, while the present-day Aa outflow is 5 km East at the city of Gravelines. Map established with SHOM data delivered to the University Lille 1 under the 205/2010 contract.

The current coastline is straight and extended by approximately 50 km. It is dominated by sandy beaches and coastal dune systems stabilised by vegetation (De Moor and Mostaert, 1989; Houthuys *et al.*, 1993). The coast is strongly affected by tides, wind, waves and eventually storms (Anthony, 2000). Maximum dune heights are located towards the east of Dunkerque where the dunes reach altitudes up to between +10 and +20 NGF (De Ceunynck, 1985; Clabaut, 2000) (Fig. 2.8).

Behind the present coastal dunes some particular feature are observed. To the west of the coastal plain, the city of Calais and the town of Marck rest directly over gravel and sand bars with an altitude around +5 NGF. These reliefs were detailed by Dubois (1924) and Sommé (1977) and constitute the “*Banc des Pierrettes*” and the “*Banc of Marck*”, respectively.

Towards the easternmost area of the French coastal plain, located 2 km inland from the present shoreline, a dunes-ridge system is observed with a notable relief (+3 to +8 NGF) (Fig. 2.9). This unit represents the Ghyvelde dune system that

has been largely studied by several authors motivated to its particular geographical position and sedimentary characteristics (Blanchard, 1906; Dubois, 1924; Briquet, 1930; Paepe, 1960; Sommé, 1977; De Ceunynck, 1985; Baeteman, 2001, 2004, 2012; Anthony *et al.*, 2010, 2012). However, the Ghyvelde dune system is still discussed due to different interpretations in terms of mechanisms of formation as well as the temporal framework.



*Figure 2.8. Coastal dunes system at the east of Dunkerque. Easternmost part of the French Flemish coastal plain.*

Behind these dunes is situated the very flat and low-lying area of De Moeren, called in French “*Les Moères*”. This area shows quite different characteristics compared to the major part of the coastal plain. It lies about 2.5 m below the present-day mean sea level measured from the general levelling of France (NGF-IGN69). The area is enclosed to the north by the Ghyvelde dunes and to the south by the inner Flanders.

The following feature, further inland, applies to the major part of the coastal plain. It is the flat lands that show a relatively homogeneous relief, with gentle slopes and small heights reaching +3 m (e.g. Bourbourg town). At a first glance, the surface appears as a monotonous topography which has been densely populated and used for agriculture.

The vertical axis of the French coastal plain is observed between the surroundings areas of Saint Omer and Gravelines, showing its largest width: about 30 km in a straight line. The Aa and Hem rivers are draining this region; together with their affluent they represent the watershed of the coastal plain (Fig. 2.2). Through centuries, this place has been embanked and drained thanks to dense networks of artificial rivers called *watergangs* that allowed reclaim land from the sea, thus,

creating a polder region. This made the region a heavily anthropised area (Tys, 2007) showing dense population, developed industry and intensive agriculture.



*Figure 2.9. Two photographs of the Ghyvelde dunes systems. A) A general vision of the current aspect of the inland dunes. B) An approach detailed the aspect of the upper part of the dunes showing aeolian cross-bedding and soil development. A pen is used as scale.*

As mentioned before, the Aa river possesses two intervals. On the lowlands of the coastal plain is observed the second interval. It represents a meandering river running through the plain seawards. With around 0.6% flatter gradients (Blanchard, 1906) its flow discharge decrease until  $4 \text{ m}^3\text{s}^{-1}$ , around the Wizernes town (I.F.R.E.M.E.R, 1986).

The river turns sharply to the NW by the Arques town, where the course has been modified by the human action. The navigable waterway is crossing the Audomarois (name of the natural region around Saint-Omer town) swamplands and receives the Houlle affluent when approaching Watten. Just after the Watten area,

the lowermost part of the watershed begins. The present-day drainage is subdivided in three main branches leading to Calais, Gravelines and Dunkerque and is spreading throughout the plain by the watergangs. Present configuration is the product of several human interventions after the creation of dykes, channelization and drained areas.

Concerning to the Hem River, in this section the river enters into the plain. The average slope around the Polincove town falls to about 1%. Crossing the coastal plain, the watercourse is modified and then separated in two arms that end in different zones of the waterway that join Calais with Saint Omer (SAGE du delta de L'Aa, 2005).

### **2.3 Hydrodynamic context**

The consideration of the hydrodynamic conditions is a key element in the study of coastal and marine environments (Callaghan *et al.*, 2010). The assessment of the current characteristics of tides, winds and waves is important to clarify the functions and impact of them on source areas, transport mechanisms and possible changes in the sedimentary processes through time. The effect of the coastal hydrodynamic conditions to the French Flemish Coastal Plain has been a remarkable point in this area because it represents one of the main controls in the Quaternary stratigraphic record and their characteristics onshore and offshore (Trentesaux, 2005).

The North Sea is a marginal sea with important tidal currents but also where the wind action plays an important role over the marine currents (Anthony, 2000). Waves action is limited because of the configuration of the coast that does not allow the intrusion of long ocean waves (Clique and Lepetit, 1986). The shallow water depths of this sea contribute to limit their formation. The entire characteristics displayed by the hydrodynamic conditions have an important seasonal component that provides different scenarios during the year in relation with the energy conditions and the occurrence of climatic events.

The French Flemish Coastal Plain is characterized by a semi-diurnal, macrotidal regime. Mean spring tidal range varies from 6.4 m in Calais to 5.4 m in Dunkerque, while mean sea level varies from 0.6 to 0.5 m above NGF- IGN69 datum in the same direction. So a large part of the plain lies below the level of the mean



high water springs (3.8 m at Calais for 3.2 m at Dunkerque), which causes the susceptibility of the area to be flooded by the sea (Fig. 2.10). Tidal currents flow parallel to the shoreline with velocities between 0.5 and 1 m/s (S.H.O.M, 1968; LeBot, 2001; Cartier, 2011). They are characterized by the asymmetric alternation of flood currents directed to the north-east and ebb currents which leads to the south-west (Fig. 2.11). Flood tide currents are faster and shorter than ebb tide currents that are dominant in duration (Clique et Lepetit, 1986; Cartier, 2011).

Because of the characteristics of the shallow sea, the wind on the North Sea has a major importance to reinforce the tidal currents and spreading the waves. Wind roses in the figure 2.12 evidence a predominant blowing direction from the south-west. A second wind direction can be distinguished coming from the north-east. Due to its intensity it may helps in building the eolian dunes extended in the area.

Regarding to the waves action, their patterns are under the control of the predominant wind direction. In this sense, the waves derived from the north and north-west zones of the North Sea. The wave heights are usually comprised between 0.5 m and 1.5 m, but may attain up to 3 m during the storms (Clique and Lepetit, 1986; Anthony *et al*, 2010). The period of waves has an average of 5 s (Le Bot, 2001).

Sediment transport patterns are dominated by tides, wind waves and wind-driven currents. Along the coast, wave-driven currents also contribute to the sediment transport (van der Molen and van Dijck, 2000). The strong tidal currents induce the transport of high amounts of sediment in the southern North Sea which generates a group of very large linear sand banks (Tessier, 1997; Trentesaux *et al.*, 1999).

The main direction of sediment transport along the coastline responds directly with the fluctuations in tidal currents. However, due to the asymmetry of tidal currents and the provenance of the waves, the resultant littoral drift is rather northward towards the Belgian coast (Cartier, 2011). Sand banks of the offshore area of the southern North Sea have represented some evidences to understand the sea-level variations and features of sedimentary units preserved (Trentesaux, 2005).

The combination between the dominant macrotidal conditions, compared with the relatively limited action of wave dynamics, leads to define this coastal plain as a tide-dominated system (Dalrymple *et al.*, 2012). However, due to the strong anthropisation, some processes have been minimized and the current coastal dynamic has been modified.

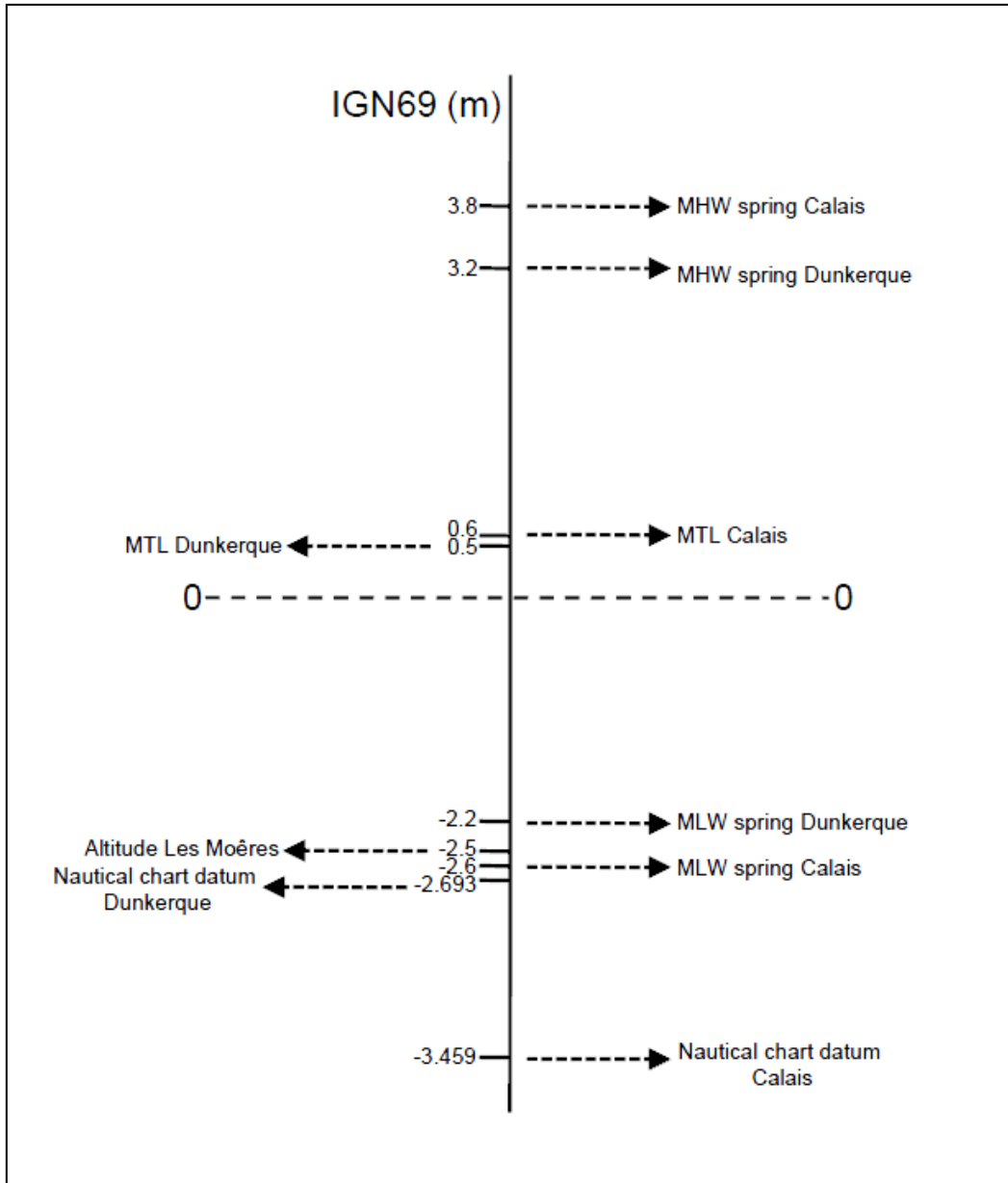


Figure 2.10. Diagram illustrating tidal levels and depths measured in the FFCP. MHW: Mean high water, MTL: Mean tide level, MLW: Mean low water.

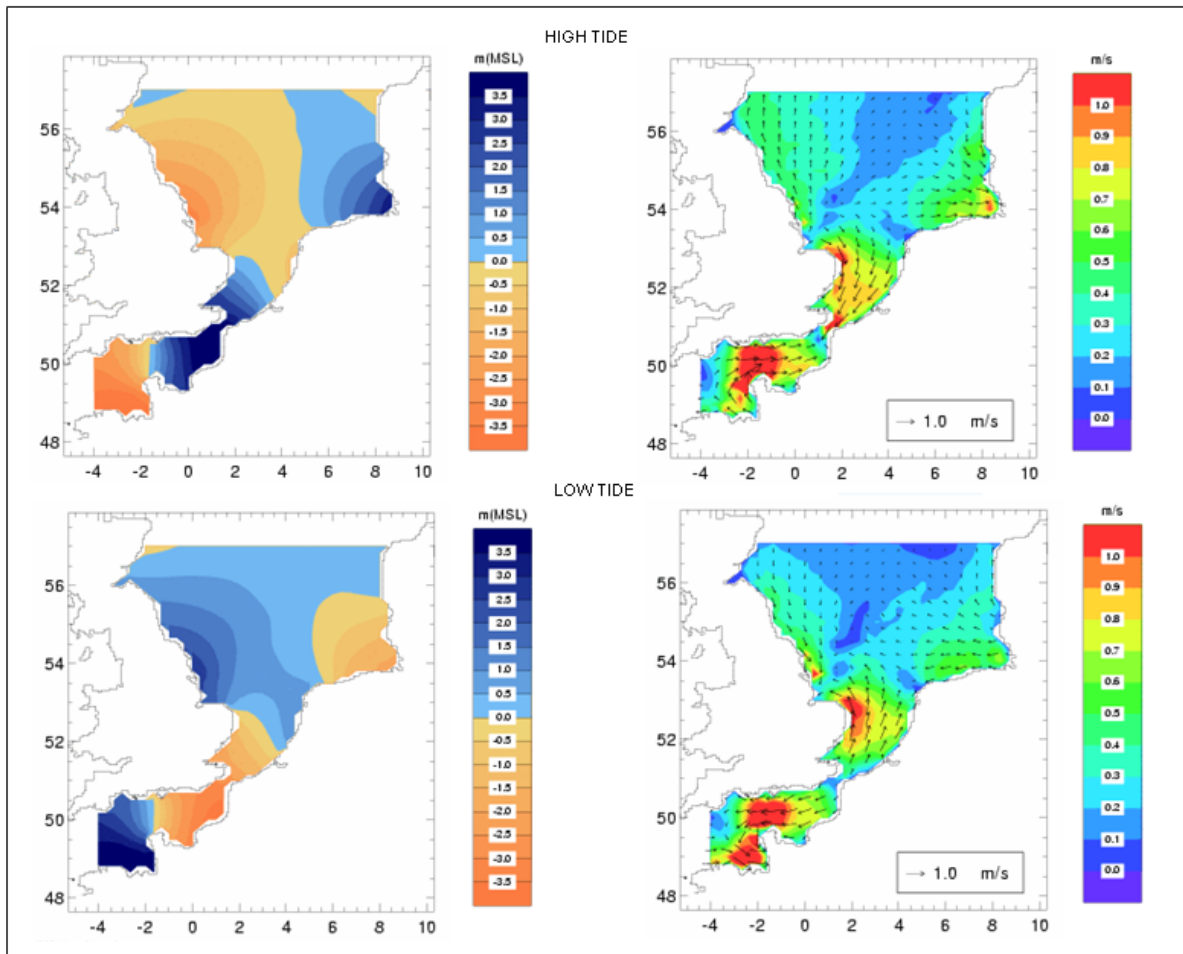


Figure 2.11. Tides and currents to the English Channel and the southern North Sea. From <http://www.mumm.ac.be>

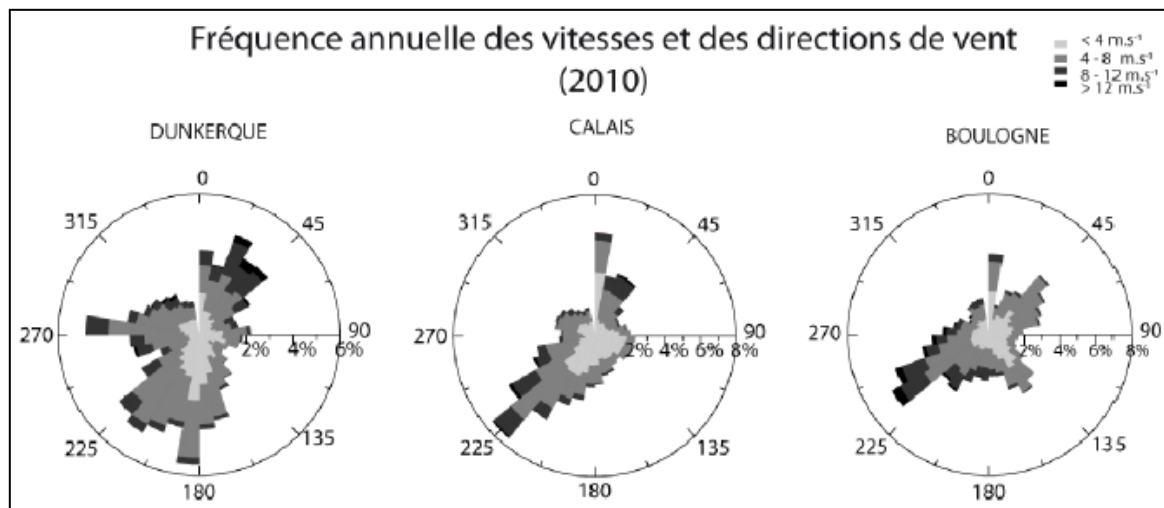


Figure 2.12. Wind direction averages to the north-western France. Data obtained of <http://www.meteofrance.com> from Cartier (2011).

## 2.4 Geologic context

The French Flemish Coastal Plain is a wedge of Quaternary sedimentary deposits bordered by Cretaceous and Palaeogene formations. The figure 2.13 shows the present-day geological configuration of the area. The coastal plain is located after the flexure of the Variscan front, in the Anglo-Brabant block, a monocline structure dipping gently towards the North and North-East (Colbeaux *et al.*, 1980; Van Vliet-Lanoe *et al.*, 2001).

The western border is limited by the Artois Hills and Boulonnais highlands that are represented by the asymmetric fold structures and striking faults belonging to the Weald-Artois axe (Mansy, *et al.*, 2003). This western part is mostly composed by Mesozoic rocks. Palaeogene and Lower Palaeozoic rocks also outcrop in the area. The main part of the bedrock corresponds to Cretaceous chalks (nodular chalk and chalk with flints), Jurassic shales, sandstones and marly limestones, Palaeogene sands and Palaeozoic carbonates and shales (Briquet, 1930; Pierre and Lahousse, 2004).

Towards the east, the coastal plain is limited by the high relief of the inner Flandres and the group of hills denominated “Mont des Flandres”. This relief represents a clastic Palaeogene unit characterized by Paleocene sandstones and Eocene clay rocks, relic of the geomorphologic changes occurred during the Neogene period (Sommé, 2009; Melliez, comm. personal).

In general, geological formations outcropping in the highlands, are dipping with the structure towards the North and North-east. Paleozoic rocks are overlain by Mesozoic and Paleogene rocks representing the basement of the North Sea shelf and the coastal plains that are covered by the Quaternary deposits (Henriet *et al.*, 1989; Liu *et al.*, 1993; Trentesaux *et al.*, 1999; Mathys, 2009).

The distribution and characteristics of the Quaternary deposits are closely linked with the exposed and submerged history, in response to the frequency and magnitude, of the glacial – interglacial periods (Mellet, 2012). These cycles were accompanied by an event very significant for the region: the breaching of the Dover Strait.

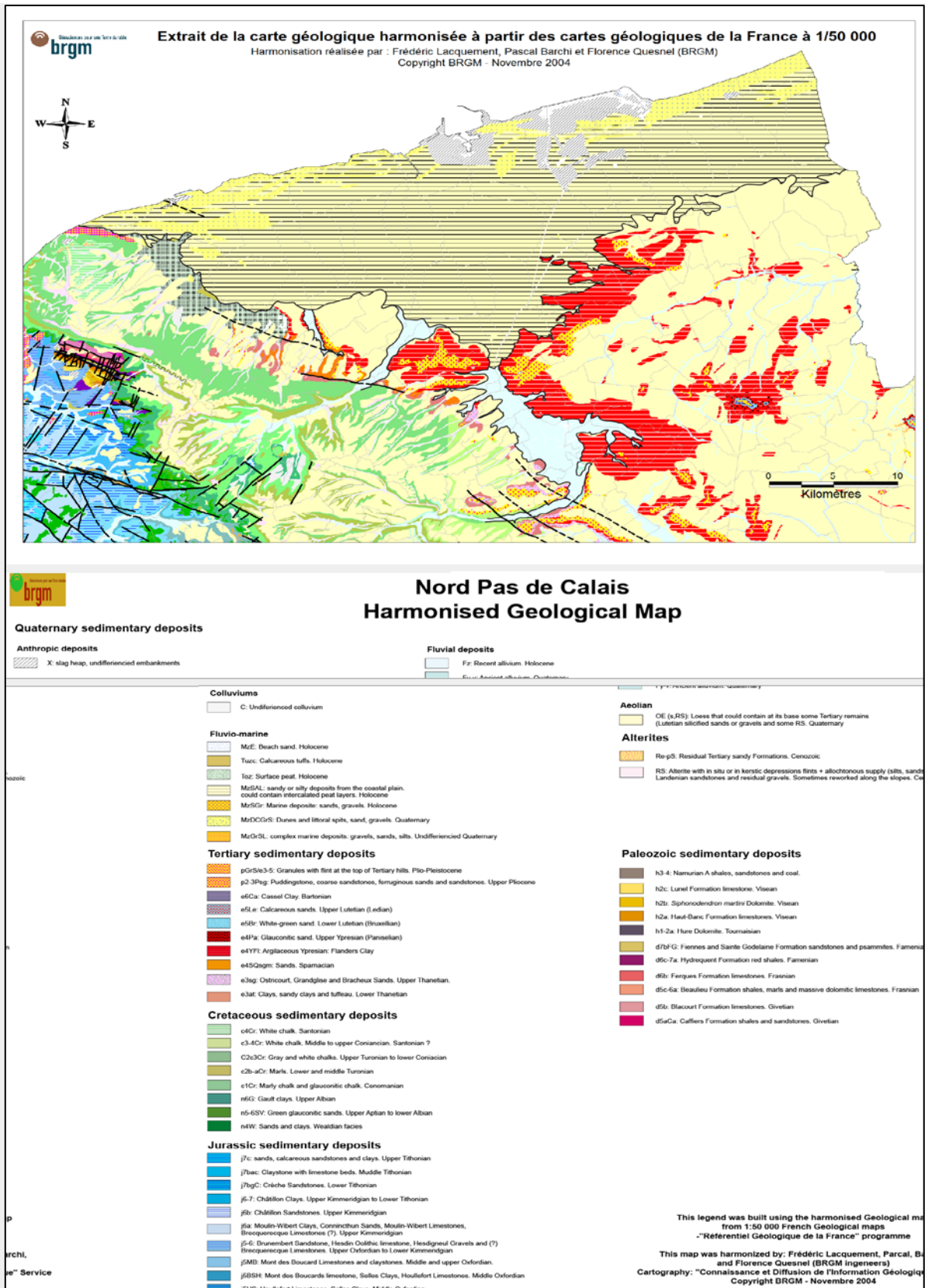


Figure 2.13. Harmonized geological map of the study area. Courtesy from Julie PICOT-2014, BRGM, Service Régional Nord- Pas de Calais. We translated the original legend from French and adapted it to the terrains outcropping in the area. Supplementary information can be found at Infoterre website: <http://infoterre.brgm.fr>

Even if the age of the definitive breaching is still debated and could be considered of Tertiary age, the changing sea level during the Quaternary radically transformed its importance and deeply transformed the sedimentary processes. Different hypotheses are expressed, and still debated, to explain the mechanism that induced the breaching of the Strait of Dover and the evolution of the English Channel. The following are some scenarios proposed to its formation:

Colbeaux *et al.* (1980) expressed a tectonic scenario where the major opening process was interpreted as due to perpendicular graben formation resulting from pulsating reactivation movements of the fault zone between the Brabant and Ardennes block (Fig. 2.14).

Another uplift and subsidence in response to glacio-isostasy adjustment due to glacial – interglacial climatic alternations (Lambeck, 1997; Van Vliet-Lanoë *et al.*, 1998; Shennan *et al.*, 2000; Antoine *et al.*, 2003a; Busschers *et al.*, 2007). In the same time some spectacular processes at the moment of reopening at one or more sea-level rise were proposed: Catastrophic overflow from the breaching of a glacial lakes (Gibbard, 1995, 2007; Gupta *et al.*, 2007) or a gentler fluvial down-cutting (Gibbard *et al.*, 1988) (Fig. 2.15)

In this sense, it is possible that interaction of higher frequency relative sea-level changes, climatic conditions and tectonics induced the morphology of the valleys around the southern North Sea that were subsequently modified during the Holocene infill (Guilcher, 1951; Jelgersma, 1979; Antoine *et al.*, 2003a).

In the Belgian coastal plain and the continental shelf, the tectonic and isostatic movement are not evident or absent during the Quaternary, indicating that the area has been relatively stable (D'Olier, 1981; Kiden *et al.*, 2002, Vink *et al.*, 2007, Mathys, 2009). Henriët *et al.* (1989) revealed an undeformed Quaternary cover from their seismic profiles offshore northern France and Belgium, thus, similar conditions could be envisaged in the French coastal plain. Despite that, it is important to note the hypothesis of the neotectonics after interpretations of modern fault reactivation in Saint Omer area (Gandouin *et al.*, 2007) and make comparison between satellite imagery and ancient cadastral register of the northern France (Colbeaux, comm. personal).

Quaternary deposits cover the whole French Flemish Coastal Plain (FFCP) area. The deposits consist of a complex variation of fluvial, aeolian and marine deposits. Most of the deposits in the plain are of Holocene age (Fig. 2.13).

However, there are some witnesses of Pleistocene deposits located in specific sectors into the plain (e.g. Coulogne), but they are more common outcropping at the landward surrounding areas of the plain (e.g. Sangatte; Sommé, 1977, 1999).

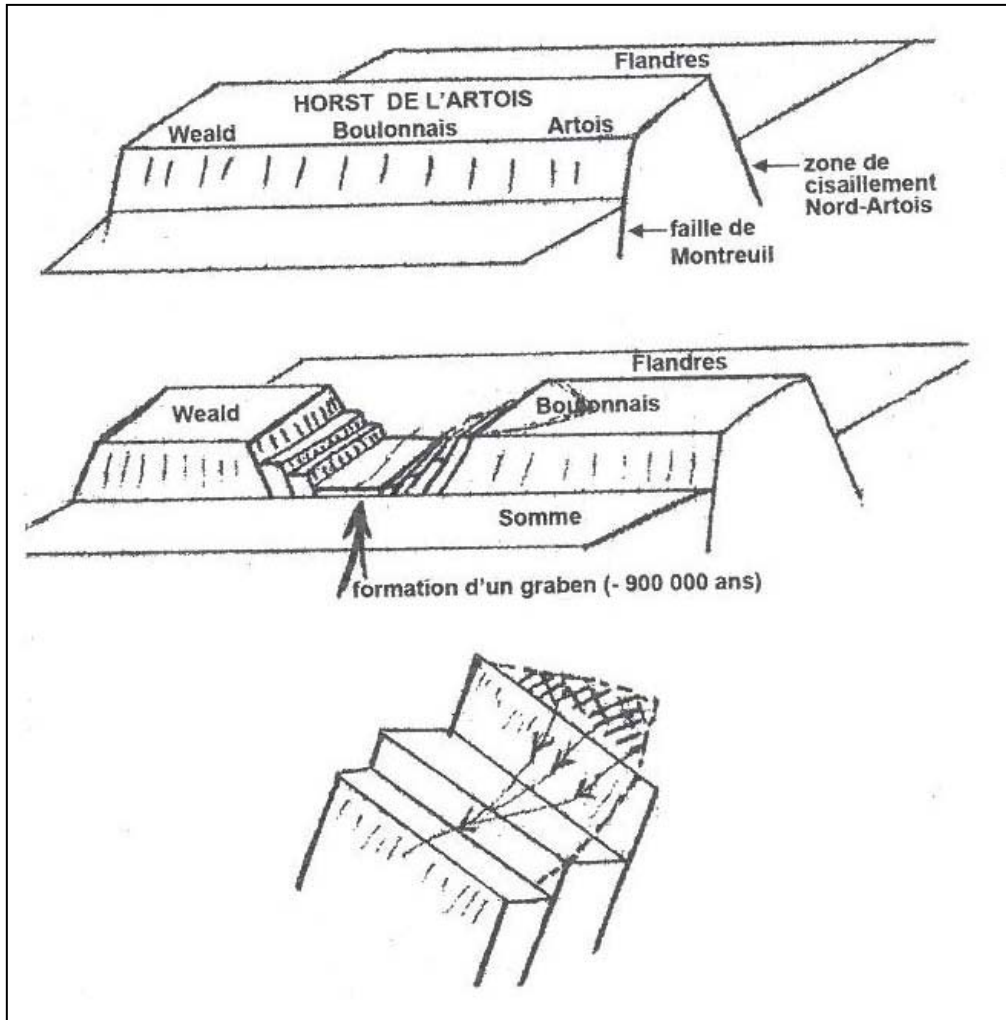


Figure 2.14. Structural model for the Dover Strait breaching (From Colbeaux, 1980). Upper: Artois horst formed around the Eocene period. Middle: Formation of the graben during the Pleistocene. Lower: Graben flank erosion caused by the rivers.

Holocene deposits respond to a variable coastal sedimentation marked by dynamic marine sand supply and tide-hydrodynamic circulation (Anthony, 2000; van der Molen, 2000). Likewise, the relevant Pre-Holocene palaeotopography (Baeteman and Declercq, 2002) and the context of the post-glacial climatic changes (Törnqvist and Hijma, 2012) were factors that affected the sediment distribution and ruled the coastal evolution.

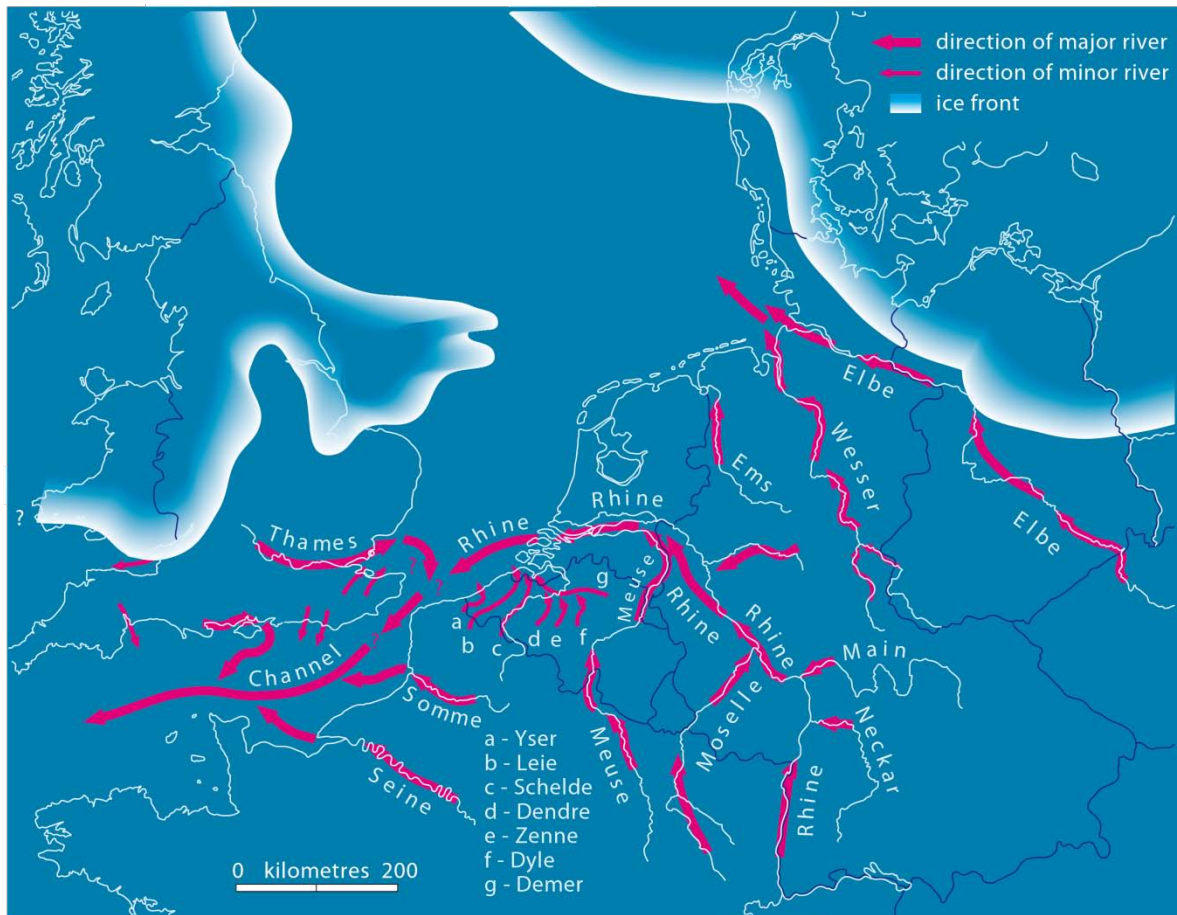


Figure 2.15. Paleogeographical map illustrating the river system of northwest Europe during the maximum extent of glaciations in the late Weichselian. Data originally published by Philip Gibbard in 1988 and updated to the NEESDI project 2001.

Map obtained from [http://www.qpg.geog.cam.ac.uk/research/projects/nweurorivers/#The\\_maps](http://www.qpg.geog.cam.ac.uk/research/projects/nweurorivers/#The_maps)

## 2.5 Development of the Quaternary stratigraphy

The evolution of the Quaternary infill in the region of the northern France has been studied by various authors since the 19<sup>th</sup> century. A brief historical overview is made in order to indicate some aspects of the conceptions and definitions of the Quaternary stratigraphy and the Holocene development of the northern France coastal plain:

As mentioned Sommé and Tuffreau (1978) the first general references in respect to the study of the Quaternary stratigraphy in the north of France were proposed by Belpaire in 1827 and Meugy between 1851 and 1854. The overture of descriptive geography is traced back to 1870. This corresponds to an open-minded and rich period in observations, research and discussions about the stratigraphic



problems present in the area. Gosselet (1873) and Ladrière (1879) conceived some ideas about the superposition of sedimentary beds and regional variations in northern France.

Keeping on with their research, Ladrière (1890) and Gosselet (1893) proposed some stratigraphic systems and evidenced the marine influence in the sedimentary deposits for the coastal region. Despite the importance of the advances by Ladrière (1890) their systems were not taken into account by Dubois (1924) due to the lack of stratigraphic organisation of the deposits. However, he considered useful their elaborate lithologic description in his stratigraphic recognition.

Because of the great emphasize in the detailed sedimentary units and thanks to its extensive work bearing new stratigraphic definitions, Dubois (1924) became the main stratigraphical reference for the area (Fig. 2.16). Describing many boreholes and similar deposits he defined three lithostratigraphic subdivisions for the Quaternary deposits associated to a major sedimentary cycle in Flanders. His work, accompanied by the excellent syntheses made by Briquet (1930) and Sommé (1977), is an essential inventory of the lithostratigraphy of northern France and provided a regional framework for the different stratigraphic units.

Dubois (1924) named “Assise d’Ostende” the lower part of the sediments that contain abundant *Corbicula fluminalis*, a bivalve mollusc. He proposed “Assise de Calais” for the thick marine grey-blue sandy deposits underlying the upper peat and containing a faunal assemblage similar to the present one. He also related the Assise de Calais to the shingle spit system of *Les Pierrettes*. A third lithostratigraphic unit was proposed as “Assise de Dunkerque” for the marine sediments corresponding to the upper part of the sedimentary succession above the upper peat and containing recent fauna such as soft-shell *Mya arenaria*. J. Cornet in 1927 made an analogy in his initial approach in Belgium (Baeteman, 1999).

A. Briquet (1930) and Tavernier (1938) associated the Dunkerque deposits to a major sea-level rise setting emphasis on the concepts of transgressions. However, Tavernier (1947, 1948) introduced the subdivision of these deposits in three transgressions (Baeteman, 2013) and discuss the relief inversion caused by the peat compaction. Moreover, from his observations, the surface peat was indexed as a separate layer above the “Assise de Calais” and below the “Assise de Dunkerque”; also the “Assise d’Ostende” deposits was attributed to an Eemian age (Sommé, 1977).

Geological time scale age Ka		France marine - estuarine lithostratigraphy (Sommé, 2013)	Belgium marine - estuarine lithostratigraphy (Gullentops et al., 2001)	Belgium lithostratigraphy (Tavernier, 1948)	Northern France lithostratigraphy (Dubois, 1924)					
11.7	HOLOCENE	FLANDRES	Dunkerque  Calais	VLAANDEREN Fm. De Haan Mbr. Dunkerque Mbr.  Calais Mbr.	Dunkerque deposits	FLANDRIEN	Upper	Assise de Dunkerque	Cardium sands	
					Surface peat		Middle	Assise de Calais	peat Sands Polder clays	
123	PLEISTOCENE	LATE	LOON	Oostende Fm.	Deeper peat		Lower	Assise de Ostende	peat	
							MIDDLE	Herzeele Slack Fart	Herzeele Fm.	

Figure 2.16. Schematic stratigraphic table of the Quaternary deposits in the French –Belgian coastal plain area.

Further investigations were carried out in the context of soil mapping using the transgression subdivisions in the Belgian coastal area after the 1950s (Baeteman, 1999; Baeteman, 2013). In the French area it would be awaited until the 1970s to get new contributions as those by Paepe and Sommé (1970), Lautridou and Sommé (1974) and Sommé (1977) for establishing comparisons with the stratigraphic framework adopted in the neighbouring countries.

In the seventies, the regional stratigraphy was marked by chronostratigraphic interpretation of the Holocene deposits (Fig 2.17). The detailed chronology is imposed in the stratigraphic description and the name of Calais and Dunkerque became used in different context as informal lithological units, formal lithostratigraphic units and transgression phases (Baeteman, 1999; Sommé, 2013). However, the characteristics of the sedimentary succession allowed the interpretation in terms of transgressive and regressive stages and their association with the post glacial sea-level changes (Sommé, 1977; 1979). In this sense, Calais and Dunkerque

units became two major transgressions without distinguishing other infill processes (Baeteman, 1999).

This vision became generalised, the stratigraphy was almost exclusively referring to the relationships of these deposits and the variability of the sea level changes. Thus, the presence of sand beds intercalated with peat levels through the entire sedimentary system, pollen-analysis data and radiocarbon dating allowed the recognition of alternating transgression - regression cycles (Sommé, 1979; Van der Woude & Roeleveld, 1985). As a consequence, the Holocene sedimentation was associated to accentuate transgressive pulses and stillstand periods after the melting of the last glacial caps.

The concept of alternating cycles of transgression and regression settled the stratigraphic framework in the plain because the deposits were often correlated with Dutch and German successions to indicate that the Holocene sea-level changes were synchronous and easily integrated within the overall North West Europe (Meurisse, 2007). However, a scientific group of Belgian and German researchers, mentioned that this adopted stratigraphic system excluded the dynamic character of the depositional processes to be considered as representative of the entire Holocene settings of the southern North Sea (Streif 1978, Baeteman, 1999, 2005).

In this sense, another perspective is proposed including the problems concerning the complexity of the stratigraphy (Streif, 1978; Baeteman, 1985; 2005b; Bertrand and Baeteman, 2005). Thus, the development of the coastal plain becomes a function of different controlling factors as rate of sea-level rise, sediment budget, accommodation space and subsequent processes that affected the sediments as peat compaction (Baeteman, 1999, 2013). This approach was continually developed in the nineties and improved with new studies which have resulted in significant differences to understand the development and evolution of the Belgian coastal Plain (Bertrand and Baeteman, 2005).

Meanwhile, during the eighties and nineties, several studies were deployed along the NW France in order to improve the palaeogeographic settings and stratigraphic features of the Pleistocene deposits (Sommé, 1992; 1994). These investigations achieved improvements in age determination, new lithostratigraphic formations and the variations related to the climatic or neotectonic controls that ruled the Pleistocene sedimentation (Sommé *et al*, 1999). However, they did not lead to significant changes in the definition of the Holocene deposits and their stratigraphic

system (Van der Woude & Roeleveld, 1985; Leplat and Sommé, 1989; Sommé *et al.*, 1992, 1994, 1996).

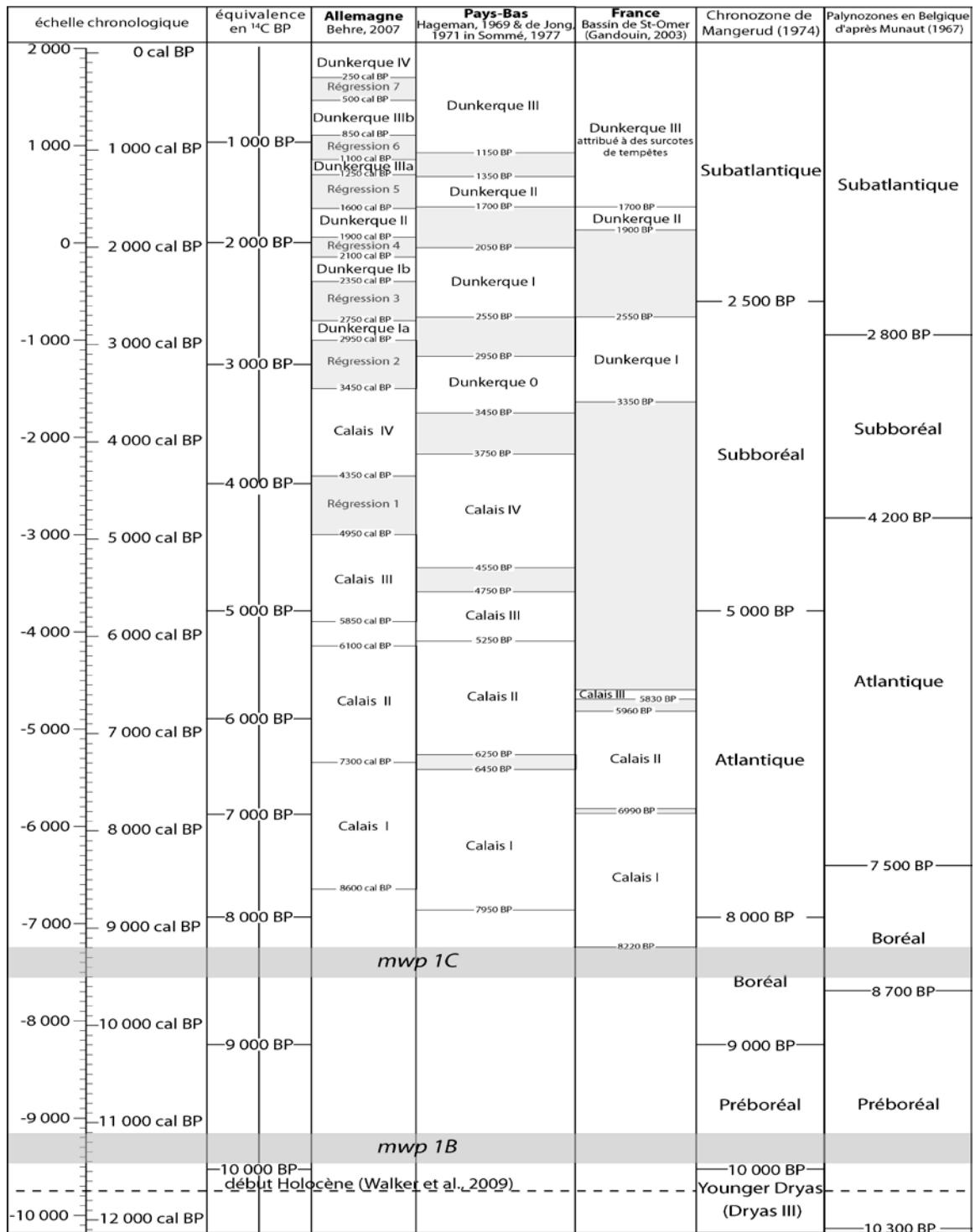


Figure 2.17. Comparative table showing the widely-used palynological Holocene subdivision and the stratigraphy of the north-western Europe according with the transgressive – regressive record. From Gosselin (2011).

New approaches in the French coastal plain have abandoned the chronological Calais – Dunkerque system using facies analysis to obtain palaeoenvironmental evolution (Mrani, 2006) or qualifying the classical patterns of sea-level changes into major palaeoenvironmental sequences to identify the general environmental trends which could be used on regional scale (Meurisse, 2007).

However, recent improvements in the lithostratigraphic charts based on inventories of detailed lithological studies (Sommé, 2013) seek to recover the lithostratigraphic sense of the “assises” and suggest a complete stratigraphic framework to the Quaternary units of the northern France. In this regard, applying “Assise de Dunkerque” to the deposits above the surface peat seems to remain valid due to the significant change in sedimentary conditions expressed across the plain. The “Assise de Calais” in spite of its variable lithology, remains a useful and simple mapping unit given the low density of detailed borehole data and relatively low knowledge of the underlying strata.

## **2.6 Holocene sea level rise**

There has been broad discussion about the interpretation of sea-level changes and the palaeoenvironmental context that supports the reconstruction of the geological setting in the southern North Sea area and specifically its control on the French Flemish coastal plain.

The sea level rise plays a key role in the Holocene sedimentation of the North-Western Europe (Törnqvist and Hijma, 2012). Palaeoenvironmental changes are strongly influenced by the sea-level conditions of the southern North Sea. Several curves have been applied through time to explain the variations of the sea level and the relationships with complex coastal stratigraphy and the distribution of depositional environments (Ters, 1973; Jelgersma, 1979; Denys and Baeteman, 1995; Lambeck, 1997; Behre, 2004, 2007).

Two contrasting models exist for the interpretation of relative sea-level changes and their influence on depositional systems in the southern North Sea Basin (Baeteman, 2008). The first suggests a fluctuating model using the Calais-Dunkerque system with data obtained from Germany and unpublished data from investigations in different points of the coastal region (Behre, 2004, 2007). The second shows a smooth and gradual sea-level rise based on data collection from coastal plains of

Netherlands (Jelgersma, 1979; Kiden, 1995) and Belgium (Denys and Baeteman, 1995). The Figure 2.18 shows the two types of curves proposed to describe the sea-level rise during the Holocene.

They look rather different and gave rise to the highly debatable question whether eustatic changes are best reflected by smooth or oscillating curves. The fluctuation curve assumes transgressive and regressive phases that can be applied throughout the southern North Sea with a terminology fairly employed in the region (Behre, 2007). However, this curve has been questioned to be used in the southern North Sea basin as a whole because of uncertainties in the age and altitude estimates (Baeteman, 2008). They dismiss compaction, changes in coastal settings as differences in tidal ranges, erosion and reworking of sediments as well as the glacio-isostatic movement that influenced differently the coast of Germany, Netherlands and Belgium (Baeteman *et al.*, 2011).

In turn, the smooth sea-level curve considers the importance and control of sedimentary processes, variations in sediment supply and accommodation space. It appears as a general rise following a very smooth declining of the acceleration rate (Denys and Baeteman, 1995; Baeteman, 1999). The trend of sea-level rise presents a fast increasing at the beginnings of the Holocene (7m/kyr) and two progressive decelerations at 7500 cal BP (2.5m/kyr) and 5500 cal BP, after which time sea-level rose at a rate of 0.7m/kyr.

Also, sediment compaction and increasing of storm activity became important in the sedimentary record for the late period of the Holocene (Meurisse-fort, 2007) considering the variations in the deposits as a result of sedimentary processes and not as fluctuations of sea level.

Holocene sea-level have been largely studied to interpret the sediment variability and palaeoenvironmental changes in the sedimentary record. Holocene deposits possess an important influence of the sea-level rise printed in their characteristics. Analyzing the sea-level reconstructions made in the southern North Sea and the sedimentary characteristics observed in the Holocene record of the French Flemish Coastal Plain we found that it seems there is no need to add some fluctuations in the sea-level rise to integrate the results that we obtained in our study.

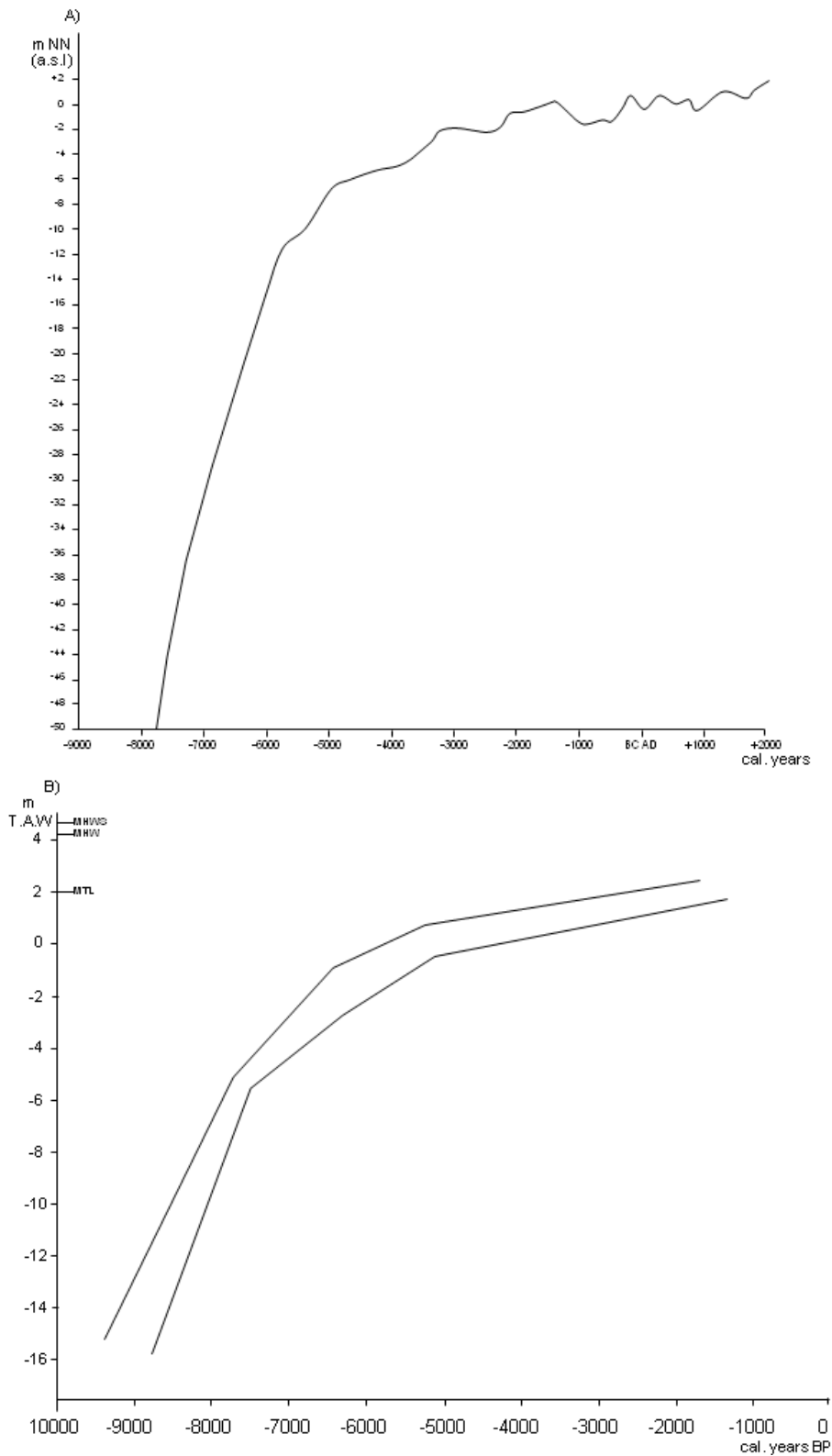


Figure 2.18. Relative sea-level curves in the southern North Sea. A) Sea-level curve by Behre (2007) showing changes in the late Holocene relative sea-level rise. German ordinance datum (NN) is similar to the French mean level (NGF). B) Sea-level curve by Denys and Baeteman (1995) showing a smooth late-Holocene relative sea-level rise. The Belgian datum (TAW) is 2.33 m lower than the French datum (NGF).

## **2.7 Comments about the literature review and vision of this research**

The northern of France has represented an historic place to understand the Quaternary regional context of the southern North Sea. Continuous improvements and new data are required to provide new clues about the development of the sedimentary succession and the processes acting in their evolution.

Many interpretations are obtained from several researches conducted in the coastal plain and surrounding areas. Through time, new conceptions and interpretations have induced replacement and abandonment of different systems and classifications providing a wide range of models, detailed or simplified. The contrasts between them will remain interesting and debated because of their usefulness to each area and the quantity of evidences or local changes that support their differences. However, it is important to know the limits and reliability of the model to be used as well as the issues that controlled the sediment variability to reflect the best approach of the sedimentary infill.

The French Flemish Coastal Plain is an area that presents a high variability in their deposits. Besides, considering the different geological investigations developed in the area and their different approaches it seems necessary to perform more research to obtain some responses to the current knowledge of the depositional history. Efforts for understanding the complex sedimentary arrangement and the distinct characteristics and distribution of the deposits should be focused onto facies assemblages that highlight the stratigraphic architecture without rigid models, identifying the variables affecting the sedimentation beyond the sea-level changes. This research is conducted having this sense in mind. We tried to use new techniques and merged different disciplines to contribute to a regional vision of the Holocene infill.



# **Chapter 3. Sedimentary facies analysis and depositional system of the French Flemish coastal plain**

## **3.1 Introduction**

A depositional environment is the result of a dynamic association among physical, chemical and biological processes operating within an area (Scholle and Spearing, 1982). These processes impart explicit characteristics to the sediments being deposited. In consequence, a sedimentary environment can be reconstructed using these parameters including distinctive features as composition, inorganic and organic sedimentary structures, textures, mineralogical composition, and faunal and floral assemblages (Nichols, 2009).

Reconstruct coastal or marginal marine environments is not an easy work (Miller, 1965). Although, these zones are well preserved in the stratigraphic record it is difficult to find the relationships between the sedimentary characteristics of the deposits and the wide range of environmental processes (Coleman and Prior, 1982, Boyd *et al*, 2006). For this reason, a detailed sedimentological examination should be conducted to develop an accurate approach for a comprehensive reconstruction of mechanism that ruled the palaeoenvironmental conditions (Reineck and Singh, 1980).

In the French Flemish coastal plain (FFCP), despite previous investigations and the abundant subsurface data derived from undisturbed cores and numerous auger hand drillings (Bosch, 1975; Bootsman, 1977; Paris, 1977; Sommé, 1977; Sommé, 1994; Gandouin, 2003; Mrani, 2006), the response to sea-level rise control, hydrodynamic behaviour, and sedimentary deposits arrangement during the Holocene still remains debated as what regards the main factor controlling the stratigraphic architecture.

This chapter shows the nature and sedimentary characteristics of the Holocene deposits from new core data acquired into the FFCP with the purpose to provide new insights for the Holocene sedimentary succession. The detailed study of these new cores seeks to help filling the gap of the changes on this coastal system.

In this sense, we divided the deposits in five sedimentary facies and environmentally significant facies assemblages as defined by Dalrymple, *et al.* (1992) and Dalrymple and Choi (2007).

Comparing with previous subsurface data, it leads to a comprehensive overview of the sedimentology, stratigraphy, palaeoenvironmental framework and depositional processes after the last glaciation and before the anthropisation of the plain. To support the interpretation of the sedimentary facies, clay mineralogical assemblages and micropaleontological data (foraminifera and pollen analysis) were integrated to the facies analysis in order to obtain a most reliable approach of the depositional conditions (Culver and Banner, 1978; Huault 1980; Chamley, 1989).

## **3.2 Methods**

### **3.2.1 Subsurface facies analysis**

Data on the subsurface of the FFCP are derived from four sources (Fig. 3.1):

- 188 borehole lithology data of previous published studies (Bosch, 1975; Bootsman, 1977; Paris, 1977; Sommé, 1977; Sommé, 1994; Gandouin, 2003; Mrani, 2006). Descriptions were carefully red to be homogenised with unique vocabulary.
- 197 boreholes from the BRGM database. Many data from the French Geological survey (BRGM) are easily available through internet via the InfoTerre website (BRGM, 2014) or directly at the regional office of the survey. The database includes: oil drills, geological and geotechnical investigations, water boreholes and hand drillings. The reliability and detail level of these descriptions is highly variable because their contents include any subsurface description associated to several studies. For this reason, data were selected with emphasis on verified and documented data. Data folders were reviewed and validated according to the level of detail and the consistency of the descriptions. In the BRGM database we found some boreholes with ancient

reference levels. Changes were done to relate them to the NGF – IGN69 datum.

- 2 sections from archaeological trenches and pits exposing the stratigraphy of the final infill of the Holocene succession (Figs. 3.2 – 3.3). In the Bierne area, we took benefit of an archaeological diagnostic to get the last few meters of a large surface open in the framework of a natural rehabilitation. These sections were described, but we also used some data from the report that was written by the archaeologists (Herbin, 2013).
- 10 undisturbed cores collected during two fieldwork campaigns at Bierne and Les Attaques areas (Figs. 3.2 – 3.4).

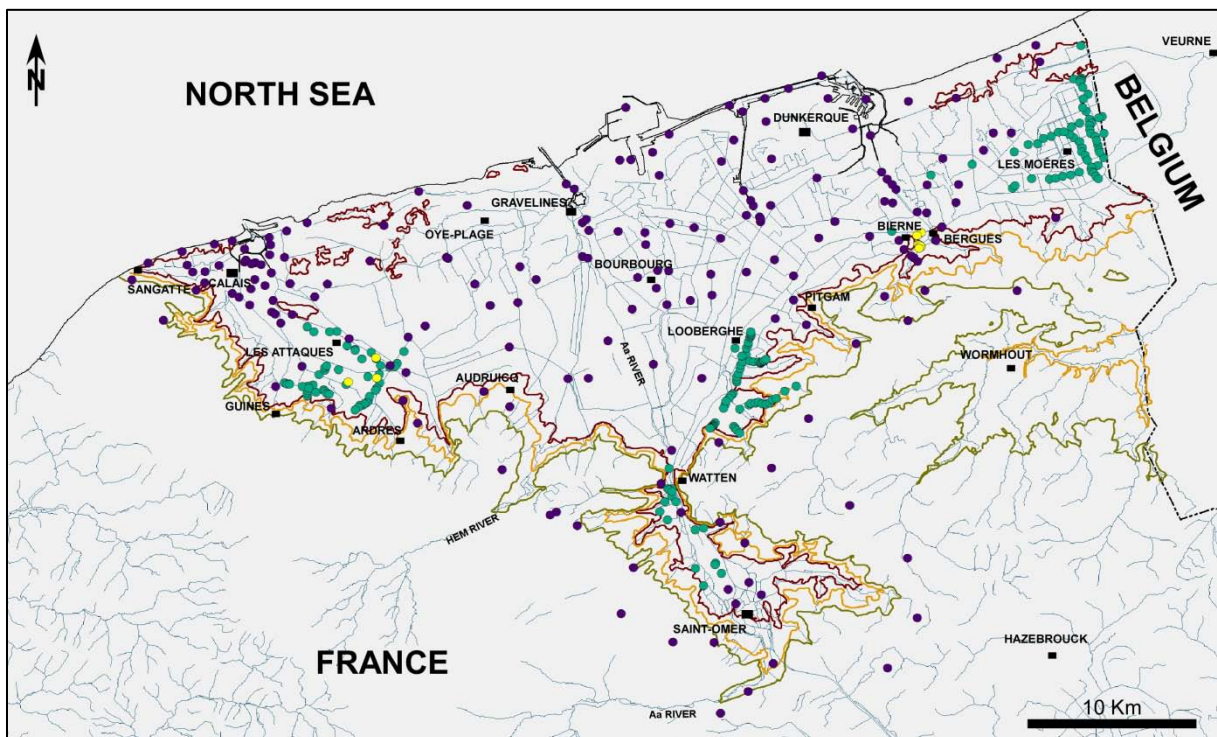


Figure 3.1. Map of available subsurface data used in this study. BRGM boreholes (●). Previous published studies (▲). Cores obtained during our fieldwork campaigns (◐). Cities and towns (■). Details on the location and name of boreholes in appendix A. Contour lines correspond to +5m NGF (red line), +10m NGF (yellow line) and +20m NGF (green line).

These two sites were chosen to provide accurate sedimentary records of the Holocene infill in selected areas (Fig. 3.2). The Bierne site was selected taking the opportunity of archaeological trenches dug by the Archaeological Service of the

General Nord Council (Fig. 3.3). This area represents an interesting zone contributing to recognize the latest sedimentary beds and to obtain the complete succession of Holocene deposits and the contact with older deposits. This place is also located along a presumed old stream linking the upper reaches of the coastal plain with the area between Bergues and Dunkerque.

The Les Attaques site was selected for the good seismic information that was recorded in the Calais – Saint-Omer canal near this locality (see figure 4.9 in chapter 4). One of the objectives was to calibrate the seismic record with lithological data. Les Attaques is also in an interesting geographic position to observe the Holocene infill of the western corner of the FFCP. Collecting new cores offers the possibility to get more detailed and robust information from an area with a significant density of data already collected.

Acquisition of coring was performed using a percussion corer developed at the University Lille 1 (Fig. 3.5). The deepest core achieved a maximum depth of 6 m below the present-day surface. Cores were split in two parts, photographed and analysed at the laboratories of the University Lille 1.

The Holocene sedimentary facies defined in this study are obtained from the new cores and archaeological pits and described trenches. They are based on lithology, grain size, physical sedimentary structures, colour (Munsell chart), faunal content and fossil-trace types. Detailed examination also took into consideration the micropaleontological and clay-mineral content. Pleistocene deposits were described from borehole data and outcrops of surrounding areas of the plain.

Results were obtained from the analysis and comparison of the new and previous data. Diagnostic sedimentary texture, mineralogy and depositional trends of sedimentary facies were compared and correlated with previous lithostratigraphic interpretations to characterise the available subsurface database of the plain after the last glaciations with emphasis in the Holocene deposits.

Sedimentary facies contact and assemblages suggested in this analysis allows the recognition of broad information about the environment of deposition and the mechanisms acting in the sedimentation along the coastal plain. Sedimentary facies addresses some of the major features of the Holocene stratigraphy with regard to the depositional features in the coastal dynamic framework.



Figure 3.2. Map showing the position of the newly acquired cores (black circles) during the FFCP fieldwork and archaeological site in the area of Bierne (black lines). Upper: Bierne site. Lower: Les Attaques site. Les Attaques 1 is very close (50 m) to the canal where seismic profile Nr. 8 was shot.



*Figure 3.3. Archaeological trenches and pits from Bierne diagnostic site. Pictures A and B show the work progress to generate the trenches and pits. Pictures A and B are courtesy of Christine Louvion from Archaeological Service of the General Council of the Nord Department. C: Example of an about 1m-deep archaeological trench. D: Disposition of parallel trenches. E: Example of the process of cleaning and description of sedimentary features in these trenches.*



Figure 3.4. Pictures of core acquisition campaigns. A Bierne; B Les Attaques area.

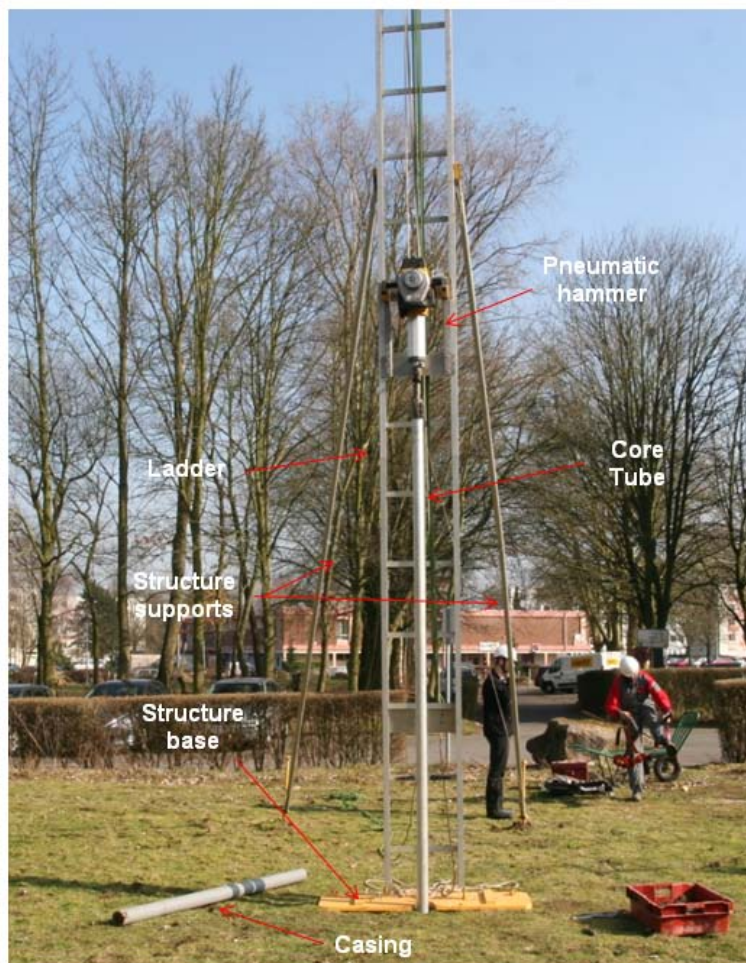


Figure 3.5. Picture showing the different parts of the percussion corer used in the FFCP.

### 3.2.2 Foraminifera

Benthic foraminifer's assemblages were used as a palaeoecological proxy, supporting the environmental interpretations proposed by the sedimentary facies. 37 samples were collected from archaeological trenches and cores from the sites of Bierne and Les Attaques, covering the entire studied time interval and the diverse facies to get a complete characterization of them. This database was compared and complemented by published data (e.g. Mrani, 2006) with the objective to use the vertical and spatial distribution of foraminifer's assemblages in order to establish a more reliable palaeoenvironmental framework of the Holocene sedimentation.

Samples were extracted from each sedimentary facies. Sample preparation corresponds to a common procedure of wet sieving (Hoenstine, 1996 using a 63- $\mu\text{m}$  sieving ignoring juvenile and small specimens, difficult to identify. However, faunal content of the sediment could be highly variable and the number of individuals limited. In this sense, the extraction of all specimens in coastal samples is often necessary to obtain a population statistically representative (>200) (De Vernal *et al.*, 1996; Kemp *et al.*, 2009). For that reason, to obtain larger quantities of individuals, the sediments were sieved through a 38  $\mu\text{m}$  mesh sieve removing only the fine silts and clays. Despite this smaller sieving limit some samples still contained very limited amount of foraminifera or eventually none.

Foraminifera were separated and concentrated from sediments by flotation on trichloroethylene ( $\text{C}_2\text{HCl}_3$ ) and counted under a binocular microscope (Olympus SZX16 - magnification up to x110). In total 29 benthic foraminifera species were identified under the supervision of Dr. Eric Armynot du Châtelet of University Lille 1 and using the work of Cimerman and Langer (1991) and Horton and Edwards (2006). Appendix B shows the foraminifera dataset with the abundance of each species and the total number by samples. The species are listed in alphabetical order. In the Appendix B is also illustrated the foraminifera individuals identified in this study.

Despite the very low content of foraminifera in some samples, qualitative microfaunal analysis revealed distinctive environmental conditions to be matched with the other parameters developed in this research. Apart from foraminifers, diatoms and ostracods were also recovered but they were not analyzed in detail in this study.



### 3.2.3 Pollen analysis

A preliminary study of pollen analysis was carried out in the French Flemish coastal plain considering the possibility to identify vegetation changes and its relation with the environmental changes. 32 samples from 2 cores were taken on the surface thick peat layer and some deeper thin organic levels to be analyzed for this study.

Sampling for Holocene sediments is very delicate because it involves a high risk of contamination from modern pollen and spores. Hence, pollen samples must be handled very carefully. Generally, sampling should be closed along the core due to the changes in ages is variable and small intervals can represent millenary intervals or some decades. In this sense, vertical sampling of 5 mm was used to obtain a detailed pollen-profile and provide data in short periods of time.

Pollen extraction procedures followed the conventional methods to remove mineral and organic matter for Quaternary sediments (Erdtman, 1954; Moore *et al.* 1991). Two methods were used to treat the samples testing alternatives to get a good concentration of pollen grains: alkali treatment by 10% potassium hydroxide (KOH), deflocculation and acid treatment using hydrochloric acid (HCl), and hydrofluoric acid (HF). Residues were then mounted on glass slides.

Pollen analysis was realised with the collaboration of Dr. Virginie Vergne of University Lille1 and using reference material from Reille (1990) and Lambidon *et al* (2004). Currently, 16 samples have been analysed giving some details on the characteristics of the surface peat. Appendix C represents the pollen dataset. It shows each type of pollen identified and their taxonomic organization.

The observed samples are poor in pollen grains. Several tests were made to enrich the residues in pollen grain, but were not fully satisfying. In certain levels 4 or 6 slides were prepared for counting but unfortunately the total of grains to be identified was generally low. In some mounted slides, many grains were observed damaged or in a bad state of conservation. Following Lowe (1982), it is possible to obtain some clues about the interpretation of deteriorated pollen grains and their assessment as palaeoenvironmental indicators.

Despite pollen counts were low for statistical study, the analysis of pollen assemblages, percentages and pollen diagrams were reported with a clear mention, reminding that interpretation is essentially qualitative. It could be used and compared with data and interpretations performed in northern France and in the close Belgian

plain (Stockmans and Vanhoorne, 1954; Van der Woude and Roeleveld, 1985; Sommé *et al.*, 1994; Vergne, 2013).

### **3.2.4 Clay mineralogy**

On the basis of core description, all sedimentary facies identified at Les Attaques and Bierne sites were sampled to determine the mineralogy of the clay fraction (particles smaller than 2  $\mu\text{m}$ ). 29 samples have been taken to characterise each sedimentary facies as long as they contain enough clay-size elements. A semi-quantitative approach was carried out having in mind that the evaluation of clay-mineral contents could be an environmental indicator or a possible signal for sediments origin.

Data were processed into the Clay laboratory of the University Lille 1. Clay mineral associations were studied using X-ray diffraction (XRD) following the protocol indicated by Bout-Roumzeilles *et al.* (1999). Identification of clay minerals was made mainly according to the position of their series of basal reflections on XRD diffractograms obtained under three measurement conditions: air-drying, ethylene-glycol saturated, and heated. Semi-quantitative calculations of each peak's parameters were carried out on the glycolated curve by using MacDiff software (Petschick, 2000). Appendix D shows the clay mineral content and distribution in the cores and facies sampled.

### **3.2.5 Radiocarbon dating**

Radiocarbon dating is based on the measure of the radiological activity of the  $^{14}\text{C}$  isotope contained in any young enough organic matter or shell containing carbon (Libby *et al.*, 1949). This technique uses the decay of  $^{14}\text{C}$  isotope to determine the age of fossils and other dead organic material.  $^{14}\text{C}$  dating has been used extensively to provide the context of sea-level evolution, testing hypothesis of fluctuating or smooth sea-level rise (Baeteman, 2008). Radiocarbon dates are commonly used to establish relationships between sea-level changes and shoreline shifts as well as to provide information to establish a chronology of the time/space reconstruction of sedimentary history (Long, 1991).

Within the context of this study, absolute ages were used as an approach to express the age of facies and infer the temporal framing of the events in the depositional record. Radiocarbon ages obtained from 60 samples of previous studies (Bosch, 1975; Bootsman, 1977; Paris, 1977; Sommé, 1994; Gandouin, 2003; Mrani, 2006) and 4 new radiocarbon data were used in this work.

The new samples (wood and peat fragments) were selected from the most important core of the Bierne area. Its importance comes from its depth, variability of facies and development of thick peat at top. The samples were sent to the Centre for climate, the Environment & Chronology (14CHRONO) at the University of Belfast according to the recommendations of Brown *et al.* (1988) and Bronk Ramsey *et al.* (2004).

Dating was made with Accelerator Mass Spectrometry (AMS) analysis. The AMS measures the isotopic ratios  $^{14}\text{C}/^{12}\text{C}$  and  $^{13}\text{C}/^{12}\text{C}$  of the sample. From these measured isotopic ratios, the  $^{14}\text{C}$  activities were calculated, including the correction for isotopic fractionation. From these activities, the  $^{14}\text{C}$  dates were calculated and reported in  $^{14}\text{C}$  BP (Mook and van der Plicht, 1999). Conventional radiocarbon ages were calibrated using the intercept method explained by Stuiver *et al.* (1993).

The calibration curve used in this study corresponds to the current international calibration curve (IntCal09) provided by the IntCal Working Group (IWG) which represent a quality controlled and statistically robust curve (Reimer *et al.*, 2009) that improve the previous version (IntCal04). To calibrate  $^{14}\text{C}$  ages, we used the CALIB software (Stuiver and Reimer, 1986) in its 2011 revised version (Calib 6.1.0). The calibrated ages are presented with a confidence range of more than 92 % ( $2\sigma$ ). Details of radiocarbon data are presented in Appendix E.

### **3.3 Sedimentary facies – Results**

Sedimentary succession presents a coastal system in which we distinguished Pleistocene and Holocene deposits. According to the detailed description of cores, archaeological trenches and borehole data, their main sedimentary characteristics are as follows:

### 3.3.1 Pleistocene deposits

Pleistocene deposits represent part of the basement for Holocene sediments. This situation is common in the inner part and along the borders of the coastal plain, where Pleistocene sediments can be differentiated. It is then possible to establish the contact with the Holocene deposits. In the central part and seaward, the Pleistocene/Holocene boundary is often missing and the Holocene succession is directly overlying Palaeogene (Ypresian or Thanetian beds) or Cretaceous bedrocks which outcropping in surrounding areas (See figure 2.13 in chapter 2).

Some sedimentary characteristics of the Pleistocene deposits in contact with the Holocene succession are expressed in borehole data, outcrops and cores. Pleistocene deposits have been reached in the lower part of some cores, as seen at Bierne location (Fig. 3.6). Sediments are composed by blue-greyish clayey silt with rust-coloured mottling and devoid of evident sedimentary structures (Fig. 3.6a). Locally, the blue-greyish mottled sediments of the Pleistocene are incised by grey fine sand layer with chalky granules. We also observed a level possibly affected by an ice wedge (Fig. 3.6b).

Clay mineralogy composition presents four minerals in decreasing proportion: smectite, illite, kaolinite and chlorite (Appendix D). As expressed in the Bierne area cores, the assemblage indicates a high concentration of smectite (>70%) while illite (15%), kaolinite (10%) and chlorite (5%) are less abundant.

Towards the inner coastal plain between Watten and St Omer, the Pleistocene was reached in boreholes and cores studied by Sommé *et al.* (1994) and Gandouin (2003) (Fig. 3.7; Appendix A). They are characterized from base to top by badly sorted clayey sands and silts; containing coarse chalk and flint debris brought by the watershed of the Aa river grading to a complexes of marly sediments and muddy and vegetated thin deposits.

In the western area of the coastal plain, the Sangatte cliff, displays a thick succession of Pleistocene deposits (See figure 2.5 in chapter 2). A brief description of these sediments in contact with Holocene deposits shows aeolian sands and mud with chalks granules underlying humiferous aeolian sands. Sommé *et al.* (1999) and Balescu (Pers. comm.) placed these deposits into the Weichselian pleniglacial period.



Figure 3.6. Core images from Bierre 3 (A) and Bierre 4 (B) showing the characteristics of the Pleistocene deposits in the subsurface of the FFCP. Scale in centimetres. A Greyish clayey silt with rust-coloured mottling (1), Holocene – Pleistocene sharp contact (2) grey sands of the basal Holocene deposits (3). B Blue-greyish mottled clays of the Pleistocene deposits (4) affected by possible ice wedge (5) and filled by grey fine sands with chalky granules (6).

Borehole data around of current shoreline and excavations during the port construction (e.g. Dunkerque ferry port, boreholes 77 and 93 in appendix A and cross-section 7) can reach deeper shelly greenish or yellowish sands and gravels deposits (around -20 and -30 m deep NGF) that have been debated by several studies as late Pleistocene or early Holocene based on faunal molluscs content (Dubois, 1924; Briquet, 1930; Sommé, 1977; Leplat and Sommé, 1989). However, molluscs and pollen assemblages mentioned by Sommé *et al*, (2004) provides a late Eemien age for these marine deposits. Actually, these deposits are correlated with the Oostende Formation in the Belgian side of the coastal plain (Paepe *et al*, 1981; Gullentops *et al.*, 2001; Sommé, 2013).

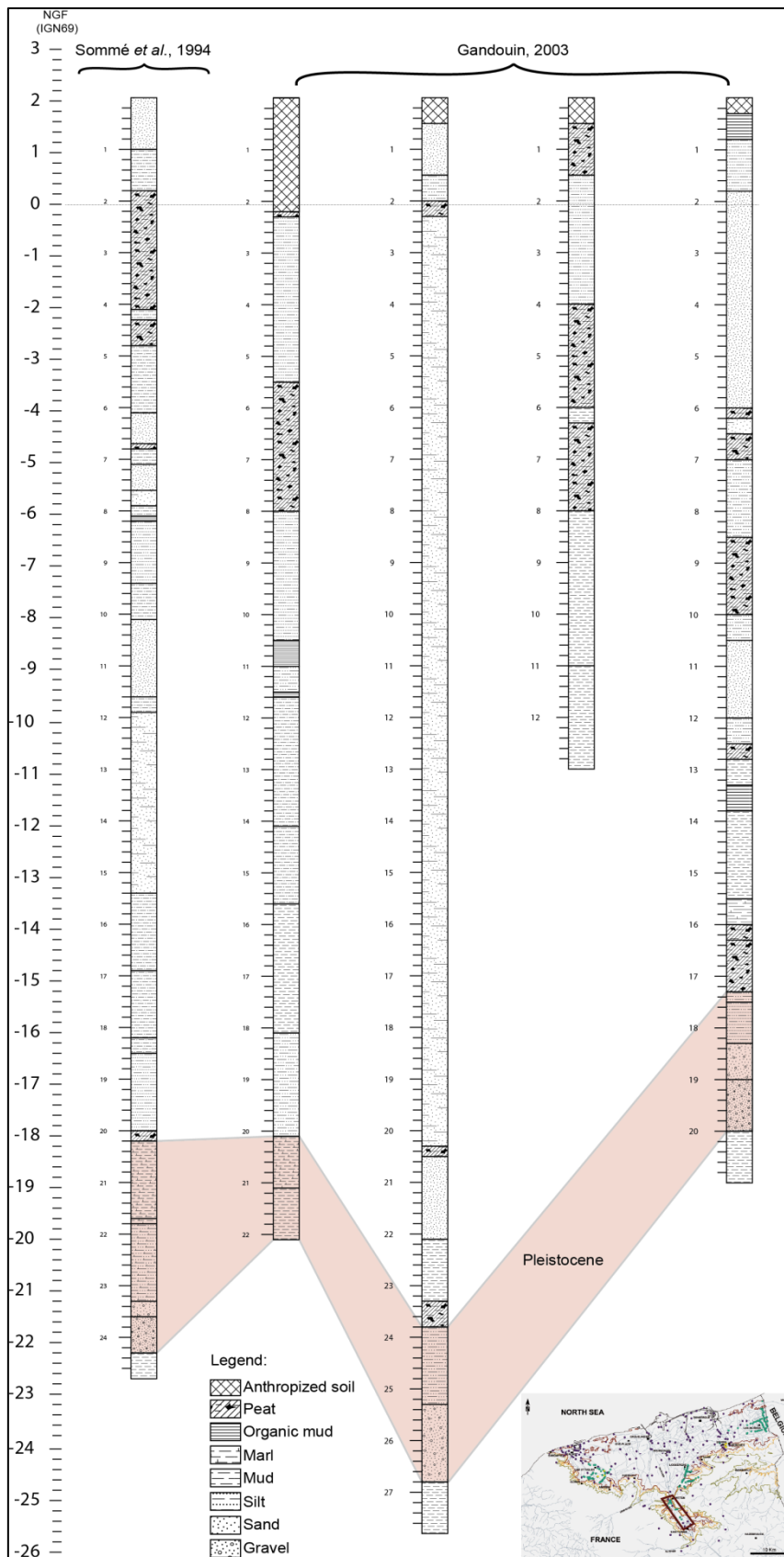


Figure 3.7. Borehole data used in this study showing the Pleistocene deposits of the southern part of the coastal plain. Pleistocene interval is highlighted to show the predominant lithology for this period. Lithology description from Sommé et al. (1994) and Gandouin (2003).

Other witnesses of Pleistocene features presented in the French Flemish coastal plain are the sand and gravel mounds located at Petite Rouge Cambre, Coulogne and Les Attaques (See figure 2.13 in chapter 2). Despite the fact that they were not observed in borehole data, it is important to mention them as a possible heritage of Pleistocene deposits in the area. These reddish, greenish and brownish sands, mixed with yellowish mud and bluish gravels were described as a continuation of the Sangatte fossil cliff and proposed a Pre-Weichselian age (Dubois, 1924; Briquet, 1930; Paris, 1977; Sommé, 1977).

### **3.3.2 Holocene deposits**

Within the Holocene sedimentary succession, five sedimentary facies showing vertical and lateral changes in lithology, sedimentological components and faunal content were described. The five sedimentary facies occurring in Holocene deposits correspond to: Organic-rich facies, Mud facies, Heterolithic facies, Sand facies and Gravel facies. These sedimentary facies can be synthesized in the Holocene sedimentary succession from cores Les Attaques 1 and Bierne 1 (Figs. 3.8 – 3.9). The rest of cores are presented in appendix F.

Clay mineral content appears as a significant indicator to give some clues about the sedimentological characteristics of the sediment supply. Figure 3.10 shows typical clay distribution in the sedimentary succession. Clay fraction for each sedimentary facies is observed in appendix D.

#### **3.3.2.1 Organic-rich facies**

These facies correspond to organic-rich beds described in the Holocene infill of the FFCP. Generally, these accumulations are important for the Holocene sedimentary arrangement. They provide clear evidences for environmental changes in Holocene deposits of the region (Vergne *et al.*, 2009) and a chronological framework that support the interpretations of the stratigraphic arrangement (Huat *et al.*, 2011; Wójcicki, 2012).

Two types of peat layers and organic-rich muds are present in the Holocene infill of the FFCP. These two types have been defined by their stratigraphic position and ages measured by <sup>14</sup>C radiocarbon dating.

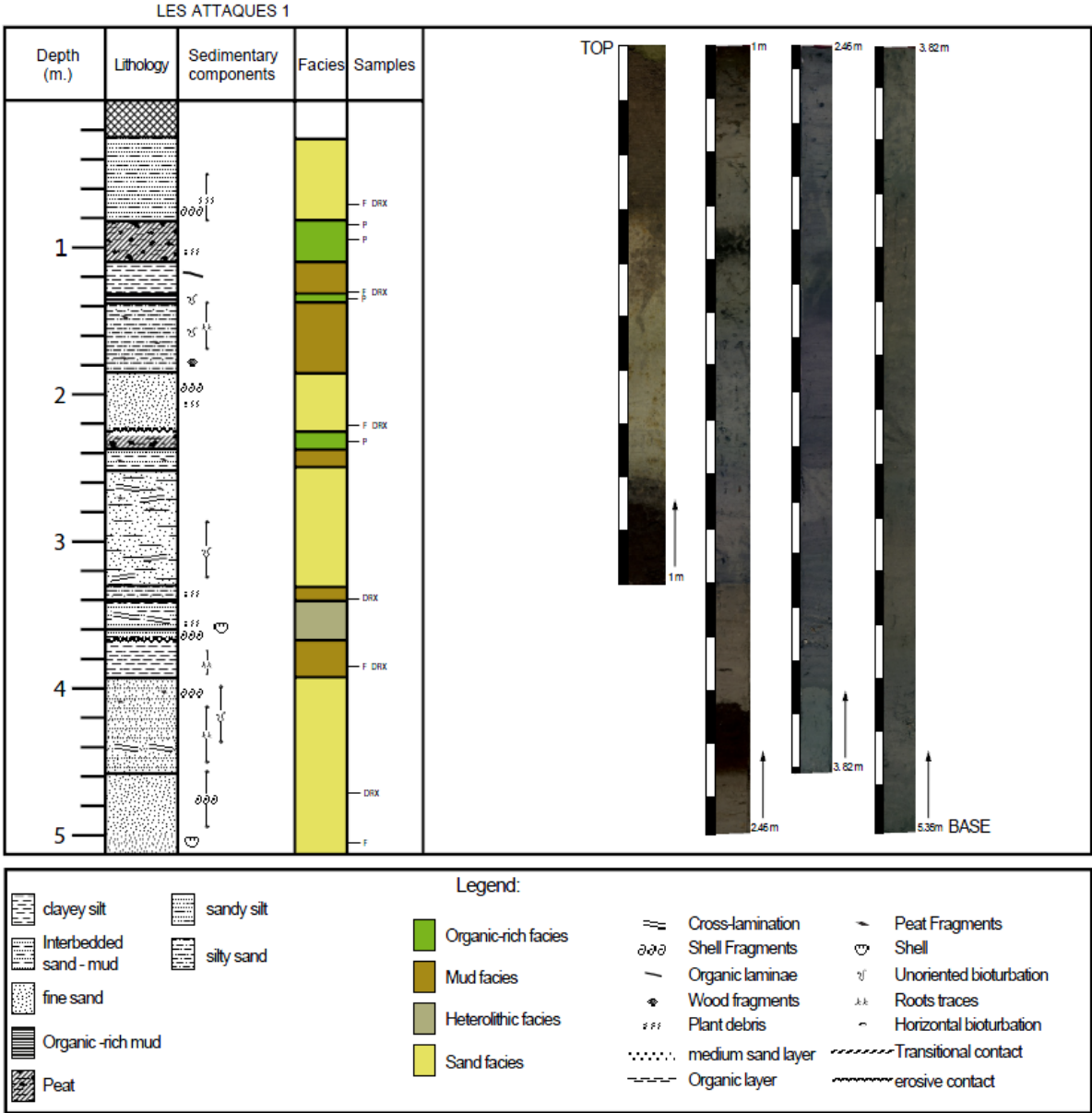


Figure 3.8. Stratigraphic succession for the Holocene deposits at Les Attaques. See location of core in figure 4.2 and appendix A.



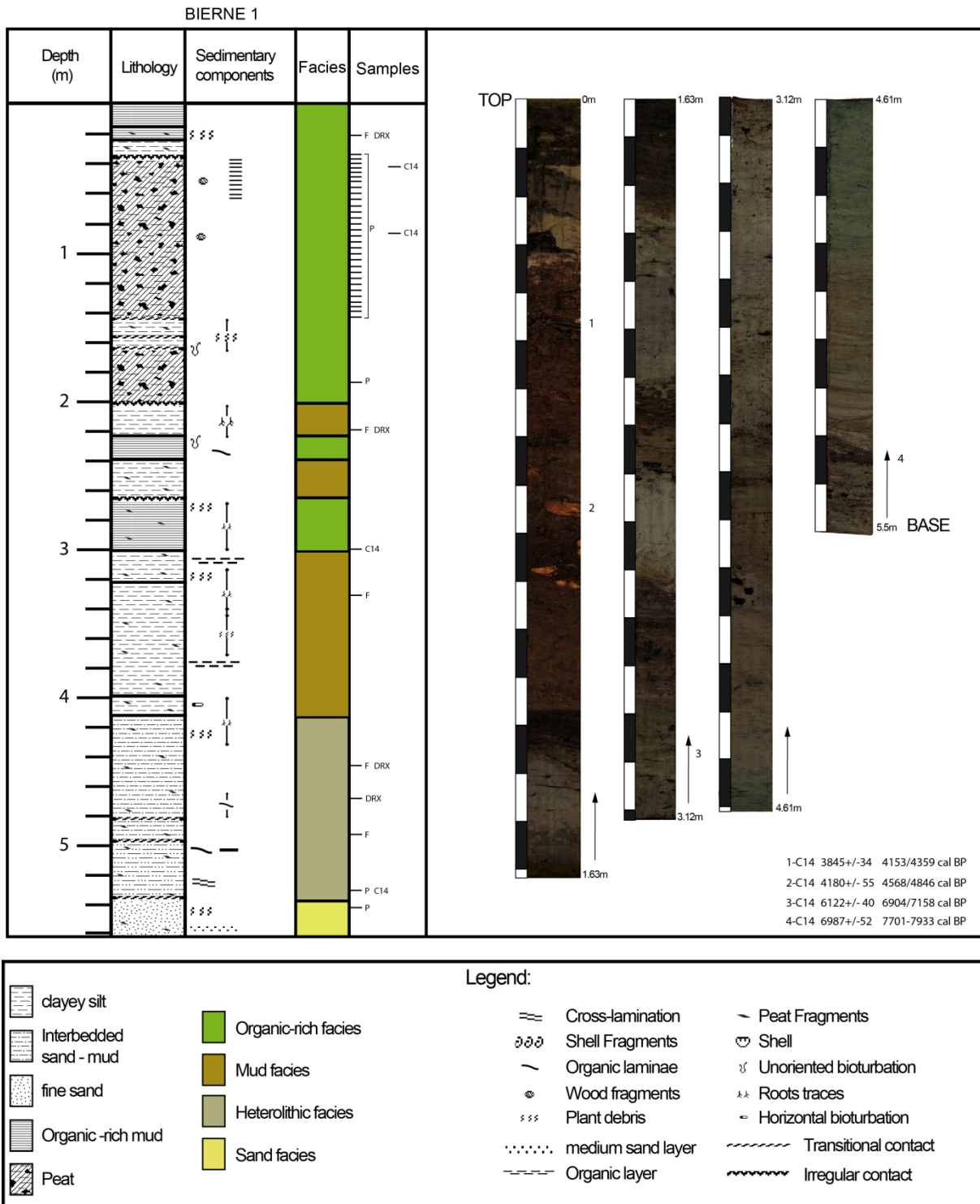


Figure 3.9. Stratigraphic succession for the Holocene deposits in Bierre. <sup>14</sup>C ages in appendix E. See location of core in figure 4.2 and appendix A.

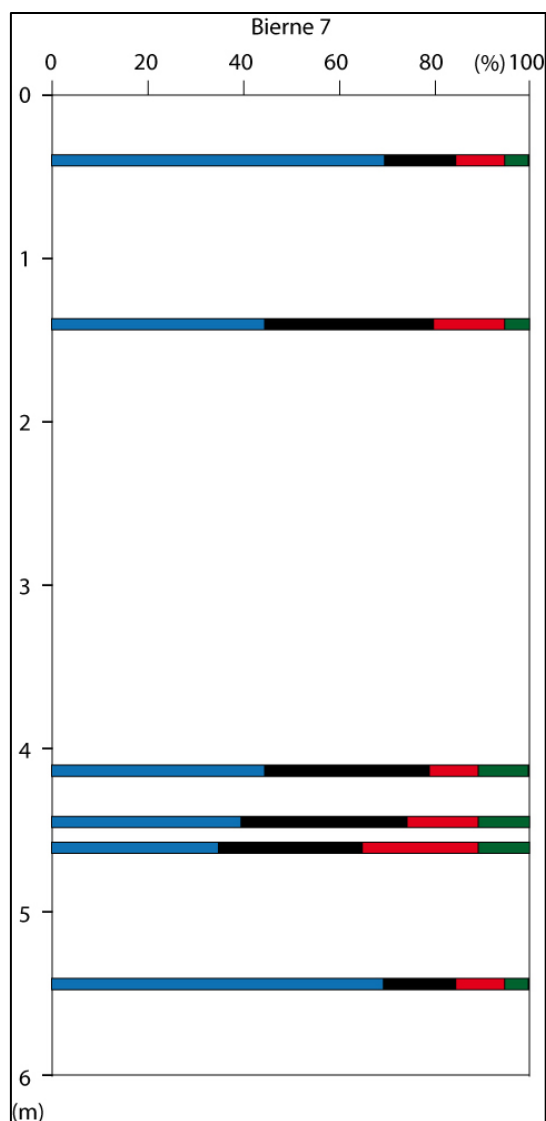


Figure 3.10. Example of typical clay mineralogy distribution along the cores of Les Attaques and Bierne sites. Clay assemblages show smectite (blue) illite (black), kaolinite (red) and chlorite (green).

The first peat bed is founded in the bottom of the Holocene infill. It was not observed into the new cores acquired in the FFCP due to its absence or limited core lengths. Its location is restricted where it has been observed within the borehole database (e.g. southern part of the coastal plain as showed in figure 3.7). Their characteristics were described mostly from the literature (Fig. 3.11).

This peat bed called in the literature “basal peat” often corresponds to the first Holocene deposits (Baeteman, 1991, 1999; Sommé *et al.*, 1992, 1994). Depth (ranges from -22 to -12 NGF) and ages (10690 cal BP – 7900 cal BP) of the basal peat are highly variable and mainly depend of the morphology of the pre-Holocene surface and rise of groundwater following the sea-level rise. It is preserved landward into the inner part and some sheltered areas at borders of the coastal plain.

Physical characteristics described in these deposits show a horizon (around 15 cm of thickness) of greenish compacted clayey peat, rich in plant fragments and some sandy laminations. Brown-yellowish organic-rich beds (*charophyte* mud) and light grey calcareous silts or tufa (Van der Woude and Roeleveld, 1985; Sommé 1992, 1994; Gandouin, 2003, 2007) were also identified. Pollen from *Corylus*, *Tilia*, *Quercus* and *Alnus* are common in this level. However, this level marked a decrease of their fluctuating changes and the progressive extension of marine influenced pollen as *Chenopodiaceae* (Sommé *et al.*, 1992, 1994).

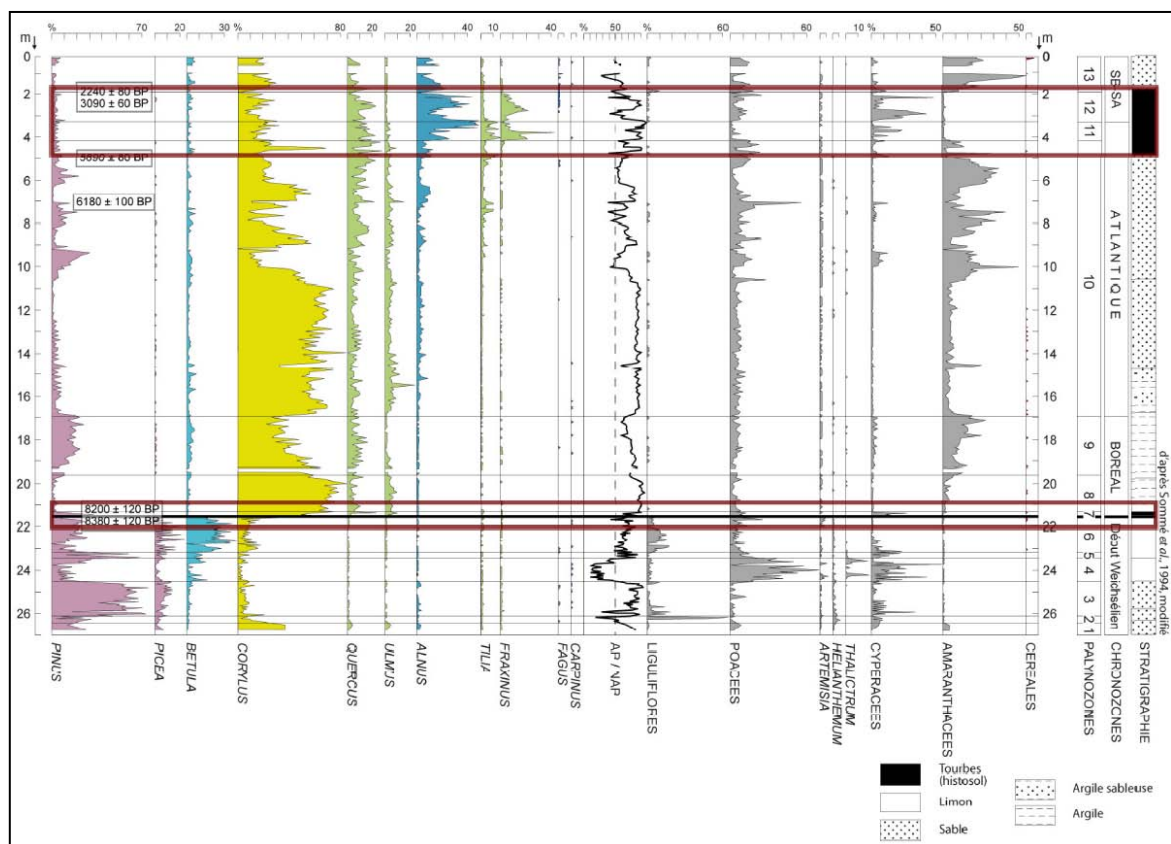


Figure 3.11. Borehole 385 showing the pollen diagram of Watten boring. Red square highlights the characteristic of peat layers. Interpretation was obtained from Sommé *et al.*, 1994 and modified by Vergne *et al.*, 2009. See location in Appendix A.

Another shallower and extensive peat layer is described in the sections cored and borehole data along the coastal plain. Its age is largely dated between 6500 cal BP and 3000 cal BP. Its base mostly appears comprised between 6000 cal BP and 5000 cal BP (Appendix E). This peat level, also called in the literature as “surface peat” or “Holland Peat” (Tavernier, 1947; Jelgersma, 1961) is intercalated between

muddy and sandy deposits. It is represented by a thick peat bed, or often consists in a series of small beds intercalated with organic-rich muds.

Peat layers present horizontal and vertical variations in their physical characteristics. They present a variable colour between black and brown-to-dark brown respectively associated with textures ranging from sapric (amorphous) to fibric (fibrous, > 67% fibre content, ASTM 1990). They also contain some roots, wood fragments and plants remains (fragment of *Cyperaceae* are identified).

Generally, the described peat beds consist of undecomposed fibrous organic materials (Fig. 3.12a). Peat can present an apparently laminated aspect but is unstructured in most cases. However, in some cases at the top of the peat bed decomposition (humification) is observed (Fig. 3.12b). In other cases, peat is totally amorphous (Fig. 3.12c), hiding the peat structure and changing the original chemical composition of the peat.

Pollen analysis made from Bierne samples show dominance of *Alnus* and sedges (*Cyperaceae*) within the pollen association along the entire interval sampled. We also noticed the presence of *Betula*, *Quercus* and *Gramineae* (Appendix C). Although their presence is scarce, it is important to indicate that pollen from aquatic plants as *Myriophyllum verticillatum* and *Potamogeton* were recognised towards the middle part of the peat and upwards. Uppermost samples (0 NGF) show some signs of anthropisation evidenced by the presence of *Plantago* grains.

Towards Watten, Sommé *et al.* (1994) described this peat. It is characterised by an important extension of *Alnus* and *Fraxinus* as well as very strong reduction of *Chenopodiaceae*. *Quercus*, *Corylus* and *Tilia* are present. Herbaceous vegetation was dominated by the ferns, among which is *Thelypteris palustris* (marsh fern) *Cyperaceae* and *Poaceae* (Fig. 3.11).

The depth of this surface peat is highly variable depending on the morphology of the underlying facies and the progressive invasion of the environmental conditions necessary for its preservation. It ranges from -7 between Saint-Omer and Watten to +0.5 NGF at areas as Bierne or Les Attaques.

Another representative lithology of this facies is the organic-rich muds. At the bottom of boreholes around Saint-Omer area, these muds are described as beds of *charophyte* mud (Gandouin, 2003; Gandouin *et al.*, 2007). In cored sections, were described organic-rich muds which are represented by thin beds of organic material (<15 cm) mainly related with the filling up of the mud facies (Fig. 3.13).

Stratigraphically, they are mostly described underlying the surface peat layer. Radiocarbon ages from some samples show earliest ages of 7500 cal BP. However, is also possible to find this type of beds in the uppermost sedimentary cover at about 1600 cal BP.

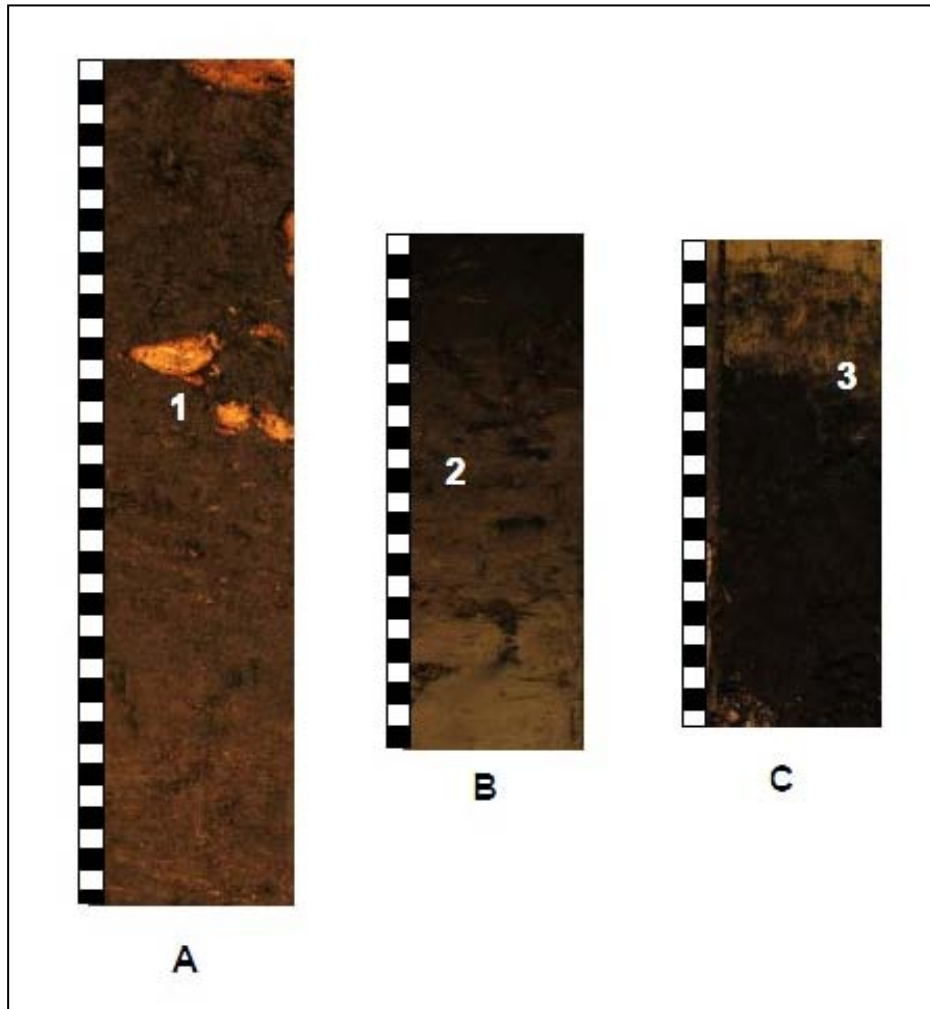


Figure 3.12. Core photo of surface peat layer. A: Fibrous peat layer of Bierne 1 core. Note the laminated aspect and the well-preserved rest of wood into the organic material (1). B: Surface peat layer of Les Attaques 1 core. It shows the process of humification of the peat bed (2). C: Surface peat layer of Bierne 7 core. It displays an amorphous aspect caused by the total decomposition of the peat (3).

They show an increase of clay content and a gradual contact with a distinct colour change upwards, from brown-greyish clayey silts to brown/black organic-rich clays (Fig. 3.13b). The organic-rich muds are characterised by faint laminations, concentration of plant debris and abundance of bioturbation. Following Gingras *et al*

(2007) and Gingras *et al.* (2012) classifications the bioturbation observed could be associated with trace fossils such as *Psilonichnus* or *Thalassinoides* and *Planolites*.

Samples from Les Attaques location, taken in the contact of the upper part of silty mud beds and transition to the organic-rich muds present a foraminifera's microfaunal content in decreasing order with: *Jadammina macrescens*, *Haynesina germanica*, *Criboelphidium gerthi*, *Criboelphidium williamsoni*, *Criboelphidium margaritaceum* at depth of 5 m (-3 m NGF) in core Les Attaques 2. In core Les Attaques 3 the assemblage is characterised by the presence of *Haynesina germanica* and *Trochammina inflata* at 1.80 m from the top of the core (+0.2 m NGF).

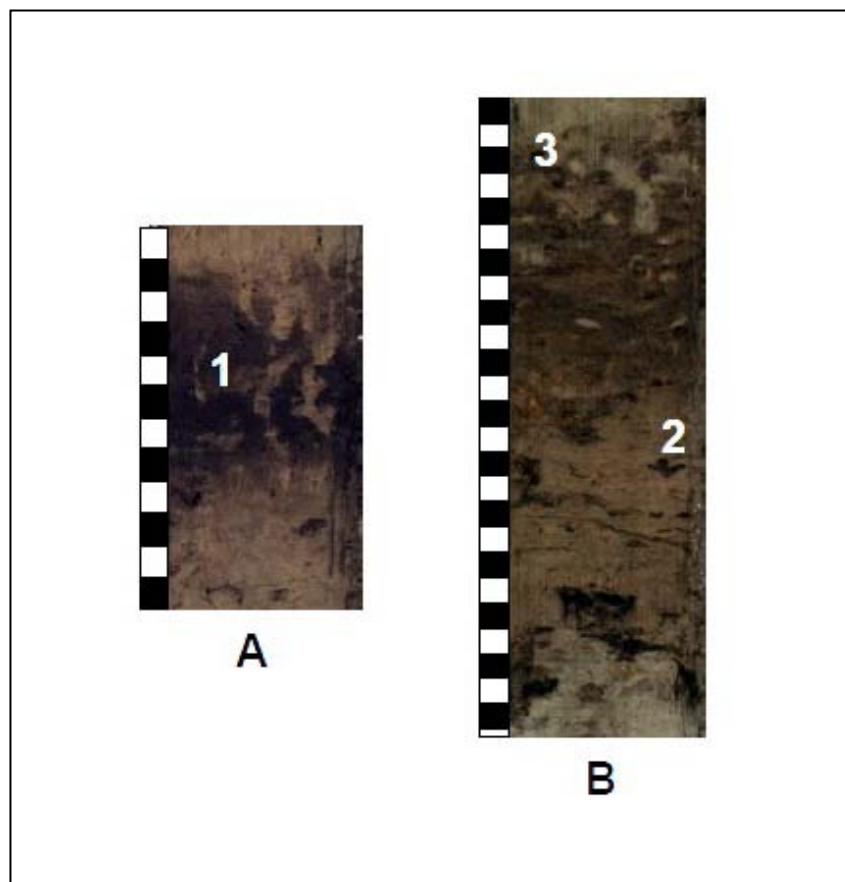


Figure 3.13. Core photo of organic-rich muds. A: Organic-rich mud of core Les Attaques 1. Bioturbation shows predominant vertical burrows (1). B: Transitional contact between the underlying mud facies and the organic-rich muds (2) of core Bierne 1. Bioturbation shows a diversity of sizes and shapes, mostly rounded and cylindrical (3).

Towards Bierne location, the recognized species are *Haynesina germanica*, *Lobatula lobatula*, *Criboelphidium williamsoni*, *Jadammina macrescens* and *Criboelphidium gerthi*, in core Bierne 1 at 2.1 m (-2.1 m NGF) Samples B1 and B8,

collected along archaeological trenches present some assemblages consisting of *Miliammina fusca*, *Trochamina inflata* and *Jadammina macrescens* (Appendix B).

Clay mineralogy from this facies in Bierne indicates that smectite dominates with 65%, being followed by illite (15%) and kaolinite (15%). Chlorite may be present, but in traces quantities (5%) (Appendix C).

### 3.3.2.2 Mud facies

This facies is widely extended in cores and borehole data of the coastal plain, mainly inland and borders areas. It was described showing variable thicknesses and stratigraphic positions. Commonly, it is disposed vertically in accreted beds, where the basal contact is generally sharp and the upper contact is gradational to the organic-rich sediments. The cores from Les Attaques, Bierne and the inner coastal plain, present similar features.

These deposits are characterised by grey bluish clayey silts with massive/structureless or slight parallel lamination (Fig. 3.14a). Most of the time, the original fabric of the sediment was modified by the intense action of roots and bioturbation (Fig. 3.14b). Some indistinct mottled texture is commonly observed. High quantity of roots traces, organic laminae, thin lenticular bedding (some single lenses of very fine sand) as well as peat and wood fragments scattered in the beds were identified. Also, scattered shell fragments and complete shells of *Cerastoderma edule* and *Hydrobia ulvae* were found

At the topmost sedimentary succession, the described mud facies corresponds to light grey to beige clayey silts. Development of soils disturbs the upper part of this facies leading to a brown colour in the upper part of this package (Fig. 3.14c). Devoid of sedimentary structures, only some laminations are observed. Scattered peat fragments and moderate bioturbation are some characteristics preserved in this package. Similar lithologic characteristics are repeated and extended in borehole data along the plain.

Micropaleontological analyses of the mud facies from Les Attaques present a foraminifera assemblage characterised by *Haynesina germanica*, *Criboelphidium gerthi*, *Criboelphidium williamsoni*, *Milliolinella subrotunda*, *Haynesina depressula*, *Ammonia tepida* and individual specimens of *Planoburlina mediterraneensis*, *Favulina melo*, *Cassidulina laevigata* at 3.80 m in core Les Attaques 1 (-1.8 m NGF). At the

top of this core, at a depth of 0.7 m (1.3 m NGF), above the peat layer, facies presents an assemblage with notable dominance of *Haynesina germanica* and presence of *Criboelphidium williamsoni*, *Bulliminella elegantissima*, *Cassidulina laevigata* and *Haynesina depressula* (Appendix B). Microfaunal assemblages from mud facies of Bierne present *Haynesina germanica*, *Haynesina depressula*, *Criboelphidium excavatum* and *Criboelphidium margaritaceum* at 3.10 m NGF in core Bierne 7.

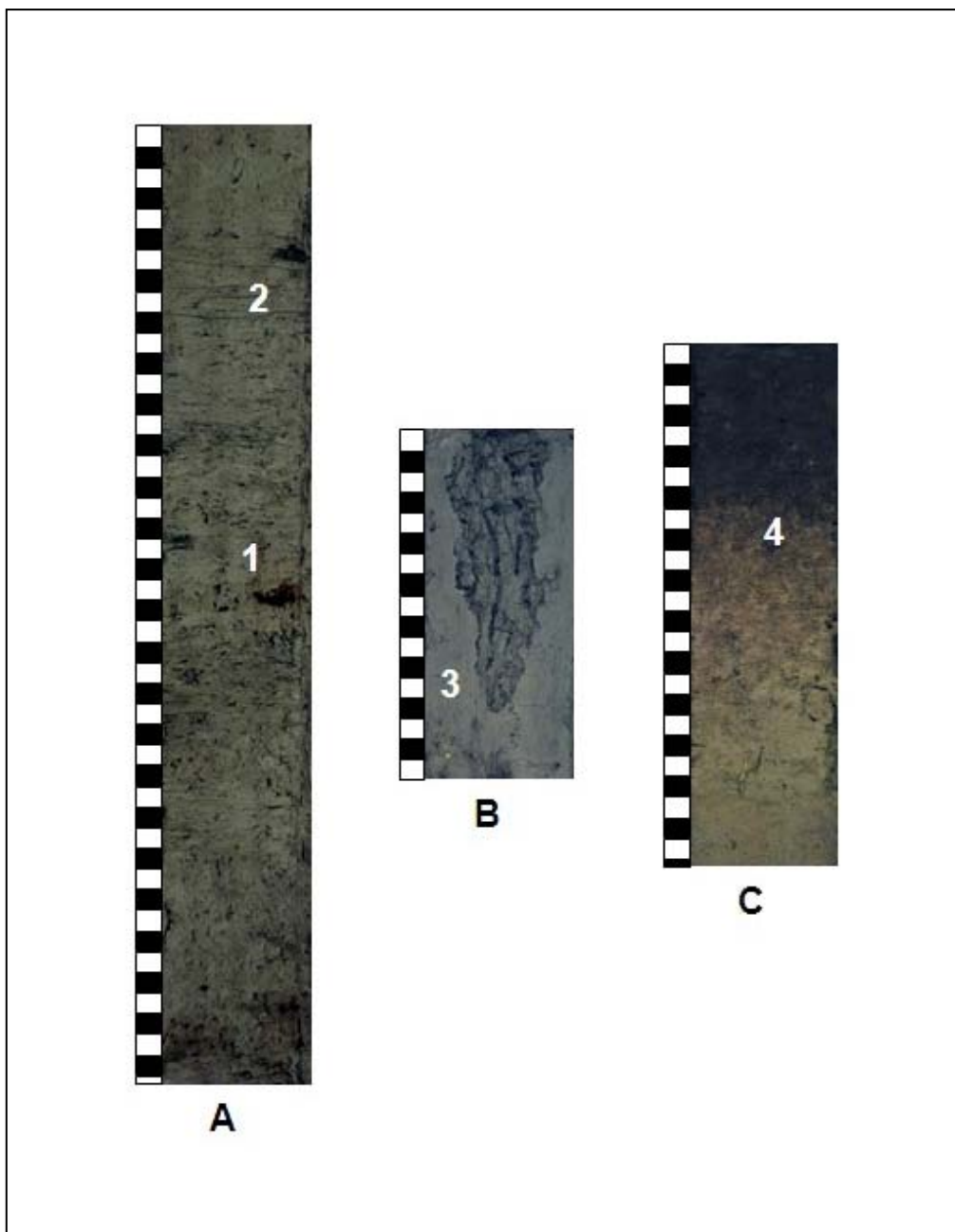


Figure 3.14. Mud facies of FFCP. A: Bierne 1 core showing a structureless part of this facies with scattered plant debris (1) and slightly parallel lamination (2). B: Bierne 7 core showing the intensity of



roots in the muddy deposits (2). C: Les Attaques 2 core showing the development of anthropized soils (3) in the uppermost part of this facies and the last sedimentary cover of the FFCP.

Clay mineral analysis of this facies was obtained from all the cores measured in both locations. It allows making the distinction between two assemblages based on the abundance of smectite, the most abundant mineral in both location, Les Attaques and Bierne. The two assemblages seem to respond to a stratigraphic reason (Fig. 4.10): mud sediments of the top most sedimentary succession have high concentrations of smectite (From 65 to 80%) while illite (15-25%), and kaolinite (10-15%) and Chlorite (0+ - 5%) are present in lower proportions. Mud sediments below the surface peat layer show relatively low values of smectite (45-50%), while illite (30-35), chlorite (5-10%) and kaolinite (10-15%) present higher contents.

### **3.3.2.3 Heterolithic facies**

Heterolithic sand-mud sediments were recognized in cores from Les Attaques and Bierne (Fig. 3.15). These deposits display thin beds (usually few with variable thickness < 5 cm) containing greyish brown light grey, well sorted, fine grained sand and greyish brown mud layers interbedded in sharply contrasting strata. Sedimentary structures include typical heterolithic tidal bedding with parallel and wavy thin bedding and sand/mud rhythmities.

Among other characteristics, the lower contact could be gradational or erosive with underlying facies. Mud layers are increasing upwards in thickness. Shell fragment layers and shells of *Cerastoderma edule* were eventually distinguished. Following the classification of Droser and Bottjer (1986) bioturbation degree is discrete and trace fossils undifferentiated in the mud layers (Fig. 3.15a).

Clay mineralogy from this facies in Bierne presents a high dominance of smectite with 75% followed by illite (15%) and kaolinite (10%). Chlorite may be present but in traces quantities (+/- 0%).

### **3.3.2.4 Sand facies**

Sand-dominated deposits are broadly extended along the entire coastal plain. They were described in cores, archaeological trenches and borehole data. In

accordance with their stratigraphic position, a distinction has been made within sand deposits outlined by their changes in sediment components, colour and occurrence of shells. From lower part until the uppermost sedimentary cover sand facies, they present different thicknesses and could be interbedded with mud and heterolithic facies or amalgamated in several stacked sand packages. The basal contact is usually erosive while the upper contact tends to be gradational or erosive, capped by new sand package. In relation with their geographical position, it is possible to describe their different characteristics:

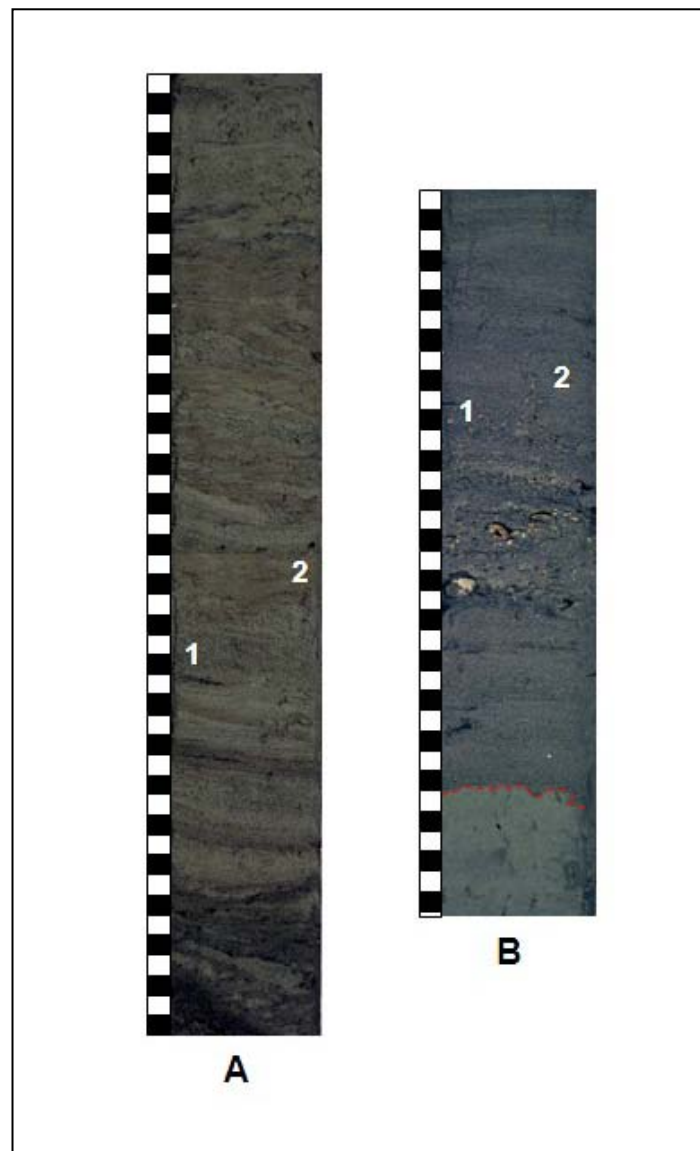


*Figure 3.15. Heterolithic facies of the FFCP. A: Bierne 1 core displaying the interbedded layers of sand (1) and mud (2) with parallel and wavy lamination. Relative quantity of mud is increasing upwards. B: Les Attaques 1 core showing heterolithic bedding and abundant shell fragments. Note the erosive contact (red line) with underlying mud facies.*

On the western part of the plain, within cores from Les Attaques area, it is possible to observe two types of sand facies mostly based on their contrasting colour in the vertical succession (Fig. 3.16). Lower sands consist of bluish grey, well-sorted, sub-rounded and medium to fine grained sand. They look massive, commonly structureless with scarce discontinuous mud laminae and shell fragments. Among the sporadic shell fragments rests of *Cerastoderma edule* (Fig. 3.16a) are distinguished.

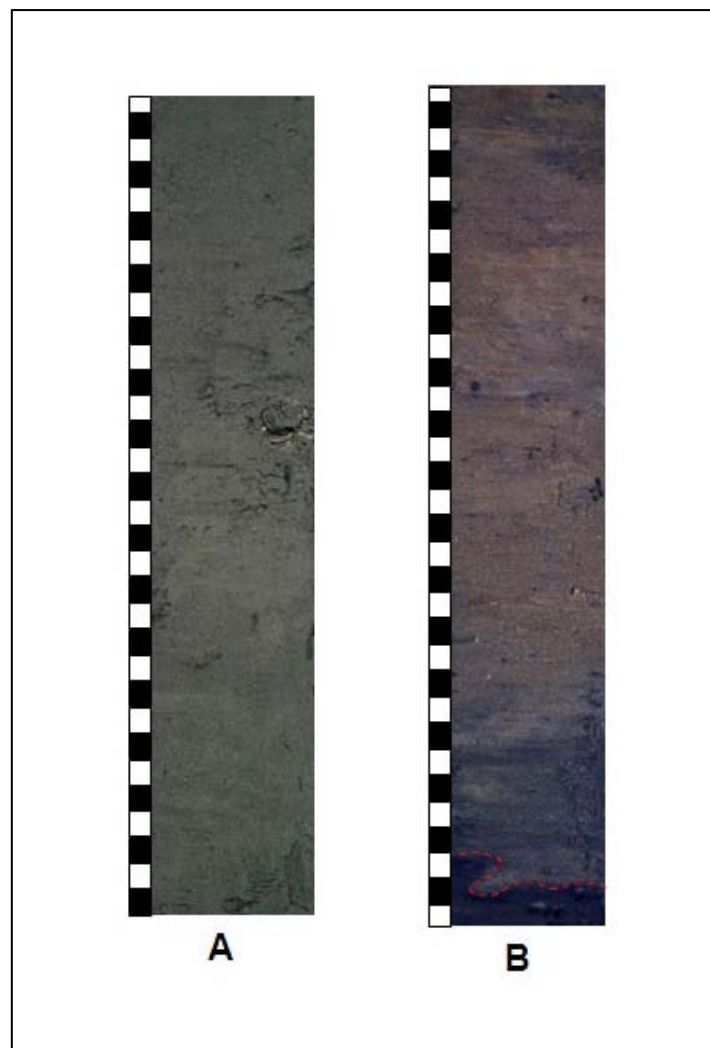


Figure 3.16. Sand facies from Les Attaques area. A: Les Attaques 1 core showing typical lower massive bluish-grey sand facies with scattered shell fragments. B: Les Attaques 3 core showing typical upper light-grey sand facies with common shell and peat fragments. Lower contact with underlying organic-rich facies is generally erosive (red line).

In general, the succession shows a fining upward trend, from medium to very fine sand and passes to clayey silt dominated sediments of the mud facies. Lower

contact is erosive or was not attained. Maximum visible thickness reached 1.2 m. Following the classification of Droser and Bottjer (1986) the bioturbation in this facies have a very discrete intensity or is rare.

In the uppermost part of cores the second type of sand was observed (Fig. 3.16b). These sands present lighter colour than the first one. A light grey/brown colour defines the change. These sands beds are silty to fine-grained, rounded and moderate to well-sorted. They present a moderate abundance of peat fragments, presence of glauconite, common shell fragments and occasional whole shells of *Cerastoderma edule*. Some parts of the beds were oxidized and affected by the anthropisation.

Micropaleontological analyses of these facies in this area present a foraminifera assemblage that, in decreasing order of content, is characterised by *Milliolinella subrotunda*, *Haynesina germanica*, *Criboelphidium gerthi*, *Triloculina trigonula*, *Haynesina depressula*, *Adelosina sp.*, *Criboelphidium excavatum*, *Criboelphidium gunteri*, *Criboelphidium williamsoni*, and *Elphidium pulvereum* at 5.05 m (-3.05 m NGF) in core Les Attaques 1.

In core Les Attaques 3 at 1 m from the top of the core (+1 m NGF) the content is characterised in decreasing order by *Criboelphidium williamsoni*, *Haynesina germanica*, *Criboelphidium gerthi*, *Ammonia tepida*, *Haynesina depressula*, *Lobatula lobatula*, *Bulimina elegans*, *Miliolinella subrotunda* and some forms of reworked Cretaceous planktonic foraminifera.

In the samples from Les Attaques cores, clay mineral content is characterised by dominance of smectite (always more than 50%) followed by illite (30%), kaolinite (15%) and chlorite (5%).

On the eastern part, towards Bierne area, the cores show sand facies that consist of bluish grey, subrounded, moderate-sorted fine sand, with thinly parallel bedding, and rare discontinuous mud laminae (Fig. 3.17). Sporadic plant debris is dispersed in the beds and some shell fragments scattered in the lower part. When the base reached the underlying Pleistocene deposits, the lower contact is generally sharp or erosive. Visible thickness can reach 1 m. The succession follows a fining upward trend, and then passes to clayey silt dominated sediments of the mud facies.

From the archaeological trenches of Bierne, sand facies was described in small channel-fill associated with the uppermost sedimentary succession (Fig. 3.18). The channel-fill facies, approximately 70-cm thick, presents decimetric sand beds

interbedded with thinly centimetres mud layers. The basal contact is erosional with the underlying mud facies and surface peat. Sands are fine to very fine grained, subrounded and well sorted. Their colour varies between light pale brown to ochre while mud is dark brown. Mud layers present some moderate bioturbation identified as *planolites*. Common sedimentary features include slight cross lamination, wavy and flaser bedding, mud clasts, presence of glauconite, shell fragments and complete shell of *Cerastoderma edule* and *Scrobicularia plana* (Figs. 3.18 – 3.19).

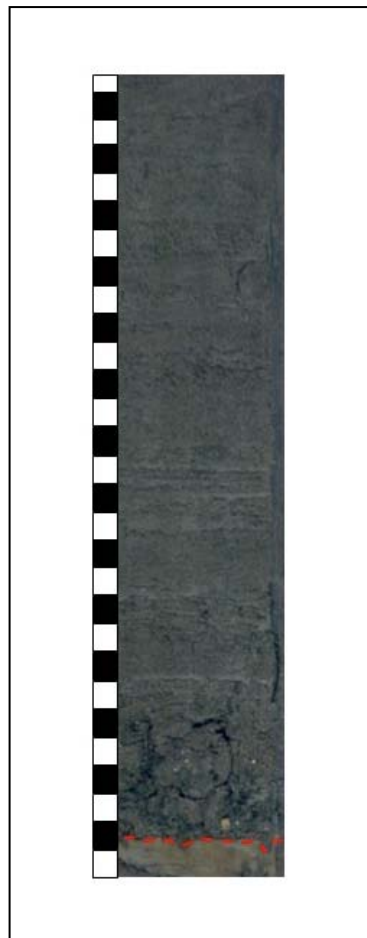


Figure 3.17. Sand facies from Bierne area. Bierne 2 core showing the typical bluish-grey sand with thinly parallel bedding and rare mud laminae. Lower contact with Pleistocene deposits is erosive (red line).

Samples B2, B6 and B9 from the archaeological trenches of Bierne location (Fig. 3.2) present a significant microfaunal assemblage with dominance of *Haynesina germanica*, and presence of species as *Miliolinella subrotunda* and *Haynesina depressula*.

In Bierne, the clay mineralogy of this facies presents quite similar characteristics than the samples from Les Attaques with dominance of smectite but more variable percentages. They indicate that smectite still dominates (40-45%) illite (30-35%), kaolinite (15-10%) and chlorite (10%).

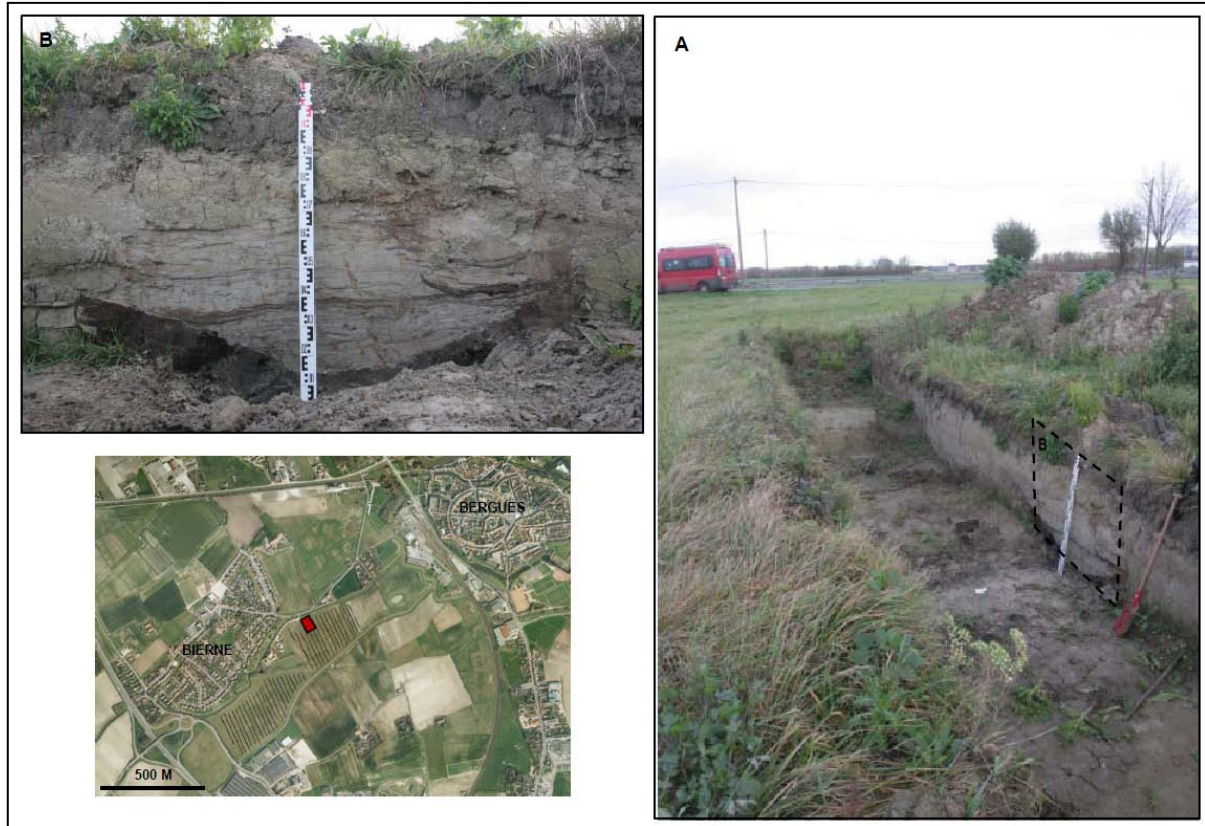


Figure 3.18. Photos of archaeological trench at Bierne location showing sand-dominated small channels detailed in B. These channels, also called creeks, exhibit an erosive lower contact with underlying organic-rich facies.

In the southern area of the plain, between Saint Omer and Watten some cores studied by Sommé *et al.* (1994) and Gandouin (2003) allowing us to define two types of sand facies and their contrast in the vertical succession. According to the vertical distribution, downwards (overlying clayey beds or the basal peat) sand facies present small thicknesses (between 1 - 2 m), fining upward trends and have poorly sorted silty grey sands with levels of coarse sands. Upwards, sand facies consist of another series of small sand bodies or punctual thick packages (more than 20 m) of grey-greenish well-sorted fine sands, with mollusc shells and erosive basal contact that incises into the previous muddy and/or grey bluish sand deposits.

In the central and northern area of the French Flemish coastal plain, this thick package (> 20 m) of grey-greenish fine sands with highest occurrence of shell

fragments is repeated and intercalated in punctual boreholes (see profiles 1 and 7 in chapter 5). However, subsurface data are mainly characterised by extended thick packages of grey-bluish fine sands and stacked silty sands (packages with thickness around 4-5 m). Overlying these deposits, yellowish sands extend in the coastal plain representing the modern sedimentary deposits of the plain.



Figure 3.19. Common shells observed widespread in the last sedimentary cover at Bierne area. *Cerastoderma edule* (upper) and *Scrobicularia plana* (lower).

#### 3.2.3.4 Gravel facies

Borehole data of the North-Western area of the French Flemish coastal plain, specifically in Calais area, show the presence of significant thicknesses of gravel in their logs (Fig. 3.20). They are constituted by rounded bluish flint pebbles and coarse to medium sand. Some chalk and sandstone pebbles are also present but in less proportion. Sand associated to this facies presents some abundance of glauconite and is mostly observed in the upper part of this accumulation (Dubois, 1924; Sommé, 1977). The basal contact is with the grey-bluish sand facies or directly overlying Pre-Holocene substrate, the top is outcropping or directly covered by coastal dunes (Sommé, 1977).

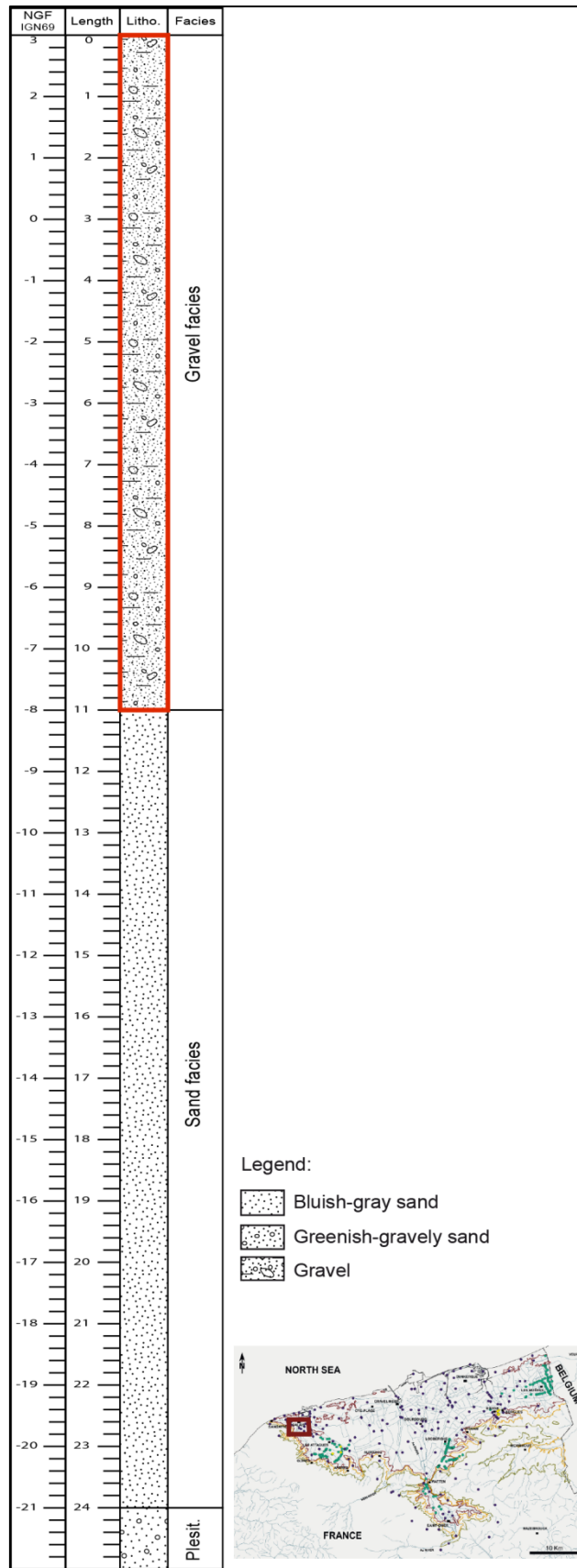


Figure 3.20. Description of borehole 174 around Calais area emphasizing (red square) the gravel facies observed in the FFCP. See location in Appendix A.



### **3.4 Sedimentary facies - interpretation**

Based on the sedimentary facies and the relationships among their sedimentological, micropaleontological and clay mineralogy information, we have interpreted the depositional facies and the possible processes that reflect the characteristics of the environment in which sediments are deposited during the Holocene period. For each sedimentary facies the following features were distinguished:

#### **3.4.1 Pleistocene deposits**

Pleistocene deposits that are preserved in the plain and surrounding areas correspond to three cycles of glacial – interglacial periods (Sommé *et al.*, 1999). However the sediments that are in contact with Holocene deposits are related with the second-to-last interglacial (Eemian) and the Last Glacial period before the Holocene (Weichselian). Non-marine environments were interpreted for Weichselian deposits (Sommé 1994; 1999; Gandouin 2003, Gandouin *et al.*, 2007) while marine environments found in deep boreholes seaward (Sommé *et al.*, 2004) and the witnesses of gravel bars from Petite Rouge Cambre, Coulogne and Les Attaques were interpreted as Eemian deposits (Sommé, 1977).

In the inner part of the coastal plain, the occurrence of sandy and gravel deposits, marly deposits, clayey and vegetated beds indicates that late Pleistocene deposits were developed in a fluvio-lacustrine environment (Fig. 3.7). Fluvial characteristics of the deposits show the influence of the river supply in the sedimentation and the environmental context of the ancient Aa River valley. In general, the sedimentary characteristics of these deposits are indicative of a late Weichselian age (Paepe and Sommé, 1970; Sommé *et al.*, 1992, 1994, 2004).

According to the vertical succession of these deposits (Fig. 3.7), we think that depositional settings could be influenced by a meandering main course of the Aa River and the action of its drainage system fed by small tributaries. Similar conditions have been interpreted by Gandouin (2003) who mentioned in his study a meander belt channels in the middle of a vast swampy region that could have developed for the Saint-Omer area during late Pleistocene. Vegetated and marly deposits may represent swamps and shallow lakes as it was also interpreted by Sommé *et al.*

(1994) which may be formed in many areas of the floodplain linked to the action of the meandering Aa River.

In Bierne area, we have interpreted as loess deposits the Pleistocene sediments that have been preserved at the bottom of the cores (Fig. 3.6). These sediments are one of the most important depositional features indicative of periglacial conditions (Paepe and Sommé, 1970). They were affected by ice wedges and evolved to water saturated soils, in which developed characteristics of gleysols (Fig 3.6b). Similar conditions are explained by Sommé *et al.* (1992) and Sommé *et al.* (2004) in the subsurface of the coastal plain near Watten and Gravelines respectively. Loess deposits were also reported by Bosch (1975) with similar characteristics in the inner part of the western side of the coastal plain.

In other parts of northern France, loess deposits present similar characteristics being modified by gelifluction processes. They were interpreted as a blotched soil resulting of saturated groundwater, a facies of loess under wet or waterlogged conditions (Lautridou, 2006; Antoine *et al.*, 2003b). This general change in the environmental context of the region shows that water saturation of soils could be induced by the sea-level rise after the last glaciation.

In terms of environmental context, some characteristics in the conditions of deposition could be estimated from the occurrence of clay mineral content (Chamley, 1989). In this sense, the smectite enrichment of the clay mineral composition that we observed along our cores is controlled by the source-rock mineralogy corresponding to the Cretaceous rocks of the Artois hills (Deconinck *et al.*, 1989; Deconinck and Chamley, 1995). They are directly distributed through the paleoflow drainage of the Aa fluvial system fed by the Hem River. The high degree of humidity of the soils and the poor drainage capacities may also contribute to the high concentration of smectite (de Visser and Chamley, 1990; Moon *et al.*, 2000) due to the increasing water table associated to the Holocene sea-level rise.

Sedimentary characteristics of the Pleistocene deposits observed in the FFCP could be compared, temporally and lithologically, with some features expressed in Pleistocene deposits in the Belgian and Dutch coastal plains. The Belgian area presents clay, silts and fine sands of fluvial origin dating from the Late Pleistocene directly covered by the Holocene basal peat (Baeteman and Declerck, 2002; Baeteman, 2004). Also, were found Weichselian periglacial coversands underlain by marine deposits of more probably Eemian age (Paepe *et al.*, 1981; Baeteman,

1985, Denys and Baeteman, 1995). The Dutch coastal plain is compound by aeolian cover sands and fluvial sediments of late Weichselian age (van der Valk, 1996).

### 3.4.2 Holocene deposits

The analysis of the Holocene sedimentary facies reveals the main sedimentological characteristics of the FFCP deposits and their variations. There are five sedimentary facies: organogenic deposits, then from finer to coarser facies. They provide evidences to reconstruct the depositional settings of the area: an often clear action of tidal currents in a macrotidal regime, an important wave action in exposed conditions and the influence of the sea-level rise.

A large proportion of the earliest Holocene sediments were accumulated in low energy conditions indicated by the basal peat and organic-rich muds as a non-erosional Holocene/Pleistocene contact (de Gans and van Gijssel, 1996; Baeteman, 1999). The basal peat presents a predominance of *Corylus*, *Tilia*, *Quercus* and *Alnus* compared to herbaceous plants (Sommé *et al.*, 1992, 1994) and muds predominance of *charophytes* (Gandouin, 2003). This suggest that deeper organic-rich facies was developed in swamps forest conditions (CORINE Biotopes, 1997) associated to the previous fluvial environment and influenced by the rising water table associated to the relative sea-level rise around 9000 cal BP during the Boreal period. It is possible to find older organic-rich bed in the Preboreal period showing ages around 10508 - 10875 cal BP in borehole 380 (Appendix A and E).

The French basal peat deposits show a relatively older deposits than those studied in Belgium where the oldest known basal peat is 9780-9040 cal BP (Denys and Baeteman, 1995). This delay in the Belgian as well as Dutch record could be associated to the flooding history of the southern bight that had an earlier effect along the French coastal areas (Beets and van der Spek, 2000).

Basal peat marks the change of exclusive terrestrial pollen dominance to progressive extension of *Chenopodiaceae* reflecting a gradual influence of marine conditions in the area, changing to marshes conditions (Sommé, *et al.*, 1994) and the response to the climatic changes progressing in early Holocene. Similar trends of inundation and beginning of marine conditions were identified by Long *et al.* (2000) with the rise of *Chenopodium* type pollen in the southern England peat accumulations.

No tectonics evidences were observed in the sedimentary succession, suggesting that subsidence and deepest basal peat could be more related to compaction by sediment load during the Holocene. It involves a good consolidation of this sedimentary accumulation (Törnqvist *et al.*, 2008; van Asselen, 2010) and the morphology of the underlying Pre-Holocene palaeotopography.

Surface peat layer is present across the cores and abundant boreholes analyzed in the coastal plain. Its formation could be associated with a considerable preservation of high water table conditions (Flint *et al.*, 1995), a variation in sedimentary conditions and climatic changes that occurred in the coastal plain around the Atlantique-Subboreal transition (Sommé, 1977; Leplat and Sommé, 1989).

In cored sections, this layer is often vertically following the underlying mud flats deposits. At the contact between mud and organic-rich sediments, foraminifera assemblages we observed indicate the presence of *Jadammina macrescens*, *Miliammina fusca* and *Trochammina inflata* that suggest supratidal conditions and the establishment of salt marsh environments (Culver, 1978; Wang and Chappel, 2001; Debenay, 2006).

Pollen analysis of the surface peat samples from Bierne shows high dominance of sedges (*Cyperaceae*) and *Alnus* into the pollen association suggesting the development of shrub swamps (CORINE Biotopes, 1997) overlying mud flats and marshes. Within these shrub swamps some wooded areas and constantly submerged zones (mostly related with freshwaters conditions) developed in a nearshore context. Occurrence of arboreal pollen and some presence of pollen from aquatic vegetation support this consideration.

These types of wetlands are highly localized in the coastal area of the Nord-Pas de Calais region (Vergne, 2013). Surface peat from Watten exhibits similar characteristics of mixture of herbaceous vegetation with *Alnus* and *Fraxinus*. Very strong reduction of *Chenopodiaceae* marks the disappearance of marine influence favouring the development and extension of the peat layer (Sommé *et al.*, 1994). The approach from diatom analyses led by Denys (1993) for the same peat layer in the western Belgian coastal plain displayed similar environmental conditions considering an evolution from low marshes to fresh fens.

Installation of this type of vegetated areas is associated with the filling-up of the transgressive succession that dominates the first part of the Holocene period.

The occurrence and thickness of this peat accumulation across the coastal plain result in an interesting evidence that the climate factors become dominant among the environmental parameters (Meurisse, 2005; Vergne *et al.*, 2009). Climatic changes were influenced by seasonally patterns, increasing of precipitation and warm climate during this time interval (Magny and Haas, 2004; Sebag *et al.*, 2006).

Peat lamination, as observed in core Bierne 1 (Fig 3.12a), could be related with the rapid peat compaction (van Asselen, 2010). Peat compaction could be associated to different factors, such as biological, chemical and physical factors. Peat compaction resulted in shallow subsidence in the area (Törnqvist *et al.*, 2008). The mechanism that drove the pre-consolidation of the peat is a function of the overlying clastic deposits facies that covering them.

The anthropisation and polderisation may also have played a significant role in the compaction of peat (Ameryckz, 1961). As a consequence of the dry bulk sediments, peat and muds were compacted and sand filled channels appear in the landscapes as ridges (Cohen, 2003; van Asselen *et al.*, 2009). Figure 3.21 shows an example of this situation into the FFCP.

Organic-rich muds represent the transition from upper mud flats to salt marsh deposits (Culver and Banner, 1978; Weimer *et al.*, 1982). Dominance of agglutinated benthic foraminifera as *Jadammina macrescens*, *Miliammina fusca* and *Trochamina inflata* suggest supratidal environments, lower salinity and the establishment of salt marsh conditions (Culver and Banner, 1978; Wang and Chappel, 2001; Debenay, 2006, Armynot du Châtelet *et al.*, 2008).

Salt marsh deposits present small thicknesses and it is constantly intercalated with mud facies. This situation is particularly common in upper intertidal zones due to changes in the hydrodynamics conditions (Mángano *et al.*, 2002) and not directly associated with changes in relative sea-level. Tidal inundation could be prolonged, flooding the tidal flat surface accompanied by a low sedimentation rate (McKenzie and Moran, 2004).

Mud facies are widely distributed in the area (see distribution further in profiles of chapter 5). They evidence deposition from suspension by low energy processes (Reineck and Singh, 1980). The clayey silt deposits and the occurrence of their components are indicative of upper intertidal flats or mud flats deposits (Desjardins *et al.*, 2012). Mud-flat deposits are more frequent inland and towards the border areas of the FFCP, where the energy of tidal currents tends to be minimal but flooding

affect the watershed of the plain, covering extended areas with a low sedimentation rate. This facies occurrence express that tidal energy penetrates further inland than wave energy and muddy sediments accumulation occurs along the sides of the length of the estuary (Dalrymple *et al.*, 1990).



Figure 3.21. Aerial picture in an area close to Bierne displaying a section of a major channel bend with connected small meandering creeks (Source [www.geosur.info](http://www.geosur.info)). This is part of the most recent tidal network before definitive anthropization of the plain.

The mud facies of the FFCP mostly present some clayey silt. It represents an interesting distinction from finer material giving some information about the depositional setting where the mud flats developed. As explained by Flemming (2012), this distinction allows discussing the transport conditions on sedimentation. Applying the grain-size parameters developed in tidal flats by Wang and Ke (1997), we estimated from the frequency of this relatively coarse grain-size that mud flats were influenced by strong tidal flows and very-high suspended sediment concentrations with active transport.

Some other depositional settings of the mud facies could be inferred from the benthic foraminifera that we gathered in cores from Les Attaques and Bierne sites.

They are dominated by *Haynesina germanica*, accompanied by some variations in the presence of *Ammonia tepida*, *Criboelphidium gerthi*, *Criboelphidium williamsoni*, *Milliolinella subrotunda* and *Bulliminella elegantissima*. This indicates slight variations between low mud flats and high mud flats conditions (Culver, 1978; Horton, 1999, Evans *et al.*, 2001; Bernasconi, 2009). The mixed assemblage of euryhaline species (e.g., *Criboelphidium williamsoni*) and stenohaline species (e.g., *Milliolinella subrotunda*) refers to brackish waters.

The mud flats of the FFCP show rapid variations in the vertical profile with gradual changes to marshes. As remarked Weimer *et al.* (1982) this variations in mud flats environments could be associated to the edge of the influence of tidal energy and the seasonal intertidal cycles that may allow rapid physical changes in providing filling material and the slow colonization of the upper mud flats surface by organism and plants.

The sedimentological characteristics of the heterolithic facies described in the plain suggest associating these sediments as mixed flats deposits, tidal channels fill or mud flats when present a mud-domination (Dalrymple *et al.*, 1992; Desjardins *et al.*, 2012). These deposits on the FFCP show a fining upward pattern where sand content decreases and pass gradually to mud deposits characteristic of mud flats.

These deposits respond directly to the hydrodynamic conditions and a strong tidal control on the sedimentation (Weimer *et al.*, 1982). Tidal bedding responds effectively to tidal cycles. These types of rhythmic deposits can be typically formed on the flank side of the main streams in shallow estuaries (Dalrymple *et al.*, 2012).

Sand facies that extend into the coastal plain can be separated in tidal channels, tidal creeks and sand flats, based on sedimentological characteristics, faunal content and geometric measurements (thickness, depth, contacts and fining-upward trends). Broadly exposed in the subsurface data, they present erosive characteristics in their basal contact, affecting previous deposits of Pleistocene (Figs 3.6 and 3.17) and earlier Holocene facies (Figs. 3.15 and 3.16).

They are greatly associated to the length of the Aa River and to the seaward part of the coastal plain (see distribution further in chapter 5). Their abundance in the French Flemish coastal plain responds to the interaction of Holocene sea-level rise, tide dominated hydrodynamic processes, wave action, abundant sediment supply from offshore and the coastal plain drainage configuration before and during the Holocene infilling.

Tidal channels constitute the main transport pathways for the marine-sediment supply associated with the development of a tidal prism and the ongoing sea-level rise during the Holocene. As we saw in chapter 2 the rivers flooding in the coastal plain have low solid flows. This is reflected in the composition of the Holocene sandy deposits that is clearly different compared to Mesozoic and Palaeogene rocks surrounding the plain. Only limited grain supply derived from hinterland can be supposed (Baak, 1936).

Sandy deposits corresponds the main building sediments of the FFCP. The sediment contribution is essentially composed of sands transferred by the coexisting strong current patterns of the North Sea to the coast (Anthony, 2000; van der Molen and de Swart, 2001). In spite of these affirmations sandy sediments correspond to the mixture of grains with well to moderate sorting and moderate to well roundness which could be the evidence of a mixture between remote and local sources. Mrani (2006) presented similar results, showing that sandy sediments have an important influence of fluvial sources, especially in the deeper (older) sands, with increasing marine origin upward.

Based on the strata succession from core description and borehole data distributed along the plain, sand facies present a vertical variation in colour, possibly associated to their mineral composition. Their characteristics suggest two main periods of deposition, where sediments are mixture of sources and reworked previous deposits. Similar sedimentological characteristics were observed on profiles of the Picardy coastal plain (Lefèvre *et al.*, 1980).

The lower grey-bluish sands are mainly related with the long source of mixed group of fluvial-glacial sediments transported through the southern North Sea after the last glaciations (Baak, 1936). These sediments are mixed with local alluvial and marine Pleistocene sediments reworked during the Holocene transgression. This type of sediment dominates the early stages of the Holocene infilling when the accommodation space was great due to the fast early Holocene sea-level rise. Leplat and Vivier (1969) mentioned grey-bluish water saturated quartzose sediments for almost the entire thick early-mid Holocene sedimentary succession of the French Flemish coastal plain.

Upper light grey or grey greenish sands also mainly correspond to a marine sand supply (Baak 1936; Schüttenhelm and Laban, 2005) which could be a mixed of distant sources with local sources and reworking of previous Holocene deposits.



Depositional conditions suggested that most influence for this last sedimentation may be associated with low accommodation space and high hydrodynamic control from tides and waves, giving more importance to reworked local sources. Presence of greenish colour could be related to enrichment in glauconite and other minerals associations practically similar to those founded in the current beach sands (Baak, 1936). Our field geological observations from the current shoreline of Calais, Gravelines and Dunkerque show the same assumption made by Baak (1936) and revisited by Schüttenhelm and Laban (2005).

In the central and northern part of the coastal plain, tidal channels form a seaward wide coalescing network with sand flats that consist of grey-bluish fine sands and silty sand deposits. High-energy conditions with strong tidal currents allow to build-up sandflats in the lower intertidal zone derived by migrating tidal channels (McCants and Zarillo, 1985; Feniès and Faugères, 1998). Sand introduced into the coastal zone also influenced the upper intertidal and supratidal areas creating landward tidal creeks networks not connected directly to the main drainage system, but affected by tidal flooding and seasonal water level rises (Feniès and Faugères, 1998).

Foraminifera assemblage founded in samples of this facies show abundance of *Milliolinella subrotunda*, *Criboelphidium excavatum*, *Triloculina trigonula* and *Haynesina depressula*. This strongly suggests subtidal settings and the influence of marine conditions in the deposits (Culver, 1978; Wang and Chappell, 2001; Debenay *et al.*, 2006). Also, the presence of calcareous fauna and stenohaline species (e.g., *Milliolinella subrotunda*) evidences open marine organisms brought from offshore during the rapidly rising relative sea-level (Brodniewicz, 1965; Scott *et al.*, 2004) in Early Holocene when the paleochannels were flooded (Baeteman, 2005a). In consequence, these deposits could be interpreted as being formed under lower intertidal to subtidal settings (Desjardins *et al.*, 2012).

Yellowish sand sediment dispersed in the northern area could be influenced by storm wave activities and aeolian processes (Anthony, 2000) which directly acted in the formation of the inland and current coastal dunes. Aeolian deposits are overlying the upper tidal flats deposits indicating that the processes that induced their development were important after the mid to late Holocene. This situation is also observed and discussed by Baeteman (2004) and Mrani and Anthony (2011).

Gravel deposits dispose morphostratigraphic and sedimentary characteristics that allow interpreting these deposits as a barrier spit formed by the wave action in the north-western area of the plain. The barrier spit, which is called *Banc des Pierrettes* in the literature, has an up to 12 km long extension until the town of Marck. The relative age of the barrier construction could be determined by its stratigraphic relationships with surface peat complex. Sommé (1977) mentioned its development during the Atlantic period.

The sandy gravel spit is directly linked to the source of gravels corresponding to the flint that are contained in the Cretaceous chalk still visible along the cap Blanc-Nez. Due to the littoral drift, the gravels are transported eastward by waves as it could be observed along the southern bank of the Somme estuary. According to Dalrymple *et al.* 2012), the construction of this type of barrier in a mostly tide-dominated system could represent the control of waves in the seaward flank of the estuary mouth or a small tidal prism.

Summarizing the information from each sedimentary facies, their changes in sedimentary content, contacts and depositional settings, it is possible illustrate the genetic relationships among them. Definitions of the depositional facies explain the environmental context in which the sedimentation taking place (Miall, 1985). In this sense, according to the vertical succession of the depositional facies interpreted, we propose differentiating the FFCP infill in Late Pleistocene alluvial valley and Holocene tidal environments (Fig. 3.22). Holocene depositional environments are described by estuarine and tidal flats units. Estuarine unit corresponds to the filling-upward packages from tidal channels to marshes/swamps and stacked tidal channels/sand flats (Figs. 3.8 – 3.9). Tidal flats unit is the last sedimentary cover with extended intertidal flats overlying the thick surface peat layer and which present changes as lighter colours, increased shell quantity, minerals and rock fragments.

To document the spatio-temporal distribution of these sedimentary units and their internal depositional facies organization, we performed a series of seismic lines (chapter 4) and several regional cross sections along the plain (chapter 5) to delineate the depositional model and fit the stratigraphic architecture of the area.

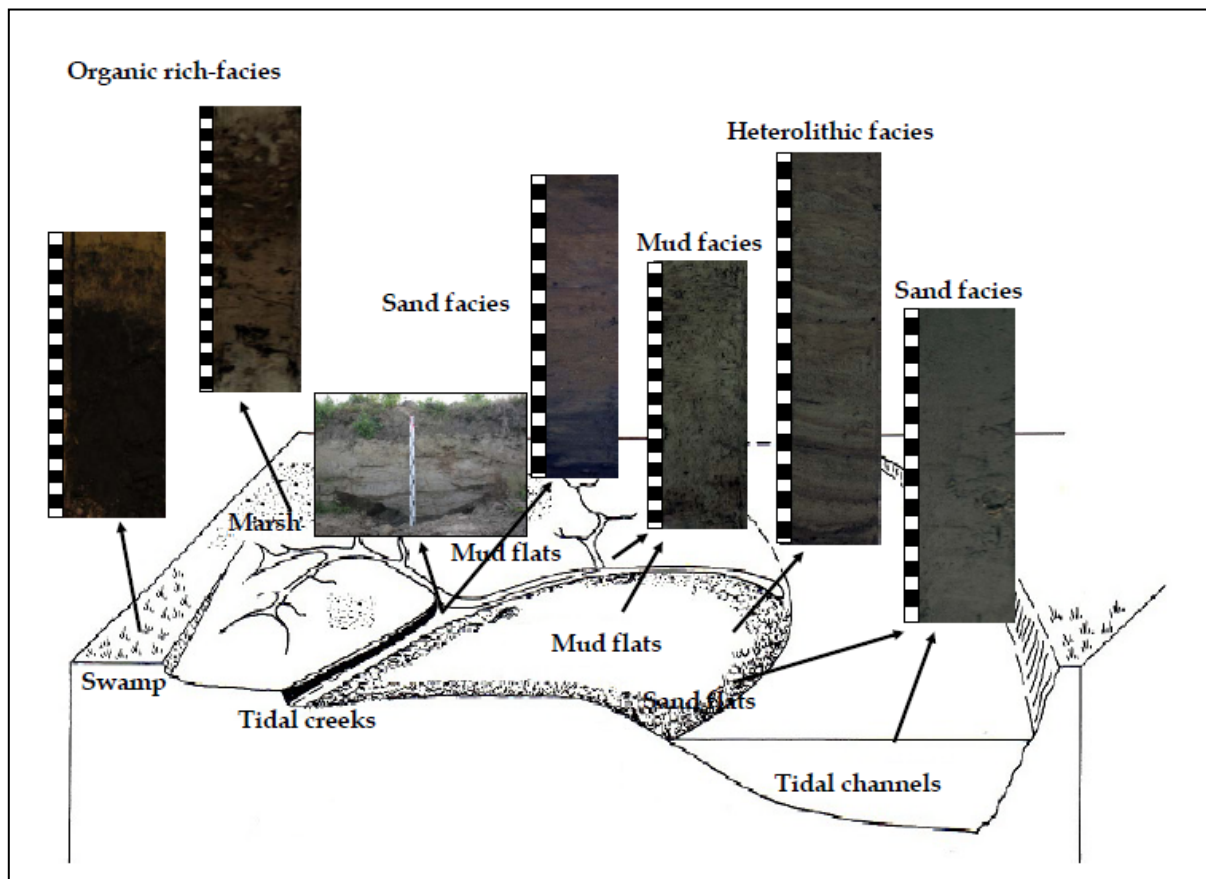


Figure 3.22. Schematic distribution of the depositional facies within the tidal environments of the FFCP during the Holocene. (Adapted and modified from Weimer et al., 1982)

### 3.5 - Conclusions

The study of sedimentary features of our cores combined with the characteristics of borehole data allow us defining five sedimentary facies. From their depositional context we grouped them in facies assemblages establishing the environmental sedimentary units that illustrate the changes in depositional environment within the plain. It started with an alluvial valley followed by Holocene tidal environments: estuarine and tidal flats units.

Sedimentary characteristics show dominant marine sediment supply and some local fine admixture during the Holocene interval. Sedimentation results from the interaction of sea-level rise and a strong role of the hydrodynamic influence. The accumulation delineates sediments from tide dominated coastal areas from shallow subtidal to swamp zones.

It is inferred from the lithologic characteristics and sedimentary patterns that most of the sediments have been deposited within a coastal prism with high accommodation space inland. However, morphosedimentary condition would be changed and a great development of peat appeared capping large part of the Holocene deposits. Subsequently, new intertidal sedimentary deposits become dominant and cover the entire area.

Tidal currents dynamic is the main sediment transport mechanism acting in the French Flemish coastal plain. It controls the water levels and inland sedimentary distribution from the tidal channels. However, coastal behaviour is not only caused by the domination of tides. Waves action has a strong influence along the littoral zone, controlling the erosion, redistribution and sedimentation of the seaward area that flanked the mouth of tidal channels.

Clay mineralogy is quite homogeneous through the Holocene sedimentary succession. Their characteristics can be associated with the current marine conditions. However, the samples present some differences in the uppermost beds which being especially rich in smectite as it was observed in the Pleistocene sediments of the bottom of cores, showing an increase in the clay fraction from hinterland contribution.

# **Chapter 4. Very High-resolution seismic: Looking to the subsurface features of the Holocene infill of the French Flemish coastal plain.**

## **4.1 Introduction**

Seismic reflection is a geophysical exploration method based on the recognition of interfaces that are detected where the acoustic properties of the rock change (Brown, 2011). This is the basis of the understanding of the nature of seismic data. Acoustic impedance of a rock layer is the product of the density and the velocity of that layer, the reflection is generated by a contrast in acoustic impedance (Brown, 2011). This method has a long and successful history in the exploration of hydrocarbons. In this activity the depths of interest are commonly several kilometres below the surface, in consolidated strata. However, the growing interest in shallow sub-surface exploration has developed the field of the high-resolution seismic profiling (Brouwer, 1988).

Very high-resolution (VHR) seismic survey is a method used in shallow or deep waters to obtain images of the first meters of the subsurface (Verbeek, 1995). The term "high-resolution" is incorporated due to the small size of the structures to be determined when compared to the deeper and larger conventional reflection seismic. This type of survey has an adaptable methodology providing solutions to wide and varied case studies, with scientific and industrial purposes, as stratigraphic models, hydrogeology, civil engineering, etc (Olsen *et al.*, 1993; Teixidó, 2000). As such, the acquired survey is designed as an initial recognising tool, to define the spatial extent of the subsurface targets (Lynn, 2009). Additionally, VHR seismic is used in combination with previous stratigraphic interpretations, using seismic and well data to maximize lateral correlation and depositional interpretation.

Greatly implemented in continental shelves (e.g., Mathys, 2009) VHR seismic reveals significant new information about the architecture of their shallow sedimentary cover, providing the opportunity to better describe the subsurface features and reconstruct the geometry of the different sedimentary layers (De Batist and Versteeg, 1999; Tessier *et al.*, 2003). In marine marginal areas, seismic surveys have progressed quickly showing valuable results; being widely used in order to

identify a large range of morphological and sedimentary evidences that provide information of the relative sea-level history, sedimentary dynamics and stratigraphic organisation of the coastal zones (Brouwer, 1988; McDowell *et al.*, 2005; Tessier *et al.*, 2010). Generally, defined as marine seismic data, it may be shot on rivers and canals using and adapting the same seismic source, receivers and the continuous-profiling acquisition technique, to be applied in non-marine waters (Verbeek *et al.*, 1994; Verbeek, 1995; Tóht *et al.*, 1997; De Batist and Versteeg, 1999).

A VHR seismic survey was performed in this study along the French Flemish waterways open to navigation. The French Flemish coastal plain (FFCP) presents a complex Holocene sedimentary arrangement and is a key place to understand the relations between relative sea-level, sedimentation controls and the link between them. Therefore, testing the seismic response of the tidal deposits may provide a better understanding of the distribution and geometry of the sedimentary bodies. The development of a series of seismic profiles shows the first metres of the subsurface with the objective to insight distinctive sediment-infilling features through the Holocene and improves the stratigraphic framework within the area.

The waterways configuration open to navigation determines the geometry of the profile network (Fig. 4.1). A major strike profile was shot between Saint-Omer and Gravelines along the canalised Aa river. Another strike profile links Bergues and Dunkerque to the East. It is one of the oldest French canals dug around the XVI<sup>th</sup> century to link the powerful city of Bergues to the North Sea. Parallel to the coast, some profiles were taken along the canal that join Veurnes with Dunkerque, and along the Bourbourg canal. Crossing the coastal plain to the border sides, the seismic survey followed the canal between Watten and Calais and between Watten and Dunkerque.

This chapter details the acquisition, processing and interpretation of seismic records. We first describe briefly the general data acquisition and processing, but a special emphasis is set on the seismic interpretation and on the stratigraphic diagnostic signatures of the shallow subsurface that had, up to now, only been studied by punctual borehole data. For more details about the VHR seismic techniques, acquisition, processing and applications, I could recommend to read some authors as Bally (1987), Brouwer (1988), Simpkin and Davis (1993), Verbeek (1995), Marsset *et al.*, (1998) and Teixidó (2000) that discuss deeply the most technical aspects for these methods.

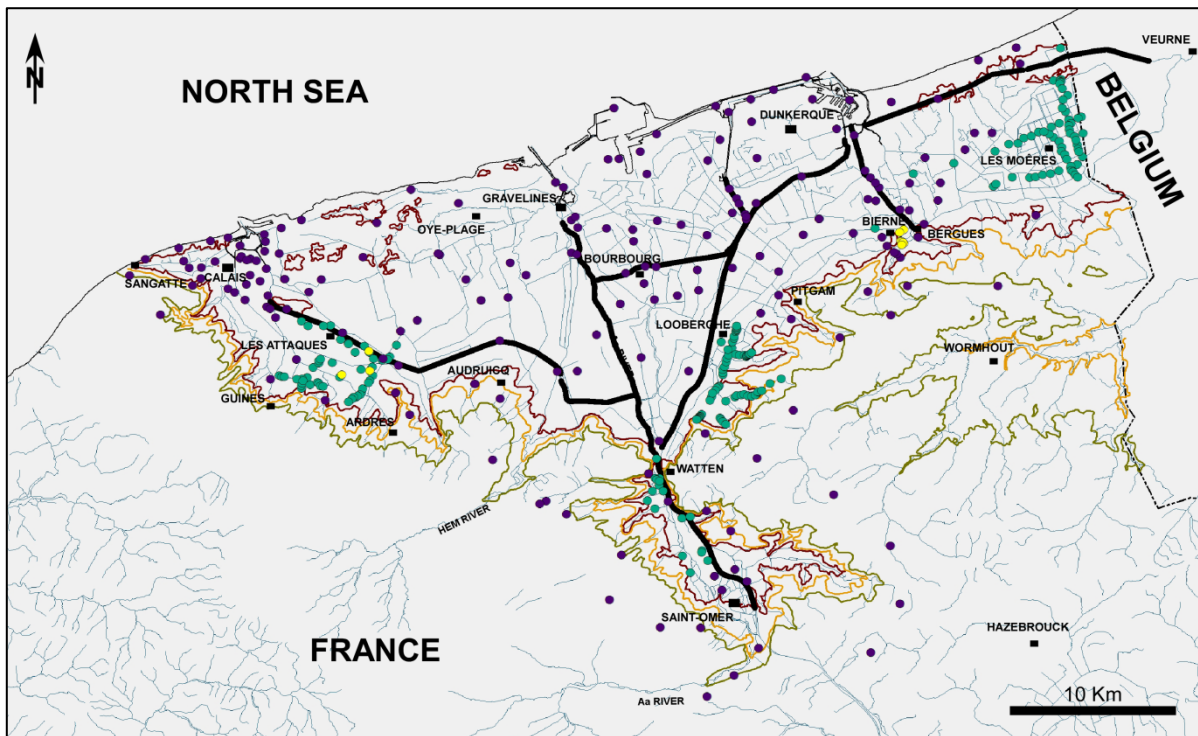


Figure 4.1. Map of the French Flemish coastal plain showing the shape of the plain, the drainage system and the seismic survey differentiated by thick black colour lines.

The seismic interpretation is based on the identification of the geometric relationships of seismic reflectors and on acoustic properties that define the seismic units (Brown, 2011). The character of a seismic-reflection profile depends on the acoustic impedance contrasts within the subsurface layers. Lithological or depositional boundaries are only detectable when these boundaries coincide with a detectable change in acoustic impedance (Brown and Fisher, 1980; Brown, 2011).

Guided by the known general settings of the coastal plain, seismic profiles can serve as a good subsurface image to obtain some clues about the stratigraphic information of the Holocene infill.

## 4.2 Material and methods

### 4.2.1 Seismic data acquisition

The seismic lines have been acquired using the Seistec boomer profiler (Simpkin and Davis, 1993) (Fig. 4.2). The "Seistec" instrument consists in a source

and a receiver mounted together on a 6-foot catamaran sled towed behind and to the side of the survey vessel (Fig. 4.2). The source is a wide band electro-mechanical "boomer" that generates a single positive pressure transient; the receiver is an in-line-cone hydrophone array oriented to maximize vertical-incidence reflection energy. The boomer plate produces a sharp (short duration) broad-spectrum pulse that gives a good trade-off of penetration vs. resolution. Theoretically, the frequency of the signal is comprised between 500 Hz – 10 KHz and the vertical resolution is better than 0.5 m to a sub-bottom depth penetration of approximately 60 m (Foster and Poppe, 2003; Childs *et al.*, 2000).



*Figure 4.2. Views of Boomer profiler used in this study. It belongs to the Renard Centre of Marine Geology (RCMG) of Ghent University.*

The procedures carried out in the French Flemish coastal plain were conducted through a BQR programme of University Lille 1 and the collaboration of the Renard Centre of Marine Geology (RCMG) of Ghent University. Following their experience, we set the survey parameters using a power of 200 J, a shooting interval of 2 seconds and a recording length of 100 ms. This range was sufficient to get the Quaternary sediments and the top of the underlying bedrock. Differential GPS determined the position of the shooting points (Fig. 4.3); all coordinates in the recorded data were converted from geographic Lat-Long to Universal Transverse Mercator (UTM) using the WGS 1984 standard for UTM zone 31N.

In total, about 125 km (80% of navigable canals of the plain) of seismic profiles were acquired into the coastal plain (Fig. 4.1). Acquired data present some problems in the seismic quality. The poor performance of the seismic profiles could be



consequence of certain factors as: ship (engine and electrical devices) noises during the acquisition, thick channel bottom bed, echoes from channel sides, wind and ship waves, bad weather or other external limitations that cannot be controlled (Verbeek, 1995; Muller *et al.*, 2002; Chaumillon *et al.*, 2004; Van Lacker *et al.*, 2009).

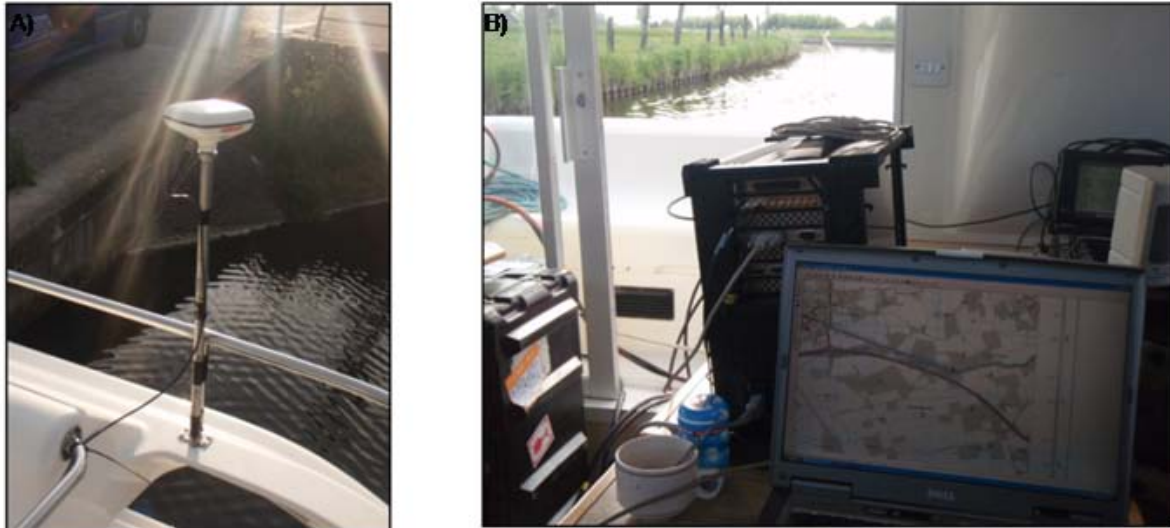


Figure 4.3. A) Differential GPS. B) Real-time position record during the seismic survey.

In the FFCP, the main problem seems to be linked to the low favourable conditions of the canals. A strong absorption of the signal in the uppermost sediments layers, the presence of organic material in the bottom sediments, eventually rich in gas, could make a mask to sound propagation. Also, recently disturbed or dredged sediments may deteriorate data acquisition (Haeni, 1986; Tóht *et al.*, 1997). Last not least, the shallowness of the waterways and their widths are at the origin of a large number of acoustic multiples that rapidly masked the deeper reflections.

#### 4.2.2 Seismic data processing

VHR seismic is more frequently used as it helps obtaining good quality data at without enormous budget. It also does not necessarily need a great processing effort. Under favourable conditions, raw data provide useful information about very shallow sediments (Tóht, 1997). However, it is usually observed in VHR seismic certain reverberations, which make difficult the interpretation and require some processing steps. Filtering tools are used to improve the seismic image, remove noise and

distinguish the near subsurface reflections (Marsset *et al.*, 1998; Chaumillon *et al.*, 2004).

The FFCP data from our survey present quite a lot of noise. Several multiples and refraction hyperboles obstruct the possibility to obtain a clear vision of the seismic reflections and prevent from an in-depth interpretation. Seismic data present a frequency range of 500 Hz – 7 KHz and a dominant frequency around 4 KHz (Fig. 4.4). Hence, the seismic data were processed following a workflow in Seismic Unix (CWP Seismic processing software) with stacking, a 1 – 6 KHz band-pass filter and automatic gain control (AGC) in 50 ms window length, obtaining some areas into the seismic profiles that were used for interpretation (Fig. 4.5). The seismic processing was carried out at the Laboratory of Continental and Coastal Morphodynamics (M2C) of the University of Caen Basse-Normandie.

#### **4.2.3 Seismic data interpretation**

Processed data were loaded into the 2d/3dPAK of Kingdom suite (SMT software) for interpretation. In order to express the interpreted sections in metres, an average seismic velocity in saturated soft sediment of 1500 m/s was used (Dalrymple and Zaitlin, 1994; McGee, 1995; Bachrach, 1998; Saito *et al.*, 1998; Novak, 2002; Lin, 2009). Time-to-depth conversion of the profiles displays a penetration around 30 m and a calculated vertical resolution up to 0.09 m. This sound velocity gives a good match when comparing the basal contact of the Holocene deposits in the borehole data with the time of the surface in the seismic lines, from where the Pre-Holocene surface is defined.

The interpretation of seismic data was focused in the qualitative analysis of the geometry and internal reflection character considering the methods outlined by Mitchum *et al.*, (1977) and Sangree and Widmier (1979). The different seismic parameters and their geological significance are described in Table 4.1 showing the scheme proposed by Mitchum *et al.* (1977). Thus, to evaluate the internal reflections features for this study, amplitude and continuity as well as the information from reflection configuration and external forms were used in order to identify the seismic facies, their spatial relationships and the approach of the depositional settings. The internal reflection patterns, reflection configuration and external forms are represented in figures 4.6 and 4.7.

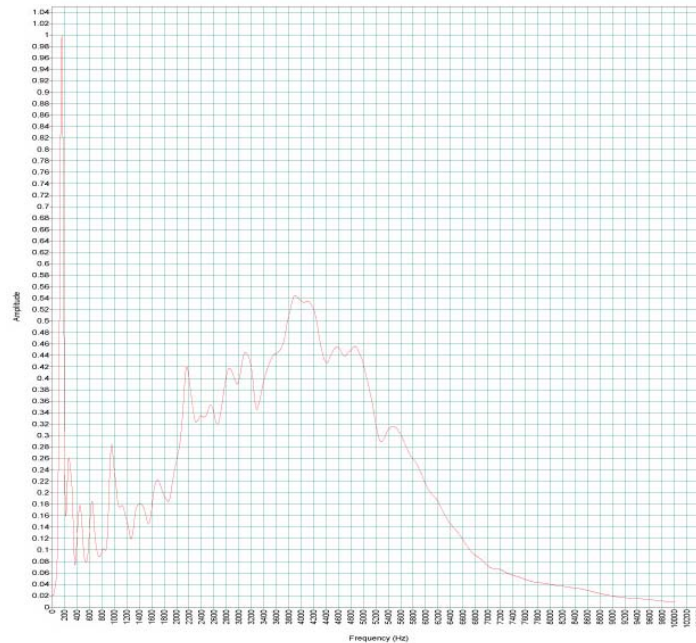


Figure 4.4. Example of spectral survey of raw seismic data (Line 8) showing the average range of frequency obtained in the FFCP.

Reflection amplitude is a function of the acoustic impedance contrast between units or layers and is described as high, moderate, or low. In general, much larger is the contrast in acoustic impedance at an interface, much larger the amplitude will be. Since acoustic impedance is a function of a material's density and the sound velocity through that material, high-amplitude reflections are marked by an important change in the deposits characteristics. This is expected for the Holocene-Pre Holocene interface. Low-amplitude reflections are expected where density or grain-size contrasts are small as observed within the Holocene infill.

Reflection continuity describes the consistency of the strata surface. Highly continuous reflectors or discontinuous reflectors are often the result of changes in the conditions of the depositional processes. Caution must be exercised following variations in these parameters as a diagnostic tool because the amplitude and continuity of a reflector is heavily influenced by interference, attenuation, and noise in the subsurface, which can be spatially non-uniform.

The integrating geophysics and core data approach in this chapter is limited because of poor quality of the seismic data and the quite weak nature of the acoustic reflectors. However, a comparison with projected boreholes allowed the calibration of reflections and some indications of depositional settings.

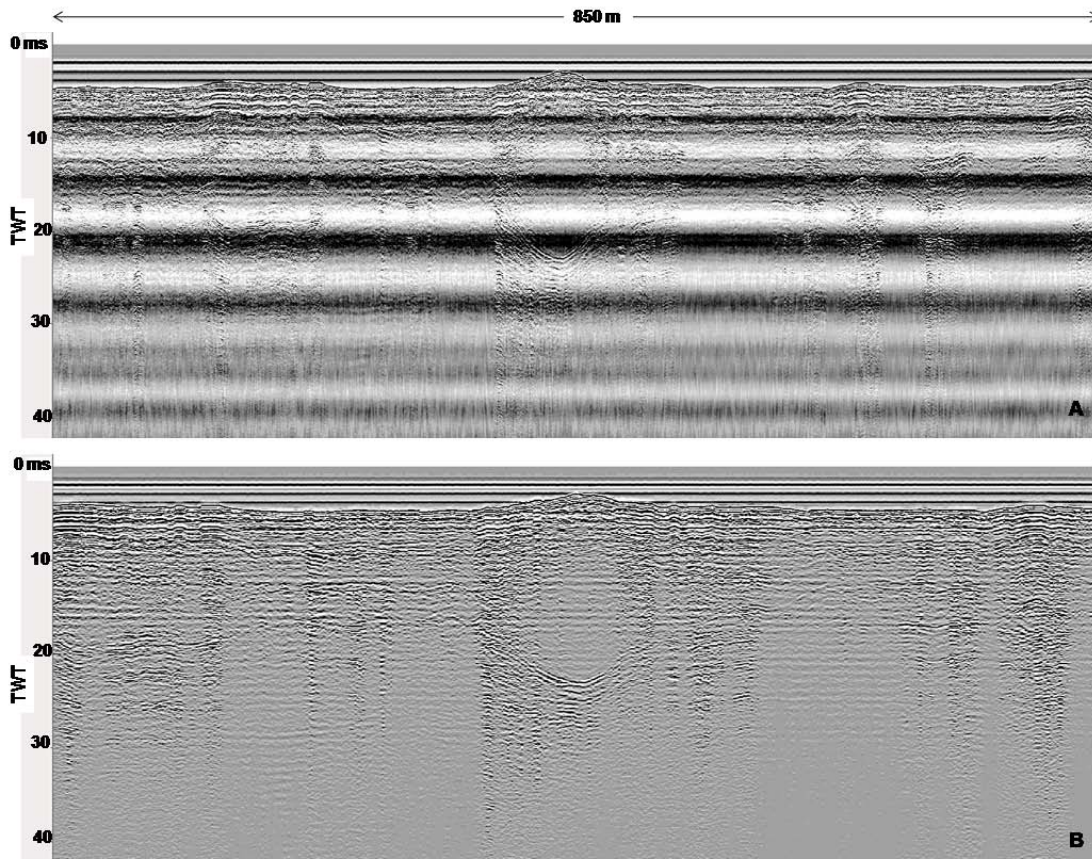


Figure 4.5. Example of seismic profile (Line 8) before and after processing. A) Pre-processed raw form. B) Result of the processing applied in the seismic line. The presence of noise is diminished in the post-processed profile.

Table 4.1. Seismic reflection attributes commonly used in seismic stratigraphy and their geological significance. Modified from Mitchum et al. (1977).

SEISMIC FACIES PARAMETERS	GEOLOGIC INTERPRETATION
Reflection configuration	Bedding patterns Depositional processes Erosion and paleotopography Fluid contacts
Reflection continuity	Bedding continuity Depositional processes
Reflection amplitude	Velocity-density contrast Bed spacing Fluid content
Reflection frequency	Bed thickness Fluid content
Interval velocity	Estimation of lithology Estimation of porosity Fluid content
External forms & Areal association of seismic facies units	Gross depositional environment Sediment source Geologic setting

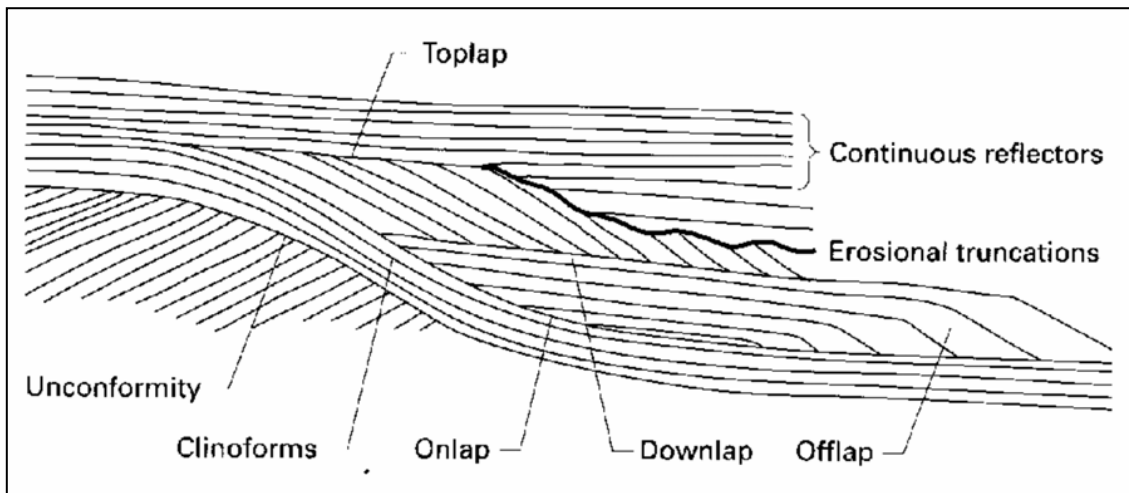


Figure 4.6. Examples of reflector relationships and termination patterns in depositional sequences.

Modified from Mitchum et al. (1977).

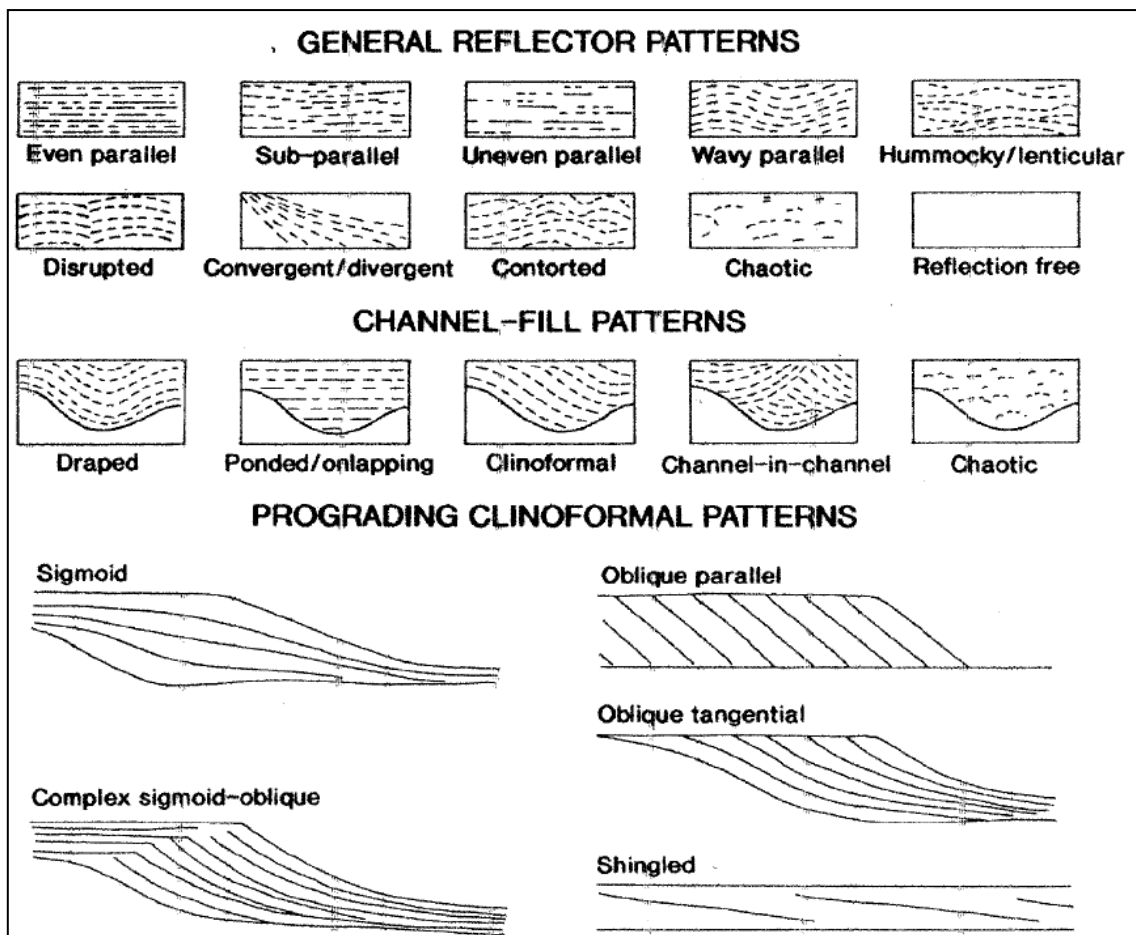


Figure 4.7. Examples of reflection configuration patterns. Source: Mitchum et al. (1977). Modified from

Stocker et al. (1997).

## 4.3 Results

### 4.3.1 Seismic Stratigraphy

The analysis of each seismic profile across the study area leads to the identification of two seismic units. Figure 4.8 depicts the seismic lines within the coastal plain selected to show the interpretation. A comparison with borehole data determines their stratigraphic position and the chronology of the surface which divides them (Fig. 4.9). The Pre-Holocene substrate and the Holocene deposits were identified and separated by a clear reflector appearing in the profiles along the entire area and corresponding to the Pre-Holocene unconformity. Among other important aspects, no faults or structures modifying the whole stratigraphic section were expressed along the profiles.

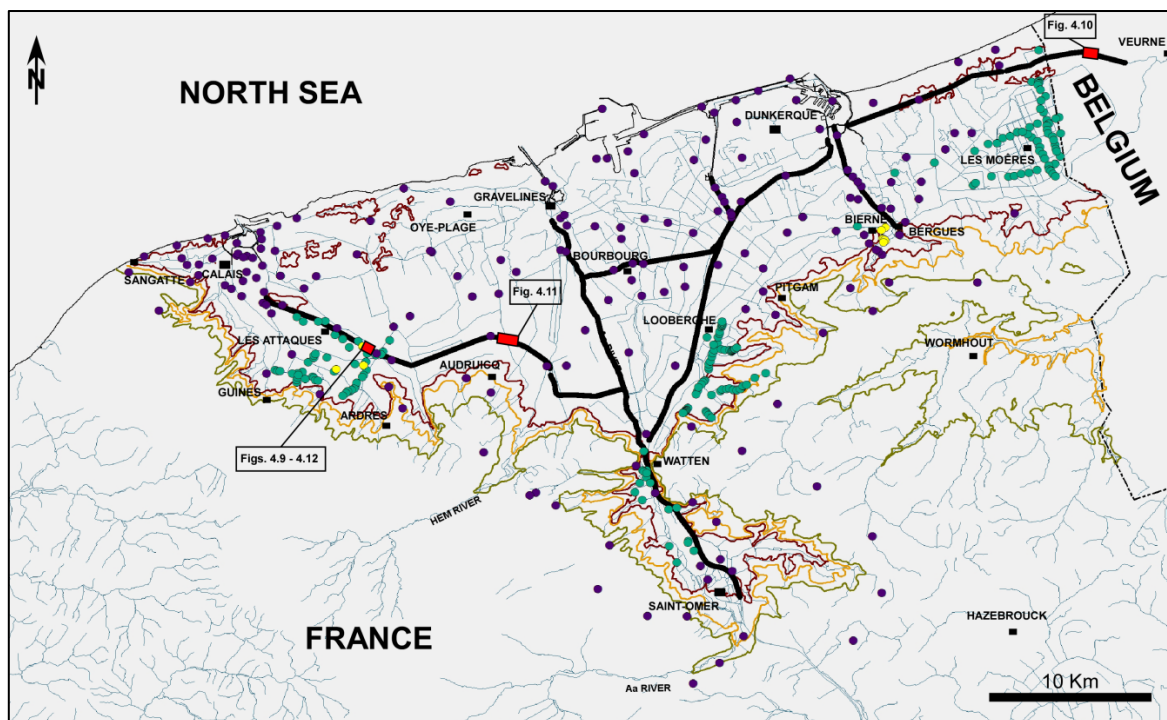


Figure 4.8. Location of seismic lines (in red) selected as examples of Pre-Holocene/Holocene subdivision of the sedimentary succession. Profiles interpreted are in the borders of the coastal plain.

### 4.3.2 Pre-Holocene unconformity

This surface is the major discontinuity distinguishable along the coastal plain. Generally, it is a well-defined, continuous and undulating, high amplitude seismic

reflector (Figs. 4.10 - 4.11). Sometimes, it is also well defined and non-continuous but as a whole, it constitutes a key surface due to its regional extent delimiting the Pre-Holocene substrate from the overlying Holocene deposits, in order to understand the sedimentary arrangement in the coastal plain.

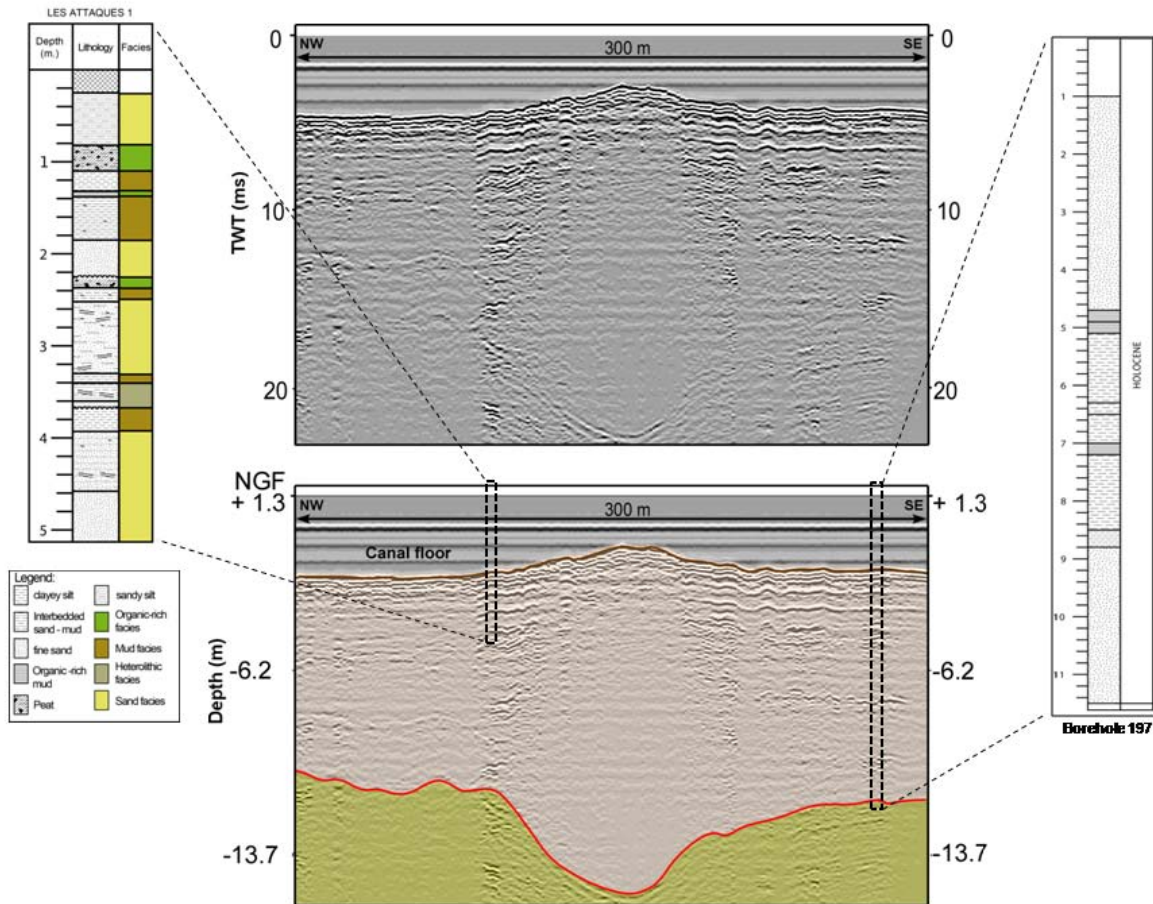


Figure 4.9. VHR seismic profile and its comparison with the boreholes described in the FFCP (Core Les Attaques 1 and borehole 197) showing the Holocene sedimentary infilling. Bottom of Borehole 197 reaches the pre-Holocene deposits.

The surface can describes incisions in some locations of the Pre-Holocene deposits (Fig. 4.12). Erosional features also could be distinguished by truncated weak reflectors. In other areas where the reflections terminations are concordant, not clear or not indicated, the strong contrast of acoustic impedance defines the discordance.

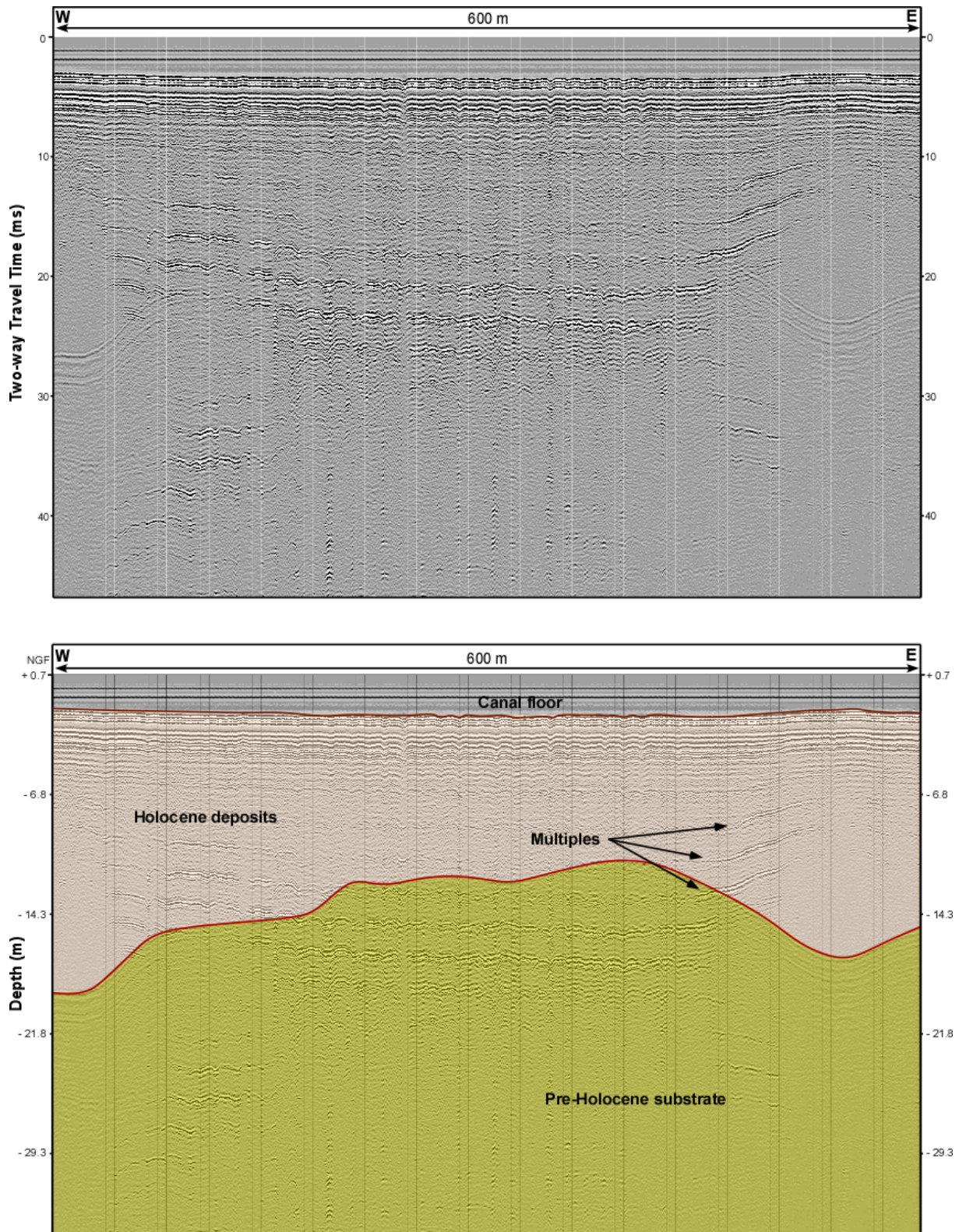


Figure 4.10. This profile depicts seismic line 1 in the FFCP subsurface. Above: non-interpreted seismic line. Below: interpreted seismic line showing the seismic unit and the Pre-Holocene unconformity. Note the high-quantity of multiples (parallel reflectors) and the low contrast impedance in the profile.



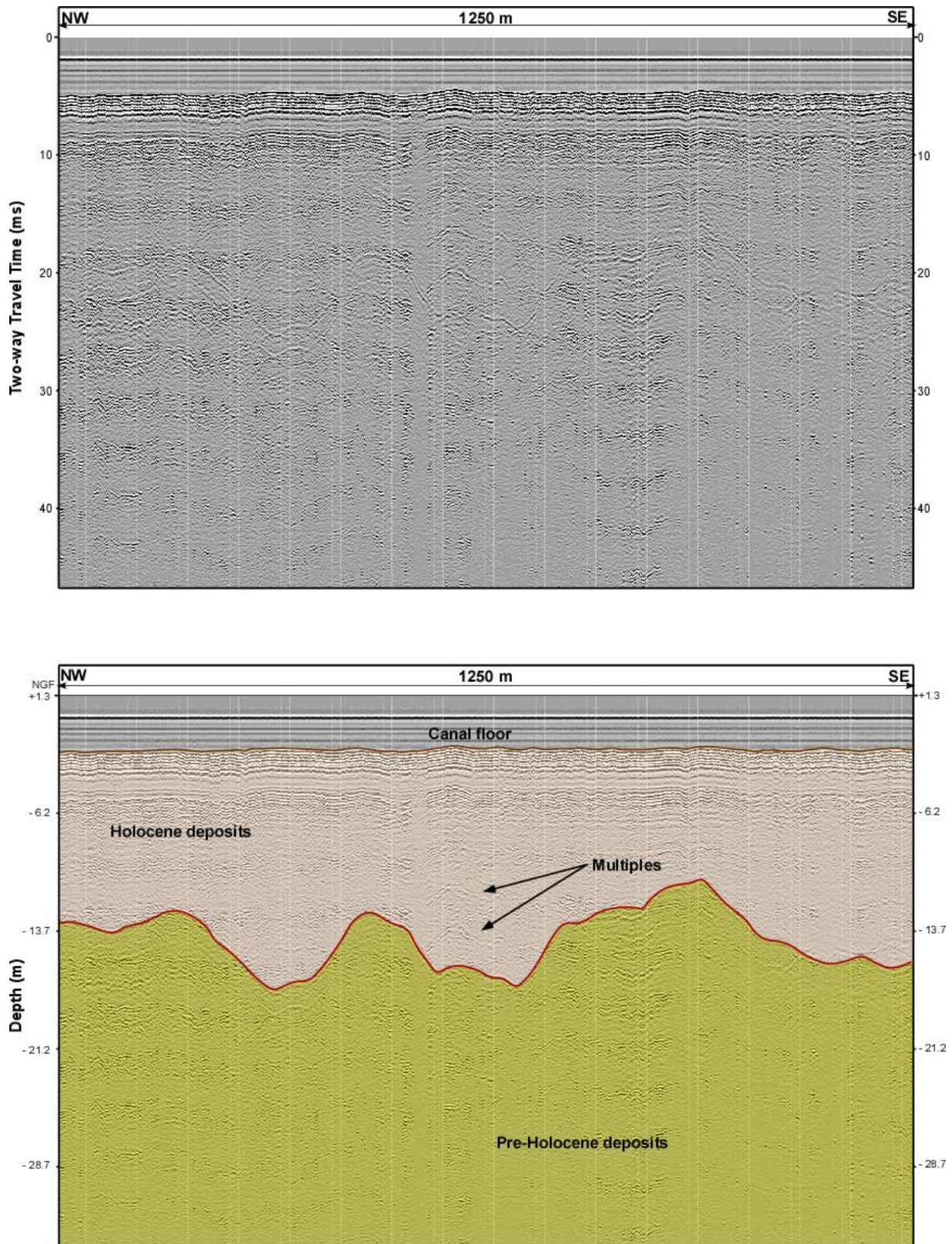


Figure 4.11. This profile depicts seismic line 8 described in the FFCP subsurface. Above: non-interpreted seismic line. Below: interpreted seismic line showing both seismic unit and the Pre-Holocene unconformity. Here it is also possible to observe the high-quantity of multiples (parallel reflectors) and the low impedance contrast of the profile.

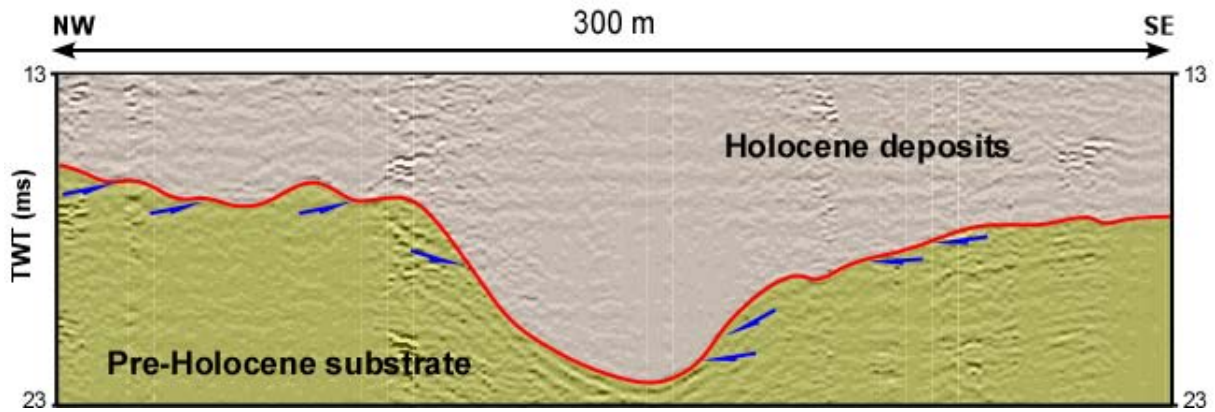


Figure 4.12. Pre-Holocene unconformity interpreted in seismic line 8. It is a good example to show how the Pre-Holocene substratum is incised and subsequently filled by Holocene deposits.

### 4.3.3 Seismic units

#### 4.3.3.1 Pre-Holocene substrate

This unit forms the acoustic basement of all the observed seismic profiles along the area. Its upper surface is marked by the Pre-Holocene unconformity. It corresponds to a truncated surface with some depressions. Its deepest part does not have remarkable characteristics, any specific geometry, structures or regularly reflection patterns. This is mostly due to a poor acoustic response or a limited sub-bottom penetration that prevent any detailed interpretation. Only some scarce diffuse reflections and sporadic small and strong reflectors could be observed in some profiles. Figure 4.13 depicts the location of seismic profiles selected to show the seismic unit interpretation while figures 4.14 and 4.15 demonstrate the feature of these units.

This basal unit is not uniform in age. According to published borehole data (BRGM, 2014) and previous documented studies (Dubois, 1924; Sommé, 1977; Houthuys *et al.*, 1993; Sommé *et al.*, 1994; 1999, Gandouin, 2003) it corresponds to Pleistocene or Palaeogene deposits in the major part of the area while towards the westernmost part of the plain it corresponds to Cretaceous deposits.

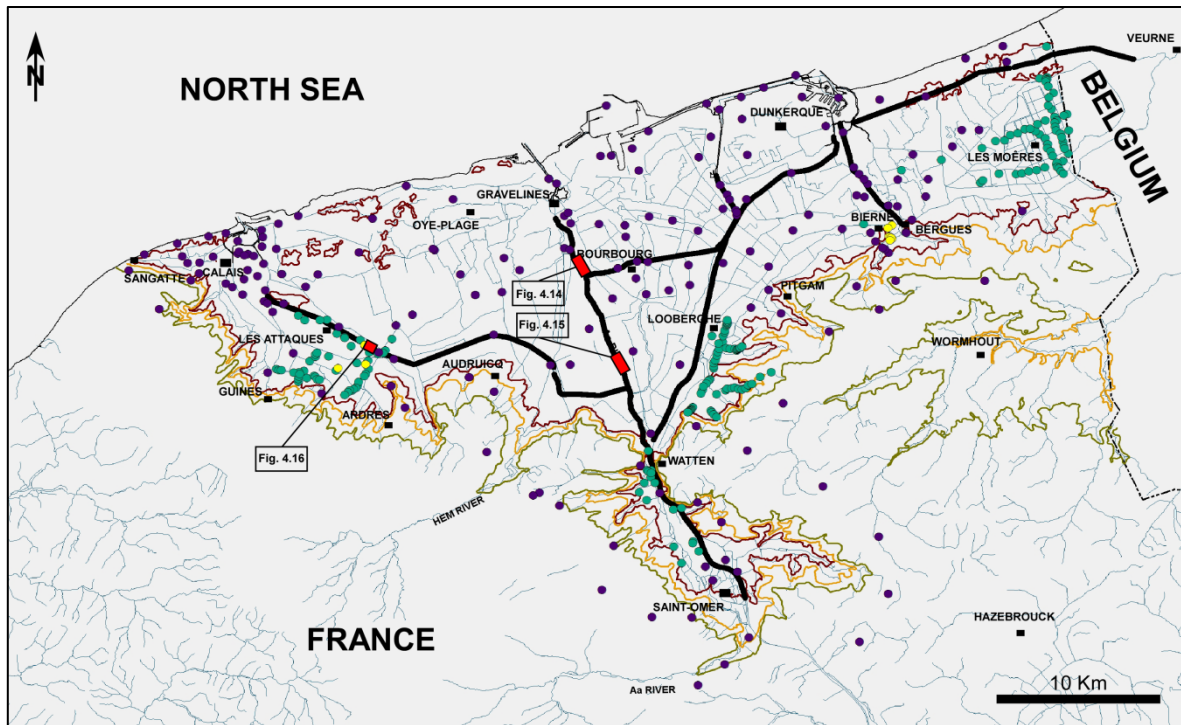


Figure 4.13. Location of seismic lines (in red) selected as exemplars to show the seismic units features. Profiles interpreted are in axial part of the coastal plain.

#### 4.3.3.2 Holocene deposits

This unit overlies the Pre-Holocene deposits with a sharp or erosive contact previously described as Pre-Holocene unconformity. Distinctive characteristics of the Holocene infilling have been represented from two seismic facies in spite of the weak impedance contrast and constant interference. They are named A and B. The combination of the character of the reflectors, the internal patterns configuration and the external geometry allows identifying these two seismic facies that indicate the arrangement of the Holocene deposits and their spatial and temporary variations (Figs. 4.14 – 4.15).

##### 4.3.3.2.1 Seismic facies A

This facies is developed above the Pre-Holocene deposits and is widespread along the coastal plain, being observed in most profiles. It is mainly distinguished on the basis of the regular channel-shaped features. It represents a stratified complex filled with a predominating multi-phase channel in channel nature. This could

correspond to the spatial migration of a series of imbricated and stacked channels (Figs. 4.14 – 4.15).

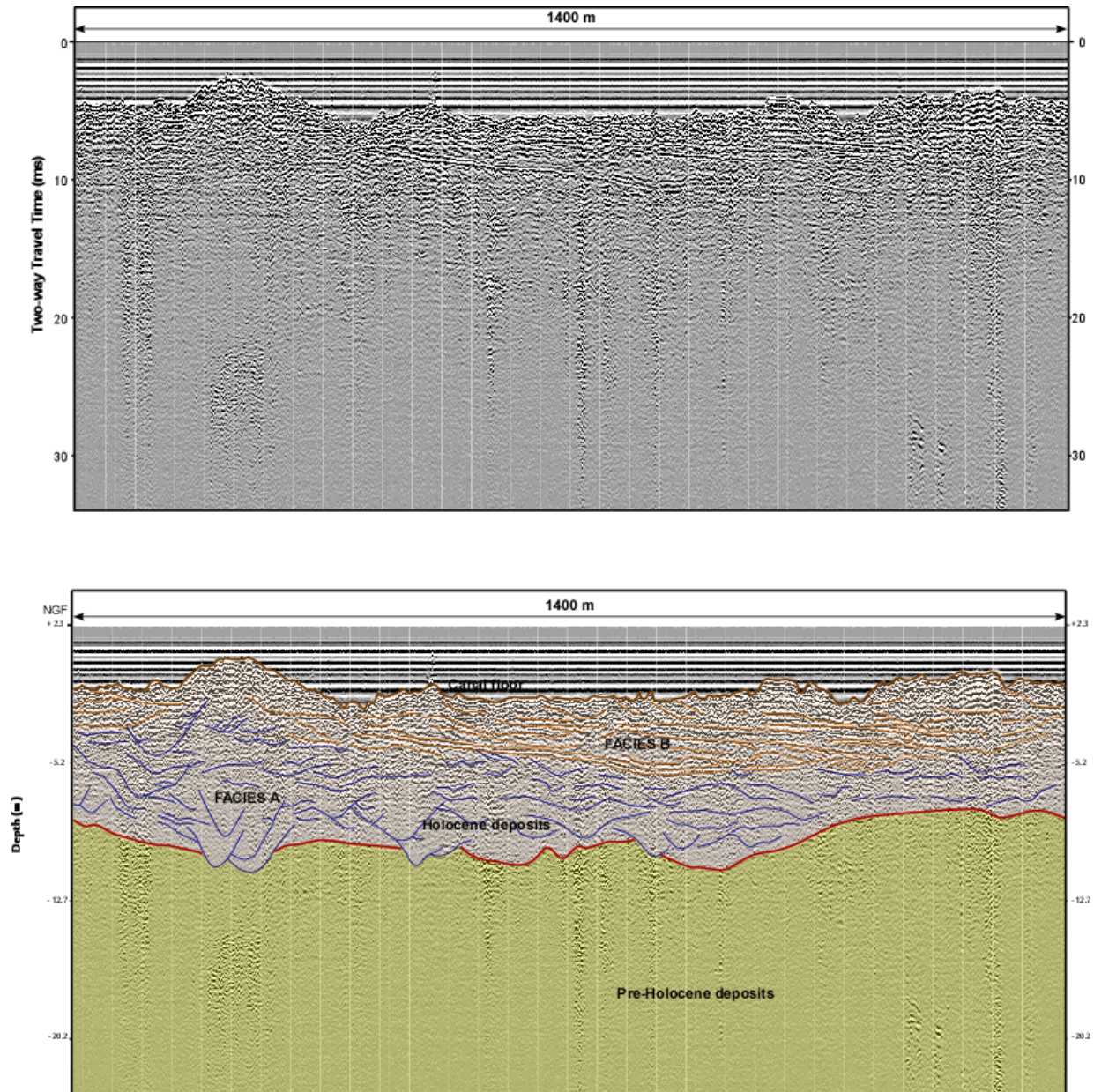


Figure 4.14 – Image of seismic profiles showing the non-interpreted seismic (above) and interpretation of the seismic units and seismic facies described in the Holocene deposits (below). The depth-time conversion uses a sound velocity in soft sediments of 1500 m/s. It is possible to distinguish the channel-fill that characterize the seismic facies A, and the slightly prograding clinoforms of the seismic facies B.

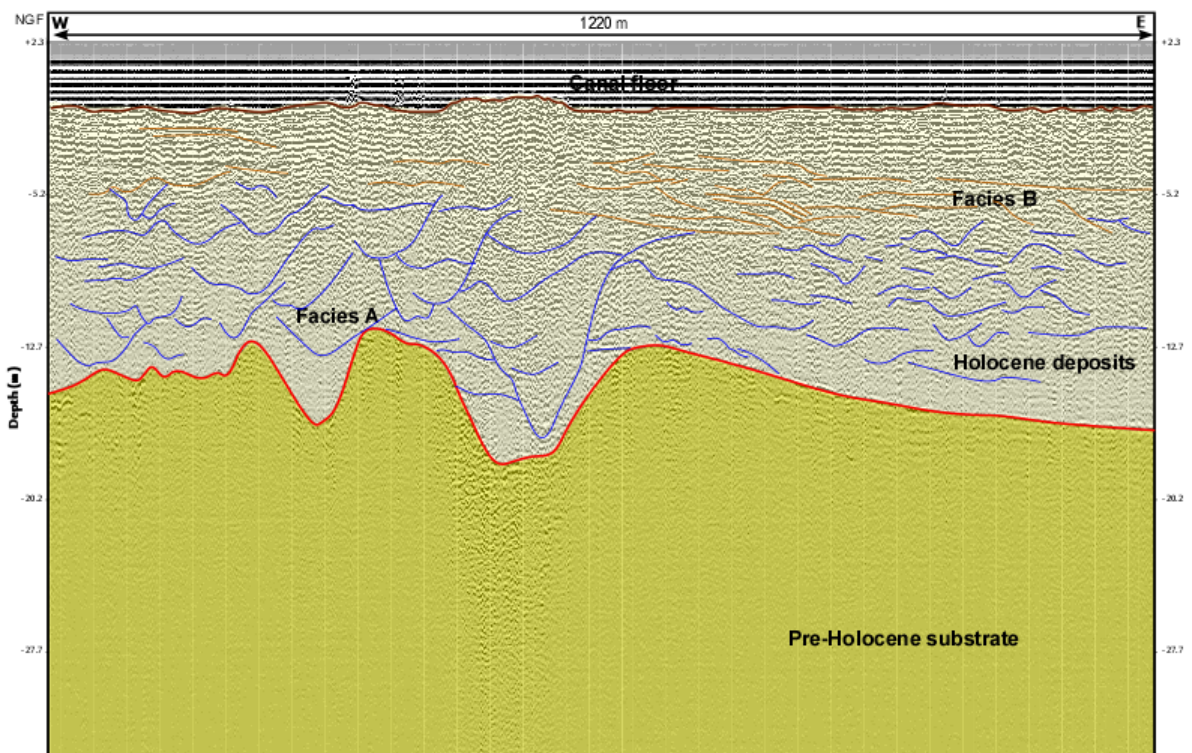
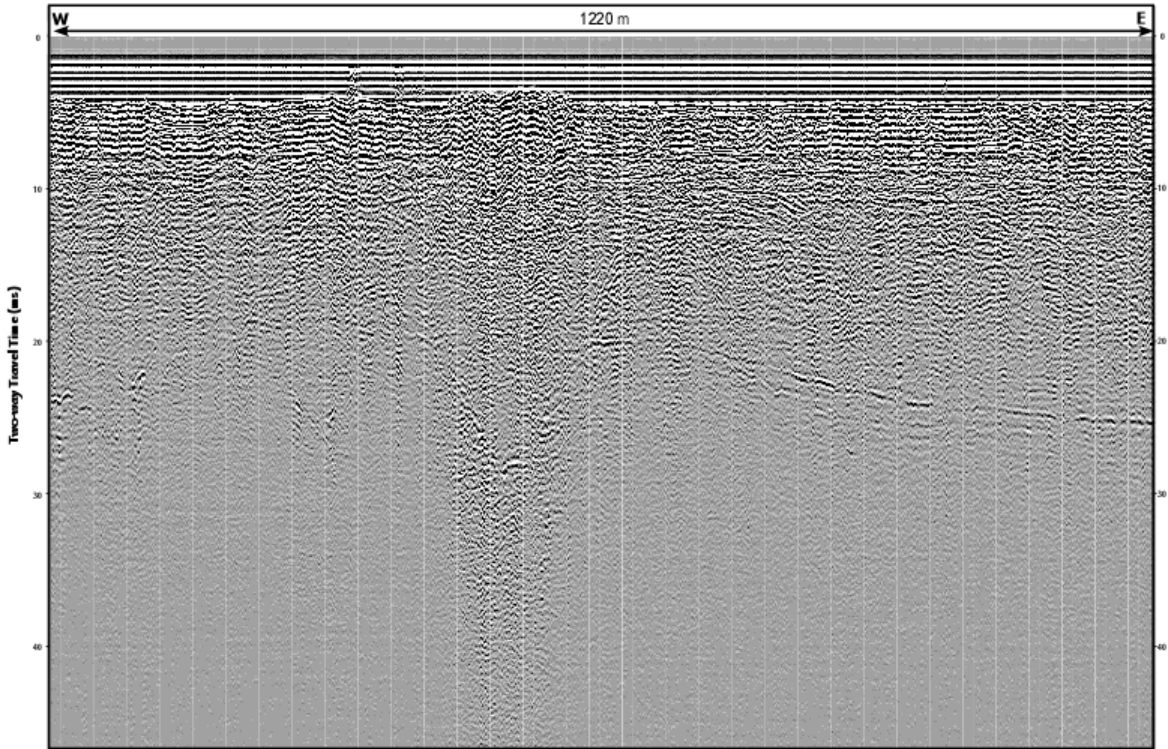


Figure 4.15 – Seismic profile showing more characteristics of the seismic unit and Holocene seismic facies. Above: non-interpreted profile. Below: interpretation of the seismic units and seismic facies described in the Holocene deposits. Holocene deposits present clear incisions into the Pre-Holocene substrate and facies A show deeper channels compared to channels observed in figure 4.14.

Reflectors show low to moderate amplitude and low or very low continuity. Internal reflection configuration exhibits hummocky and oblique patterns that describe sinuous and oblique cut-and-fill configurations respectively. Bottom area becomes concordant or present onlap terminations onto the lower boundary surface. Upper bounding surface is variable and can be merged with the present river floor. It can also be truncated with onlap and concordant terminations by overlying seismic facies B.

The channels present variable vertical and horizontal distribution besides different depths and shapes. Their thicknesses are variable, small thicknesses of 1 or 2 meters will be linked to the channel-fill configuration created by the flow regime and the behaviour of the main-stream system (Figs. 4.14 – 4.15). The coalescence of these channels creates important thicknesses of sand deposits as shown in the same figures. Another type of channels incises deeply the Pre-Holocene deposits. They may reach around 15 m as shown figure 4.16.

#### **4.3.3.2.2 Seismic facies B**

The second seismic facies is limited to the north-central section of the plain, along the Aa river towards Gravelines (Figs. 4.14 – 4.15). It is observed in the upper part of the Holocene unit, overlying the channelized facies A with gently onlapping, downlapping and concordant terminations. The main features of this facies show stratified prograding clinoforms forming a wedge shaped fill.

This facies is apparently thinner than facies A, showing a maximum thickness of 8 m. Reflections show moderate to high amplitude and moderate continuity. The internal character patterns display low angle tangential oblique patterns, indicating slightly dipping seaward reflectors as prograding foresets (Figs. 4.14 – 4.15). Upper bounding surface coincides with the present-day canal floor.

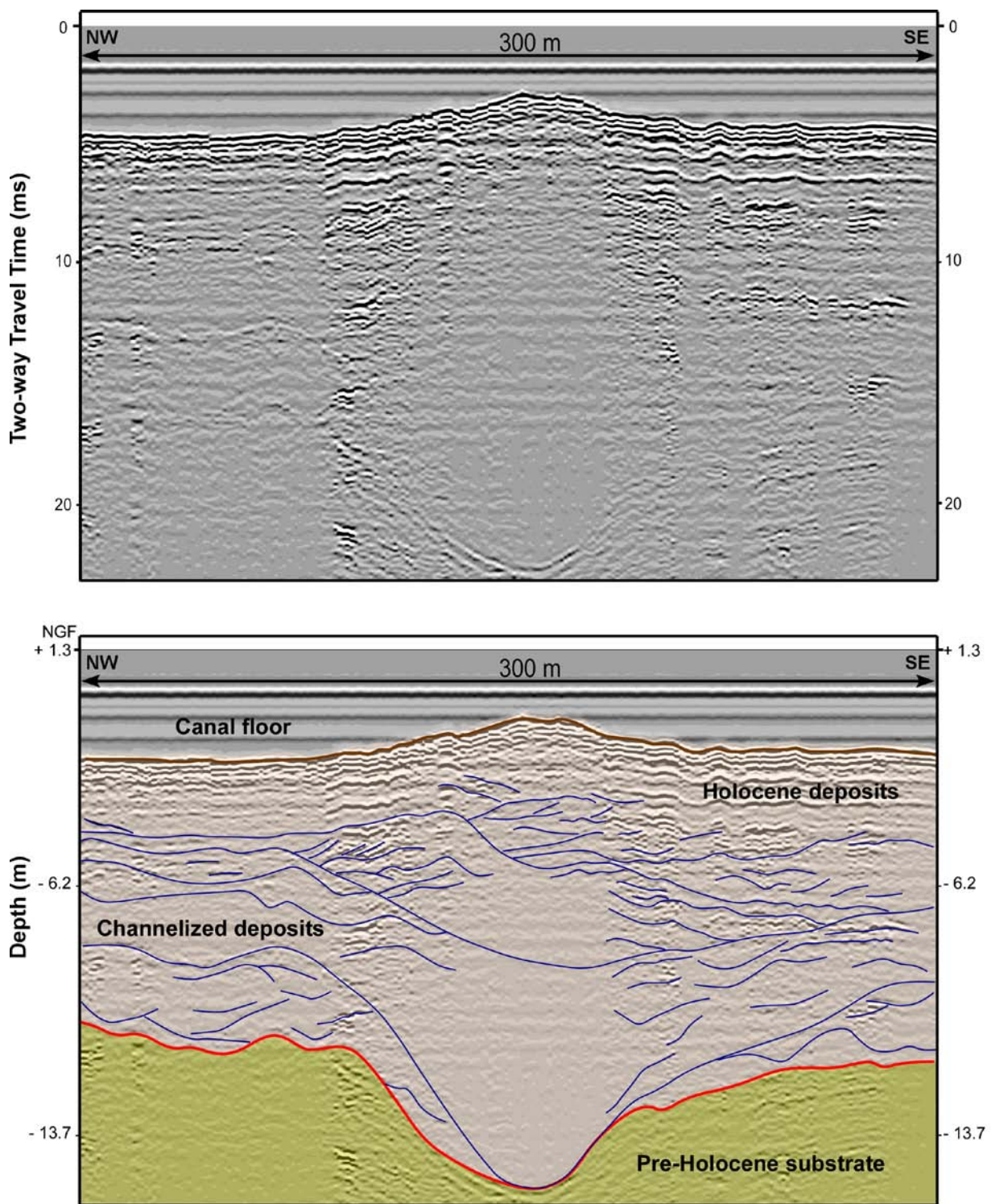


Figure 4.16. Seismic profile showing details of the facies A and its channel fill characteristics. Above: non-interpreted profile. Below: interpretation of the seismic units and seismic facies described in the Holocene deposits.

#### 4.4 Seismic approach to the Holocene sedimentary arrangement

Identification of the different seismic facies and recognition of their geometric-spatial arrangement helps understanding some characteristics of the depositional context of the FFCP. The seismic character and the geometry of reflections reveal some aspects of the dynamic evolution that took place in the area.

According to the outlined seismic units and considering the complex Quaternary geological settings explained in Chapters 2 and 3, an approach to the stratigraphic arrangement can be drawn from the depositional features expressed through the seismic profiles. Using the reflection patterns we defined two seismic units, divided by the Pre-Holocene unconformity: the pre-Holocene substrate corresponds to the acoustic basement of this stratigraphic section and the Holocene deposits the infilling of the shallow palaeotopography, that reach a thickness around 20 m (Fig. 4.10).

Subsurface images show some depressions in the Pre-Holocene substrate representing evidences of the incisions which may be controlled by the lowstand sea level during the last glacial age in the Weichselian period (Lambeck, 1997; Anthony, 2002; Baeteman and Declerck, 2002; Antoine *et al.*, 2003b; Laban *et al.*, 2011) and affect the palaeotopography and palaeodrainage configuration. This period shows a degradation of the landscapes in the entire southern North Sea making them susceptible to erosion (Mellet, 2012).

Subsequently, the post-glacial transgression covered these depressions with marine sediments that came from the southern North Sea being associated with the Holocene sea-level rise and strong tidal currents operating in the area (Jelgersma, 1979; Beets and Van der Spek, 2000; van der Molen and van Dijck, 2000). Fast sea-level rise and sea invasion probably could modify previous morphology of the channels (Brew *et al.*, 2000).

This means that the Pre-Holocene unconformity probably possesses a polyphasic development (Baeteman, 1999), with a time hiatus between the incision and deposition of the Holocene infilling. The morphology expressed at the surface of the Pre-Holocene substrate is a morphological inheritance shaped during the lowstand Weichselian times and the transgression started at the beginning of the Holocene. Some erosional features as small incisions into the Pre-Holocene sediments (Fig. 4.14) could be related to tidal scours generated by the tide-



dominated conditions occurring during the Holocene (Baeteman, 1999; Cleveringa, 2000).

The Holocene deposits unit is characterised by two seismic facies. The difference between their geometries is related with the environmental factors that determine the nature of the infill. Facies A is mainly channelized and extends across the area showing a cut-and-fill configuration interpreted as a result of tidal-channel migration and vertical stacking (Figs. 4.14 to 4.16). Channel-fill sedimentation with different widths and shapes suggests an onshore infill of the estuarine system (Kerr *et al.*, 1999) where the extended geometry could be related with the accommodation space created by the sea-level rise and the important role of the tidal dynamic (Dalrymple *et al.*, 2012).

Channelized facies present low contrasting impedance inferring quite homogeneous sandy deposits, probably related with the broad middle part of the estuary (Yang *et al.*, 2006). They could indicate a consistent energy regime with a complex architecture of sand-to-sand accretion during the shoreline transgression and lateral expansion of subtidal and intertidal environments (Dalrymple and Zaitlin, 1994; Catuneanu, 2006; Dalrymple *et al.*, 2012).

Sinuuous or undulating reflectors are also present in this facies, indicating a lateral variability of depositional conditions (Brown and Fisher, 1980; Zecchin *et al.*; 2009). This type of reflections represents poorly stratified prograding sediments that may be linked with the lenticular to chaotic arrangement of the reflection resulting from the variations in the energy conditions. In the environmental conditions handled during the Holocene in the coastal plain, these reflection patterns could be associated with the control of the hydrodynamics conditions, which induces changes in the energy flux and channels overflows that may be evidenced by interbedded deposits (Brown and Fisher, 1980).

Above this channelized configuration we observed the Facies B. It is characterised by prograding low-angle foresets patterns. Given the flat morphology of the reflection configuration, it is possible to infer a ravinement surface, possibly associated with new marine sedimentation. This new phase may have develop in response to variation in climatic conditions, the energy of sedimentation, compaction, tidal and/or storm scours and smoothly declining rate of sea level stand in late Holocene (Allen, 2000; Anthony and Orford, 2002; Baeteman, 2005a; Long *et al.*,

2006; Mrani-Alaoui and Anthony, 2011). The upper limit coincides with the current bottom sediments of the waterways recently disturbed or dredged by human activity.

To summarize, the relationships established between the Holocene seismic facies can be considered, in essential, as a shallow palaeovalley infill. Reflector characteristics present a vertical stacking that implies at least two phases of deposition which could be compared with the two sedimentary units that we defined for the Holocene deposits of the FFCP. This deposition is complex and is marked by reflector patterns that represent erosion, aggradation, lateral accretion and progradation of sediments bodies within the valley. Seismic configuration could correspond to interactions between the pre-existing topography and the flooding started with the the post glacial sea-level rise. The coastal area was inundated and tidal environments where developed by the interactions of sedimentary processes and slowing sea-level rise.

#### **4.5 Conclusions**

This study describes a new vision of the subsurface of the French Flemish coastal plain from a seismic stratigraphy study testing VHR seismic methods on the waterways. Dataset of the survey show that this technique becomes limited on this type of onshore and human-modified environments. It is difficult to identify several detailed units or to compare detailed lithologies with the Holocene sedimentary facies but it highlighted some major depositional processes in terms of palaeoenvironmental interpretation and of, deposits extension and thickness.

Along the axial Watten – Gravelines (Aa canal) profile, the features of the deposits are strongly influenced by the behaviour of the Aa drainage system, performing the best images of the seismic facies defined in the area. The other branches of the current Aa drainage system (Watten – Calais and Watten – Dunkerque) are quite close to the southern extension of the coastal plain, showing incisions of the small streams and other characteristics associated to the Aa watershed, which were affected by the hydrodynamic conditions during the Holocene evolution. The easternmost profile (Dunkerque - Veurnes) shot parallel to the coastline enhances the characteristics of the Pre-Holocene unconformity but it is difficult to establish some attributes about the Holocene deposits. Last not least, the three next main profiles (Bourbourg canal, Bergues canal and Saint-Omer – Watten

connexion) displayed quite bad profiles, probably due to insufficiently dredging effort and limited size (especially width).

The results confirm the importance of the inherited morphology of the Pre-Holocene unit and climate changes after last glaciation, that strongly influence the Holocene sedimentary infill and its stratigraphic disposition. The shape of the shallow valley has a significant control on the nature and spatial distribution of the seismic facies developed, particularly in the early stages of the infilling when interglacial conditions drove the rapid sea-level rise. The evolution of the seismic facies and their architecture is linked to the contrast of tidal processes and slowing sea-level rise.

The seismic-profile network is insufficient to display all the coastal plain heterogeneities. However, the integration of the contacts, reflector terminations, geometry and internal reflector characteristics suggest that the Holocene infill is not a single depositional interval. Following the displaying reflection features we proposed the idea that it was filled in two intervals. The first interval is dominated by an aggrading channels-fill deposits widely developed in the area and related with the evolution of the main drainage network (Aa watershed) in transgressive conditions. The second interval is limited to the north-central area due to the location of the seismic profiles but it could be more extended along the plain. It is dominated by wedge or sheet shaped deposits that may be linked to prograding deposits representing the last sedimentary cover during the Holocene.

Associations with sedimentary facies were difficult due to the resolution of both seismic facies and borehole data. However, their comparison improves the understanding of the morphodynamic processes and depositional settings during the Holocene. The possibility to combine the main features from both approaches are considered to construct the stratigraphic architecture of the French Flemish coastal plain in the next chapter.



# Chapter 5. Stratigraphy architecture of the Holocene deposits of the French Flemish Coastal Plain

## 5.1 Introduction

Holocene sedimentary succession in the French Flemish Coastal Plain has been interpreted as a tide-dominated coastal system as defined by Boyd *et al.* (1992) and Dalrymple *et al.* (1992). Depositional facies are belonging to estuarine and tidal flats units covering a former shallow alluvial valley. Holocene sedimentary units are closely similar in terms of facies assemblages, but reflect some changes in sedimentary trends, sediment composition and their depositional settings.

In this sense, to show the stratigraphic architecture, a reconstruction using cross-sections over large areas through this wide coastal plain were considered to expose the entire distribution and spatial relationships of the depositional facies, their variability and the control factors operating therein in a regional-scale approach. The cores and borehole data collected, offer the opportunity to delineate each sedimentary unit and to map their changes giving a 2D-3D context.

Cross-sections were chosen in order to obtain a grid covering most of the plain with transects that are perpendicular or parallel to the general flow direction (Fig 5.1). Vertical succession of  $^{14}\text{C}$  dates taken from peat layers, paleosols and mollusc shells precise the time control to determine the temporal changes in the architecture of the Holocene infill. Appendix E indicates the series of radiocarbon ages, dataset sources and distribution in the boreholes we used to precise the correlations.

Subtle changes in lithology and sedimentary components of boreholes reflect the transition between the sedimentary units. This information, combined with a comparison of the seismic stratigraphic criteria (see Chapter 4) and depositional facies succession (see Chapter 3) was used to improve the spatial organization of the sedimentary units, overcoming the difficulty to correlate the variable lithological sedimentary facies and gaining a better understanding of the depositional evolution of the Holocene infill.

The correlations and the diverse features explained in the FFCP give us the opportunity to generate an approach of the palaeogeographic context in which the coastal system was developed during the Holocene. To perform this task, we used

the Pre-Holocene substrate geometry, the available sea level curve (Denys and Baeteman, 1995) and some  $^{14}\text{C}$  radiocarbon dating (Appendix E). We then discuss the relative influence of the different hydrodynamics agents as well as the changes in the interaction between sediment supply and accommodation space.

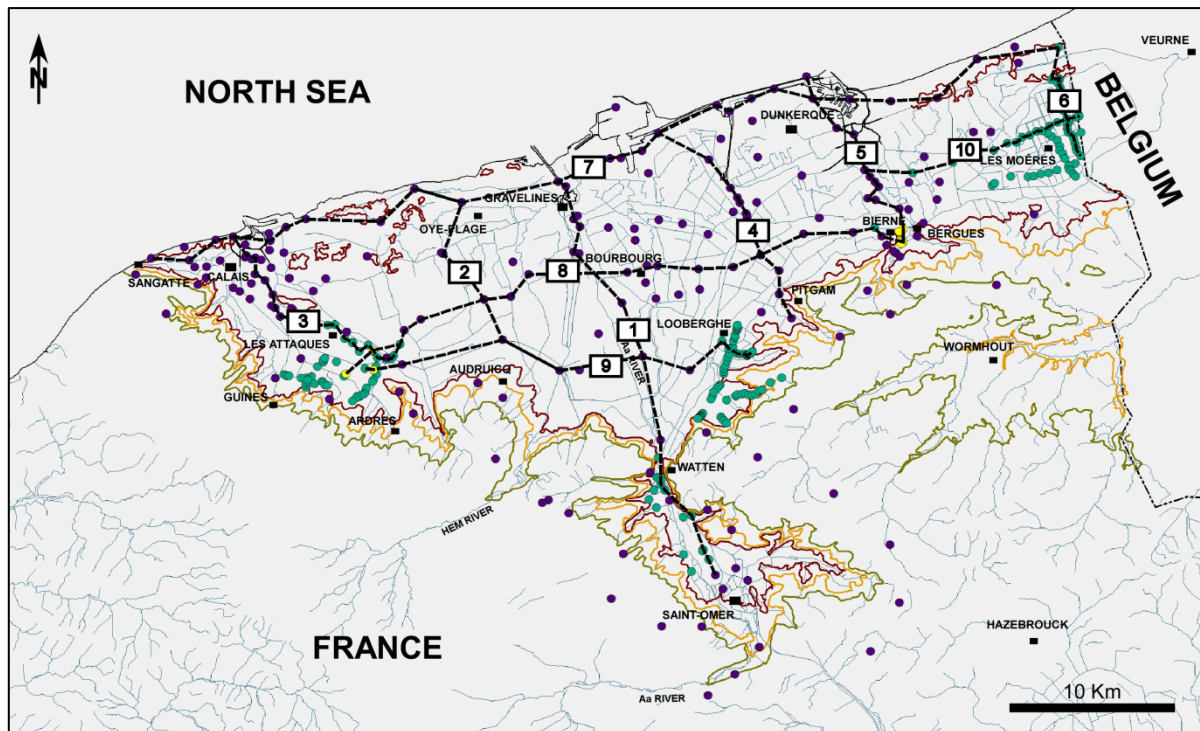


Figure 5.1. Location map of FFCP correlation profiles. Saint-Omer – Gravelines (1), Audruicq – Oye-Plage (2), Les Attaques – Calais (3), Pitgam – Dunkerque Ferry port (4), Bierne – Dunkerque (5), Les Moères – Bray – Dunes (6); Calais – Dunkerque (7); Les Attaques – Bierne (8); Les Attaques – Looberghe (9) and Bergues – Les Moères (10). Names and location of boreholes are shown in the profiles and appendix A.

## 5.2 Stratigraphic framework

Ten (10) cross sections were constructed to reveal the spatial and temporal distribution for the three sedimentary units recognizable throughout the area (Fig. 5.1). Two series of cross-sections were carried out to explore the architecture of the sedimentary units. N-S direction is used to describe these correlations perpendicular to the current shoreline. They were organized from the axis of the coastal plain towards the western and eastern sides. E-W profiles are parallel to the coastline and we decided organize them from distal to proximal. The main characteristics of the Holocene stratigraphy are described below:

## 5.2.1 N-S oriented profiles

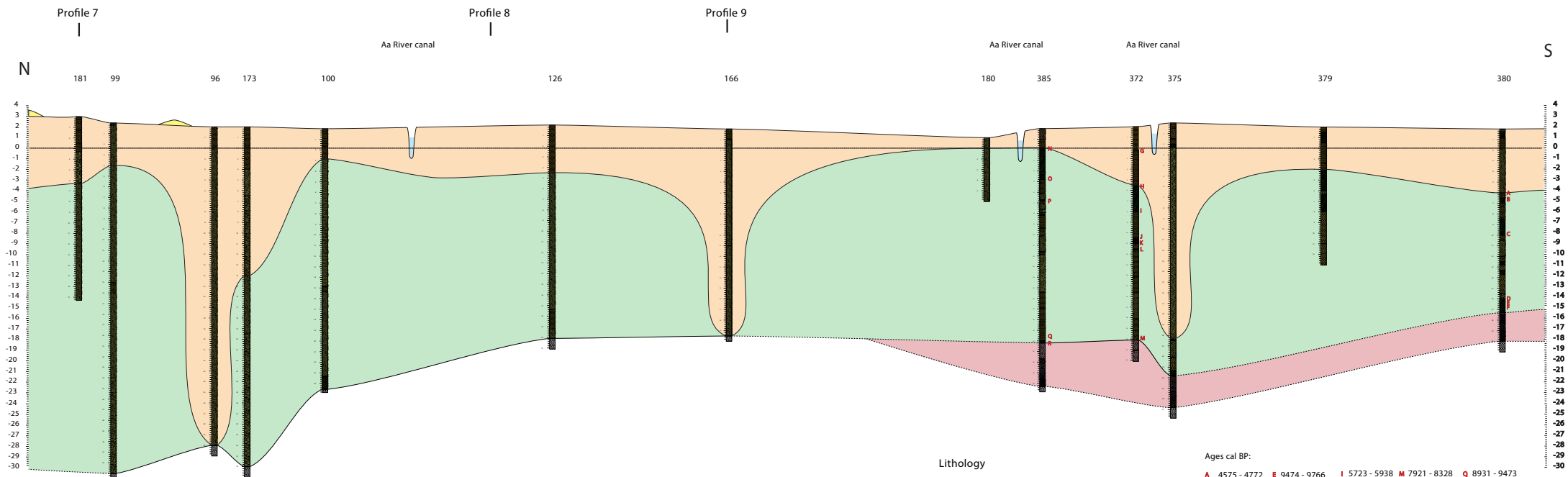
### 5.2.1.1 Profile 1: Saint - Omer – Gravelines

This profile runs through the main axis of the coastal plain and stretches from Saint Omer to the current coast towards Gravelines. It uses thirteen (13) boreholes. This correlation shows a view in dip direction of the distribution of the late Pleistocene deposits and Holocene sedimentary units along the central axis of the valley of the Aa River (Fig. 5.2).

Pleistocene deposits were distinguished in the southern part of the section, between Saint-Omer and Watten. They occupy the lower part of the section underlying the Holocene deposits and capping the Palaeogene bedrock, being the only place of the coastal plain where this subdivision can be clearly distinguished. These deposits represent the main evidence of the alluvial plain which comprise the fining-upward fluvio-lacustrine sediments of late Weichselian age. Their maximum thickness reaches 4.5 m and was recorded in borehole 385.

In this southern part, the Pleistocene unit is capped by the basal organic-rich facies and peat accumulation. This peat layer has been dated between 10508-10875 cal BP and 7921-8328 cal BP and their characteristics represent the gradual change to the initial infill of the Holocene succession. The basal peat layer was preserved and extended in the southern part of the coastal plain while to the northern area it was absent, eroded or replaced by the development of estuarine deposits which become dominant through the entire cross-section.

In the southern part, the estuarine succession shows a transgressive trend with the development of low-energy deposits of mud flats overlying the basal peat and being subsequently covered by sand facies associated to tidal channels. These tidal channels have a gradational shift to dominantly mud flats that were capped by the development of intercalated peat beds, organic-rich muds or a thick surface peat level (maximum thickness around 2 m) showing a fining-upward succession. Estuarine deposits show a vertical change of depositional conditions from intertidal to supratidal (combination of marshes and swamps).



Modern deposits

- Coastal dunes
- Anthropized soil
- Dunes
- Peat behind coastal dunes

Sedimentary unit

- Tidal flat unit
- Tide-dominated estuarine unit
- Pleistocene deposits

Depositional facies

- Marsh/Swamp
- Mud flats
- Tidal creeks
- Tidal channels/Sand flats
- Barrier spit

Lithology

- Peat
- organic-rich mud
- Clay
- Clayey silt
- Silt
- clayey sand
- shelly sand
- Sand

Ages cal BP:

- |                      |                        |                      |                      |                      |
|----------------------|------------------------|----------------------|----------------------|----------------------|
| <b>A</b> 4575 - 4772 | <b>E</b> 9474 - 9766   | <b>I</b> 5723 - 5938 | <b>M</b> 7921 - 8328 | <b>Q</b> 8931 - 9473 |
| <b>B</b> 5659 - 5906 | <b>F</b> 10508 - 10875 | <b>J</b> 7415 - 7577 | <b>N</b> 1999 - 2366 | <b>R</b> 9078 - 9545 |
| <b>C</b> 6493 - 6734 | <b>G</b> 1476 - 1713   | <b>K</b> 7477 - 7671 | <b>O</b> 6313 - 6654 |                      |
| <b>D</b> 8410 - 8609 | <b>H</b> 1693 - 1997   | <b>L</b> 7592 - 7938 | <b>P</b> 6797 - 7279 |                      |

Figure 5.2. Profile 1 Saint-Omer - Gravelines

**PROFILE 1**  
SAINT-OMER - GRAVELINES

1 KM



Organic-rich muds were developed, approximately, since 7592-7938 cal BP and thick peat layers occur from 5723-5938 cal BP. They show variable stratigraphic position; maximum depth can reach -8 m NGF in the southernmost part (Borehole 380) becoming closer to the surface northward (0 m NGF) in surroundings areas of Watten. This peat layer is absent or eroded further North after Watten, where estuarine succession is represented by vertically stacked sand bodies.

In the central and northern part of the profile, the internal geometry of the estuarine unit shows an amalgamated, long system of tidal channels and sand flats. This unit increases seaward where it reaches around -30 m NGF. The sedimentary trends are not evident as well as lithostratigraphic data are usually homogenous which does not allow a clear vision of the internal geometry of the sand bodies. Channelized seismic facies described in chapter 4 (see figures 4.15 – 4.16) gave some clues about the internal patterns of this area, indicating aggrading tidal channels with cut and fill infilling.

The deposits of the estuarine unit in the northern part are overlaid directly by new mud flats and deep tidal channels of the uppermost sedimentary unit represented by the tidal flats unit. This upper unit is broadly extended through the entire section overlying and eroding the previous Holocene estuarine deposits. Its sediments are characterised by mud flats deposits and deep tidal channels; mud flats represent the dominant fill of this succession.

These tidal channels are punctual and repeated from south to north, mostly related with the main channel of the Aa River. They present a narrow and deep geometry that generates variable incisions into the previous deposits reaching depths that affect not only the Holocene, but also the Pre-Holocene surface in some cases.

In the southern area, tidal flat unit is represented by rapid changes between mud flats, main tidal channels and creeks and the development of fresh-water marshes silted up by the muddy deposits. Towards the north it is laterally extended adjacent to the deep tidal channels.

#### **5.2.1.2 Profile 2: Audruicq – Oye-Plage**

This N-S cross-section is one of the western visions of the coastal plain (Fig. 5.3). It is composed of 7 boreholes along a section starting near Audruicq and ending close to Oye-Plage. From south to north the section shows a seaward-thickening

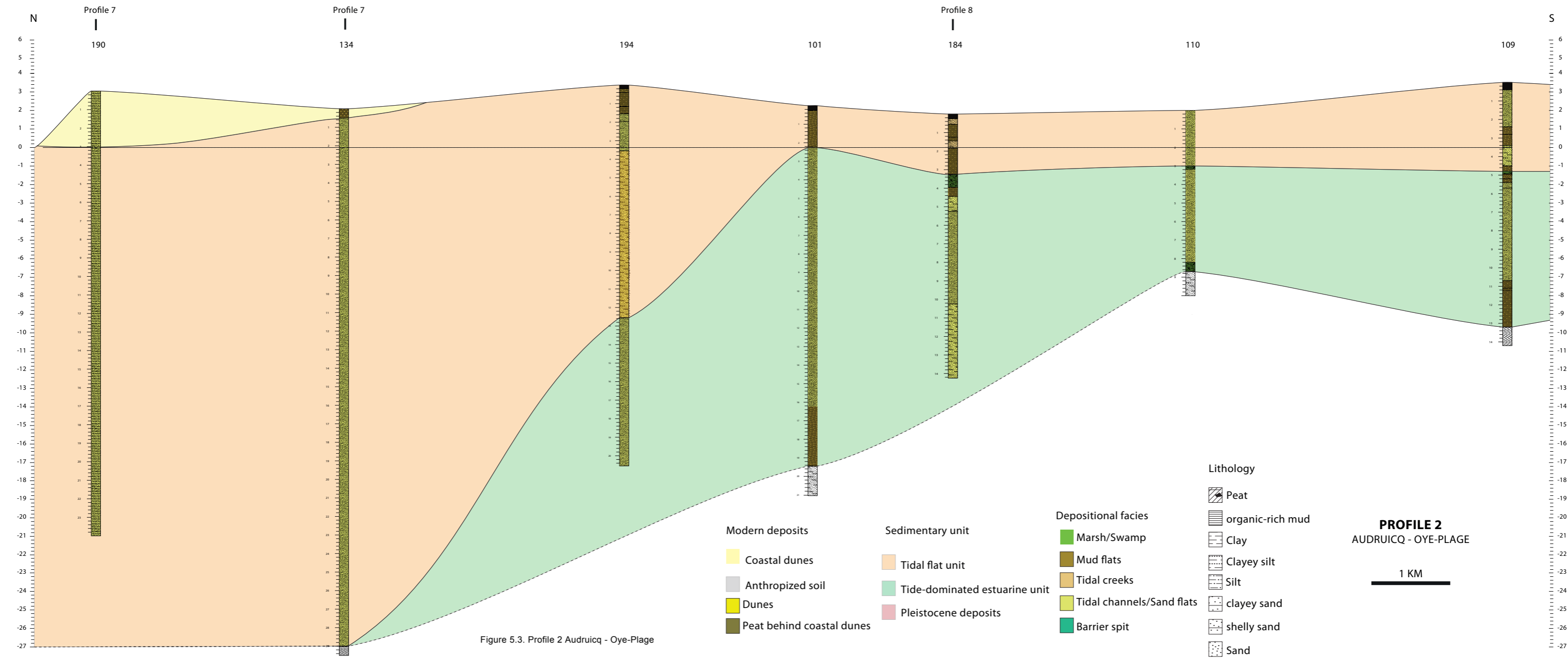


Figure 5.3. Profile 2 Audruicq - Oye-Plage

wedge. The top of the Pre-Holocene surface reaches -7 m NGF in the southern part and is deepening until - 27m NGF seaward. Pleistocene deposits were not differentiated in this profile.

The Holocene succession is directly overlying in erosive contact the Pre-Holocene substrate in the northern part. Towards the south, mud flats deposits (boreholes 101 and 109) and basal peat (borehole 110) shows low energy sedimentation. The most volumetrically significant deposits correspond to the estuarine facies unit. This well-preserved unit shows a sand-dominated package linked to the sand flats and aggrading tidal channels in the middle estuary valley. Towards the south of the section, sand bodies between boreholes 109 and 110 are related to the tidal channels associated to the Hem river drainage. It is also interesting to note that in the bottom of borehole 110 the estuarine deposits are covering a non-dated basal peat, evidence of the previous early Holocene wetland associated to the Hem River.

The estuarine unit is capped by a non-dated thin surface peat unit (< 1 m) between boreholes 380 and 385. As we observed along profile 1, this layer is absent in the northernmost area. The uppermost tidal flat unit covers the entire section overlying the peat unit in the south and resting directly above the thick sand packages of the estuarine unit in the north. This unit mainly presents a low energy deposition setting: mudflats north and shallow tidal channel interbedded with mudflats towards the south.

### **5.2.1.3 Profile 3: Les Attaques – Calais**

It is the westernmost profile of the French Flemish coastal plain. Comprising 21 boreholes this section extends from the Ardres bridge (crossing the canal of Calais – Saint Omer) to the shoreline next to the port of Calais (Fig. 5.4).

The section being a border of the coastal plain presents an elevated Pre-Holocene substrate because of its proximity to the high reliefs that bounded the plain in the western side. The Holocene deposits are relatively thin with an average thickness of 8 m, except in borehole 121 (around 20 m). In this case, it corresponds to a narrow deep depression associated with small streams descending from Artois hills. In boreholes 84 and 171, the thickness also increases. We are there in the northernmost area close to the shoreline where the Holocene base is dipping.

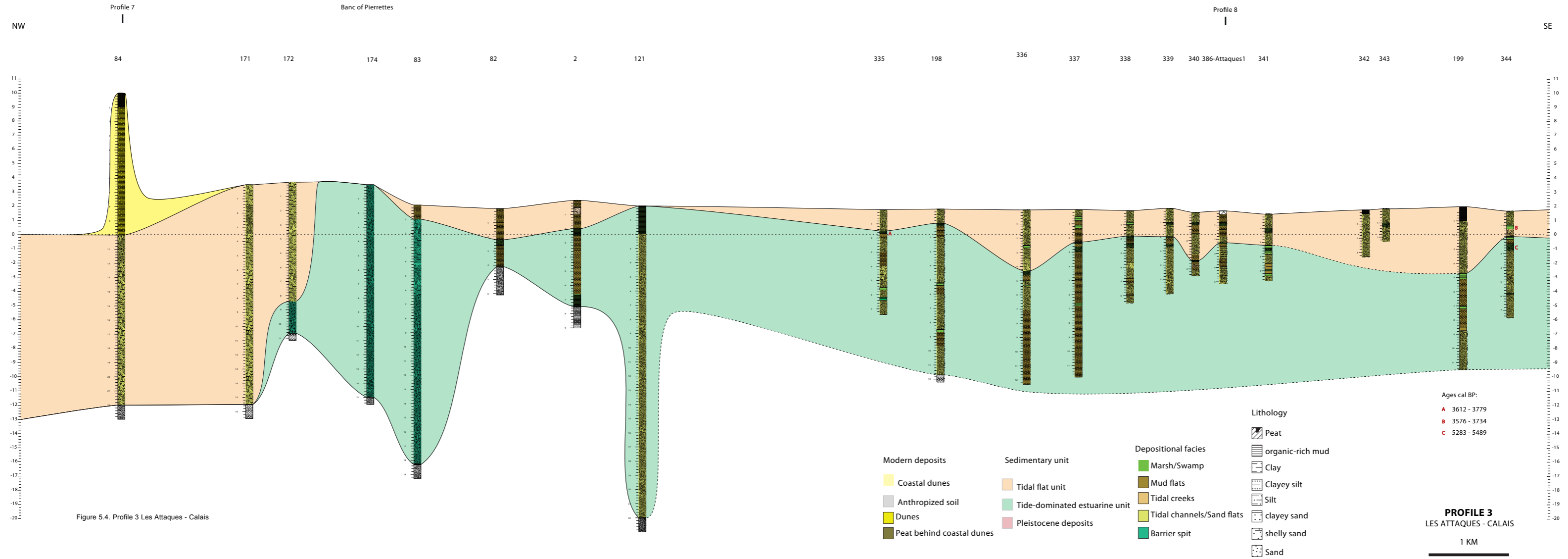


Figure 5.4. Profile 3 Les Attaques - Calais

The estuarine unit highlight tidal flat deposits sheltered by a sand-gravel spit seaward (Boreholes 174 - 83). The gravel spit extends and is recognised only in this profile. It shows that waves strongly influenced the depositional processes and facies distribution in the western side of the plain.

Tidal channels, mud flats and marshes deposits were developed behind the gravel spit, showing fining-upwards trends and being related with the small coastal streams, descending from the Artois hills affected by tidal currents. It is evidenced by channelized seismic facies observed in chapter 4 (Fig. 4.16). In the area, intertidal deposits prevailed until they were filled by supratidal levels with development of peat and organic-rich mud beds, which are spreading regularly behind the gravel bar.

Peat and organic-rich mud beds show a variable morphology and depths (maximum depth -2 m NGF). Their accumulation is well developed behind the gravel spit where it exhibits until 2 m of thickness. Its thickness decreases towards the central area of the section. The base of these organic-rich sediments was dated at 5283-5489 cal BP and 3612-3779 cal BP respectively.

In the upper part of the Holocene deposits, the tidal flats unit occurs along the entire section. In front part and close behind the spit, sand flats and washover deposits were developed respectively. Sand flats occupy the entire Holocene succession in front of the spit showing that the Holocene deposits seawards are associated to the last sedimentary cover of the FFCP. For its part, washover deposits are associated with the breaching of the spit. Southernmost tidal flat unit present a variable organization of mud flats, marshes and tidal channels cutting slightly the previous estuarine units.

At the current shoreline, already modified by the anthropization, a series of coastal dunes cap locally the sand flats associated to the tidal flat unit. They represent a recent morphological feature that generate low-elevated coastlines and a close relationship from the interaction of natural and human factors,

#### **5.2.1.4 Profile 4: Pitgam – Dunkerque ferry**

This cross-section is one of the eastern profiles of the coastal plain. It consists of 12 boreholes from the Pitgam village to the ferry port of Dunkerque located close to Loon-Plage town (Fig. 5.5). In this section the Pre-Holocene surface is the highest (-1 m NGF) and is dipping more abruptly.

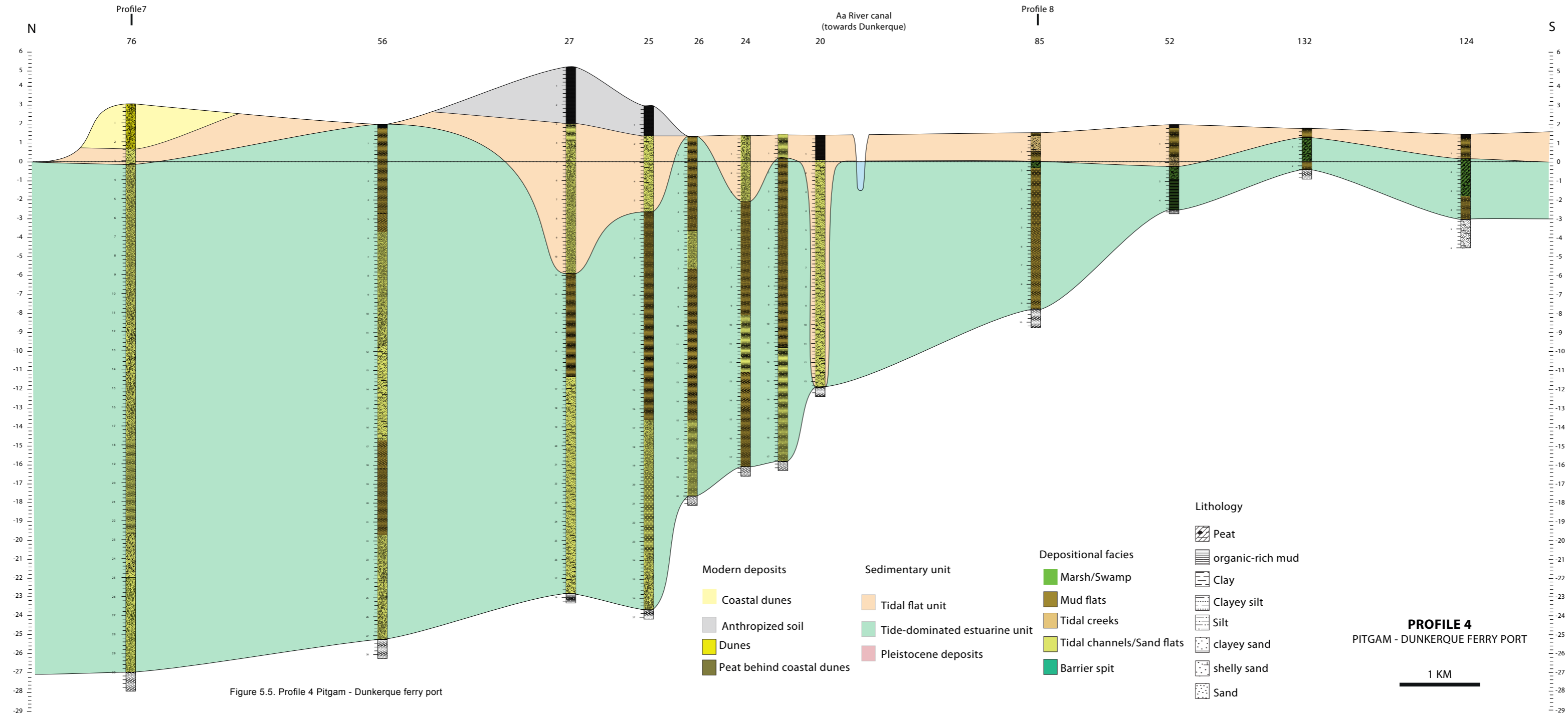


Figure 5.5. Profile 4 Pitgam - Dunkerque ferry port

Similar to profile 2, the section shows a seaward-thickening wedge and volumetrically significant deposits of the estuarine unit overlying the Pre-Holocene substrate. It presents a maximum depth that reaches -27m NGF. The facies assemblage of this first unit is composed by stacked sets of dominant sand bodies of tidal channels and sand flats seaward and mudflats landward.

The dominant sandy deposits are progressively replaced southwards where mud flats prevail. This suggest a progressively change to supratidal levels and a decrease of tidal energy. Mudflats deposits were silted up and overlaid by the surface peat layer. This peat layer grew until 2 m of thickness in the southernmost area of the section. It is extended and decreases in thickness towards the North, where it only corresponds to a thin bed that disappears after the borehole 85. The upper tidal flat unit has some similarities to those presented in the profile 1. Deeply scouring and narrow tidal channels associated with the main drainage of the Aa River incised the previous estuarine deposits.

#### **5.2.1.5 Profile 5: Bierne – Dunkerque**

This section incorporates 12 boreholes from Bierne village in adjacent areas of the Bergues town to Dunkerque port (Fig. 5.6). Southward, the pre-Holocene substrate is relatively near to the surface (-5 m NGF) and gently slopes seaward. The Holocene succession presents a maximum depth towards the north where it reaches -25m NGF in borehole 14.

As along previous profile, the estuarine unit presents changes from lower intertidal to supratidal zones. They exhibit stacked sandy packages in the north while to the south the assemblage is grading to fining-upward trend with small tidal channels separated and covered by mudflats and marsh deposits (e.g. Borehole Bierne 1 and Bierne 7). Mud laminae from the base of these fining-upward deposits were dated 7701-7933 cal BP. A surface peat layer capping the estuarine unit was dated, near the base of the bed, at 4568-4846 cal BP. It develops from the south towards the north, where the intertidal deposit of the upper tidal flat unit interrupts it.

The upper tidal flat unit covers the entire section and is composed of mud flats and shallow tidal channels towards the south and sand flats seawards above the previous estuarine unit. In the northern area, on the top of the tidal flat unit Aeolian

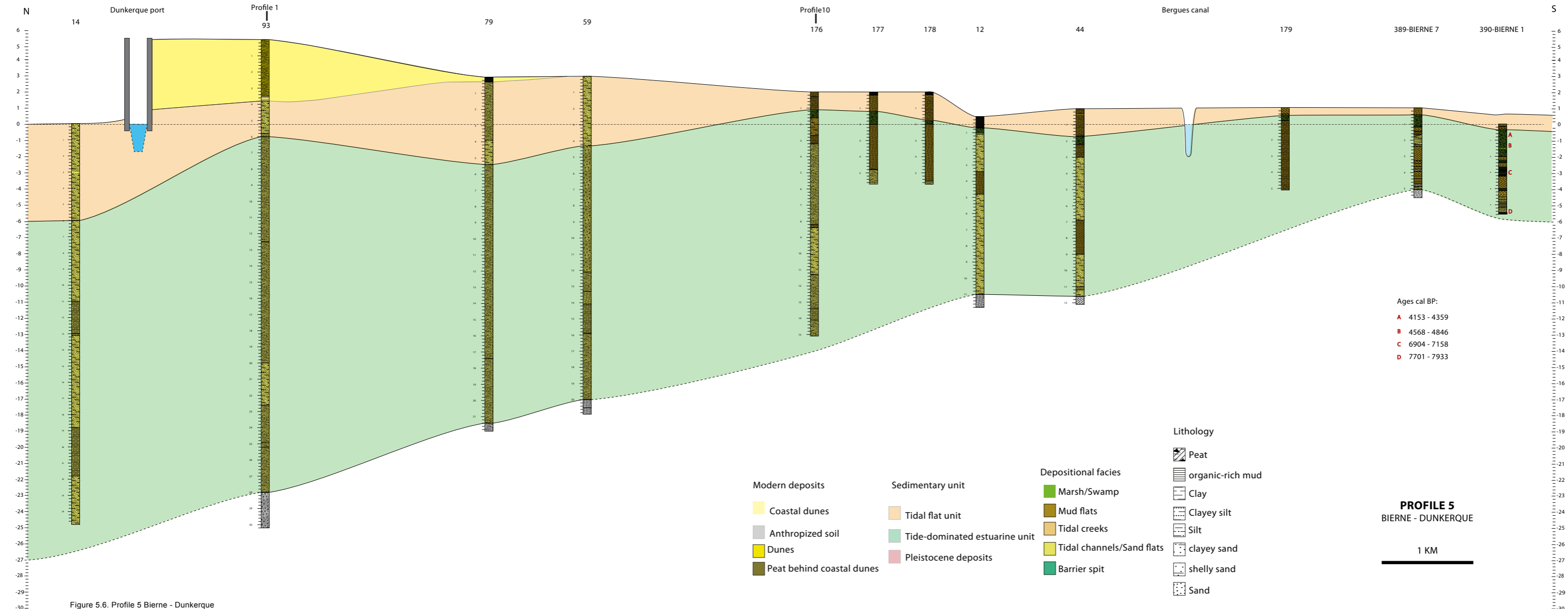


Figure 5.6. Profile 5 Bierre - Dunkerque



deposits are encountered. They are linked to the modern dunes complex extended along the current shoreline.

#### **5.2.1.6 Profile 6: Les Moères – Bray-Dunes**

This is the easternmost profile of the French coastal plain. It runs next to the French-Belgian border along the lowest areas in the coastal plain. It comprises 23 boreholes showing the common seaward-thickening Holocene succession (Fig. 5.7). As previous profiles 4 and 5, the Pre-Holocene substrate is near the surface (-3 m NGF) in the southward area and gently dips seaward.

The borehole data do not reach great depths. The initial Holocene infill begins with the basal peat in landward boreholes and scattered in some other wells in the middle part. Above the basal peat significant mud flats deposits developed and are covered by thin marsh intervals in the southern area. Towards the north the sedimentary succession mainly consists of sand flats deposits. The aggraded mud flats deposits of the southern part were eroded by younger sand flats and/or tidal channels tidal deposits belonging to the upper tidal flats unit which is extending and affecting the previous Holocene deposits along the entire section. Shells in living position from these new sandy deposits (Mrani, 2006) were dated in borehole 329 and given ages around 3442-3642 cal BP.

Surface peat unit expressed in the other profiles is absent in this section. However, in the northern part a thin sandy peat layer is developed overlying the sand flats deposits of the estuarine unit. This peat layer, mentioned as “peat behind dunes” (Mrani, 2006; Dewaide, 2007) has not been dated but is possibly associated with the formation of the inland dunes observed in the northern area. The development of the dunes is dated from a paleosoil in borehole 332 that indicates an age of around 3462-3635 cal BP and could be related to the development of the upper sand flats also dated with similar ages.

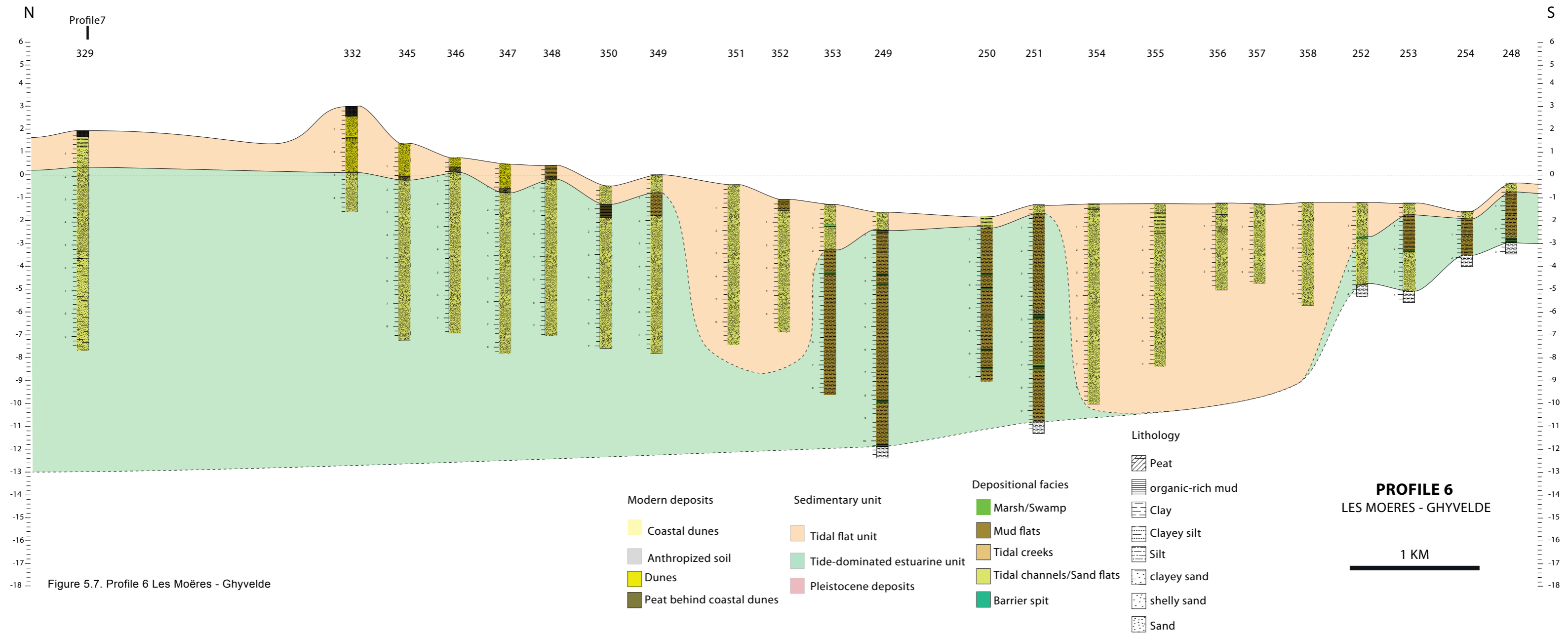


Figure 5.7. Profile 6 Les Moères - Ghyvelde

## 5.2.2 E-W oriented profiles

### 5.2.2.1 Profile 7: Calais – Dunkerque

Oriented perpendicular to the general flow direction this profile is located close to the current shoreline of the coastal plain. Using 23 boreholes, the section shows the outer visual of the architecture of the Holocene sedimentary units (Fig. 5.8).

The pre-Holocene substrate underlies and bound the Holocene succession showing a variable paleo-topography. The morphology of the pre-Holocene surface presents an extended depression which forms a wide valley in the eastern area. Towards the western part, the topography tends to decrease in depth and presents some small and narrow depressions. These valley shapes could be related with the main branch and network of the of the Aa-Hem river system. As a function of the previous morphology, the Holocene succession is variable and can reach a thickness of 34 m.

Holocene infilling highlighted a series of stacked sand packages of tidal channels and sand flats of estuarine unit and tidal flat units. Peat layers in this section are absent. The vertical and lateral expansion of the estuarine unit shows the aggrading sand bodies of grey-bluish sand which were explained in chapter 4 that filled the available accommodation space created at the begins of the Holocene. These deposits are scattered and mainly preserved in the eastern part of the cross-section. In the rest of the area, they were affected by the upper tidal flat unit,

The upper tidal flat unit shows deep tidal channels and sand flats deposits, which eroded and reworked previous Holocene deposits and reaching pre-Holocene substrate. This unit presents a large volume in this profile showing the domination of marine dynamic processes acting in the stacking and distribution of the sand deposits. Deep and narrow incisions are observed in the central part of the section, as seen in previous profiles. They are possibly related with the main Aa River channel network.

The last sedimentary cover observed in the cross-section corresponds to aeolian sediments commonly displayed along the current shoreline and associated to the modern coastal dunes.

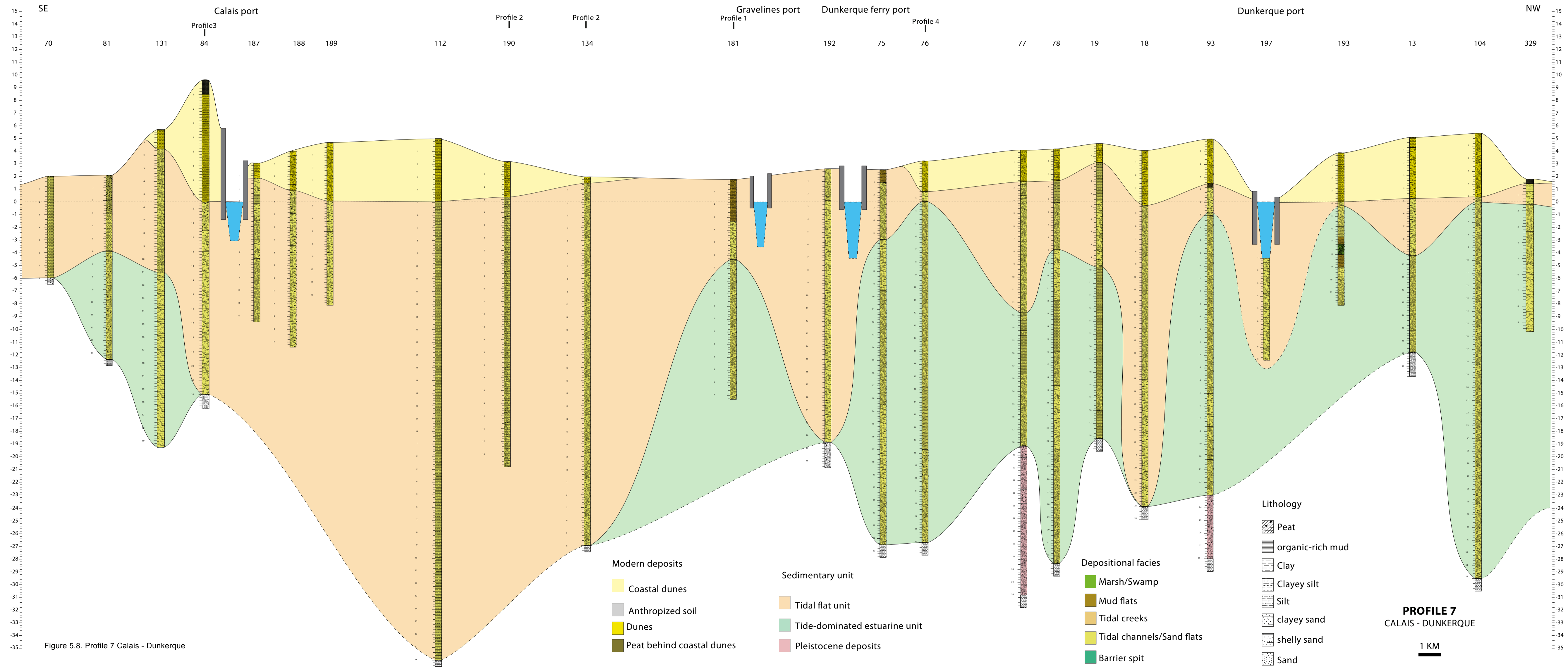


Figure 5.8. Profile 7 Calais - Dunkerque

### **5.2.2.2 Profile 8: Les Attaques – Bierne**

This profile is made of 18 boreholes (Fig. 5.9). It crosses the central part of the coastal plain and display some interesting characteristics explaining the arrangement of the sedimentary units and their spatial distribution.

The transversal positions of the section allows to observe a pre-Holocene substrate forming a wide and shallow valley with a maximum depth -17 m NGF in the axial part of the sections; and decreasing towards the borders responding to the landward enclosure of the coastal wedge.

Pre-Holocene deposits are covered by the extended estuarine unit. This unit shows the vertical and lateral expansion of the estuarine unit with an aggrading channel-belt infill in the central part of the section. This channel belt is laterally extended grading to mud flats interbedded with small channels that flanked the elongated sand bodies. Mudflats are capped at both sides by the surface peat layer; this peat layer is dated between 5283-5489 cal BP (west side) and 4568-4846 cal BP (east side) in their base. In the central part, the surface peat layer is absent and the upper tidal flat unit, which have been developed along the entire section, directly overlies the estuarine unit.

The upper tidal flat unit is composed of mud flats overlying the stacked sandy bodies of the central estuarine valley. To the west and east sides mud flat were cut by tidal creeks and small tidal channels, the morphology of deep tidal channels or strong incisions associated with the main drainage of the Aa river is not well expressed on this section.

### **5.2.2.3 Profile 9: Les Attaques – Looberghe**

It is located south of Profile 8, and goes from Les Attaques to Looberghe. A total of 19 boreholes were used to construct the section (Fig. 5.10). It displays deposits of the pre-Holocene outcrop at the east side and gently dips westward. The central part displays a valley shape reaching -17 m NGF. It then begins to rise towards the west until -8 m NGF and stays flat to Looberghe.

The Holocene succession in this cross-section starts with a dispersed basal peat observed in some wells to the east (boreholes 285, 286 and 288) and in

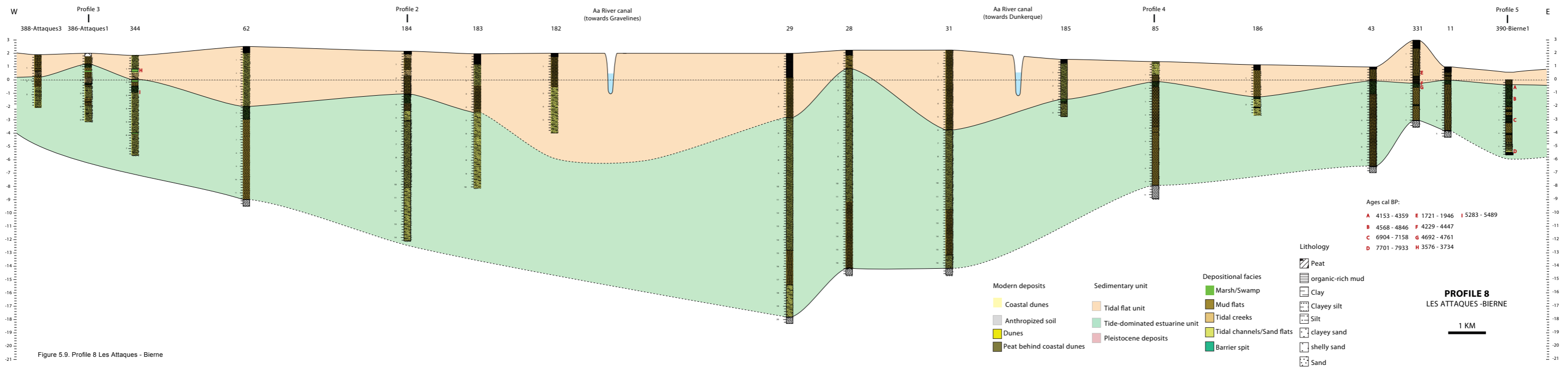


Figure 5.9. Profile 8 Les Attaques - Bierre

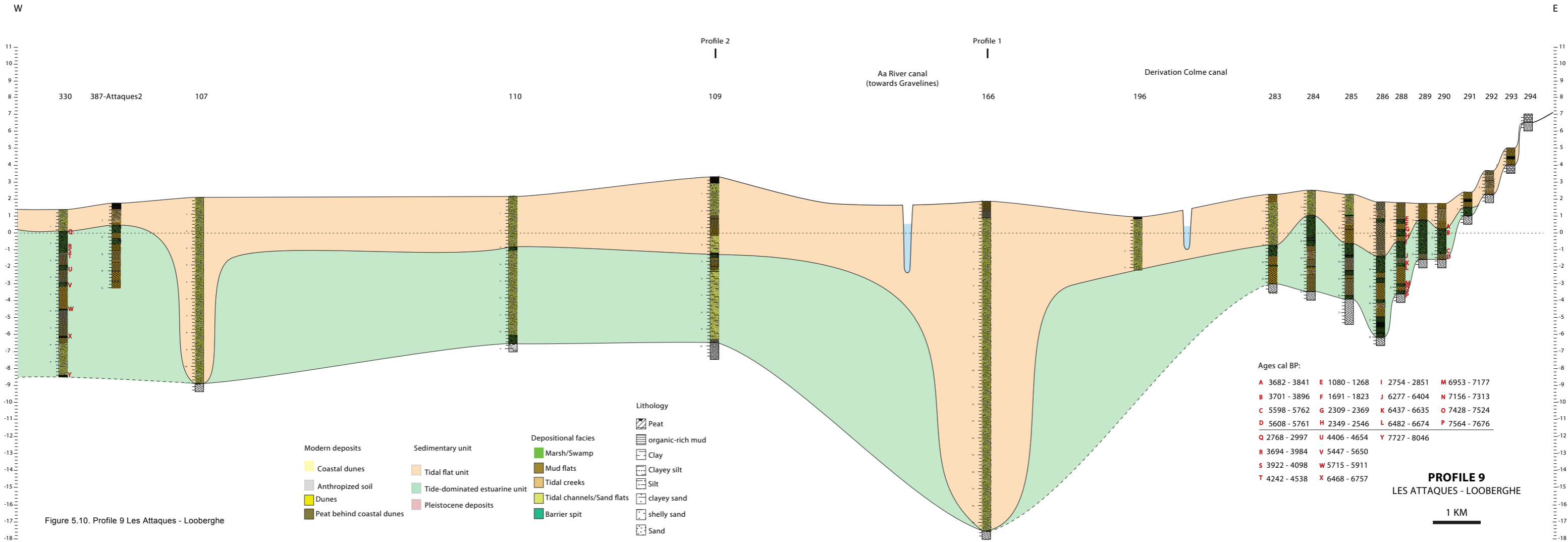


Figure 5.10. Profile 9 Les Attaques - Looberghe

borehole 330 at the west side. East side displays an age of 7564-7676 cal BP, fairly similar to the basal peat from the west side, dated at 7727-8046 cal BP.

Subsequently, the estuarine unit presents some characteristics in its facies succession that resembles the profile 8. Tidal channels/sand flats deposits dominate the central part of the shallow valley and are associated to the main drainage system while intertidal flats correspond to the development of small tidal channels and mud flats flanking these sandy deposits.

The surface peat layer silted up intertidal deposits of both sides. In the east side, peat layers are particularly thick and numerous. They are indicative of an area with usually supratidal conditions, constantly vegetated and which has been sheltered from the tidal floods. Significant accumulation of peat beds, as seen in boreholes 289 and 290, show a maximum thickness of 2 m. Variable stratigraphic position and decrease of thickness is observed from the borders towards the central part overlying the sandy deposits. The base of the thick surface peat layer begins at 6277-6404 cal BP (Borehole 288).

In the western side, the surface peat layer presents an age of 4242-4538 cal BP and largely extend from the border toward the central part where it turns to thin until the upper tidal flat units and estuarine unit interrupt it by the coalescing tidal channel complexes.

The extended upper tidal flats unit overlies the estuarine deposits. It shows a good development of deep tidal channels, sand flats and mud flats covering the previous estuarine deposits. Development of deep tidal channels is observed in the central and western part of the section, deeply scouring and reaching the pre-Holocene substrate. Adjacent to these tidal channels the intertidal deposits dispersed along the cross-section are widely developed.

#### **5.2.2.4 Profile 10: Bergues – Les Moères**

This E-W oriented cross-section reveals the easternmost distribution of the sedimentary units from Bergues to the central part of Les Moères thanks to 16 cores. It also expresses the topographic change between the average level of the French coastal plain and the low-lying area of Les Moères (Fig. 5.11).



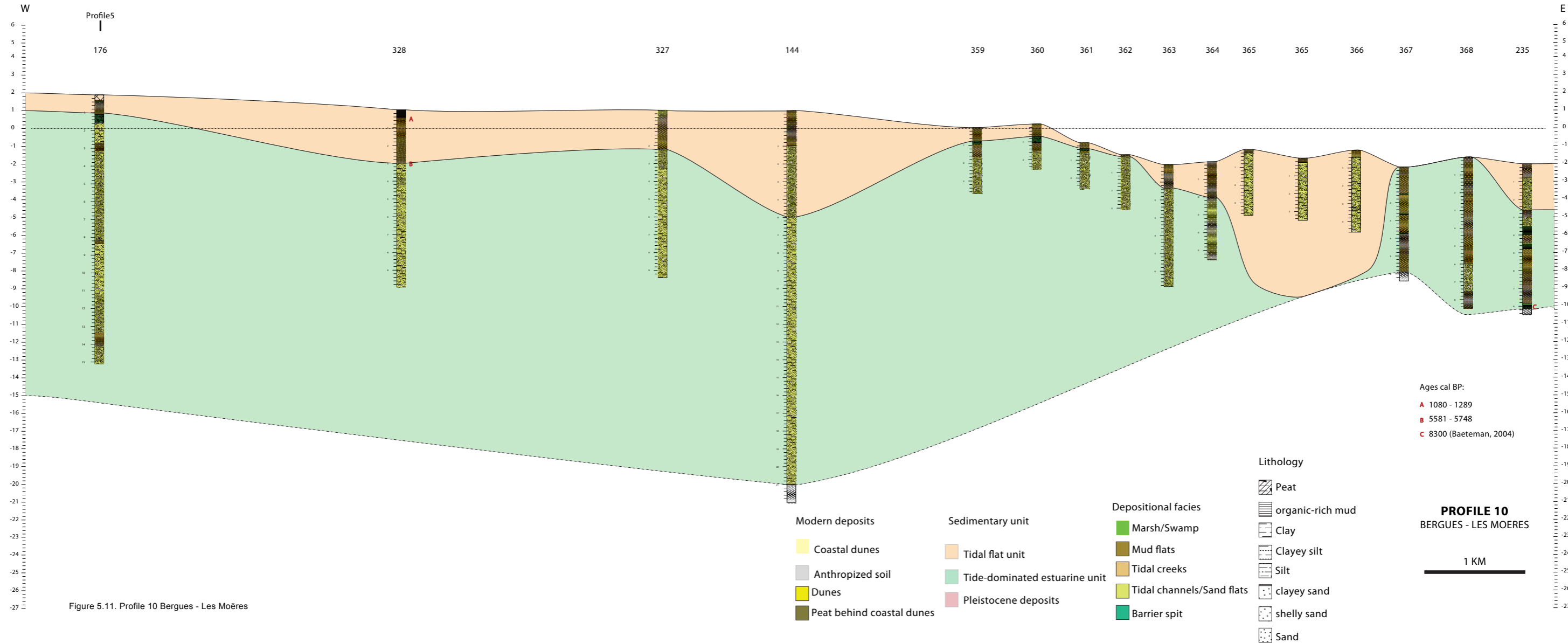


Figure 5.11. Profile 10 Bergues - Les Moères

The pre-Holocene substrate illustrates the same characteristics displayed by the other eastern profiles. It is shallower (maximum depth of -18 m NGF) than in the central and western profiles in their seaward position.

The Holocene succession begins with the estuarine unit, mainly composed by small tidal channels and sand flats deposits developed in the central and western parts of the section and which changes laterally to mudflats and tidal creeks in the central part of Les Moères. Mud flats in Les Moères developed over thin basal peat accumulations only preserved in the easternmost part of the profile at the Belgium border.

Towards western part of the section, the sand deposits show fining-upward patterns, filling up by thin deposits of the surface peat. This surface peat is not observed in boreholes of the central and eastern part towards Les Moères. Above these units the tidal flat unit with new mud flats and sand flats developed. It covered and eroded the previous intertidal deposits associated to the estuarine unit. The sand flats deposits that occur in Les Moères area erode the previous mud flats infill while outside, in the central and western part of the section mudflats and tidal creeks developed overlying the previous thick sand flats deposits.

## **5.3 Discussion**

### **5.3.1 Stratigraphic architecture depositional history of FFCP**

Longitudinal and transversal profiles illustrate the sedimentary units and the organization of depositional facies along the coastal plain, allowing to reconstruct the regional sedimentary environments and to explain their evolution. The sedimentary units from base to top, recording the Holocene evolution of a coastal prism that switches from alluvial valley to transgressive and vertical accreted estuarine deposits and to coastal progradation and expansion of tidal flats (Fig. 5.12).

Considering their spatial distribution and comparing with the characteristics of seismic facies, the two sedimentary units perform the regional Holocene sedimentary arrangement. A lower estuarine unit and an upper tidal flats unit, as a response of sea-level rise, accommodation space variations and interaction of hydrodynamic processes represent them. The stratigraphic architecture is presented in figure 5.13.

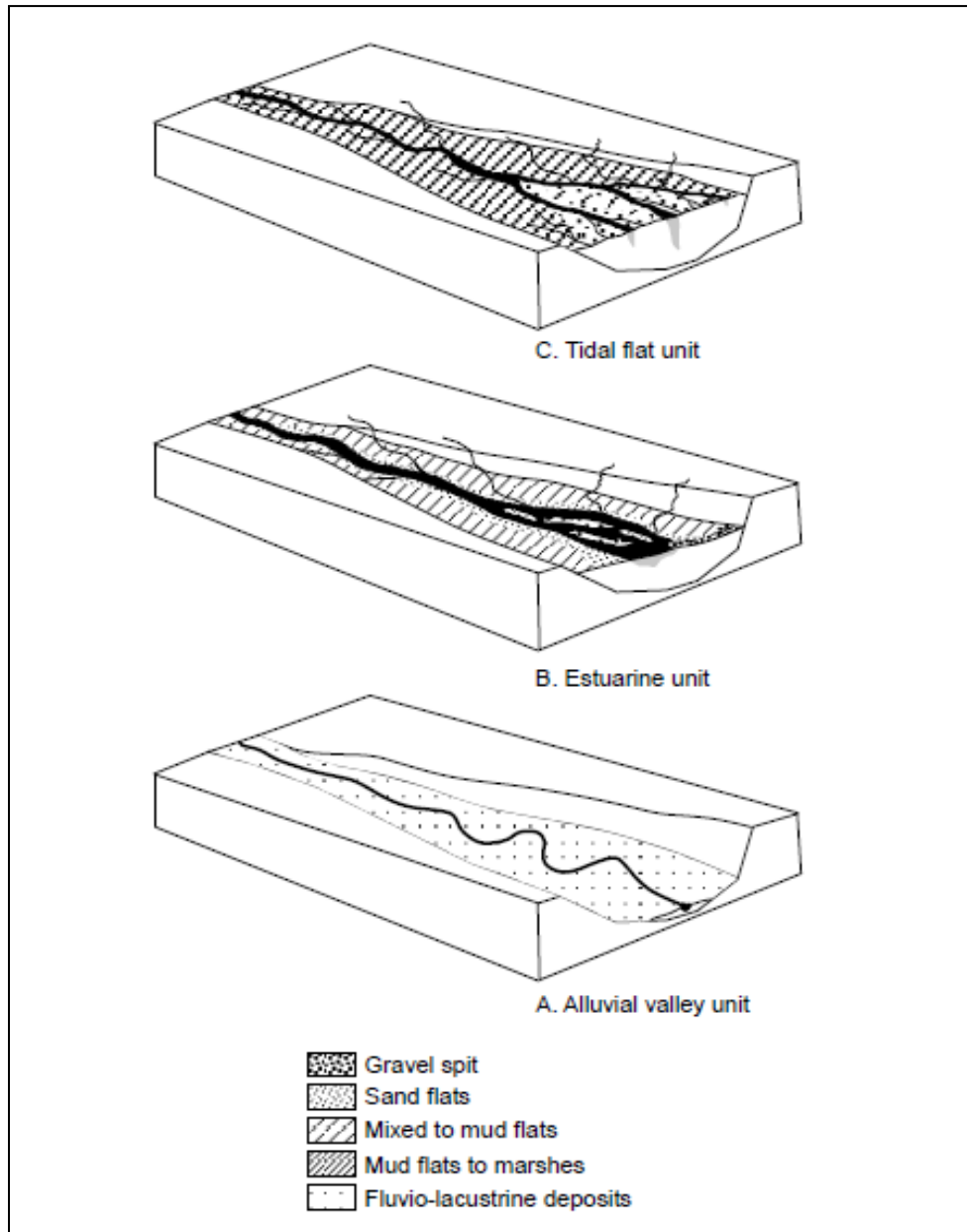


Figure 5.12. 3D blocks of idealised coastal depositional environments interpreted into the FFCP. From base (A) to top (C) the vertical succession of sedimentary units and evolution of the coastal system. (Adapted and modified after Plink-Björklund, 2005 and Dalrymple and Choi, 2007).

Estuarine unit is widespread along the entire area of the FFCP; it is well developed and preserved landward (Fig. 5.13). It is linked to the rapid sea-level rise at the beginning of the Holocene that creates a great accommodation space available for sediments mostly of marine origin. The palaeotopography played a fundamental role in the distribution of depositional facies during these transgressive conditions. Some organic-rich facies of this unit were dated and present similarities in their ages of accumulation but variable stratigraphic position. They can be influenced by the morphology of Pre-Holocene surface and the action of compaction which affect the final stratigraphic arrangement.

The characteristics of sedimentary development are described as aggradation of a combination of sand flats-tidal channels, mud flats and marsh-swamp facies (see figures 3.8 – 3.9 in chapter 3) which were developed along the margins that flanked the sand-dominated axial network of the Aa-Hem River system. Sand flats/tidal channels facies dominated the axial zone and are equivalent to seismic facies A (See figures 4.14 – 4.15 in chapter 4).

Tidal flats unit represent a change in depositional setting of the coastal system (Fig. 5.13). Due to low accommodation space, peat developed in the most internal zones and sediment deposition occurs seaward, indicating an infilling dominated by progradational trends. Seismic facies B can show part of the prograding features of this unit (See figures 4.14 – 4.15 in chapter 4).

The action of tidal channels incised along the main branches of the active drainage system (Aa-Hem River system) and reworked previous deposits, affecting the estuarine unit and eventually the Pre-Holocene deposits. Depositional facies of this unit are represented by sand flats-tidal channels and mud flats facies on the flanks. They cover the upper part of the Holocene deposits (See figure 3.8 in chapter 3) and are influenced by marine sediment supply and some contribution, at least for the clay fraction (See figure 3.10 in chapter 3), of mainland reliefs carried by the river system.

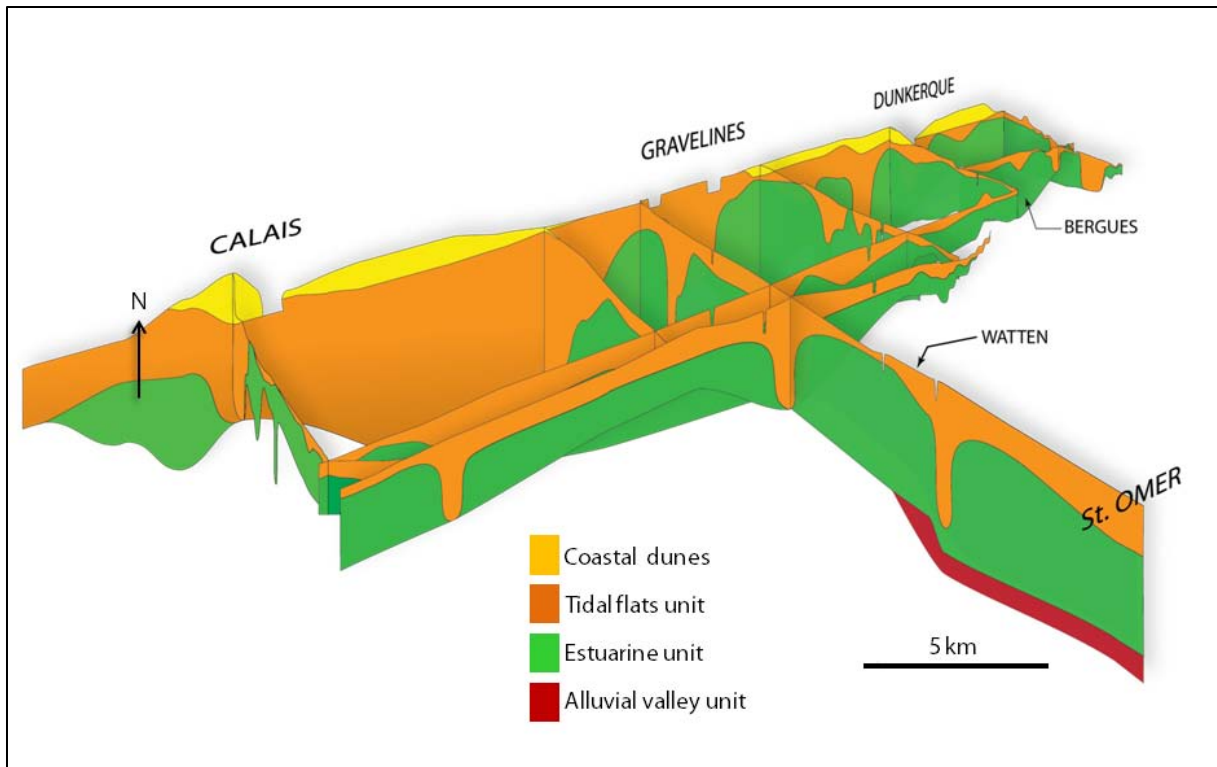


Figure 5.13. Fence diagram giving a simplified regional picture of the 3D vertical and lateral stratigraphic relationships between Holocene sedimentary units of the FFCP. For location see figure 5.1.

### 5.3.2 Depositional history of French Flemish Coastal Plain

The shape of the pre-Holocene substrate gives some clues for the shallow paleovalley of the French coastal plain (Fig. 5.14). The valley shape is associated with the ancient fluvial network of the Aa-Hem River system and some other more modest coastal streams that contributed to the local drainage, mainly from the western highlands of Artois hills. The morphology of the paleovalley responds to the low sea level and the regional environmental conditions controlled by climatic factors during the Weichselian last glacial period in north-western Europe (Lambeck, 1997; Anthony, 2002; Antoine *et al.*, 2003; Ehlers *et al.*, 2011; Laban *et al.*, 2011).

In this sense, we suggest that the paleovalley of the FFCP being part of a series of paleovalleys developed along the eastern side of the southern North Sea as the Ijzer valley in Belgium (Baeteman and Declerck, 2002; Baeteman, 2005a) or the large Rhine-Meuse system in the Netherlands (Beets *et al.*, 1992, Donselaar and Geel, 2007).

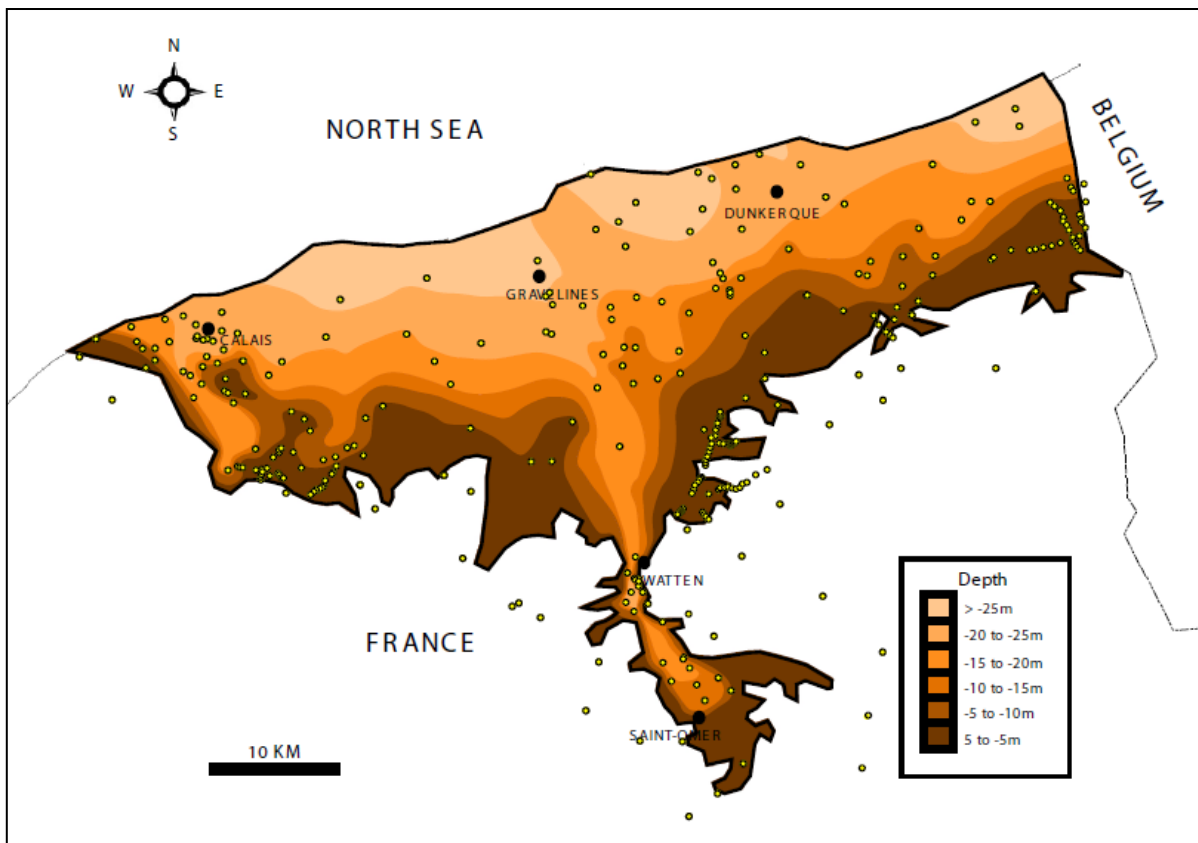


Figure 5.14. Pre-Holocene surface obtained from boreholes and seismic data. Contour interval 5 m relative to NGF.

### 5.3.2.1 Late Pleistocene to early Holocene

Fluvio-lacustrine sediments of the alluvial plain unit developed during the late Weichselian or *Tardiglaciaire* and earliest Holocene. This represents the first infill covering this shallow valley morphology (Fig. 5.15). In terms of sequence stratigraphy these deposits could reflect a lowstand fluvial profile as explained Allen and Posamentier (1993) and Boyd *et al.* (2006) that was flooded and scoured during subsequent transgression.

Due to the erosive action of post-glacial marine transgression (Jelgersma, 1979; Beets and Van der Spek, 2000) most of these deposits were eroded, especially, in the outer part of the plain and were replaced and later covered with estuarine and tidal flats deposits (Profile 1). Some of these characteristics could be illustrated in the seismic lines where incised Pre-Holocene surface can also be modified by following erosive features (see figures 4.12 - 4.14 in chapter 4). Likewise, a great part of boreholes through the wide plain present in the subsurface the

Holocene deposits directly overlying Cretaceous and Palaeogene rocks (BRGM, 2014) lacking the Late Pleistocene deposits.

Fluvio-lacustrine sediments were only preserved in the inner part of the coastal plain associated with the paleothalweg of the Aa River (Profile 1) and in sheltered areas on the sides of the coastal plain where lithology of pre-Holocene substrate is distinguished as Pleistocene deposits. The main remnants of these deposits are located towards the western corner between Audruicq and Guines, and close to the French-Belgian border.

Some other witnesses of the fluvial drainage could be observed offshore when processing bathymetric data (see figure 2.7 in chapter 2). These locally empty paleovalleys possibly indicate that during the transition from the late Pleistocene to Holocene period, the fluvial Aa-Hem system extended along all the plain but also further North, when the shoreline was some kilometres away associated to the English Channel downstream fluvial drainage system (Busscher *et al.*, 2007; Gibbard, 2007).

Organic-rich facies at the base of some boreholes marks the beginnings of the Holocene infilling. They were preserved in the inner part of the estuary (Profile 1) and extended to the borders where low energy environments dominated (Profiles 6 and 9). Oldest ages around 10500 cal BP obtained in these deposits and pollen assemblages mentioned by Van der Woude and Roeleveld (1985) and Sommé *et al.* (1994) (for details of these deposits see organic-rich facies in chapter 3) expressed their development in the fluvial network affected by the action of transgressive flooding.

The groundwater level rose since the influence of sea-level rise and vegetated areas were constantly fed by water. The features of these accumulations changed and marine influence increased that allow us infer an area more connected with the seaward conditions. This change is documented in the characteristics of the sediments showing marine-influenced and salinity optima species of flora over more continental species as explained by Sommé *et al.* (1994). Some similarities were evidenced for the same level using flora for the Seine estuary (Huault and Lefebvre, 1974) and using diatom proxy in the Belgian coastal plain (Denys, 1999).

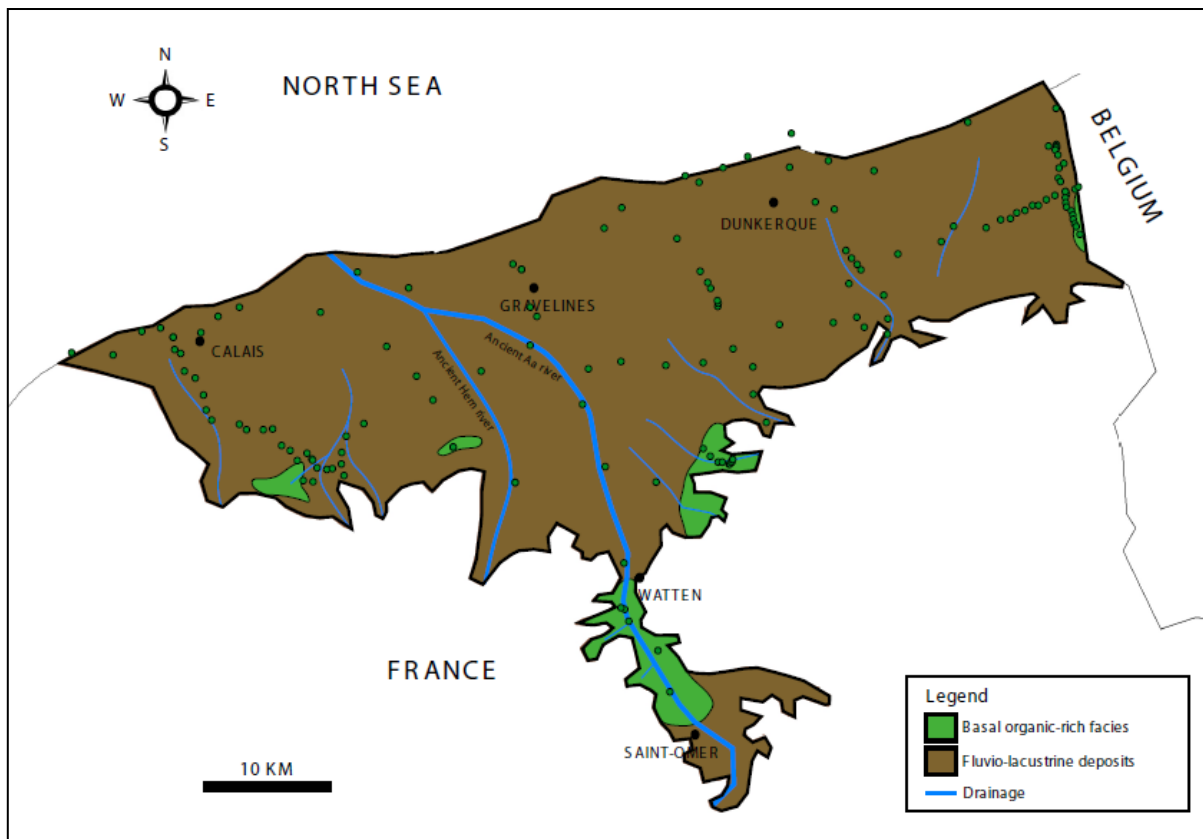


Figure 5.15. Early Holocene around 9000 (MSL around -17m NGF). It shows the dispersed distribution of organic-rich facies included basal peat accumulation. The position of the main Aa River and the other small coastal streams were inferred from the morphology of the Pre-Holocene surface and valleys observed in the profiles. Shoreline should be some kilometres offshore than its current location.

### 5.3.2.2 Early to mid-Holocene

The sea-level rise after the last glacial period induces the flooding of the fluvial network and the development of new depositional conditions in the coastal plain. During the early Holocene sea level rise rate was high with up to 7m/ka (Denys and Baeteman, 1995) generating strong geomorphologic and sedimentologic changes on the French coastal plain, gaining a lot of accommodation space and setting estuarine conditions. As explained Van Wagoner *et al.* (1990) the shift from fluvial to estuarine deposits evidences the transgression within a coastal system.

The behaviour of the area evolved to transgressive conditions while landward infilling and broad sediment contribution from offshore sources characterized this early stage of sedimentation. The main channels and adjacent lower areas, located in the axial part of the coastal plain, were the first affected for this transgressive



backfilling, controlling the entire axial area. This filling gradually extended and widens the estuarine sedimentation to surrounding zones.

The timing of transgressive flooding was dated of the Boreal period around 9500 cal BP (Jelgersma, 1979; Beets and Van der Spek, 2000) which marks the generalised presence of estuarine conditions along the coastal plain. Comparing with the western Belgian coastal plain, ages of flooding into the IJzer paleochannels were also dated around 9500 cal BP (Baeteman and Declerck, 2002; Baeteman *et al.*, 2011). However, the flooding in the eastern side seems to be younger (Cleveringa, 2000; Mathys, 2009; Hijma, 2009) inferring that the action of flooding by sea-level rise of the southern bight as showed Beets and Van der Spek (2000) impacted earlier and probably stronger in the southernmost part of the North Sea.

According to the spatial distribution and ages of basal organic-rich facies, the sediments in the French coastal plain do not present a gradual shift landward as mentioned by Baeteman (1991; 1999) in Belgium. This difference could be referred to erosion due to the progressive entry of sandy deposits during the transgression or indicates some non-deposition conditions due to the constant high tidal dynamics in the drainage network. Likewise, catchment zones for the axial part of the coastal plain and adjacent areas maintained subtidal and lower intertidal conditions.

The tide-dominated estuarine unit is the most volumetrically significant Holocene sedimentary deposits (all the profiles, but profile 7). Depositional features were driven by the combination of a high accommodation space, mainly marine sediment supply, strong tidal currents and storm waves and wind activity. Within this type of framework, Dalrymple *et al.* (2012) mentioned the importance of considering the increasing size of the tidal prism to develop extensive estuarine environment.

They pointed out that, although tidal range is an important control factor, to generate the tidal influence further inland the tidal prism should become larger, generating tide-domination along the axis of the estuary while waves action influence the seaward flanks. This type of suggestions represents an important input to be considered among the parameters that ruled the development of this type of coastal plain considering the weak discharge of rivers and the important contribution from offshore sediments.

Because of changes in coast configuration, the tidal regime was affected after post glacial period (Shennan *et al.*, 2000) rapidly increasing during early Holocene and reaching the macrotidal range as present-day around 7500 cal BP (van der

Molen and van Dijk, 2000). The sea-level rise deceleration around 7500 cal BP (Denys and Baeteman, 1995) and the interaction with marine sediment supply and the incidence of the hydrodynamic processes became more explicit as a function of the balance between accommodation and sediment supply. Within this overall setting, most of the estuarine unit developed its sedimentation and erosion processes (Fig. 5.16).

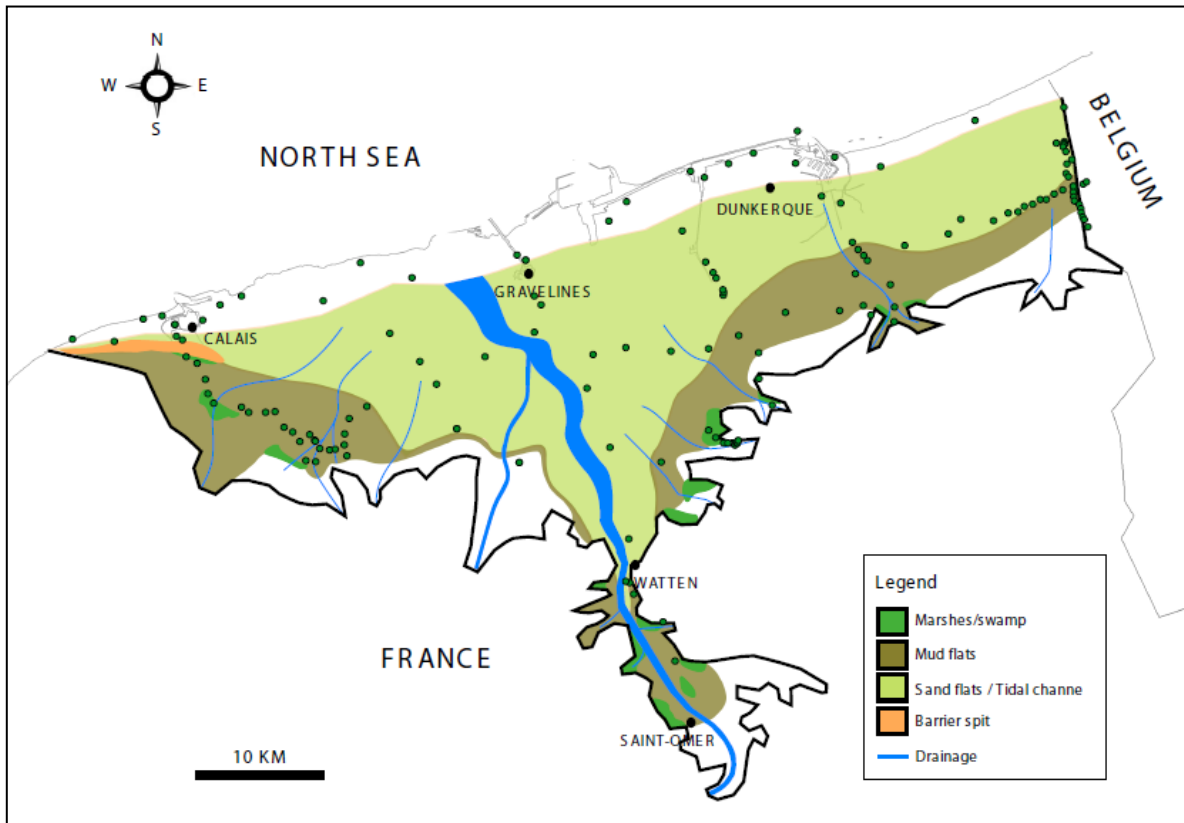


Figure 5.16. Paleogeography around 7000 BP (MSL around -7m NGF) showing the development of the estuarine unit, increase of the tidal prism and the change of the Aa River mouth towards the East. Shoreline may be further inland than present-day location.

The facies assemblages of the estuarine unit present variable organisation along the FFCP. The characteristics are the following:

### 5.3.2.2.1 Axial zone

The axial part could be explained in two sectors the inner part and the central-outer part (As examples profiles 1, 4 and 5). Landward, the ascending stratigraphic order illustrates that the mud flats were the first sediments covering the fluvio-

lacustrine deposits. They show the low-energy conditions of the initial transgression and could reach ages of 8000 cal BP. Mud flats were overlaid by tidal channels defining a retrogradational set. Sand facies and the influence of marine conditions become common landward due to the conquest of tidal channels in inland areas.

Retrogradational stacking evolved fast and intertidal sediments were deposited in aggrading conditions after decelerating of sea-level rise around 7500 cal BP (2.5 m/ka; Denys and Baeteman, 1995). Intertidal sedimentary conditions were dominant and extended. Tidal channels together with interbedded mud flats present fining upward successions that were capped by organic-rich muds and thick peat layers dated around 6500 – 5500 cal BP. The effects of this change and the development of fining-upward could be considered as the fully development of estuarine deposits and the beginnings of a transition to progradational settings.

The upper part of this unit shows the change from intertidal to supratidal low-energy conditions in relation to the cessation of tidal impact in the sedimentation as well as the second decelerating period of sea-level rise dated around 5500 cal BP (0.7 m/ka; Denys and Baeteman, 1995) in the mid-Holocene. As seen in the Belgian coastal plain (Baeteman, 2004) sea level was close to its maximum and sediment supply exceeded the creation of accommodation space. Organic-rich muds and peat accumulations developed largely and marked a progressive diminishing of the marine influence installing wet swamp conditions always drained by the main channel of the Aa River (Profiles 1, 3, 4 and 5).

Towards the central and outer zones of the axial part, the estuary presents sand facies organized as amalgamated tidal channels and sand flats deposits (Profiles 1, 2, 4 and 8). No fining-upward trend or organic-rich sediments are found here. Only stacked sandy deposits were preserved showing the high energy to which this area was subjected. In this macrotidal regime, high currents energy and the migration of large-scale sand bodies within subtidal and lower intertidal environments were characteristic.

Through the development of this unit, tidal channels aggraded and laterally migrated, creating a broad sandy channel fill succession always associated with the main channel of the Aa river (Profiles 1, 2, 4, 8, 9) mainly fed by marine sand supply (Anthony, 2000; van der Molen and van Dijck, 2000) and minimal river contribution. Since the arrangement of the depositional facies, the sedimentation could be considered as flood-dominated, especially in the sides. Because the main channel

network was always active. The central part of the coastal plain could have ebb-dominance and the main river probably had a low meandering path.

#### 5.3.2.2.2 Western zone

To the west, the development of a gravel-sand spit (*banc des Pierrettes*) infers high-energy, wave-dominated conditions and a strong eastward littoral drift controlling the seaward margin of the estuary mouth (Profile 3). This is still the case along the southern margin of the Somme or the Slack estuaries further south. The spit shows a migration of gravel sediments from the closest cliff after later Boreal and a maximum development during the Atlantic transgression (Sommé, 1977, Pierre, 2007).

The pathway assumed from sediment distribution in this margin has been strongly wave-driven during the Holocene coastal development (Anthony, 2000, Héquette *et al.*, 2013). The shape of the gravel spit presents spatial variations that could be attributed to the non-linear function of the wave parameters and variations of longshore transport.

In spite of macrotidal regime and larger tidal prism, waves can coexist and influence the outer flanks of the estuary mouth allowing the constant growth of the spit during the infilling of the tide-dominated estuary. Gravel-sand barrier in macrotidal environments suggests that grain size could have played an important role for their occurrence and stability (Hayes, 1994). As no gravel is available from the rivers, the extension of the spit could be defined by the amount of coarse-sized material accumulated at the foot of the Cretaceous and Pleistocene cliff during interglacial ages and its Holocene retreat.

In the middle part of the spit, another branch was developed seaward. This later spit, contrary to the previous one, mostly consists in sandy deposits with seldom gravels. This sand spit is directly related to climatic changes (Sommé, 1977) and the effects of the wave influence on the hydrodynamic conditions and nearshore sedimentation during the Holocene (Anthony *et al.*, 2010; Héquette *et al.*, 2013) that modified the direction of the shoreline. The development of this sand spit was temporally related with the formation and extension of the surface peat layer along the western area of the plain behind the barrier. It suggests a manifestation of the climatic change from the Atlantic to Subboreal period (Sommé, 1977).

The sedimentary succession behind the spit complex, presents typical depositional characteristics of back-barrier tidal flats (profile 3). They comprise tidal channels (fed by small coastal streams affected by flooding), mud flats and marshes showing fining-upward patterns controlled by the construction of the barrier. Considering the hydrodynamic conditions and depositional facies organisation displaying extensive tidal flat deposits behind the spit, the sediments of this part define a quite classical estuarine back-barrier system as explained Flemming (2012).

#### **5.3.2.2.3 Eastern zone**

To the East, the sedimentary succession of the estuarine unit contrasts with the clear wave-dominated western side. As shown along profiles 5, 6, and 10 extended tidal flat deposits separate the main estuarine paleochannels of the Aa and the Ijzer rivers. This area does not present large coastal rivers, but only some short streams draining the catchment area from the low-hill slopes.

The sedimentation was totally dominated by the progressive transgression and its relationships with tidal discharge and wave action. This mixed action was more evident after the balance generated by the first deceleration of the sea-level rise (Denys and Baeteman, 1995). Extended tidal flat environment, as observed in this part, could be directly related to the development of macrotidal conditions and the interaction of tide and wave parameters in the adjacent areas for the estuaries of small rivers as explained Fan (2012).

Intertidal deposits of this side of the FFCP show a predominant variable arrangement of fining-upward successions with small tidal channels, mixed flats, mud flats and marshes or vertical accreted mud flats inland, while seaward, near to the current coastline, deposition is dominated by a wide coalescing sand flats/tidal channels deposits system (profile 5). Mrani and Anthony (2011) presented some similarities with this sedimentary distribution. Using a core succession, they show muddy deposits inland, while the bulk of the deposits consist of homogeneous sands seaward.

Environmental conditions interpreted by previous investigations in the area suggested different sedimentation settings: coastal barrier settings (Paepe, 1960; Sommé 1969, 1977), a wide tide-dominated back barrier infilling (Baeteman, 2001,

2004, 2012) or mixed tide-wave dominated shoreface (Mrani, 2006; Anthony *et al.*, 2010; Mrani and Anthony, 2011).

In essence, the environmental interpretations from these different interpretations suggest an important control of tidal dynamic for inland infilling, but differ in the mechanisms (giving different emphasis for tides and waves controls acting in the environmental context) that welded the accretion of subtidal/lower-intertidal sandy deposits and constructed the root of the dunes complex of Ghyvelde described seaward.

Offshore deposits, capped by the recent tidal sand banks (< of 1000 years) (Tessier, 1997) present sedimentological characteristics that give some clues about the possible extension of tidal flat related to early mid-Holocene (Trentesaux *et al.*, 1999; Mathys, 2009). In addition, very high-resolution seismic provides some insights about the migration and attachment of banks (Tessier, 1997; Mathys, 2009), which are related to the occurrence of the homogeneous sandy cover and changes in the morphology of the estuary mouth.

Unfortunately, our new data evidence the tide-dominated sedimentation for inland deposits, but do not provide new clues to solve the seaward divergence. The perspective to perform some cores in the French offshore would be interesting to compare and resolve some aspects of the sand to sand contacts, ages and sedimentological characteristics of the deposits.

### **5.3.2.3 Mid to late-Holocene**

High rate of sediment supply, flood-dominant hydrodynamics conditions, and sea-level rise deceleration contributed to fill up with transgressive estuarine deposits the significant accommodation space created during early to mid-Holocene period by the fast sea-level rise. After mid-Holocene, in the whole coastal plain, environmental changes were associated with the second decrease of sea-level rate and low accommodation space. This led to a stabilisation of the coastline and to the development of new depositional settings linked to low-accommodation conditions and a diminishing size of the tidal prism.

Surface peat layers testify into their characteristics the change from salt marshes to fens and shrub swamps (see organic-rich facies in chapter 3), as well as the widespread development over the intertidal deposits (Fig. 5.17). However, some

part of the eastern side as Les Moères zone remained tidally influenced, without peat accumulation (Profiles 6 and 10).

This wetlands evolution shows that low-energy conditions prevailed in the area. This is linked to the stabilisation of the transgressive conditions when the retrogradation of the barrier finally stabilized (Baeteman, 2001, 2004, 2012) or when shoreface sandbodies welded to the shoreface (Mrani, 2006; Anthony *et al.*, 2010; Mrani and Anthony, 2011). This is synchronous with the beginning of shifts to progradation features (Holz *et al.*, 2002) and migration of supratidal environments seaward. During this change the tidal energy lost influence at the border sides of the plain, the major tidal channel remained open concentrating the tide energy.

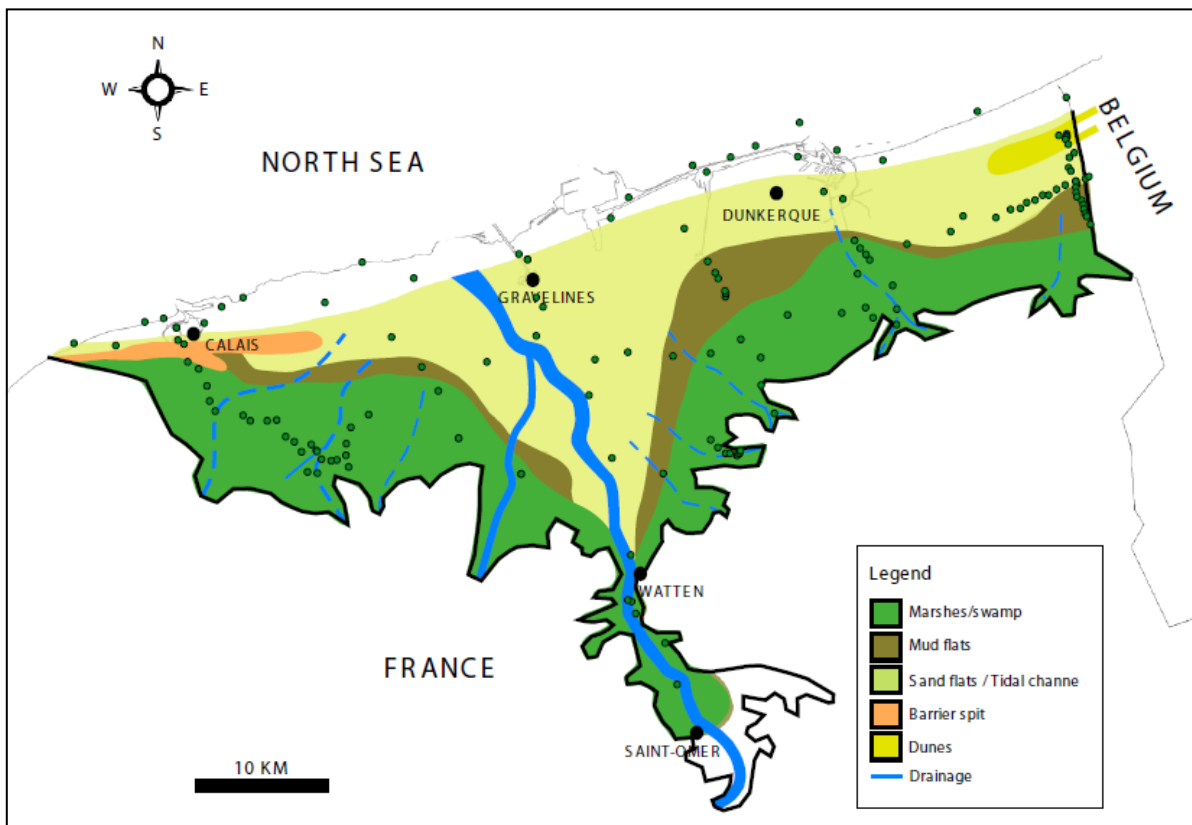


Figure 5.17. Paleogeography around 5000 BP (MSL around -2m NGF). It is showing the extent of the surface peat layer, decreasing of tidal prism and the change in the position of the Aa River mouth towards the East.

Later, the infilling is associated with the re-entrance of tidal flats extended through the coastal plain. In areas with limited available space for internal infilling, a low fluvial input and a high marine supply in macrotidal conditions resulted in conditions favourable for tidal flats establishment (Tessier *et al.*, 2010). This is a good

definition to characterize the new depositional settings for the upper sedimentary cover of the Holocene infill.

Renewed tidal flats were established around 3000 cal BP where tidal deposits reached inland areas, eroding and covering the marsh and peat accumulations (Fig. 5.18). Although surface peat was still growing in scattered areas, even after anthropisation, tidal flats unit affected a large surface by this widening re-entry.

Tidal channels incise, rework and coalesce with the previous tidal channels, creating deeper and narrower channels affecting the estuarine unit and eventually the Pre-Holocene deposits (profile 1, 4, and 7). Land-sea interaction becoming progradational, persistent marine sediment supply (van der Molen and van Dijck, 2000) maintained a steady contribution from the sea. Ebb-dominated conditions play the predominant role in the inner and middle part of the plain while mixed wave and tidal currents handle the transport and sedimentation coastward where sand bodies are attached to the coast.

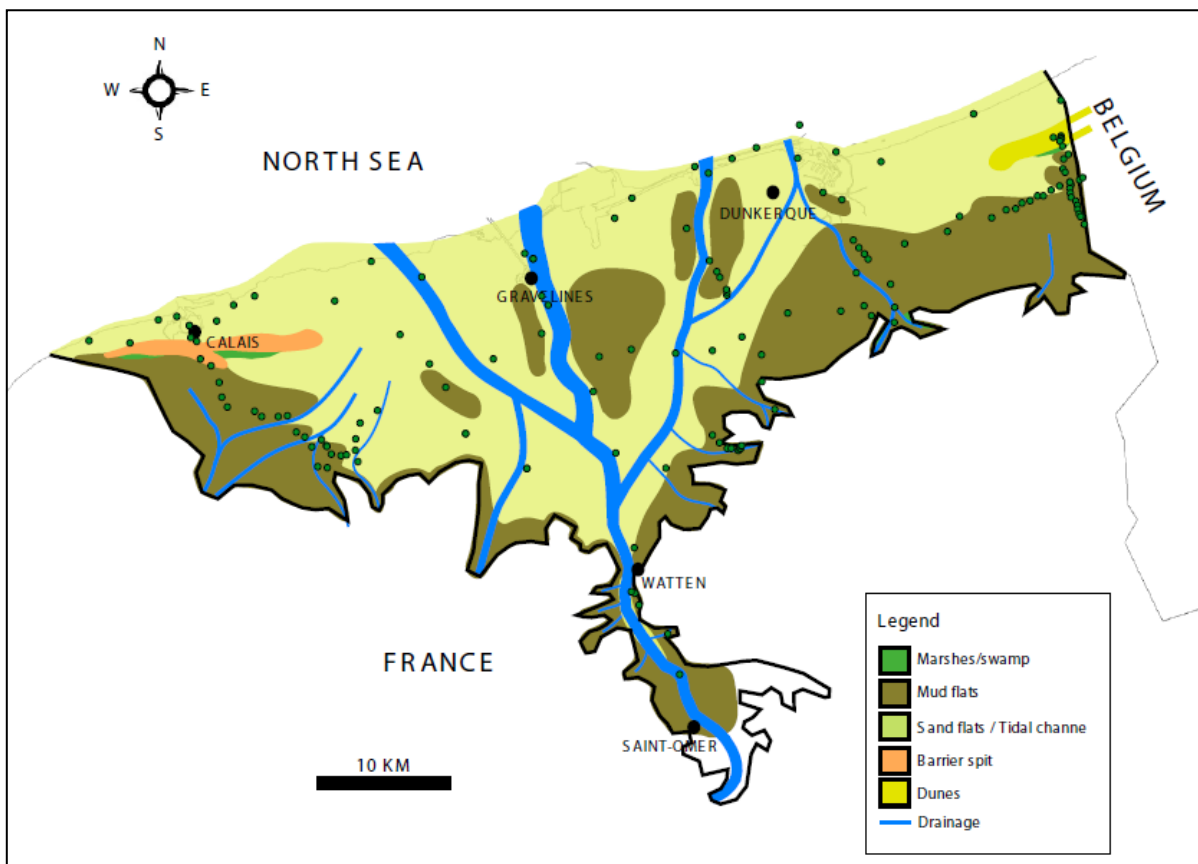


Figure 5.18. Paleogeography around 3000 BP (MSL around -2m NGF) showing the expansion of intertidal deposits along the FFCP. Aa River present small distributaries separated by intertidal flats.



Tidal channels progressively increased the tidal prism and tidal conditions extended to the entire coastal plain affecting the previous deposits. Some features of their characteristics along the coastal plain are as follows:

#### **5.3.2.3.1 Axial zone**

In the axial part and adjacent areas the main action could be related to the progressive increase of tidal prism and ebb-dominated flow which eroded, drained and compacted the surface peat layers and previous mud flats. Sand flats and tidal channels dominated the area in which progradational bodies developed. In the seismic profiles reflections patterns showing slightly progradational settings were recognized in the last sedimentary cover, which can be compared and assumed to describe the migration of sandy deposits seaward.

#### **5.3.2.3.2 Western zone**

The development of an extended peat layer capped the upper part of the estuarine deposits. The peat developed seaward, showing a prograding trend, with earliest ages around 6000 BP inland and late-Holocene ages of about 3500 BP to the North. Its extension could be correlated, as seen in the inner part of the estuary, by the interaction of the second decelerating phase of sea-level rise, accommodation space filled and the environmental change where marshes prograded over intertidal deposits.

In the inner western part, the tidal flats unit overlain surface peat layer. It is represented by interbedded mud flats and scoured small tidal channels and creeks that could reflect the action of fluvial floods associated to the amplification of some climatic conditions as the heavy rainfall in the subboreal period (Clavé, 2001) creating shallow networks which subsequently were connected to the main channel drainage and were flooded. Seaward, new sand flats eroded and reworked previous intertidal deposits disposed during the transgression (Profile 3).

In the outer western side, washover deposits were associated with the breaching of the spit linked to storm waves generating marine sandy deposits behind the spit. Likewise, an extended shoreface tide- and wave- dominated was created

and maintained during late Holocene, serving as a main source to aeolian dunes formation (Anthony *et al.*, 2010, Anthony *et al.*, 2012).

#### **5.3.2.3.3 Eastern zone**

As seen in the western side, the surface peat accumulation capped inland succession and extended seaward, covering the intertidal deposit of the estuarine unit. Ages from the base of these sediments started around 5600 cal BP and as observed in the other areas of the coastal plain, its development and signature suggest some changes in the depositional trend.

The renewed tidal deposits extended inland through tidal channels with tidal creeks networks, eroding previous mud flats and marshes (Profile 5). Mud flats, as Les Moères zone, were not reached by the widespread surface peat layer. This area has been eroded due to the increasing efficiency of ebb-dominated channels and infilled with sand bodies brought from the surrounding sand flats, which are extended seaward. Previous works from the French-Belgian border (Baeteman 2001, 2004; Mrani, 2006; Mrani and Anthony, 2011) also suggest significant changes in tidal dynamics controlling flooding and contributing to peat compaction as a parameter to gain accommodation space for tidal inundation.

The widespread conditions of this upper unit have been discussed and attributed to different alternatives of driving mechanisms affecting in different ways the entire coastal plain. Important features of the uppermost tidal flat successions over freshwater peat were also identified in other studies performed in northwest Europe (Baeteman, 2005; Long *et al.*, 2006; Mrani, 2006) proposing the penetration of tidal sediments from morphodynamic processes dominated by the interaction of energy fluxes abandoning the earlier works reflecting sea-level fluctuations (e.g. Houthuys *et al.*, 1993).

In the entire plain, peat compaction corresponds to an important parameter responsible of the creation of this tidal flat unit and the last natural landscape of the coastal plain. . Despite peat compaction was not quantified in this study we think this process influences the sedimentation of the last sedimentary cover. As shown Asselen (2010) in many Holocene basins containing peat accumulation, the peat compaction contribute to the total subsidence of the coastal areas, and can locally

provide up to 40% of the accommodation space, deeply affecting the sedimentary patterns.

Peat compaction can deform in a complex form the entire stratigraphic column, as well as generate remarked problems to plot sea-level curves and complicate efforts to reconstruct paleogeographic perspectives (Long, *et al.*, 2006). However, the process of compaction impacts directly the geomorphologic dynamic, especially in coastal lowlands where it plays an important role in the deformation and the distribution of the deposits (Long, *et al.*, 2006; Törnqvist *et al.*, 2008).

Changes in the tidal prism of the main drainage may be induced, as explained Mrani and Anthony (2011), by peat compaction. These changes in tidal prism are leading a progressive infilling with ebb-dominated channel flow and bed incision consequence of drained and compacted peat layers. However, this should not be the only cause to the loss of volume. Auto-compaction by climatic changes (Allen, 2000) and drainage modification by anthropogenic activities (Paepe, 1960; Baeteman, 2005) must also be considered as other variables.

For this last sedimentary cover, other parameters should be integrated to the morphosedimentary development of the plain before the anthropogenic activities became the main factor explaining the evolution of the present-day landscape. Storm surges and active aeolian accumulations have been related to the large sand flats open to the sea, over which mixed tide- and wave-energy construct modern coastal banks (e.g the Dunkerque offshore bank system).

## **5.4 Conclusions**

The interplay between hydrodynamic conditions and the sea-level rise are clearly the main factors that control and modify the sedimentation of the French Flemish coastal plain during the Holocene. Dominant macrotidal settings were established after early Holocene, characterizing the deposition of estuarine and tidal units. The tidal range is an important factor in this type of environment, but the wide morphological features with small fluvial contribution observed in the French Flemish coastal plain show that the tidal prism, partly linked to the tidal range, has a great significance in the development and distribution of depositional facies.

The general context evolved from estuarine aggradational deposits until 5500 cal BP to progradational tidal flats deposits. High accommodation space and high rate of sedimentation favoured the transgressive deposits in estuarine conditions until mid-Holocene. Sedimentation changed when sediment supply was unable to fill the area leading to regressive conditions. Changes in the sedimentation do not depend exclusively on one parameter, as sea-level rise or hydrodynamic processes but rather on the interaction and relative influences between them.

The sea-level rise was the most important parameter during earlier Holocene and became less important when it decelerated. The balance between sediment supply and hydrodynamic conditions then had the maximum impact in the sedimentation. However, sea level was still rising and continued to be an active factor to the current sedimentary dynamics. This is an important factor to take into account to formulate predictive modelling.

## Chapter 6. General conclusions and further research

This research described the Holocene coastal evolution of the French Flemish coastal plain (FFCP) from the combination of cores, boreholes and, for the first time, VHR seismic profiles on the waterways of the study area. The analysis of 125 km of seismic profiles, 383 boreholes, 10 cores, a series of archaeological trenches and samples for micropaleontology, clay mineralogy and radiocarbon dating provides us the opportunity to build a reconstruction of the internal architecture of the infill of the plain. It highlights the sedimentological characteristics and the succession of depositional environments of this southernmost part of the continental southern North Sea coastal plain.

Coastal deposits from FFCP reflect the cumulative effects of processes that have been ongoing during the Holocene. This coastal system does not represent a sedimentation dominated by eustatic transgressive-regressive cycles as some previous studies mentioned. We think that Holocene sea-level has served as the major agent in causing the transgression and the creation of the inland high accommodation space in early Holocene. Consecutively, between the end of the early-Holocene and the beginning of the mid-Holocene (see figure 1.4 in chapter 1) it is the balance between the sea-level rise slowdown associated with the other coastal factors that mostly generated the filling of the shallow valley.

Sedimentation is related to the dynamic interaction of (1) the changing rate of sea-level rise and the influence of the strong macrotidal regime, (2) variations in tidal prism, (3) abundant and dominant marine sediment supply and (4) nearshore waves action. In addition, other natural, then anthropogenic, factors such as peat compaction and human activity impacted the final configuration of the sedimentary infill and the current coastland.

Following the evidence obtained by the seismic reflection patterns, sedimentary facies composition, clay mineralogy, foraminifera and pollen grains assemblages, the sedimentary infill described in the area consists of a heritage of the last Pleistocene fluvial deposits and Holocene marine influenced deposits; a strong sedimentary input from North Sea is developed during this period.

Reconstructing the sedimentary conditions of the Holocene infill, tidal channels, sand flats, mud flats, marshes, swamps and barrier spit were recognised.

Tide domination and waves influence exert a strong control in the distribution of these depositional facies. Pre-Holocene palaeotopography is also an important parameter that influences the distribution of these depositional facies. Other signatures as climatic changes could also affect the development of extended peat accumulation along this period. Peat compaction, having an effect in the geometry of the facies organisation, is another important control, which might be considered among the different factors involved in the natural evolution of the coastal plain.

The development of the Holocene infill presents the estuarine unit and tidal flat unit in a vertical succession. According to this arrangement the Holocene was characterised by a framework that displays transgressive and progradation settings. Transgressive features were developed during Early and Mid Holocene. They present aggradation of tidal depositional facies associated to a transgressive estuarine conditions which overlain the Late Pleistocene fluvio-lacustrine deposits. Tidal channels-sand flats, mud flats and marshes are distinguished in the inner and border sides of the coastal plain while tidal channels-sand flats are stacked in the central and outer area.

Progradational features are suggested during the seaward extension of the surface peat accumulation overlying the previous intertidal deposits and the wide deposition of sand bodies seaward. Tidal flat unit re-entry inland during Late Holocene. Previous Holocene deposits are affected by incision, erosion and compaction, specially the extended surface peat layer. This unit is considered the last environmental configuration before the changes induced by the human action.

This study illustrates a regional approach of the Holocene subsurface arrangement of the French Flemish coastal plain. Based on the accurate analysis of the dataset we developed our sedimentological-stratigraphic standpoint subdividing the sedimentary succession in environmental significant facies assemblages and depositional sedimentary units. However, improvements could be envisaged with further acquisition of core data, especially for radiocarbon dating and detailed sedimentological study of the thick sand bodies.

Although seems correctly abandoning the Calais-Dunkerque stratigraphy as transgressive-regressive cycles we think that the lithostratigraphic character of these deposits should be considered for further investigation. The vertical succession that we found inland, where the surface peat layer is developed, may be concordant with the characteristics that defined these units. Nevertheless, in the areas where the

contact corresponds to sand on sand they cannot be easily defined. Promoting this study could be interesting to map and design these units as valid lithostratigraphic units for the Quaternary of the northern of France.

The integration of the dataset used in this study allows us, with limitations, to propose some palaeogeographic reconstructions through the Holocene stratigraphic record. However, using the same dataset knowing the factors controlling the sedimentary setting of this coastal area, it can be interesting to test other tools as 3D stratigraphic modelling (e.g. Dionisos software developed by IFP). Some attempts have been realized during this study but it is necessary to continue its development for the millennial scale. Contributing to this development will be a significant new approach for the use of this sort of software to sedimentary models with shorter time scales. Also, it could be a useful tool to achieve a subtle model for the infilling of the FFCP.

The stratigraphic architecture of the French Flemish coastal plain and its detailed description and interpretation of data collected, reveals the geological factors that controlled the regional behaviour and the coastal evolution through the Holocene. This investigation can serve as a basis or complementary information to face of new developments and project management conducted in this fragile littoral zone of northern France. In our understanding, a constant improvement about the sedimentation and the characteristics of the different factors operating in the area is required, because they continue to influence the development of the coastal system.





## References

- Allen, G. P., & Posamentier, H. W. (1993). Sequence stratigraphy and facies model of an incised valley fill: the Gironde estuary, France. *Journal of Sedimentary Petrology*, 63(3), 378–391.
- Allen, J. R. L. (2000). Morphodynamics of Holocene salt marches: a review sketch from the Atlantic and Southern North Sea coast of Europe. *Quaternary Science Reviews*, 19, 1155-1231.
- Ameryckx, J. (1961). La genèse des polders maritimes belges. *De Aardrijkskunde*, 13(1) : 3-16.
- Anthony, E. J. (2000). Marine sand supply and Holocene coastal sedimentation in northern France between the Somme estuary and Belgium. In: K. Pye & J.R.L. Allen (Editors), Coastal and Estuarine Environments: sedimentology, geomorphology and geoarchaeology. *Geol. Soc. of London, Special publication*, 175(1): 87-97.
- Anthony, E. (2002). Long-term marine bedload segregation, and sandy versus gravely Holocene shorelines in the eastern English Channel. *Marine Geology*, 187, 221-234.
- Anthony, E. J., & Orford, J. D. (2002). Between Wave- and Tide-Dominated Coasts: the Middle Ground Revisited. *Journal of Coastal Research*, 36, 8-15.
- Anthony, E. J., Mrani-Alaoui, M., & Héquette, A. (2010). Shoreface sand supply and mid-to late Holocene aeolian dune formation on the storm-dominated macrotidal coast of the southern North Sea. *Marine Geology*, 276, 100-104.
- Anthony, E., Mrani-Alaoui, M., & Héquette, A. (2012). Reply to the comment on Shoreface sand supply and mid- to late Holocene Aeolian dune formation on the storm dominated macrotidal coast of the southern North Sea” by E.J. Anthony, M. Mrani-Alaoui and A. Héquette [Marine Geology 276 (2010) 100–104]. *Marine Geology*, 311-314, 67–70.
- Antoine, P., Catt, J., Lautridou, J.-P., & Sommé, J. (2003a). The loess and coversands of northern France and southern England. *Journal of Quaternary Science*, 18, 309–318.
- Antoine, P., Coutard, J.-P., Gibbard, P., Hallegouet, B., Lautridou, J.-P., & Ozouf, J.-C. (2003b). The evolution of the Dutch and Belgian coasts and the role of sand supply from the North Sea. *The Pleistocene rivers of the English Channel region. Journal of Quaternary Science*, 18(3-4), 227-243.

- Armynot du Chatelet, E., Recourt, P., & Chopin, V. (2008). Mineralogy of agglutinated benthic foraminifera; implications for paleo-environmental reconstructions. *Bull. Soc. géol. Fr.*, 179(6), 583-592.
- ASTM. (1998). Standard practice for establishing allowable properties for visually-graded dimension lumber from Ingrade tests of full-size specimens. *Annual book of ASTM standards. Wood. West Conshohocken, PA: American Society for Testing and Materials*, 04.10, 287-311.
- Baak, J. A. (1936) *Regional petrology of the southern North Sea*. PhD thesis, Leyden University, Wageningen. 127p.
- Bachrach, R. (1998). *High resolution shallow seismic subsurface Characterization*. PhD thesis. Stanford University. California. 155p.
- Baeteman, C. (1985). Development and evolution of Sedimentary Environments during the Holocene in the Western Coastal Plain of Belgium. *Eiszeitalter u. Gegenwart*, 35, 23-32.
- Baeteman, C. (1991). Chronology of coastal plain development during the Holocene in West Belgium. *Quaternaire*, 2(3-4), 116-125.
- Baeteman, C. (1999). The Holocene depositional history of the IJzer palaeo-valley (Western Belgian coastal plain) with references to the factors controlling the formation of intercalated peat beds. *Geologica Belgica*, 2(3-4), 39-72.
- Baeteman, C. (2001). Holocene depositional history of the Inland Dunes and De Moeren. Excursion Guide Field Meeting Geologica Belgica, 2 June 2001. *Belgian Geological Survey*. 39p.
- Baeteman, C. (2004). The Holocene development of a tide-dominated coastal lowland. Western coastal plain of Belgium. Field Guide. The QRA Third International Postgraduate Symposium Fieldtrip, September 17th 2004. *Belgian Geological Survey*. 76p
- Baeteman, C. (2005a). How subsoil morphology and erodibility influence the origin and pattern of late Holocene tidal channels: Case studies from the Belgian coastal lowlands. *Quaternary Science Reviews*, 24, 2146-2162.
- Baeteman, C. (2005b). The Streif classification system: a tribute to an alternative system for organising and mapping Holocene coastal deposits. *Quaternary International*, 133-134, 141-149.
- Baeteman, C. (2008). Radiocarbon-dated sediment sequences from the Belgian Coastal Plain: testing the hypothesis of fluctuating or smooth late-Holocene relative sea-level rise. *The Holocene*, 18, 8, 1219-1228.

- Baeteman, C. (2013). History of research and state of the art of the Holocene depositional history of the Belgian coastal plain, *in*: Thoen, E. et al. (2013). *Landscapes or seascapes? The history of the coastal environment in the North Sea area reconsidered*, 13, 11-29.
- Baeteman, C., & Declercq, P.-Y. (2002). A synthesis of early and middle Holocene coastal changes in the Western Belgian lowlands. *Belgeo*, 2, 77-107.
- Baeteman, C., Waller, M., & Kiden, P. (2011). Reconstructing middle to late Holocene sea-level change: A methodological review with particular reference to 'A new Holocene sea-level curve for the southern North Sea' as presented by K.-E. Behre. *Boreas*, 40(4), 557-572.
- Bally, A. W. (1987). Atlas of Seismic Stratigraphy. *AAPG studies in geology series*, #27, volume 1.
- Beets, D. J., & Van der Spek, A. J. F. (2000). The Holocene evolution of the barrier and the back-barrier basins of the Belgium and the Netherlands as a function of late Weichselian morphology, relative sea-level rise and sediment supply. *Neth. J. Geosc.-Geol. Mijnbouw*, 79, 3-16.
- Beets, D. J., van der Valk, L., & Stive, M. J. F. (1992). Holocene evolution of the coast of Holland. *Marine Geology*, 103, 423-443.
- Behre, K.-E. (2007). A new Holocene sea-level curve for the southern North Sea. *Boreas*, 36(1), 82-102.
- Behre, K.-E. (2004). Coastal development, sea-level change and settlement history during the later Holocene in the Clay District of Lower Saxony (Niedersachsen), northern Germany. *Quaternary International*, 112, 37-53.
- Bernasconi, E., & Cusminsky, G. (2009). Estudio paleoecológico de Foraminíferos de testigos del de Golfo Nuevo (Patagonia, Argentina). *Geobios*, 42, 435-450.
- Bertrand, S., & Baeteman, C. (2005). Sequence mapping of Holocene coastal lowlands: the application of the Streif classification system in the Belgian coastal plain. *Quaternary International*, 133-134, 151-158.
- Blanchard, R., (1906). La Flandre, étude géographique de la plaine flamande, en France, Belgique et Hollande. *Societe Dunkerquoise pour l'encouragement des Sciences, Des Lettres et des Arts*. 530p.
- Bootsman, C. (1977) De geologische opbouw van de kustvlakte bij Ghyvelde (noord-frankrijk). Study report. Instituut voor aardwetenschappen. Vrije universiteit, Amsterdam, 74p.
- Bosch, J. H. A. (1975) Verlasg veldwerk Calaisis. Study report. Instituut voor aardwetenschappen. Vrije universiteit, Amsterdam, 41p.

- Bout-Roumazielles, V., Cortijo, E., Labeyrie, L., & Debrant, P. (1999). Clay mineral evidence of nepheloid layer contribution to the Heinrich layers in the Northwest Atlantic. *Palaeogeography, Palaeoclimatology, Palaeoceanography*, 146, 211-228.
- Boyd, R., Dalrymple, R. W., & Zaitlin, B. A. (1992). Classification of coastal sedimentary environments. *Sedimentary Geology*, 80, 139–150.
- Boyd, R., Dalrymple, R. W., & Zaitlin, B. A. (2006). Estuary and incised valley facies models. In: Posamentier, H.W., Walker, R.G. (Eds.), *Facies Models Revisited. SEPM Special Publication*, 84, 171–234.
- Brew, D. S., Holt, T., Pye, K., & Newsham, R. (2000). Holocene sedimentary evolution and palaeocoastlines of the Fenland embayment, eastern England. *Geological Society, London, Special Publications*, 166, 253-273.
- Briquet, A. (1930). *Le littoral du Nord de la France et son évolution morphologique. PhD Thesis. Université d'Orléans, Orléans*, 439p.
- BRGM, 2014 <http://infoterre.brgm.fr/>.
- Brodniewicz, I. (1965). Recent and some holocene foraminera of the Southern Baltic Sea. *Acta Paleontológica Polonica*, X(2), 129p.
- Bronk Ramsey, C., Higham, T., Bowles, A., & Hedges, R. (2004). Improvements to the pretreatment of bone at Oxford. *Radiocarbon*, 46, 155-163.
- Brouwer, J. (1988). High-resolution seismic profiling: development of acquisition, processing, and interpretation for the practical implementation of the method in shallow sub-surface exploration and engineering. *Geologica Ultraiectiona*, 55, 1 - 136.
- Brown, A. R. (2011). Interpretation of Three-Dimensional Seismic Data. *Published jointly by American Association of Petroleum Geologists and the Society of Exploration Geophysicists*, 646p.
- Brown, L. F., & Fisher, W. L. (1980). Seismic Stratigraphic Interpretation and Petroleum Exploration. *Aapg Continuing Education Course Notes*, 16. AAPG, Tulsa, 56p.
- Brown, T. A., Nelson, D. E., Vogel, J. S., & Southon, J. R. (1988). Improved Collagen Extraction by Modified Longin Method. *Radiocarbon*, 30, 171-177.
- Busschers, F. S., Kasse, C., Van Balen, R. T., Vandenberghe, J., Cohen, K. M., Weerts, H. J. T, Bunnik, F. P. M. (2007). Late Pleistocene evolution of the Rhine-Meuse system in the southern North Sea basin: imprints of climate change, sea-level oscillation and glacio-isostasy. *Quaternary Science Reviews*, 26, 3216-3248.

- Callaghan, D. P., Boumab, T. J., Klaassenb, P., Van der Walb, D., Stivec, M. J. F., & Hermanb, P. M. J. (2010). Hydrodynamic forcing on salt-marsh development: Distinguishing the relative importance of waves and tidal flows. . *Estuarine, Coastal and Shelf Science.*, 89(1), 73-88.
- Cartier, A. (2011). Evaluation des flux sédimentaires sur le littoral du Nord Pas de Calais : Vers une meilleure compréhension de la morphodynamique des plages macrotidales. *Université du Littoral cote d'opale, Dunkerque*, 376p.
- Catuneanu, O. (2006). *Principles of Sequence Stratigraphy*. Amsterdam, 387p.
- Chamley, H. (1989). *Clay sedimentology*. Springer-Verlag Berlin Heidelberg, Germany, 623p.
- Chaumillon, E., Tessier, B., Weber, N., Tesson, M., & Bertin, X. (2004). Buried Sandbodies within Present-Day Estuaries (Atlantic Coast of France) Revealed by Very High Resolution Seismic Surveys. *Marine Geology*, 211, 189-214.
- Childs, J. R., Hart, P., Bruns, T. R., Marlow, M. S., & Sliter, R. (2000). High-resolution marine seismic reflection data from the San Francisco Bay Area. *U.S. Geological Survey Open-File Report 00-494*.
- Cimmerman, F., & Langer, M. R. (1991). Mediterranean Foraminifera. Slovenska Akdemija Znanosti in Umetnosti. . *Classis IV: Historia Naturales dela Opera 30, Ljubljana*, 119p.
- Clabaut, P., Chamley, H., & Marteel, H. (2000). Évolution récente des dunes littorales à l'est de Dunkerque (Nord de la France). Recent coastal dunes evolution, East of Dunkirk, Northern France. *Géomorphologie: relief, processus, environnement*, 2, 125-136.
- Clavé, B. (2001). *Evolution des paleo-environnements cotiers a l'holocene : exemple de l'aquitaine septentrionale.*, Université Bordeaux I. Bordeaux, 297p.
- Cleveringa, J. (2000). *Reconstruction and Modelling of Holocene Coastal Evolution of the Western Netherlands*. Utrecht University, Utrecht, 198p.
- Clique, P.-M., & Lepetit, J.-P. (1986). De la Frontière belge à la baie de Somme. *Catalogue sédimentologique des côtes françaises. Côte de la Mer du Nord et de la Manche. Collection de la Direction des Etudes et Recherches d'Electricité de France*, 61, 11-133.
- Cohen, K. M. (2003). *Differential subsidence within a coastal prism: late-Glacial – Holocene tectonics in The Rhine-Meuse delta, The Netherlands*. Utrecht University. Netherlands Geographical Studies, 316p.
- Colbeaux, J. P., Dupuis, C., Robaszynski, F., Auffret, J., Haesaerts, P., & Sommé, J. (1980). Le détroit du Pas de Calais: un élément dans le tectonique de blocs de l'Europe Nord occidentale. *Bull. Info. Géol.*, 17(4), 41-54.

- Coleman, J. M., & Prior, D. B. (1982). Deltaic environments, in P. A. Scholle and D. R. Spearing, eds. *Sandstone depositional environments: AAPG Memoir, 31*, 139–178.
- CORINE Biotopes. (1997). Types d'habitats français – ENGREF. 175 p.
- Culver, S. J., & Banner, F. T. (1978). Foraminiferal assemblages as flandrian palaeo-environmental indicators. *Palaeogeography, Palaeoclimatology, Palaeoecology, 24*, 53-72.
- Dalrymple, R., & Choi, K. (2007). Morphologic and facies trends through the fluvial-marine transition in tide-dominated depositional systems: a systematic framework for environmental and sequence-stratigraphic interpretation. *Ear Sci Rev, 81*, 135-174.
- Dalrymple, R., Knight, R., Zaitlin, B., & Middleton, G. (1990) Dynamics and facies model of a macrotidal sand bar complex. *Sedimentology, 37*, 577–612.
- Dalrymple, R., & Zaitlin, B. (1994). High-resolution sequence stratigraphy of a complex, incised valley succession, the Cobequid Bay Salmon River estuary, Bay of Fundy, Canada. *Sedimentology, 41*, 1069–1091.
- Dalrymple, R., Zaitlin, B., & Boyd, R. (1992). Estuarine facies models: conceptual basis and stratigraphic implications. *J Sediment Petrol, 62*, 1130–1146.
- Dalrymple, R. W., Mackay, D. A., Ichaso, A. A., & Choi, K. S. (2012). Processes, Morphodynamics, and Facies of Tide-Dominated Estuaries. In: R.A. Davis, Jr. and R.W. Dalrymple (eds.), *Principles of Tidal Sedimentology*, Springer Science+Business Media B.V, 79-107.
- Davis, R. A. J., & Hayes, M. O. (1984). What is a wave dominated coast? *Marine Geology, 60*, 313–329.
- De Batist, M., De Bruyne, H., Henriët, J. P., & Mostaert, F. (1989). Stratigraphic analysis of the Ypresian off the Belgian coast. *The Quaternary and Tertiary geology of the Southern Bight, North Sea. (Eds J.P. Henriët and G. De Moor)*, 75-88.
- De Batist, M., & Versteeg, W. (1999). Seismic stratigraphy of the Mesozoic and Cenozoic in northern Belgium: main results of a high-resolution reflection seismic survey along rivers and canals. *Geologie en Mijnbouw, 77(1)*, 17-37.
- De Ceunynck, R. (1985). The evolution of coastal dunes in the western Belgian coastal plain *Eiszeitalter und Gegenwart, 35*, 33-41.
- De Gans, W., & Van Gijssel, K. (1996). The Late Weichselian morphology of the Netherlands and its influence on the Holocene coastal development. *Mededelingen Rijks Geologische Dienst, 57*, 11-25.

- De Moor, G., & Mostaert, F. (1989). Geologie et Geomorphologie de la vallee flamande et de la plaine maritime belge. *La Flandre de part et part*, 281p.
- De Rikj, S. (1995). Salinity control on the distribution of salt marsh Foraminifera (Great Marshes, Massachusetts) *Journal of Foraminiferal Research*, 25, 156-166.
- De Vernal, A., Henry, M., & Biladeau, G. (1996). *Notes de cours destinées aux étudiants du cours SCT 5220* (Vol. 3): Département des Sciences de la terre, UAQM. 43p.
- De Visser, J. P., & Chamley, H. (1990). Clay mineralogy of the Pliocene and Pleistocene of Hole 653A, western Tyrrhenian Sea (ODP Leg 107). *In* Kastens, K.A., Mascle, J., *et al. Proceedings of the Ocean Drilling Program - Scientific Results*, 323-332.
- De Visser, J. P., & Chamley, H. (1990). Clay mineralogy of the Pliocene and Pleistocene of Hole 653A, Westerns Tyrrhenian Sea (ODP LEG 107). *Proceedings of the Ocean Drilling Program, Scientific Results.*, 107, 323-332.
- Debenay, J.-P., Bicchi, E., Goubert, E., & Armynot du Chatelet, E. (2006). Spatio-temporal distribution of benthic foraminifera in relation to estuarine dynamics (Vie estuary, Vendée, W France) *Estuarine, Coastal and Shelf Science*, 67, 181-197.
- Deconinck, J. F., & Chamley, H. (1995). Diversity of smectite origins in late cretaceous sediments: example of chalks from Northern France. *Clay Minerals*, 30, 365-379.
- Deconinck, J. F., Holtzapffel, T., Robaszynski, F., & Ami~dro, F. (1989). Données minéralogiques, géochimiques et biologiques comparées dans les craies cénomaniennes h santoniennes du Boulonnais. *Geobios*, 11, 179-188.
- Denys, L. (1989). Observations on the transition from Calais deposits to surface peat in the Western Belgian coastal plain: results of a paleoenvironmental diatom study, *in*: Baeteman, C. (Ed.) (1989). *Quaternary sea-level investigations from Belgium: a contribution to IGCP Project 200. Geological Survey of Belgium*, 6(241), 20-43.
- Denys, L. (1999). A diatom and radiocarbon perspective of the palaeoenvironmental history and stratigraphy of Holocene deposits between Oostende and Nieuwpoort (Western Coastal Plain, Belgium). *Geologica Belgica*, 2, 1-2.
- Denys, L., & Baeteman, C. (1995). Holocene evolution of relative sea level and local mean high water spring tides in Belgium-a first assessment. *Marine Geology*, 124(1-4), 1-19.

- Desjardins, P. R., Buatois, L. A., & Mangano, M. G. (2012). Tidal Flats and Subtidal Sand Bodies *Developments in Sedimentology*, 64, 1-924.
- Donselaar, M., & Geel, C. (2007). Facies architecture of heterolithic tidal deposits: the Holocene Holland Tidal basin. *Netherlands Journal of Geosciences: Geologie en Mijnbouw*, 86, 389-402.
- Droser, M., & Bottjer, D. (1986). A semiquantitative field classification of ichnofabric. *Journal of Sedimentary Petrology*, 56(4), 558-559.
- Dubois, G. (1924). Recherches sur les terrains quaternaires du Nord de la France. *Mémoires de la société géologique du Nord*, VIII(I), 356p.
- D'Olier, B. (1981). Sedimentary events during Flandrian sea-level rise in the south-west corner of the North Sea. In: S.-D. Nio, R.T.E. Schüttenhelm and T.C.E. van Weering (Editors) *Holocene Marine Sedimentation in the North Sea Basin. Spec. Publs. int. Ass. Sediment*, 221-227.
- Ehlers, J., Gibbard, P. L., & Hughes, P. D. (2011). Introduction. Quaternary Glaciations. *Extent and Chronology Developments in Quaternary Science*, 1-15.
- Eisma, D., Jansen, J. H. F., & Van Weering, T. C. E. (1979). Sea-floor morphology and recent sediment movement in the North Sea. In: Oele, E., Schüttenhelm, R.T.E., & Wiggers, A.J. (eds): *The Quaternary history of the North Sea*. Paper presented at the Acta of Symposium Annum Quingentesimum Celebrantis (Upsala), 217-231.
- Erdtman, G. (1954). *An introduction to pollen analysis*. U.S.A.: Chronica Botanica Company. 239p.
- Evans, J. R., Kirby, J. R., & Long, A. J. (2001). The litho- and biostratigraphy of a late Holocene tidal channel in Romney Marsh, southern England. *Proceedings of the Geologists' Association*, 112, 111-130.
- Fan, D. (2012). Open-Coast Tidal Flats. In R.A. Davis, Jr. and R.W. Dalrymple (eds.), *Principles of Tidal Sedimentology*, Springer Science+Business Media B.V, 231-267.
- Fenies, H., & Faugeres, J.-C. (1998). Facies and geometry of tidal channel-fill deposits (Arcachon Lagoon, SW France), *Marine Geology*, 150, 131–148.
- FitzGerald, D., Fenster, M., Argow, B., & Buynevich, I. (2008). Coastal Impacts Due to Sea-Level Rise (Vol. 36, pp. 601-647): Annual Review of Earth and Planetary Sciences.
- Flemming, B. W. (2012). Siliciclastic Back-Barrier Tidal Flats. . In R.A. Davis, Jr. and R.W. Dalrymple (eds.), *Principles of Tidal Sedimentology*, Springer Science+Business Media B.V, 231-262.



- Flint, S., Aitken, J., & Hampson, G. (1995). Application of sequence stratigraphy to coal-bearing coastal plain successions: implications for the UK Coal Measures. *From Whateley, M. K. G. & Spears, D. A. (eds). European Coal Geology, Geological Society Special Publication, 82, 1-16.*
- Foster, D., & Poppe, L. (2003). High-resolution seismic-reflection surveys in the nearshore of outer Cape Cod, Massachusetts. . *US Geological Survey Open-File Rep 03-235.*
- Gandouin, E. (2003). *Enregistrement paléoclimatique de la transgression Holocène; signature paléoenvironnementale des Chironomidae (Diptères) du bassin de Saint-Omer (France)*. PhD Thesis. Université Lille 1. Lille, 246p.
- Gandouin, E., Van Vliet-Lanoë, B., Franquet, E., Andrieu-Ponel, V., Keen, D. H., Ponel, P, Brocandel, M. (2007). Analyse en haute résolution de la transgression holocène dans un secteur subsident du littoral français : le bassin-marais de St Omer (Pas de Calais, France). *Géologie de la France 1, 11-32.*
- Garlan, T. (1990). L'apport des levés bathymétriques pour la connaissance de la dynamique sédimentaire. L'exemple des "Ridens de la rade" aux abords de Calais. *Eurocoast, 90p.*
- Gibbard, P. (2007). Palaeogeography: Europe cut adrift. *Nature, 448(7151), 259-260.*
- Gibbard, P. L. (1995). The formation of the Strait of Dover. In: Preece, R.C. (Ed.). *Island Britain: a Quaternary perspective Geological Society, London, Special Publications, 96, 15-26.*
- Gibbard, P. L., Rose, J., & Bridgland, D. R. (1988). The history of the great Northwest European rivers during the past three million years. *Philosophical Transactions of the Royal Society of London. Series B. . Biological Sciences, 318(1191), 559-602.*
- Gingras, M., Bann, K., MacEachern, J., Waldron, W., & Pemberton, S. (2007). A conceptual framework for the application of trace fossils. . *In MacEachern JA, Bann KL, Gingras MK, Pemberton SG (eds) Applied ichnology. SEPM Short Course Notes, 52, 1-25.*
- Gingras, M., MacEachern, J., & Dashtgard, S. (2012). The potential of trace fossils as tidal indicators in bays and estuaries. *Sedimentary Geology, 279, 97–106.*
- Gosselet, J (1873) Considérations historiques relatives aux tourbières des environs de Calais, *Annales de la Société Géologique du Nord, I, pag 21.*
- Gosselet, J. (1893). Géographie physique du Nord de la France et de la Belgique : la Flandre. *Annales de la Société Géologique du Nord, 21, 176-197.*
- Gosselin, G. (2011). PhD Thesis. *in prep.* Université Lille 1. Lille.

- Guilcher, A. (1951). La formation de la mer du Nord, du Pas-de-Calais et des plaines maritimes environnantes. . *Revue de géographie de Lyon*, 26(3), 311-329.
- Gullentops, F., Bogemans, F., De Moord, G., Paulissen, E., & Pissart, A. (2001). Quaternary lithostratigraphic units (Belgium). *Geologica Belgica*, 4(1-2), 153-164.
- Haeni, F. (1986). Application of continuous seismic reflection methods to hydrologic studies. *Groundwater*, 24(1), 23–31.
- Harris, P. T., Heap, A. D., Bryce, S. M., Porter-smith, R., Ryan, D. A., & Heggie, D. T. (2002). Classification of Australian clastic coastal depositional environments based upon a quantitative analysis of wave, tidal, and river power. *Journal of sedimentary research*, 72(6), 858-870.
- Hayes, M. O. (1994). The Georgia Bight barrier system. In: R.A. Davis, Jr. (Editor). *Geology of Holocene Barrier Island Systems*. Springer-Verlag: 233-304.
- Heim, J. (1970). *Les relations entre les spectres polliniques récents et la végétation actuelle en Europe occidentale*. PhD Thesis, Université de Louvain, Louvain, 181p.
- Henriet, J.-P., De Batist, M., D'Olier, B., & Auffret, J. P. (1989). A northeast trending structural deformation zone near North Hinder, in: *Henriet, J.-P. et al. (Ed.)*. Geological survey, Brussels, 241p.
- Héquette, A., Anthony, E., Ruz, M.H., Maspataud, A., Aernouts, D., & Hemdane, Y. (2013). The influence of nearshore sand banks on coastal hydrodynamics and sediment transport, Northern coast of France. *Coastal dynamics 2013* 801-810.
- Herbin, P., Louvion, C., & Pilard, V. (2013). Bierne, Création d'une zone humide au Bieren Dyck Houck. Diagnostic archéologique, rapport final d'opération. . *Service archéologique départemental du Nord, Service Régional de l'archéologie NPDC* (In corrections).
- Hijma, M. P. (2009). *River Valley to Estuary: The Early-Mid Holocene Transgression of the Rhine–Meuse valley, The Netherlands*. . Utrecht, The Netherlands.: Utrecht University. 189p.
- Hodson, F., & West, I. (1972). Holocene deposits of Fawley, Hampshire, and the development of Southampton Water. *Proceedings of the Geologists Association*, 83, 421-442.
- Hoestine, R. (1966). Microfossil sample preparation and techniques. *Florida Geological Survey*, 57, 20p.

- Holz, M., Kalkreuth, W., & Banerjee, I. (2002). Sequence Stratigraphy of paralic coal-bearing strata: an overview. *International Journal of Coal Geology*, 48, 147-179.
- Horton, B. P. (1999). The contemporary distribution of intertidal foraminifera of Cowpen Marsh, Tees Estuary, UK: Implications for studies of Holocene sea level changes. . *Palaeogeography, Palaeoclimatology, Palaeoecology Special Issue* , 149, 127-149.
- Horton, B. P., & Edwards, R. J. (2006). Quantifying Holocene Sea Level Change Using Intertidal Foraminifera: Lessons from the British Isles. *Cushman Foundation for Foraminiferal Research, Special Publication*, 40, 97.
- Houthuys, R., De Moor, G., & Somme, J. (1993). The Shaping of the French-Belgian North Sea Coast throughout Recent Geology and History. *In Coastal Zone 93' (Series Edit.: O.T. Magoon), Spec. Volume 'Coastlines of the Southern North Sea' (Volume edit.: R. Hillen en H.J. Verhagen), New York, American Society of Civil Engineers*, 27-40.
- Huat, B. B. K., Kazemian, Sina., Prasad, A., & Barghchi, M. (2011). State of an art review of peat: General perspective. *International Journal of the Physical Sciences*, 6(8), 1988-1996.
- Huault, M.-F. (1980). Nouvelles recherches palynologiques sur le Marais Vernier. . *Bulletin de l'Association française pour l'étude du quaternaire* , 17(1-2), 53-56.
- Huijzer, B., & Vandenberghe, J. (1998). Climatic reconstruction of the Weichselian Pleniglacial in northwestern and Central Europe. *Journal of Quaternary Science*, 13(5), 391-417.
- IFREMER. (1986). Le Littoral de la Région Nord-Pas de Calais qualité du milieu marin. *RAPPORTS SCIENTIFIQUES ET TECHNIQUES DE L'IFREMER. Convention de Coopération Région Nord - Pas de Calais*, 3, 136p.
- Jelgersma, S. (1961). Holocene sea level changes in the Netherlands. *Meded. Geol. Sticht.*, C(VI), 100.
- Jelgersma, S. (1979). Sea-level changes in the North Sea basin. In: Oele, E., Schu"ttenhelm, R.T.E., Wiggers, A.J. \_Eds. *The Quaternary History of the North Sea. Acta Univ. Ups., Uppsala*, 233–248.
- Kemp, A. C., Horton, B. P., Corbett, D. R., Culver, S. J., Edwards, R. J., & van de Plassche, O. (2009). The relative utility of foraminifera and diatoms for reconstructing late Holocene sea-level change in North Carolina, USA *Quaternary Research*, 71, 9-21.

- Kerr, D., Ye, L., Bahar, A., Kelkar, B. G., & Montgomery, S. (1999). Glenn Pool field, Oklahoma: a case of improved prediction from a mature reservoir. *American Association of Petroleum Geologists Bulletin* 83(1), 1–18.
- Kiden, P. (1995). Holocene relative sea-level change and crustal movement in the southwestern. Netherlands, *Marine Geology*, 124(1-4), 21-41.
- Kiden, P., Denys, L., & Johnston, P. (2002). Late Quaternary sea-level change and isostatic and tectonic land movements along the Belgian-Dutch North Sea coast: geological data and model results. *Journal of Quaternary Science*, 17, 535-546.
- Laban, C., & van der Meer, J. J. M. (2011). Pleistocene Glaciation in the Netherlands. *Developments in Quaternary Science*, 15, 247-260.
- Ladrière, J. (1879). Le terrain quaternaire du Nord *Annales de la société géologique du Nord*, VII, 11-32.
- Ladrière, J. (1890). Etude stratigraphique du terrain quaternaire du Nord de la France *Annales de la société géologique du Nord XVIII*, 93-149, 205-276.
- Lambeck, K. (1997). Sea-level change along the French Atlantic and Channel coasts since the time of the Last Glacial Maximum. *Palaeogeography, Palaeoclimatology, Palaeoecology*, 129,1-22.
- Lautridou, J.-P., & Cliquet, D. (2006). Le pléistocène supérieur de Normandie et peuplements paléolithiques. *Quaternaire*, 17(3), 187-206.
- Lautridou, J. P., & Sommé, J. (1974). Les loess et les provinces climatosedimentaires du Pleistocène supérieurdans le Nord-Ouest de la France. *Essai de corrélation entre le Nord et la Normandie- Bulletin de l'association française pour l'étude du Quaternaire*, 40-41, 237-241.
- Le Bot, S. (2001). *Morphodynamique de dunes sous-marines sous influence des marées et des tempêtes: Processus hydro-sédimentaires et enregistrement. Exemple du Pas de-Calais*. PhD thesis, Université Lille 1. Lille, 264p.
- Lefèvre, P., Rouvillois, A., Gaffet, M. A., & Bignot, G. (1980). Alternances de sédimentation marine et continentale durant l'Holocène en Plaine maritime picarde. *Bulletin de l'Association française pour l'étude du quaternaire*, 17(1-2), 25-33.
- Leplat, J., & Sommé, J. (1989). Notice explicative de la feuille Calais. *BRGM*, 19. 21p.
- Libby, W. F. & Arnold, J. R., (1949). Age Determinations by Radiocarbon Content: Checks with Samples of Known Age. *Science*, 110 (2869), 678-680.

- Lin, Y.-T., Schuettpeiz, C. C., Wu, C. H., & Fratta, D. (2009). A combined acoustic and electromagnetic wave-based techniques for bathymetry and subbottom profiling in shallow waters. *Journal of Applied Geophysics*, 68, 203-218.
- Liu, A. C., De Batist, M., Henriët, J. P., & Missiaen, T. (1993). Plio-Pleistocene scour hollows in the Southern Bight of the North Sea. *Geologie & Mijnbouw*, 71, 195-204.
- Long, A., Waller, M., & Stupples, P. (2006). Driving mechanisms of coastal change: Peat compaction and the destruction of late Holocene coastal wetlands. *Marine Geology*, 225, 63-84.
- Long, A. J., Scaife, R. G., & Edwards, R. J. (2000). Stratigraphic architecture, relative sea level, and models of estuary development in southern England: new data from Southampton Water. In: Pye, K., Allen, J.R.L. (Eds.). *Coastal and Estuarine Environments: Sedimentology, Geomorphology and Geoarchaeology. Special Publications*, 175, 253–279.
- Long, A. J., Waller, M. P., & Plater, A. J. (2006). Coastal resilience and late Holocene tidal inlet history: The evolution of Dungeness Foreland and the Romney Marsh depositional complex (U.K.). *Geomorphology*, 82(3-4 ), 309-330.
- Lowe, J. J. (1982). Three Flandrian pollen profiles from the teith valley, Perthshire, Scotland. II. Analysis of deteriorated pollen. *New Phytologist*, 90(2).
- Lynn Gary, J. (2009). *Characterizing the discharge features of glacial lake agassiz during the post-marquette period using marine seismic-reflection methods*. MSc thesis, University of Minnesota, Minnesota, 89p.
- MacKenzie, W. H., & Moran, J. R. (2004). Wetlands of British Columbia: a guide to identification *Land Management Handbook*, 52, 295.
- Magny, M., & Haas, J. N. (2004). A major widespread climatic change around 5300 cal. yr BP at the time of the Alpine Iceman. *Journal of Quaternary Science*, 19, 423–430.
- Mansy, J. L., Manby, G. M., Averbuch, O., Everaerts, M., Bergerat, F., Van Vliet, L. B., & Lamarche, J. (2003). Dynamics and inversion of the mesozoic basin of the Weald-Boulonnais area: role of basement reactivation. *Tectonophysics*, 373, 161-169.
- Marsset, B., Missiaen, T., De Roeck, Y. H., Noble, M., Versteeg, W., & Henriët, J. P. (1998). Very high resolution 3D marine seismic data processing for geotechnical applications. *Geophysical Prospecting*, 46, 105-120.
- Mathys, M. (2009). *The Quaternary geological evolution of the Belgian Continental Shelf, southern North Sea*. PhD Thesis, Ghent University, Ghent. 371p.

- McCants, C. Y., & Zarillo, G. A. (1985). Evolution and Stratigraphy of a Sandy Tidal-Flat Complex Within a Mesotidal Embayment: ABSTRACT. *The AAPG/Datapages Combined Publications Database*, 69(2), 285.
- McDowell, J. L., Knight, J., & Quinn, R. (2005). *High-resolution geophysical. Investigations seaward of the bann Estuary, northern ireland coast. : In high resolution Morphodynamics and Sedimentary Evolution of Estuaries*. Springer. 11-33.
- McGee, T. M. (1995). High-resolution marine reflection profiling for engineering and environmental purposes. Part A: Acquiring analogue seismic signals. *Journal of Apphed Geophysics*, 33, 271-285.
- Mellet, C. L. (2012). *Drowned landscapes of the eastern English Channel: records of Quaternary environmental change*. PhD Thesis, University of Liverpool, Liverpool, 229p.
- Meurisse-Fort, M. (2007). *Enregistrement haute résolution des massifs dunaires ; Manche, mer du Nord et Atlantique - Le rôle des tempêtes*. PhD thesis, Université de Lille1, Lille, 299p.
- Miall, A. D. (1985). Architectural element analysis: a new method of facies analysis applied to fluvial deposits. *Earth-Science Reviews*, 22, 261–308.
- Miller, J. (1965). Recognition and classification of marginal marine environements *Sedimentation of late cretaceous and tertiary outcrops, Rock Springs uplift; 19th Annual Field Conference Guidebook*, 1965. 209-218.
- Mitchum Jr, R. M., Vail, P. R., & Sangree, J. B. (1977). Seismic stratigraphy and global changes of sea level, Part 6: stratigraphic interpretation of seismic reflection patterns in depositional sequences. *AAPG Special Volumes*, 165, 117-133.
- Mook, W. G., & Van der Plicht, J. (1999). Reporting 14C activities and concentrations. *Radiocarbon*, 41, 227-239.
- Moon, J. W., Song, Y., Moon, H.-S., & Lee, G. H. (2000). Clay minerals from tidal flat sediments at Youngjong Island, Korea, as a potential indicator of sea-level change. . *Clay Minerals*, 35, 841-855.
- Moore, P. D., Webb, J. A., & Collinson, M. E. (1991). *Pollen Analysis*. Oxford: Blackwell Scientif Publications. 21p.
- Mrani Alaoui, M. (2006). *Evolution des environnements sédimentaires holocènes de la plaine maritime flamande du Nord de la France : eustatisme et processus*. PhD thesis, Université du Littoral, Dunkerque, 158p.

- Mrani Alaoui, M., & Anthony, E. J. (2011). New data and a morphodynamic perspective on Mid- to Late Holocene palaeoenvironmental changes in the French Flanders coastal plain, southern North Sea. . *The Holocene*, 21, 445–453.
- Mángano, M. G., Buatois, L. A., West, R. R., & Maples, C. G. (2002). Ichnology of a Pennsylvanian Equatorial Tidal Flat: The Stull Shale Member at Waverly, Eastern Kansas *Kansas Geological Survey*, 245, 1–133.
- Nichols, G. (2009). *Sedimentology and Stratigraphy, 2nd Edition* Wiley-Blackwell. 432p.
- Novak, B. (2002). Early Holocene brackish and marine facies in the Fehmarn Belt, southwest Baltic Sea: depositional processes revealed by high-resolution seismic and core analysis. *Marine Geology*, 189, 307-321.
- Olsen, H., Ploug, G., Nielsen, U., & Sorensen, K. (1993). Reservoir Characterization Applying High-Resolution Seismic Profiling, Rabis Creek, Denmark. *Groundwater*, 31(1), 84-90.
- Paepe, R. (1960a). La plaine maritime entre Dunkerque et la frontière belge. *Bulletin de la Société Belge d'Etudes Géographiques*, 29, 47-66.
- Paepe, R., Baeteman, C., Mortier, R., Vanhoorne, R., & quaternary., C. f. (1981). The marine pleistocene sediments in the flandrian area - a 'mise au point' on the nomenclature and stratotypes. *Geologie en Mijnbouw*, 321-331.
- Paepe, R., & Sommé, J. (1970). Les loess et la stratigraphie du Pleistocene récent dans le Nord de la France et en Belgique. *Annales de la société géologique du Nord*, XC, 191-201.
- Paris, P. (1977). *Verslag van het fysich-geografisch veldwerk in the omgeving van Calais, gedurende de Zomer van 1973*. Vrije universiteit, Amsterdam. 26p.
- Petschick, R. (2000). Age determination by radiocarbon content: world-wide assay of natural radiocarbon. *Science*, 4, 227–228.
- Pierre, G. (2007). Durée de l'évolution marine et recul holocène d'un littoral à falaises, l'exemple du nord boulonnais (France). . *Quaternaire*, 18(3), 219-231.
- Pierre, G., & Lahousse, P. (2004). L'évolution des falaises argilo-crayeuses et limoneuses du nord du Boulonnais (Strouanne, Sangatte, France). *Evolution of the clay-chalk and silt cliffs in northern Boulonnais (Strouanne, Sangatte, France)*. *Géomorphologie : relief, processus, environnement.*, 3, 211-224.
- Pirazzoli, P. A. (1991). *World atlas of holocene sea-level changes*. Elsevier. Amsterdam. Vol. 58. 300p.

- Plink-Björklund, P. (2005). Stacked fluvial and tide-dominated estuarine deposits in high-frequency (fourth-order) sequences of the Eocene Central Basin, Spitsbergen. *Sedimentology* 52, 391-428.
- Rasmussen, S. O., Andersen, K. K., Svensson, A. M., Steffensen, J. P., Vinther, B. M., Clausen, H. B., & Ruth, U. (2006). A new Greenland ice core chronology for the last glacial termination. *Journal of Geophysical Research*, 111. D06102.
- Reed, D. J., Davidson-Arnott, R., & Perillo, G. M. E. (2009). *Estuaries, coastal marshes, tidal flats and coastal dunes*: Cambridge, University Press. 130-157.
- Reille, M. (1990). Leçons de palynologie et d'analyses polliniques. *Editions du C.N.R.S.*, 206p.
- Reimer, P. J., Baillie, M. G. L., Bard, E., Bayliss, A., Beck, J. W., Blackwell, P. G., Weyhenmeyer, C. E. (2009). IntCal09 and Marine09 Radiocarbon Age Calibration Curves, 0-50,000 Years cal BP. *RADIOCARBON*, 51 (4), 1111-1150.
- Reineck, H. E., & Singh, I. B. (1980). *Depositional Sedimentary Environments*. Berlin: Springer-Verlag. Berlin-Heidelberg-New York. 549p.
- SAGE Delta de l'Aa, (2005). Compte-rendu du SAGE de l'Aa. 159p.
- S.H.O.M. (1968). Courants de marée dans la Manche et sur les côtes françaises de l'Atlantique. Paris. 287p.
- Saito, Y., Katayama, H., Ikehara, K., Kato, Y., Matsumoto, E., Oguri, K., . . . Yumoto, M. (1998). Transgressive and highstand systems tracts and post-glacial transgression, the East China Sea *Sedimentary Geology* 122 217-232.
- Sangree, J. B., & Widmier, J. M. (1979). Interpretation of depositional facies from seismic data. *Geophysics*, 44(2), 131-160.
- Scholle, P. A., & Spearing, D. (1982). Introduction. *Sandstone depositional environments* in: P. A. Scholle and D. R. Spearing Sandstone Depositional Environments. *AAPG Special Publication*. 31p.
- Schüttenhelm, R. T. E., & Laban, C. (2005). Heavy minerals, provenance and large scale dynamics of seabed sands in the Southern North Sea: Baak's (1936) heavy mineral study revisited *Quaternary International*, 133-134, 179-193.
- Scott, D. B., Medioli, F. S., & Schafer, C. T. (2004). Monitoring in Coastal Environments Using Foraminifera and Thecamoebian Indicators. *Cambridge University Press*, 193p.



- Sebag, D., Copard, Y., Di-Giovanni, C., Durand, A., Laignel, B., Ogier, S., & Lallier-Verges, E. (2006). Palynofacies as useful tool to study origins and transfers of particulate organic matter in recent terrestrial environments. Synopsis and prospects. *Earth-Science Reviews*, 79, 241–259.
- Shennan, I., Lambeck, K., Flather, R., Horton, B., McArthur, J., Innes, J., & Wingfield, R. (2000). Modelling western North Sea palaeogeographies and tidal changes during the Holocene. *Geological Society, London, Special Publications*, 166, 299-319.
- Simpkin, P., & Davis, M. (1993). For Seismic profiling in very shallow water, a novel receiver. *Sea Technology* 34, 5p.
- Sommé, J. (1969). La plaine maritime. *Ann. Soc. Géol. Nord*, 89, 117-126.
- Sommé, J. (1977). *Les plaines du Nord de la France et leur bordure. Etude géomorphologique*. Paris. 801p.
- Sommé, J. (1979). Quaternary coastlines in Northern France », in E. Oele, R.T.E. Schüttenhelm and A.J. Wiggers (ed.). *The Quaternary History of the North Sea. Acta Universitatis Upsaliensis, Uppsala*, 141-158.
- Sommé, J. (2013). Unités lithostratigraphiques quaternaires du Nord de la France : un inventaire. *Quaternaire*, 24, 1, 3-12.
- Sommé, J., Antoine, P., Cunat-Bogé, N., Lefèvre, D., & Munaut, A. V. (1999). Le Pléistocène moyen marin de la mer du Nord en France : falaise de Sangatte et formation d'Herzeele [The marine middle pleistocene of the north ssa in France : Sangatte cliff and Herzeele formation] *Quaternaire*, 10, 2-3, 151-160.
- Sommé, J., Cunat-Bogé, N., Vanhoorne, R., & Wouters, K. (2004). La Formation de Loon : les dépôts pléistocènes marins profonds de la plaine maritime du Nord de la France. *Quaternaire*, 15, 4, 319-327.
- Sommé, J., Munaut, A., Emontspohl, A. F., Limondin, N., Lefèvre, D., Cunat-bogé, N., . . . Gilot, E. (1992). Weichselien ancien et Holocène marin à Watten (Plaine maritime, Nord, France). *Quaternaire*, 3, 2, 87-89.
- Sommé, J., Munaut, A.-V., Puisségur, J.-J., Cunat-Bogé, N., Heyvaert, F., Leplat, J., & . (1996). L'Eemien sous les formations fluvatiles Weichseliennes et holocènes du sondage d'Erquinghem (Nord de la France) dans la plaine de la Lys. *Quaternaire*, 7,1, 15-28.
- Sommé, J., Munaut, A. V., Emontspohl, A. F., Limondin, N., Lefèvre, D., Cunat-bogé, N., & Gilot, E. (1994). The Watten boring – an Early Weichselian and Holocene climatic and palaeocological record from the French North Sea coastal plain. *Boreas*, 23, 231-243.

- Sommé, J., & Tuffreau, A. (1978). Historique des recherches sur le Quaternaire de la région du Nord de la France. *Bulletin de l'Association française pour l'étude du quaternaire* 15, 1-3, 5-13.
- Stockmans, F., & Vanhoorne, R. (1954). Étude botanique du gisement de tourbe de la région de Pervijze (Flandre maritime belge). *Museum Geological Survey of Belgium*. 75p.
- Stocker, M. S., Pheasant, J. B., & Josenhans, H. (1997). Seismic Methods and Interpretation. 9-26.
- Streif, H. (1978). A New Method for the Representation of Sedimentary Sequences in Coastal Regions. *Paper presented at the Coastal Engineering. Hamburg*. 1245-1256.
- Stuiver, M., & Reimer, P. J. (1986). A computer program for radiocarbon age calibration *Proceedings of the 12th International Conference. Radiocarbon*, 28(2B), 1022-1030
- Stuiver, M., & Reimer, P. J. (1993). Extended 14C data base and revised CALIB 3.014C age calibration program. *RADIOCARBON*, 35 (1), 215-230.
- Swift, D. J. P., & Thorne, J. A. (1991). Sedimentation on continental margins, I: a general model for shelf sedimentation. *International Association of Sedimentologists. Special Publication*, 14, 3–31.
- Syvitski, J. P. M., Harvey, N., Wolanski, E., Burnett, W. C., Perillo, G. M. E., & Gornitz, V. (2005). *Dynamics of the coastal zone. In Coastal Change and the Anthropocene: The Land-Ocean Interactions in the Coastal Zone Project of the International Geosphere-Biosphere Programme: Global Change - The IGBP Series*, 39-94.
- Tavernier, R. (1947). L'évolution de la plaine maritime belge. *Bulletin de la société belge de Géologie.*, 56, 332-343.
- Tavernier, R. (1948). Les formations quaternaires de la Belgique en rapport avec l'évolution morphologique du pays. *Bulletin de la société belge de Géologie, de Paléontologie et d'Hydrologie.*, LVIII, 609-641.
- Teixidó Ullod, M. T. (2000). *Caracterización del subsuelo mediante sismica de reflexión de alta resolución*. Unpublished PhD tesis. Universidad de Barcelona. Barcelona. 275p.
- Ters, M. (1973). Les variations du niveau marin depuis 10000 ans, le long du littoral atlantique français. . *Actes du colloque: 9e Congrès international de l'INQUA : Le Quaternaire Géodynamique, stratigraphie et environnement. INQUA (Editor)*. , 114-136.
- Tessier, B. (1997). *Expressions sédimentaires de la dynamique tidale*. Mémoire d'Habitation à Diriger des Recherches. Université Lille 1. Lille. 177p.

- Tessier, B., Baltzer, A., Certain, R., D., M., & Chaumillon, E. (2003). Very high resolution seismic imaging of shallow water sedimentary bodies: application to coastal evolution and management. *Eurodelta conference abstract*.
- Tessier, B., Delsinne, N., & Sorrel, P. (2010). Holocene sedimentary infilling of a tide-dominated estuarine mouth. The example of the macrotidal Seine estuary (NW France). *Bulletin de la Societe Geologique de France*, 181, 87-98.
- Trentesaux, A. (2005). Enregistrement de processus sédimentaires pléistocènes exemples de plates-formes détritiques et de bassins profonds Mer du Nord et mers de chine. Mémoire d'Habitation à Diriger des Recherches. Sciences Naturelles. Université Lille 1. Lille. 82p.
- Trentesaux, A., Stolk, A., & Berne, S. (1999). Sedimentology and stratigraphy of a tidal sand bank in the southern North Sea. *Marine Geology*, 159, 253–272.
- Tys, D. (2007). *La formation du littoral flamand et l'intervention humaine. In Villes et campagnes en Neustrie: sociétés, économies, territoires, christianisation ; actes des XXVe Journées Internationales d'Archéologie Mérovingienne de l'AFAM. Verslype, Laurent Pub. Montagnac*, 211-219.
- Tóth, T., Simpkin, P. G., Vida, R., & Horva' th, F. (1997). Shallow water single and multichannel Seismic profiling in a riverine environment. *Special Issue of the Leading Edge, Society of Exploration Geophysicists, November edition. Vol. 16, 11, 1691-1695*.
- Törnqvist, T. E., & Hijma, M. P. (2012). Links between early Holocene ice-sheet decay, sea-level rise and abrupt climate change. *Nature Geoscience*, 5, 601-606.
- Törnqvist, T. E., Wallace, D. J., Storms, J. E. A., Wallinga, J., L. van Dam, R., Blaauw, M., Snijders, E. M. A. (2008). Mississippi Delta subsidence primarily caused by compaction of Holocene strata. *Nature Geoscience*, 1, 173 - 176.
- Van Asselen, S. (2010). *Peat Compaction in Deltas: Implications for Holocene Delta Evolution*. PhD thesis. Universiteit Utrecht, Utrecht, 180p.
- Van Asselen, S., Stouthamer, E., & van Asch, Th.W.J. (2009). Effects of peat compaction on delta evolution: a review on processes, responses, measuring and modeling. *Earth Science Reviews*, 92, 35-51.
- Van der Molen, J., & Van Dijck, B. (2000). The evolution of the Dutch and Belgian coasts and the role of sand supply from the North Sea. *Global and Planetary Change*, 27, 1, 223-244.
- Van der Valk, L. (1996). Coastal barrier deposits in the central Dutch coastal plain. In: D.J. Beets, M.M. Fischer and W. de Gans (eds.), *Coastal Studies on*

- the Holocene of the Netherlands. . *Mededelingen Rijks Geologische Dienst.*, 57, 133-199.
- Van der Woude, J., & Wim, R. (1985 ). Paleoeological evolution of an interior coastal zone : the case of the Northern France coastal plain [Evolution paléoécologique d'une zone côtière interne : le cas de la plaine maritime du Nord de la France.]. *Bulletin de l'Association française pour l'étude du Quaternaire*, 22, 1, 31-39.
- Van Lancker, V., Du Four, I., Mathys, M., Versteeg, W., & De Batist, M. (2009). Towards a high-resolution 3D-analysis of sand-bank architecture on the Belgian Continental Shelf (RESOURCE-3D). Final Report. Brussels: Belgian Science Policy. 36p.
- Van Veen, J. (1936). Onderzoekingen in de Hoofden. *Algemene Landsdrukkerij, 's Gravenhage*, 252p.
- Van Vliet-Lanoë, B., Bergerat, F., Csontos, L., Everearts, M., Laurent, M., Manby, G., Meilliez, F. (2001). *Neogene and Quaternary Flexural Activity, NW Paris Basin* Paper presented at the Symposium RCM1 EUG XI/The Causes and Consequences of Uplift at Continental Margins, Strasbourg. Abstract.
- Van Vliet-Lanoë, B., Mansy, J.-L., Margerel, J.-P., Vidier, J.-P., Lamarche, J., & Everaerts, M. (1998). Le Pas de Calais, un détroit cénozoïque à ouvertures multiples. *Comptes Rendus de l'Académie des Sciences - Series IIA - Earth and Planetary Science*, 326(10), 729-736.
- Van Wagoner, J. C., Mitchum, R. M., Jr., C., K.M., & Rahmanian, V. D. (1990). Siliciclastic Sequence Stratigraphy in Well Logs, Cores, and Outcrops: Concepts for High-Resolution Correlation of Time and Facies *American Association of Petroleum Geologists Methods in Exploration Series* 7, 55.
- Verbeek, N. H. (1995). Aspects of High Resolution Marine Seismics. *University of Utrecht – Gelogica Ultraiectina*, 125.
- Verbeek, N. H., OldeMonnikhof, C. M., Koktas, M., McGee, T. M., deGans, W., & Zwaan, H. (1994). Canal seismics in The Netherlands. *2nd European conference, Underwater acoustics*, 937-942.
- Vergne, V. (2013). Paysages forestiers du Nord de la France : approches géohistoriques et paléoécologiques. . *La forêt domaniale du Nord-Pas-de-Calais. Bilan de 15 ans d'échanges*, 109-152.
- Vergne, V., Deschodt, L., & Delangue, B. (2009). Géohistoire de la tourbe et des tourbières du nord de la France. *Histoire économique et sociale de la tourbe et des tourbières æstuarialia*, 14, 251-276.

- Vink, A., Steffen, H., Reinhardt, L., & Kaufmann, G. (2007). Holocene relative sea-level change, isostatic subsidence and the radial viscosity structure of the mantle of northwest Europe (Belgium, the Netherlands, Germany, southern North Sea) *Quaternary Science Reviews*, 26(25-28), 3249-3275.
- Voris, H. K. (2000). Maps of Pleistocene sea levels in Southern Asia: shorelines, river systems and time durations. *Journal of Biogeography*, 27, 1153-1167.
- Walker, M. J. C., Berkelhammer, M., Björck, S., Cwynar, L. C., Fisher, D. A., Long, A. J., & Weiss, H. (2012). Formal subdivision of the Holocene Series/Epoch: a Discussion Paper by a Working Group of INTIMATE (Integration of ice-core, marine and terrestrial records) and the Subcommittee on Quaternary Stratigraphy (International Commission on Stratigraphy). *Journal of Quaternary Science*, 27, 7, 649–659.
- Wang, P., & Chappel, J. (2001). Foraminifera as Holocene environmental indicators in the South Alligator River, Northern Australia. *Quaternary International*, 83-85, 47-62.
- Wang, X., & Ke, X. (1997). Grain-size characteristics of the extant tidal flat sediments along the Jiangsu Coast, China. *Sedimentary Geology*, 112, 105-122.
- Weimer, R. J., Howard, J. D., & Lindsay, D. R. (1982). Tidal Flats and Associated Tidal Channels in M 31: Sandstone Depositional Environments. *AAPG Special Publication*, 191 – 245.
- Woodroffe. (2002). *Coasts: form, process and evolution*. University of Wollongong, Cambridge University Press. 623p.
- Wójcick, K. (2012). Stratigraphy of organic-rich deposits in floodplain environments: examples from the upper odra river basin. *Quaestiones Geographicae*, 31, 3, 107-118.
- Yang, B., Robert., W. D., Chun, S., & HeeJun., L. (2006). Transgressive sedimentation and stratigraphic evolution of a wave-dominated macrotidal coast, western Korea. *Marine Geology*, 235, 35–48.
- Zecchin, M., Civile, D., Caffau, M., & Roda, C. (2009). Facies and cycle architecture of a Pleistocene marine terrace (Crotone, southern Italy): a sedimentary response to late Quaternary, high-frequency glacio-eustatic changes. *Sedimentary Geology*, 216, 138-157.



## **APPENDIX A**

Available subsurface data. Name FFF refers to this study.

Name FFF	x	y	Original name	Source
1	420353.2861	5641779.186	00061X0459/F1	BRGM
2	420565.7455	5641651.357	00061X0205/R1	BRGM
3	460410.9468	5647013.764	00038X0017/P2	BRGM
4	459497.3184	5647891.596	00037X0170/E8	BRGM
5	458950.5144	5644887.701	00037X0069/S4M	BRGM
6	458732.4232	5645109.627	00037X0029/S8	BRGM
7	458573.8699	5645220.989	00037X0028/S7	BRGM
8	458137.5331	5645635.97	00037X0027/S6	BRGM
9	460022.067	5646208.265	00038X0008/S2	BRGM
10	460041.5742	5646188.097	00038X0007/S1	BRGM
11	457842.7518	5646177.725	00037X0026/S5	BRGM
12	457652.971	5649332.064	00037X0181/S4	BRGM
13	461239.5511	5654982.302	00034X0041/S2	BRGM
14	453700.67	5656818.44	00033X0048/S	BRGM
15	441505.9682	5654399.594	00031X0001/SC	BRGM
16	411799.335	5645404.629	00018X0026/T340B	BRGM
17	411295.512	5644989.444	00018X0025/R337B	BRGM
18	451241.551	5655561.909	00032X0022/S199	BRGM
19	449846.2776	5654955.813	00032X0027/S205	BRGM
20	449552.4614	5647326.145	00036X0099/PS5-1R	BRGM
21	450180.1931	5648351.002	00036X0450/PS10	BRGM
22	440447.0953	5639985.934	00064X0056/F2	BRGM
23	454001.2527	5647346.988	00037X0371/F1	BRGM
24	449520.427	5647641.188	00036X0113/SPT8	BRGM
25	448979.8589	5648641.838	00036X0461/SPT163	BRGM
26	449136.7838	5648324.45	00036X0110/SPT5	BRGM
27	448555.6987	5649258.819	00036X0260/S2C	BRGM
28	444078.2877	5644301.755	00035X0063/R2	BRGM
29	442220.4576	5643899.52	00035X0083/P9	BRGM
30	446668.5905	5642799.776	00071X0070/P3	BRGM
31	446599.7585	5644099.445	00035X0082/P2	BRGM
32	447153.0955	5628783.356	00076X0205/F	BRGM
33	457473.398	5648489.454	00037X0167/C5	BRGM
34	447625.3647	5624660.512	00076X0088/S	BRGM
35	441047.0807	5646738.704	00035X0109/P12	BRGM
36	442645.2365	5646664.037	00035X0110/P13	BRGM
37	442709.5021	5645934.872	00035X0156/PS1	BRGM
38	444159.6379	5647220.239	00035X0132/P70	BRGM
39	445606.3291	5646976.851	00035X0117/P33	BRGM
40	447179.5738	5646323.315	00036X0280/P31	BRGM
41	448731.6415	5647747.918	00036X0286/P67	BRGM
42	454001.2527	5647346.988	00037X0371/F1	BRGM
43	456080.9332	5646442.586	00037X0316/PS1	BRGM
44	456985.0107	5648593.579	00037X0166/D7	BRGM
45	459522.7877	5649621.812	00037X0171/G6	BRGM
46	461401.6058	5649643.041	00038X0039/18	BRGM
47	460456.6007	5651240.47	00038X0040/P189	BRGM
48	463478.8535	5652822.984	00038X0043/07	BRGM
49	464548.3984	5652824.433	00038X0004/S	BRGM
50	461241.6531	5648525.476	00038X0038/P105	BRGM
51	467211.1682	5647593.446	00045X0048/F	BRGM
52	451536.582	5644015.345	00036X0264/H5	BRGM
53	445377.1008	5642481.806	00071X0069/P4	BRGM
54	443964.3988	5642214.398	00071X0068/P5	BRGM
55	439264.1864	5637684.157	00064X0055/F1	BRGM



Name FFF	x	y	Original name	Source
56	447232.8114	5651060.451	00036X0275/P20	BRGM
57	447965.9462	5652378.686	00036X0429/PS26	BRGM
58	449893.398	5653525.155	00032X0041/S3145	BRGM
59	456142.1697	5652668.733	00037X0185/S1	BRGM
60	443506.807	5650194.524	00035X0127/P62	BRGM
61	450222.4814	5651213.198	00036X0466/PS1	BRGM
62	429509.6022	5640897.054	00063X0012/S	BRGM
63	421560.005	5641617.319	00061X0250/S1-4	BRGM
64	416351.6225	5643560.626	00061X0443/PZ1	BRGM
65	417191.2437	5644647.173	00025X0178/SD5	BRGM
66	417984.3779	5642906.112	00061X0416/SD6	BRGM
67	419106.3607	5643189.906	00061X0312/PZ1	BRGM
68	415822.2927	5643119.837	00061X0449/F1	BRGM
69	416356.4787	5644253.49	00025X0164/S1-35	BRGM
70	412953.0634	5644784.48	00018X0014/F9GETM	BRGM
71	420213.9841	5645288.234	00025X0103/R1	BRGM
72	421122.2026	5645139.746	00025X0090/111111	BRGM
73	422150.8666	5638404.089	00062X0053/F	BRGM
74	441804.8601	5651176.517	00035X0160/PS1	BRGM
75	443119.7527	5651626.767	00035X0135/P73	BRGM
76	444109.1423	5652747.032	00035X0091/SC7	BRGM
77	447697.1703	5654514.479	00032X0083/SC1	BRGM
78	448489.3187	5654147.299	00032X0048/P3	BRGM
79	455068.3062	5653066.084	00037X0059/SC11T	BRGM
80	414989.9183	5645507.014	00018X0043/SD9	BRGM
81	415301.9564	5644654.35	00018X0040/F1	BRGM
82	420428.6963	5642478.74	00061X0248/PZ4	BRGM
83	419947.2362	5643391.518	00061X0134/111111	BRGM
84	417978.1458	5646152.894	00025X0138/S1	BRGM
85	450406.4867	5645004.694	00036X0529/SRB	BRGM
86	449556.2253	5647496.263	00036X0112-SPT7	BRGM
87	446805.5249	5621369.246	00121X0015/111111	BRGM
88	448082.5009	5623756.265	00076X0189/F1	BRGM
89	448878.9826	5625069.553	00076X0193/F1	BRGM
90	448619.5759	5627509.797	00076X0002/F1	BRGM
91	444808.1097	5629389.309	00075X0184/PZS2	BRGM
92	443625.4227	5631172.461	00075X0083/111111	BRGM
93	453604.1167	5654960.727	00033X0001/F1	BRGM
94	443343.8624	5643249.865	00071X0065/P8	BRGM
95	466016.0244	5658217.095	00034X0015/F61201	BRGM
96	438918.6761	5647281.638	00028X0005-S020	BRGM
97	439136.0465	5647494.837	00028X0022/111111	BRGM
98	435179.8348	5644552.219	0028X0096/s-p23	BRGM
99	438436.3986	5649357.089	00028X0062/S12	BRGM
100	438913.8927	5645208.629	0028X0098/S-P25	BRGM
101	432491.4726	5643499.939	00063X0066/SP36	BRGM
102	412005.2823	5643754.932	00054X0064/111111	BRGM
103	450317.2076	5620078.006	00122X0157/F1	BRGM
104	463699.9704	5657438.833	00034X0042/F	BRGM
105	449611.4153	5624318.442	00076X0179/F	BRGM
106	466247.6134	5657205.796	00041X0016/111111	BRGM
107	428384.4635	5638027.429	00063X0041/F2	BRGM
108	447076.3911	5633710.743	00072X0044/111111	BRGM
109	438066.4753	5637650.479	00064X0048/S1-3	BRGM
110	434555.3531	5639602.01	00064X0032/F	BRGM

Name FFF	x	y	Original name	Source
111	421447.6402	5643527.617	00061X0068/111111	BRGM
112	427057.472	5647104.825	00026X0004/111111	BRGM
113	452931.9704	5650051.245	00036X0171/S2	BRGM
114	462899.4808	5651738.375	00038X0002/2	BRGM
115	434573.1389	5635932.76	00064X0002/F	BRGM
116	433031.3389	5636866.603	00063X0007/SO17	BRGM
117	428189.0717	5636309.566	00063X0002/F	BRGM
118	428503.8104	5640205.684	00063X0030/F1	BRGM
119	424964.9525	5640127.742	00062X0007/S1	BRGM
120	421447.6402	5643527.617	00061X0068/111111	BRGM
121	420895.3937	5641093.538	00061X0085/111111	BRGM
122	423686.0377	5643487.509	00062X0060/CAL101	BRGM
123	443423.7904	5644327.765	00035X0185/SRBOUR	BRGM
124	452298.9613	5640970.007	00072X0056/S3	BRGM
125	450463.6594	5641356.426	00072X0055/S9	BRGM
126	441893.0158	5641953.597	00071X0066/P7	BRGM
127	459404.2532	5643090.335	00073X0063/F1	BRGM
128	456981.9491	5642727.309	00073X0043/F1	BRGM
129	433031.3389	5636866.603	00063X0007/SO17	BRGM
130	420205.1785	5646358.353	00025X0005/111111	BRGM
131	416933.176	5645949.318	00025X0179/SD10	BRGM
132	451553.3928	5642506.059	00072X0052/S8	BRGM
133	426227.964	5644924.396	00026X0002/111111	BRGM
134	432046.3549	5648349.338	00027X0003/F	BRGM
135	430887.1844	5645081.484	00027X0022/111111	BRGM
136	419360.6351	5644806.493	00025X0006/111111	BRGM
137	420324.0683	5644177.631	00025X0002/F1	BRGM
138	418392.638	5642676.108	00061X0086/111111	BRGM
139	419036.6322	5642189.97	00061X0070/F4	BRGM
140	415638.1318	5644241.775	00025X0177/SD4	BRGM
141	418718.2106	5645641.824	00025X0013/111111	BRGM
142	413871.7229	5641248.765	00054X0063/111111	BRGM
143	420579.9965	5637158.822	00061X0075/F4	BRGM
144	428189.0717	5636309.566	00063X0002/F	BRGM
145	429055.8524	5634904.092	00063X0006/111111	BRGM
146	433031.3389	5636866.603	00063X0007/SO17	BRGM
147	434116.9305	5632028.175	00067X0097/F	BRGM
148	437362.5513	5629430.173	00068X0120/S	BRGM
149	436980.3942	5629233.487	00068X0149/F7B	BRGM
150	438613.7384	5628578.951	00068X0126/F13	BRGM
151	450220.9047	5632152.788	00076X0016/F1	BRGM
152	458364.2553	5641245.851	00073X0068/F1	BRGM
153	452426.6257	5635181.494	00072X0028/111111	BRGM
154	455278.0363	5639814.701	00073X0065/F1	BRGM
155	464892.0646	5643096.976	00074X0048/F1	BRGM
156	444331.8466	5621400.597	00121X0147/F1	BRGM
157	448837.0624	5618341.892	00122X0038/F1	BRGM
158	447186.2453	5617007.142	00122X0036/F	BRGM
159	457167.5714	5619807.158	00123X0129/F1	BRGM
160	458924.6236	5622890.093	00123X0128/F1	BRGM
161	458347.4058	5626573.342	00077X0080/F1	BRGM
162	454908.7997	5629823.622	00077X0102/F	BRGM
163	441224.8887	5623159.53	00121X0160/PZ1	BRGM
164	441980.154	5625990.29	00075X0082/F15	BRGM
165	423906.246	5635828.876	00062X0008/F1	BRGM

Name FFF	x	y	Original name	Source
166	443170.047	5638541.885	00071X0074/F	BRGM
167	427448.6277	5638465.278	00062X0066/S1	BRGM
168	439242.6039	5645085.763	00028X0099/S-X36	BRGM
169	419709.4778	5644693.188	00025X0007/111111	BRGM
170	418730.7974	5644831.905	00025X0010/111111	BRGM
171	418791.9974	5644971.089	00025X0012/111111	BRGM
172	419129.9852	5644748.914	00025X0011/111111	BRGM
173	439298.457	5646794.494	00028X0095/S-P13	BRGM
174	419341.2552	5643786.861	00025X0008/F1	BRGM
175	422919.6535	5642705.828	00062X0159/S1-30	BRGM
176	456811.2362	5650395.518	00037X0127/R1	BRGM
177	457126.987	5649971.405	00037X0294/H28	BRGM
178	457435.1285	5649639.679	00037X0299/H33	BRGM
179	458938.8748	5647937.143	00037X0366/PZ1	BRGM
180	444243.4125	5633236.558	00075X0098/S2B	BRGM
181	437955.0742	5649664.236	00028X0057/111111	BRGM
182	436143.1623	5643763.966	00028X0077/SH31	BRGM
183	435050.4425	5642355.077	00064X0001/S	BRGM
184	433414.6799	5642174.518	00063X0010/S	BRGM
185	448729.9317	5644240.305	00036X0028/F	BRGM
186	453046.9979	5646330.19	00036X0020/F	BRGM
187	420285.1864	5645897.762	00025X0114/RB	BRGM
188	421247.4314	5646768.39	00025X0100/R1	BRGM
189	422452.6654	5647287.414	00026X0084/PZ1	BRGM
190	429146.6211	5649205.693	00027X0069/F	BRGM
191	437955.0742	5649664.236	00028X0057/111111	BRGM
192	441156.7804	5651134.916	00035X0009/S	BRGM
193	458399.3399	5654777.528	00033X0014/S1	BRGM
194	430783.96	5645137.36	00027X0054/S1	BRGM
195	433414.6799	5642174.518	00063X0010/S	BRGM
196	446052.4719	5637678.161	00071X0036/S9B	BRGM
197	455806.13	5655340.44	00033X0110/R6	BRGM
198	424239.6485	5640586.1651	552-C27	Mrani, 2006 - Paris, 1977
199	427848.1771	5638582.8132	548	Mrani, 2006
200	422449.0468	5636593.3349	521	Mrani, 2006
201	422453.0854	5636767.6184	520	Mrani, 2006
202	422499.0437	5636927.3326	519	Mrani, 2006
203	422808.7781	5637282.7001	517	Mrani, 2006
204	422510.1577	5637205.7701	516	Mrani, 2006
205	423169.5260	5637909.2782	433	Mrani, 2006
206	423517.5683	5638178.1352	538	Mrani, 2006
207	423515.6018	5638336.4620	539	Mrani, 2006
208	423638.3877	5638436.0374	540	Mrani, 2006
209	424342.7778	5638207.9219	541	Mrani, 2006
210	425318.5207	5639451.9768	452	Mrani, 2006
211	421114.2492	5637394.2477	863	Mrani, 2006
212	421254.9442	5637318.8461	856	Mrani, 2006
213	421415.9648	5637321.0142	572	Mrani, 2006
214	422172.1368	5637168.5343	857	Mrani, 2006
215	422550.3036	5637063.9451	518	Mrani, 2006
216	422993.5924	5636826.6661	565	Mrani, 2006
217	423441.7308	5636979.0589	864	Mrani, 2006
218	423533.5748	5636898.7086	567	Mrani, 2006
219	423635.3640	5636736.2102	859	Mrani, 2006
220	423773.6661	5636712.1359	860	Mrani, 2006

Name FFF	x	y	Original name	Source
221	424798.2439	5637299.8583	578	Mrani, 2006
222	426774.4208	5637924.1054	464	Mrani, 2006
223	426811.0484	5637411.5497	466	Mrani, 2006
224	426636.9751	5637068.6432	470	Mrani, 2006
225	426552.4946	5636933.1674	474	Mrani, 2006
226	425770.7052	5636013.7960	476	Mrani, 2006
227	426118.7510	5636296.2169	477	Mrani, 2006
228	426186.6889	5636559.1068	478	Mrani, 2006
229	426041.9271	5636177.2949	479	Mrani, 2006
230	425885.8924	5636098.2020	480	Mrani, 2006
231	425647.1034	5636024.7648	544	Mrani, 2006
232	425531.0942	5635895.1371	507	Mrani, 2006
233	425337.5449	5635732.8168	506	Mrani, 2006
234	469239.2827	5653585.8513	276	Mrani, 2006
235	469976.3836	5653837.1661	88	Mrani, 2006
236	468271.0851	5652543.5069	280	Mrani, 2006
237	470075.1259	5652796.3125	104	Mrani, 2006
238	464625.8479	5649406.0646	163	Mrani, 2006
239	465768.0858	5649985.3912	172	Mrani, 2006
240	464771.8983	5649559.8591	171	Mrani, 2006
241	466837.5237	5649977.8651	235	Mrani, 2006
242	467188.9099	5650035.4448	236	Mrani, 2006
243	467626.5693	5650137.4397	242	Mrani, 2006
244	468101.1080	5650230.6913	243	Mrani, 2006
245	468611.0296	5650409.1650	244	Mrani, 2006
246	469335.4578	5650606.9956	245	Mrani, 2006
247	469724.4192	5650810.2366	239	Mrani, 2006
248	470050.4367	5651284.1600	292	Mrani, 2006
249	469008.3425	5654168.8776	272	Mrani, 2006
250	469233.9910	5653644.0600	276	Mrani, 2006
251	469350.1238	5653428.6275	744	Mrani, 2006
252	469717.4974	5652045.6421	287	Mrani, 2006
253	469780.3997	5651767.7810	288	Mrani, 2006
254	469835.1643	5651628.2695	289	Mrani, 2006
255	468026.6927	5652744.4517	221	Mrani, 2006
256	468628.1399	5652287.4884	285	Mrani, 2006
257	468798.6419	5651896.9790	290	Mrani, 2006
258	468765.2860	5651643.0156	232	Mrani, 2006
259	468974.5422	5651446.7452	233	Mrani, 2006
260	469101.4575	5651133.3421	238	Mrani, 2006
261	469340.7495	5650712.8290	245	Mrani, 2006
262	469382.4130	5650433.4345	248	Mrani, 2006
263	469484.4763	5650342.2454	257	Mrani, 2006
264	469601.3788	5650161.8417	258	Mrani, 2006
265	469762.4110	5649987.9016	259	Mrani, 2006
266	448129.3124	5637443.6876	329	Mrani, 2006
267	448136.8234	5637589.4000	328	Mrani, 2006
268	448148.5114	5637769.4600	327	Mrani, 2006
269	448231.6511	5637956.8908	326	Mrani, 2006
270	448333.4591	5638258.3344	325	Mrani, 2006
271	448397.2726	5638484.0034	324	Mrani, 2006
272	448499.3400	5638690.8774	323	Mrani, 2006
273	448693.5821	5639163.0318	322	Mrani, 2006
274	448721.1127	5639522.2040	320	Mrani, 2006
275	448820.8124	5639771.9038	319	Mrani, 2006

Name FFF	x	y	Original name	Source
276	448827.4336	5639899.5023	318	Mrani, 2006
277	448934.9367	5640190.8888	317	Mrani, 2006
278	448953.6243	5640266.2319	316	Mrani, 2006
279	449013.9520	5640322.4840	315	Mrani, 2006
280	448977.0805	5640395.7971	314	Mrani, 2006
281	448987.5551	5640481.5762	313	Mrani, 2006
282	448980.8004	5640558.6053	312	Mrani, 2006
283	448050.9855	5639525.8320	330-j119	Mrani, 2006 - Jacobs, 1978
284	448448.9259	5639051.7507	331-j118	Mrani, 2006 - Jacobs, 1978
285	448934.5859	5638740.8235	332-j152	Mrani, 2006 - Jacobs, 1978
286	449156.3263	5638688.0666	333-j115	Mrani, 2006 - Jacobs, 1978
287	449470.9733	5638690.2265	334	Mrani, 2006 - Jacobs, 1978
288	449561.4627	5638592.6911	866-j114	Mrani, 2006 - Jacobs, 1978
289	449598.2859	5638645.2787	335	Mrani, 2006 - Jacobs, 1978
290	449620.3034	5638668.2444	865-j113	Mrani, 2006 - Jacobs, 1978
291	449658.4949	5638682.6698	336-j112a	Mrani, 2006 - Jacobs, 1978
292	449704.3056	5638707.8970	337-j111	Mrani, 2006 - Jacobs, 1978
293	449753.7047	5638747.2902	338-j110	Mrani, 2006 - Jacobs, 1978
294	449792.8905	5638774.3212	339-j109	Mrani, 2006 - Jacobs, 1978
295	449890.4593	5638852.3843	340	Mrani, 2006
296	447921.3241	5636750.9580	361	Mrani, 2006
297	447868.9921	5636688.6799	362	Mrani, 2006
298	447790.6962	5636600.6030	363	Mrani, 2006
299	447676.0913	5636447.4458	364	Mrani, 2006
300	447460.2430	5636049.4875	369	Mrani, 2006
301	447342.4523	5635826.6519	372	Mrani, 2006
302	446839.5175	5634925.1864	373	Mrani, 2006
303	446763.7325	5634808.3906	374	Mrani, 2006
304	446724.7929	5634771.9731	375	Mrani, 2006
305	446683.4310	5634738.5828	376	Mrani, 2006
306	446646.5030	5634703.0729	377	Mrani, 2006
307	446607.7159	5634662.1497	378	Mrani, 2006
308	446565.0042	5634617.8825	379	Mrani, 2006
309	446528.6025	5634594.1591	380	Mrani, 2006
310	447957.5920	5634708.7678	386	Mrani, 2006
311	448045.8409	5634600.3773	387	Mrani, 2006
312	448145.8313	5634473.5771	388	Mrani, 2006
313	448329.1146	5634296.8884	389	Mrani, 2006
314	447512.1513	5636287.8920	368	Mrani, 2006
315	448329.6652	5635783.0920	390	Mrani, 2006
316	448868.6362	5636028.2499	392	Mrani, 2006
317	448977.2744	5636139.9213	393	Mrani, 2006
318	449260.8725	5636166.4496	394	Mrani, 2006
319	449446.0850	5636203.3981	402	Mrani, 2006
320	449670.9845	5636115.3559	403	Mrani, 2006
321	449881.4966	5636070.6987	404	Mrani, 2006
322	450110.1111	5636157.0199	405	Mrani, 2006
323	450272.3686	5636361.1843	406	Mrani, 2006
324	450513.6730	5636445.4643	407	Mrani, 2006
325	451020.7374	5636888.6540	409	Mrani, 2006
326	451686.2187	5637188.3750	418	Mrani, 2006
327	462206.5784	5650897.093	S4	Mrani, 2006
328	459752.6743	5650214.989	S2	Mrani, 2006
329	468705.5297	5658204.529	S7	Mrani, 2006
330	426080.4789	5637773.877	494-h48	Mrani, 2006 - Paris, 1977

Name FFF	x	y	Original name	Source
331	457417	5646738	S5	Mrani, 2006
332	468286.8519	5656139.029	SD	Mrani, 2006
333	422461.8835	5640860.903	427	Mrani, 2006
334	422864.9012	5640554.379	428	Mrani, 2006
335	423814.443	5640553.738	429-R6	Mrani, 2006 - Paris, 1977
336	424856.032	5639683.678	545-18	Mrani, 2006 - Paris, 1978
337	425336.3373	5639412.439	453-k29	Mrani, 2006 - Paris, 1979
338	425731.2743	5638876.104	546-h19	Mrani, 2006 - Paris, 1980
339	426290.5955	5639270.833	547-h18	Mrani, 2006 - Paris, 1981
340	426603.9328	5638884.171	456-k28	Mrani, 2006 - Paris, 1982
341	426861.012	5638466.034	462-h55	Mrani, 2006 - Paris, 1983
342	427398.904	5638372.193	550	Mrani, 2006
343	427726.1296	5638414.202	551-h60	Mrani, 2006 - Paris, 1977
344	428257.0995	5639319.947	549-k42	Mrani, 2006 - Paris, 1977
345	468727.3545	5656225.04	295	Mrani, 2006
346	468696.5717	5656135.369	296	Mrani, 2006
347	468745.9128	5656064.971	297	Mrani, 2006
348	468695.6792	5656035.437	298	Mrani, 2006
349	468654.814	5655935.863	300	Mrani, 2006
350	468804.1399	5655646.703	311	Mrani, 2006
351	469157.8629	5655191.816	266	Mrani, 2006
352	468865.7398	5654934.58	269	Mrani, 2006
353	468820.859	5654385.309	271	Mrani, 2006
354	469231.0025	5653309.285	278	Mrani, 2006
355	469258.4756	5653028.206	279	Mrani, 2006
356	469296.4328	5652802.001	282	Mrani, 2006
357	469574.3723	5652589.644	283	Mrani, 2006
358	469664.1882	5652350.982	284	Mrani, 2006
359	464738.8347	5651653.421	154	Mrani, 2006
360	465562.3131	5652095.795	179	Mrani, 2006
361	466129.5262	5652156.685	178	Mrani, 2006
362	466485.1766	5652476.317	214	Mrani, 2006
363	466936.0912	5652608.208	215	Mrani, 2006
364	467361.175	5652869.254	216	Mrani, 2006
365	467708.1216	5652886.142	217	Mrani, 2006
366	468160.6766	5653201.911	273	Mrani, 2006
367	468632.4138	5653427.562	274	Mrani, 2006
368	469782.6744	5653757.092	277	Mrani, 2006
369	444093.94	5632117.90	p20	Gandouin, 2003
370	444284.44	5630866.95	p10	Gandouin, 2003
371	444024.09	5630860.60	p21	Gandouin, 2003
372	444093.94	5630784.40	S1	Gandouin, 2003
373	444259.04	5630409.75	p12	Gandouin, 2003
374	443837.40	5630065.58	p19	Gandouin, 2003
375	444504.79	5630061.77	p18	Gandouin, 2003
376	443542.76	5629458.52	p1	Gandouin, 2003
377	444006.31	5628931.47	p2	Gandouin, 2003
378	445650.96	5628321.87	p17	Gandouin, 2003
379	446146.27	5628426.64	p9	Gandouin, 2003
380	446882.13	5626278.64	p14	Gandouin, 2003
381	445670.33	5625945.27	p3	Gandouin, 2003
382	446839.79	5626162.23	S2	Gandouin, 2003
383	447220.79	5625643.64	p22	Gandouin, 2003
384	446151.87	5624865.77	p6	Gandouin, 2003
385	444266.9002	5630696.241	Somme et al., 1994	Somme et al., 1994

Name FFF	x	y	Original name	Source
386	426564	5638945	Les Attaques1	Margotta, 2014
387	426628.3273	5637710.498	LesAttaques2	Margotta, 2014
388	424923	5637441	LesAttaques3	Margotta, 2014
389	459176	5646660	Bierne7	Margotta, 2014
390	459167	5645809	Bierne1	Margotta, 2014
391	458984.000	5645962.000	Bierne4	Margotta, 2014
392	459038.920	5645931.180	Bierne3	Margotta, 2014
393	459115.73	5645866.38	Bierne2	Margotta, 2014
394	459026.03	5645706.14	Bierne5	Margotta, 2014
395	458909.2	5646497.96	Bierne8	Margotta, 2014





## **APPENDIX B**

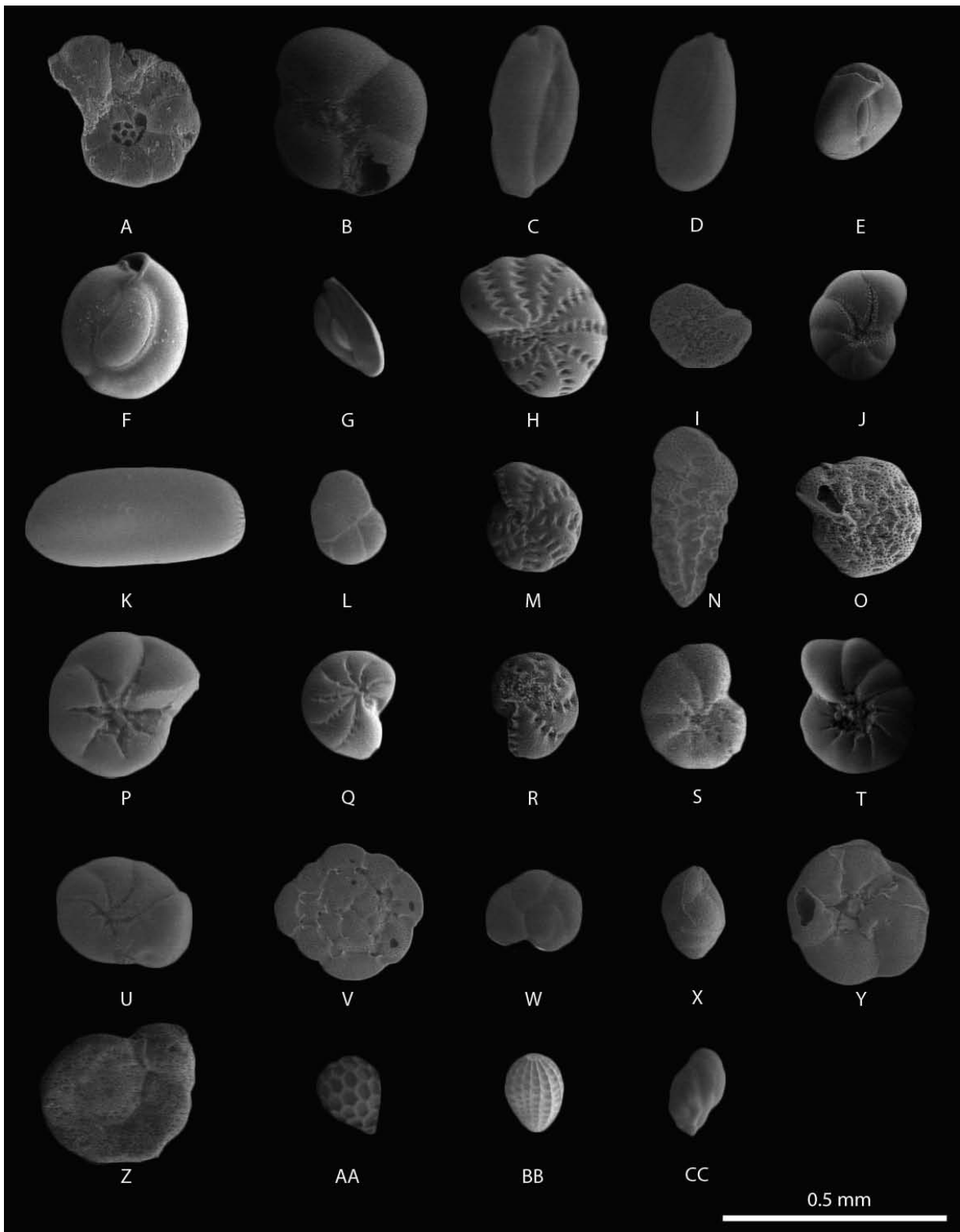
1. Benthic foraminifera data from cores of the French Flemish Coastal Plain. Samples from cores and archaeological trenches.
2. Scanning electron microscope (SEM) image of benthic foraminifera from samples of the French Flemish Coastal Plain

Benthic foraminiferal data/Samples (m NGF)	Les Attaques 1					Les Attaques 2				Les Attaques 3		
	1.3	0.7	-0.2	-1.8	-3.05	1.02	-0.5	-2	-3	1	0.2	-0.8
<i>A delosina</i> sp					1							
<i>Ammonia tepida</i>	2			2		1				3		
<i>Brizalina variabilis</i>												
<i>Bulimina elegans</i>										1		
<i>Bulminella elegantissima</i>	1											
<i>Cassidulina laevigata</i>	1			1								
<i>Criboelphidium excavatum</i>					1	1						
<i>Criboelphidium gerthi</i>	2			21	4	1		6		5		
<i>Criboelphidium gunteri</i>					1							
<i>Criboelphidium margaritaceum</i>								2				
<i>Criboelphidium williamsoni</i>	2			12	1			4		11		
<i>Elphidium pulvereum</i>					1							
<i>Favulina hexagona</i>												
<i>Favulina melo</i>				1								
<i>Gavelinopsis praegeri</i>												
<i>Haynesina depressula</i>	1			4	3					3		
<i>Haynesina germanica</i>	17			39	4	23		7		6	5	
<i>Jadammina macrescens</i>								11				
<i>Lobatula lobatula</i>										2		
<i>Miliammina fusca</i>												
<i>Miliolinella subrotunda</i>				7	5					1		
<i>Neocorbina nitida</i>												
<i>Nonion pauperatum</i>												
<i>Planorbulina mediterraneensis</i>				1								
<i>Polymorphina</i> sp	1											
<i>Rosalina vilarde boana</i>								1				
<i>Triloculina trigonula</i>					3							
<i>Trochammina inflata</i>											2	
Total	27			88	24	26		31		32	7	
Number of species	8			9	10	4		6		8	2	

Benthic foraminiferal data/Samples (m NGF)	Bierne 1					Bierne 7					B1	B2	B6	B8	B9	
	-0.2	-2.1	-3.3	-4.45	-4.9	-0.4	-1.4	-3.1	-4.15	-4.8	-5.45	0.5	0.5	0.5	0.3	0.5
<i>Adelosina</i> sp												3	14	3	5	9
<i>Ammonia tepida</i>														3		
<i>Bizalina variabilis</i>																
<i>Bulimina elegans</i>																
<i>Buliminella elegantissima</i>																
<i>Cassidulina laevigata</i>																
<i>Cribolephidium excavatum</i>								2								1
<i>Cribolephidium gerthi</i>	1											1		27	9	17
<i>Cribolephidium gunteri</i>																
<i>Cribolephidium margaritaceum</i>												1				1
<i>Cribolephidium williamsoni</i>	2							2				1	2	15	17	28
<i>Ephidium pulvereum</i>															1	
<i>Favulina hexagona</i>														1		
<i>Favulina melo</i>																
<i>Gavelinopsis praegeri</i>														1		
<i>Haynesina depressula</i>								2				3	18	22	4	7
<i>Haynesina germanica</i>	7							11				101	84	75	113	62
<i>Jadammina macrescens</i>	2											3			3	
<i>Loxostoma lobatula</i>	2											1		1	1	
<i>Millammina fusca</i>															3	
<i>Miliolinella subrotunda</i>														1	1	
<i>Neobulimina nitida</i>														1		
<i>Nonion pauperatum</i>														1	1	
<i>Planorbulina mediterraneensis</i>																
<i>Polymorphina</i> sp																
<i>Rosalina viardeboana</i>																1
<i>Tribouletina trigonula</i>																
<i>Trochammina inflata</i>																
Total	14							17				114	118	151	159	125
Number of species	5							4				7	4	12	12	7

**Foraminifera – Plate:**

<i>Adelosina</i> sp (image G)
<i>Ammonia tepida</i> (image P)
<i>Brizalina variabilis</i> (image N)
<i>Bulimina elegans</i> (image X)
<i>Buliminella elegantissima</i> (image CC)
<i>Cassidulina laevigata</i> (image L)
<i>Criboelphidium excavatum</i> (image Q)
<i>Criboelphidium gerthi</i> (image H)
<i>Criboelphidium gunteri</i> (image O)
<i>Criboelphidium margaritaceum</i> (image S)
<i>Criboelphidium williamsoni</i> (image M)
<i>Elphidium pulvereum</i> (image R)
<i>Favulina hexagona</i> (image AA)
<i>Favulina melo</i> (image BB)
<i>Gavelinopsis praegeri</i> (image Y)
<i>Haynesina depressula</i> (image T)
<i>Haynesina germanica</i> (image J)
<i>Jadammina macrescens</i> (image A)
<i>Lobatula lobatula</i> (image Z)
<i>Miliammina fusca</i> (image C)
<i>Miliolinella subrotunda</i> (image F)
<i>Neocorbina nitida</i> (image I)
<i>Nonion pauperatum</i> (image U)
<i>Planorbulina mediterranensis</i> (image V)
<i>Quinquelocuilna</i> sp (image D)
<i>Polymorphina</i> sp (image K)
<i>Rosalina vilardeboana</i> (image W)
<i>Triloculina trigonula</i> (image E)
<i>Trochammina inflata</i> (image B)



## **APPENDIX C**

Pollen analysis dataset. Pollen grains present a taxonomic organization from forest (left) to aquatic species (right).

Depth (m - NGF)	Arboreal pollen (AP)															Non-arboreal pollen (NAP)															Total						
	Pinus	Betula	Juniperus	Corylus	Quercus	Ulmus	Fraxinus	Tilia	Sambucus	Fagus	Ainus	Salix	Populus	Carpinus	Juglans	Calluna	Urtica	Chenopodiaceae	Apiaceae	Borraginaceae	Rumex	Pantago	Liguliflores	Tubuliflores	Graminaeae	Cyperaceae	Myriophyllum	Myriophyllum v eritic	Hottonia	Alismatacea		Sparganium	Potamogeton	Polypodium	Lycopodium	Equisetum	Spores triletes
-0.4	1	1	1	8	14	1	1	1	1	23	3	3	5	1	1	5	4	6	6	11	44	1	1	1	11	44	1	1	2	1	1	1	1	4	4	4	140
-0.45				1	1	1	1	1	1	1	1	1	2			2	3			1	8				1	8									1	15	
-0.5	5	3	1	8	1	1	1	1	1	21						2	3			1	25				10	25			1						18	2	105
-0.55																					3				1	6							1			1	4
-0.6		1		1						1	1	1				2					14				1	6			2						2	1	12
-0.65																																				2	22
-0.7																																				1	3
-0.75																																				1	1
-0.8																																				1	3
-0.85	2	10	7	14	8					1	117	1	1			3	1		8	16	69	3			16	69	3	16	1				9	2	2	338	
-0.9				4	4					7	7	3							1		4		1			4							1	1		2	28
-0.95	1			6	1	1				6	6	1							3		3					1	1	1	1				1	1		2	24
-1				5	3	1				15									19		1	1				2	1	2	1				1	1		1	49
-1.05	2	1		1	1					1						3	1		1	1	1				2	4						1			2	19	
-1.1	1	5	6	1	1	1	1	1	1	12	5	4	4			5			8	2	8				5	30						5	1	1	8	8	
-1.15																13			8	2	8	2			5	30						5	1	3	6	113	



## **APPENDIX D**

X-ray diffraction of Bierne and Les Attaques samples. Semi-quantitative estimates  
fraction less than 2  $\mu\text{m}$ .



<b>sm</b>	<b>ill</b>	<b>kaol</b>	<b>chl</b>	<b>Core</b>	<b>Facies</b>
70	20	10	0+	ATTAQUES-I-070G -	Sand facies
35	40	15	10	ATTAQUES-I-130G -	mud facies
50	30	15	5	ATTAQUES-I-225G -	mud facies
50	30	15	5	ATTAQUES-I-340G -	mud facies
50	30	15	5	ATTAQUES-I-470G -	Sand facies
65	25	10	0+	ATTAQUES-II-098G -	mud facies
55	30	10	5	ATTAQUES-II-250G -	Sand facies
45	30	15	10	ATTAQUES-II-400G -	mud facies
25	50	15	10	ATTAQUES-II-406G -	mud facies
50	35	10	5	ATTAQUES-II-420G -	mud facies
50	35	10	5	ATTAQUES-II-500G -	mud facies
65	15	15	5	BIERNE-01-020G -	organic-rich mud facies
45	35	10	10	BIERNE-01-210G -	mud facies
80	15	5	0+	BIERNE-01-445G -	mud facies
75	15	10	0+	BIERNE-01-545G -	Heterolithic facies
65	15	10	10	BIERNE-02-010G -	mud facies
60	15	15	10	BIERNE-02-470G -	Sand facies
25	30	30	15	BIERNE-03-030G -	mud facies
80	15	5	0+	BIERNE-03-223G -	Pleistocene
60	20	15	5	BIERNE-04-080G -	Sand facies
90	10	0+	0	BIERNE-04-224G -	Pleistocene
65	20	10	5	BIERNE-05-030G -	mud facies
70	15	10	5	BIERNE-07-040G -	Sand facies
45	35	15	5	BIERNE-07-140G -	mud facies
45	35	10	10	BIERNE-07-415G -	Sand facies
40	35	15	10	BIERNE-07-445G -	Sand facies
35	30	25	10	BIERNE-07-460G -	Sand facies
70	15	10	5	BIERNE-07-544G -	Pleistocene
70	20	10	0+	BIERNE-08-090G -	Pleistocene

## **APPENDIX E**

Radiocarbon ages performed on the French Flemish coastal plain. The calibrated ages are based on the intercept method of Stuiver *et al.* (1993) using the current calibration curve (IntCal09) provided by the IntCal Working Group (IWG).

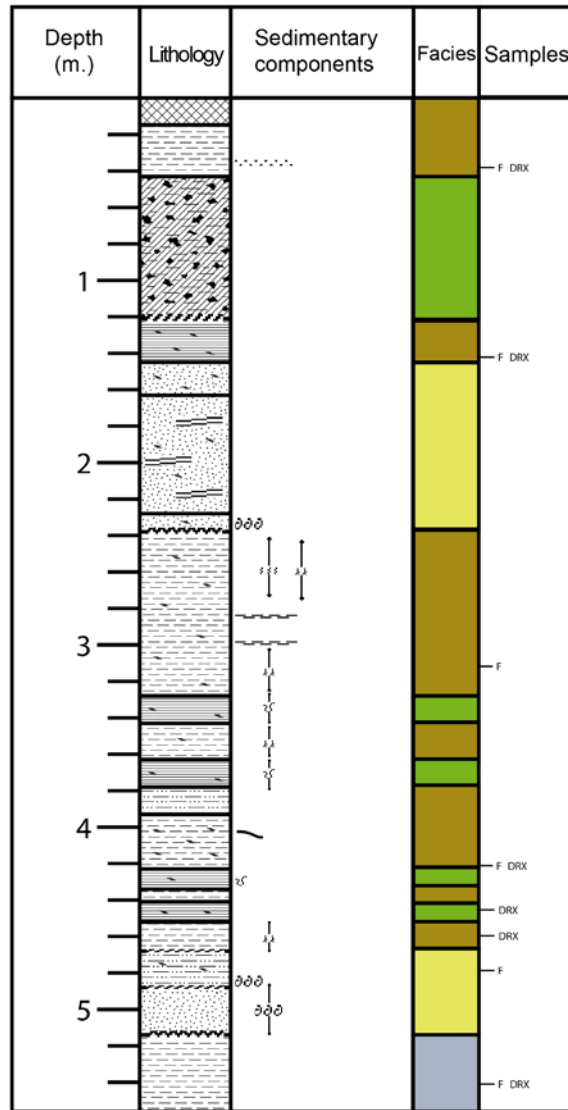
Location	Borehole (source)	Borehole (This study)	Material	Referential numbe	Depth ( m IGN69)	Conventional radiocarbon age (yr)	Radiocarbon age Cal BP	
Saint Omer	P14 (Gandouin 2003)		Peat	Beta - 161067	-15	9450 +/- 70	10508 - 10875	
	P14 (Gandouin 2003)		Peat	Beta - 161066	-14.3	8610 +/- 70	9474 - 9766	
	P14 (Gandouin 2003)		Peat	Beta - 161055	-14	7740 +/- 60	8410 - 8609	
	P14 (Gandouin 2003)		Peat	Hv - 24806	-8	5810 +/- 50	6493 - 6734	
	P14 (Gandouin 2003)		Peat	Hv - 24807	-5	5040 +/- 55	5659 - 5906	
	P14 (Gandouin 2003)		Peat	Hv - 24808	-4.5	4180 +/- 45	4575 - 4772	
Watten	Sommé 1994		Peat	LV - 1938	-18	8380 +/- 120	9078 - 9545	
	Sommé 1994		Peat	LV - 1737	-17.8	8200 +/- 120	8931 - 9473	
	Sommé 1994		Peat	LV - 1936	-6	6180 +/- 100	6797 - 7279	
	Sommé 1994		Peat	LV - 1935	-4	5690 +/- 80	6313 - 6654	
	Sommé 1994		Peat	LV - 2046	-1.3	3090 +/- 60	3157 - 3445	
	Sommé 1994		Peat	LV - 1934	-0.9	2240 +/- 80	1999 - 2366	
	S1 (Gandouin 2003)		Peat	Hv - 24811	-18	7250 +/- 110	7921 - 8328	
	S1 (Gandouin 2003)		Peat	Beta - 166492	-10	6920 +/- 100	7592 - 7938	
	S1 (Gandouin 2003)		Peat	Beta - 166491	-9.65	6710 +/- 60	7477 - 7671	
	S1 (Gandouin 2003)		Peat	Beta - 166490	-9.3	6570 +/- 60	7415 - 7577	
	S1 (Gandouin 2003)		Peat	Beta - 166493	-6.6	5100 +/- 50	5723 - 5938	
	S1 (Gandouin 2003)		Peat	Beta - 166494	-3.6	1900 +/- 70	1693 - 1997	
	S1 (Gandouin 2003)		Peat	Beta - 166495	-0.4	1680 +/- 60	1476 - 1713	
	Les Attaques	R6 (Paris 1975)		Peat	7167	-0.05	3435 +/- 35	3612 - 3779
		K42 (Paris 1975)		Peat	7161	0.65	3425 +/- 40	3576 - 3734
K42 (Paris 1975)			Peat	7308	-0.85	4650 +/- 60	5283 - 5489	
H48 (Paris 1975)			Peat	6971	-0.35	2780 +/- 50	2768 - 2997	
H48 (Paris 1975)			Peat	6970	-1.05	3560 +/- 55	3694 - 3984	
H48 (Paris 1975)			Peat	6969	-1.2	3690 +/- 35	3922 - 4098	
H48 (Paris 1975)			Peat	6968	-1.35	3965 +/- 55	4242 - 4538	
H48 (Paris 1975)			Peat	6967	-2.05	4030 +/- 55	4406 - 4654	
H48 (Paris 1975)			Peat	6966	-2.85	4800 +/- 60	5447 - 5650	
H48 (Paris 1975)			Peat	6965	-4.3	5060 +/- 40	5715 - 5911	
H48 (Paris 1975)			Peat	6964	-5.95	5820 +/- 65	6468 - 6757	
H48 (Paris 1975)			Peat	6963	-9.15	7095 +/- 75	7727 - 8046	
Looberghe	866 (Mrani 2006)		Peat	KIA 28097	1	1245 +/- 30	1080 - 1268	
	866 (Mrani 2006)		Peat	KIA 28103	0.6	1810 +/- 30	1691 - 1823	
	866 (Mrani 2006)		Peat	KIA 28096	0.2	2330 +/- 30	2309 - 2369	
	866 (Mrani 2006)		Peat	KIA 28100	-0.09	2425 +/- 45	2349 - 2546	
	866 (Mrani 2006)		Peat	KIA 28090	-0.46	2695 +/- 30	2754 - 2851	
	866 (Mrani 2006)		Peat	KIA 28110	-1.66	5525 +/- 40	6277 - 6404	

Location	Borehole (source)	Borehole (This study)	Material	Referential numbe	Depth ( m IGN69)	Conventional radiocarbon age (yr BP)	Radiocarbon age Cal BP
Looberghe	866 (Mrani 2006)		Peat	KIA 28302	-1.92	5725 +/- 35	6437 - 6635
	866 (Mrani 2006)		Peat	KIA 28901	-2.26	5785 +/- 40	6482 - 6674
	866 (Mrani 2006)		Peat	KIA 28104	-3.44	6185 +/- 45	6953 - 7177
	866 (Mrani 2006)		Peat	KIA 28102	-3.55	6215 +/- 45	7002 - 7251
	866 (Mrani 2006)		Peat	KIA 28092	-3.58	6225 +/- 50	7000 - 7258
	866 (Mrani 2006)		Peat	KIA 28105	-3.72	6285 +/- 40	7156 - 7313
	866 (Mrani 2006)		Peat	KIA 28089	-3.8	6330 +/- 45	7165 - 7331
	866 (Mrani 2006)		Peat	KIA 28308	-3.97	6415 +/- 55	7256 - 7429
	866 (Mrani 2006)		Peat	KIA 28094	-4.15	6585 +/- 45	7428 - 7524
	866 (Mrani 2006)		Peat	KIA 28099	-4.47	6750 +/- 45	7564 - 7676
	865 (Mrani 2006)		Peat	KIA 28073	0.19	3480 +/- 35	3682 - 3841
	865 (Mrani 2006)		Peat	KIA 28074	0.21	3530 +/- 35	3701 - 3896
	865 (Mrani 2006)		Peat	KIA 28076	-0.98	4970 +/- 50	5598 - 5762
	865 (Mrani 2006)		Peat	KIA 28075	-1.2	4985 +/- 40	5608 - 5761
	Bierne	S5 (Mrani 2006)		Peat	KIA 19510	-0.3	4220 +/- 30
S5 (Mrani 2006)			<i>Scrobicularia plana shell</i>	KIA 19486	0.3	3918 +/- 50	4229 - 4447
S5 (Mrani 2006)			<i>Cerastoderma edule shell</i>	KIA 19487	1.3	1903 +/- 47	1721 - 1946
N/A		Bierne1	Peat	UBA - 22259	-5.34	6987 +/- 52	7701 - 7933
N/A		Bierne1	Peat	UBA - 22258	-3	6122 +/- 40	6904 - 7158
N/A		Bierne1	Peat	UBA - 22257	-0.8	4180 +/- 55	4568 - 4846
N/A		Bierne1	Peat	UBA - 22256	-0.45	3845 +/- 34	4153 - 4359
Herbin 2013*			<i>Cerastoderma edule shell</i>	N/A	0.5	N/A	2798 - 2547
Herbin 2013*			Peat	N/A	-0.5	N/A	4031 - 3888
Herbin 2013*			Peat	N/A	-0.5	N/A	4574 - 4467
Téteghem	S2 (Mrani 2006)		<i>Cerastoderma edule shell</i>	KIA 19485	-2	4908 +/- 53	5581 - 5748
	S2 (Mrani 2006)		Peat	KIA 19478	0.3	1270 +/- 48	1080 - 1289
Ghyvelde	SD (Mrani 2006)		Soil	KIA 19480	1.3	3315 +/- 35	3462 - 3635
	S7 (Mrani 2006)		<i>Scrobicularia plana shell</i>	KIA 19498	-0.4	3308 +/- 50	3442 - 3642

## **APPENDIX F**

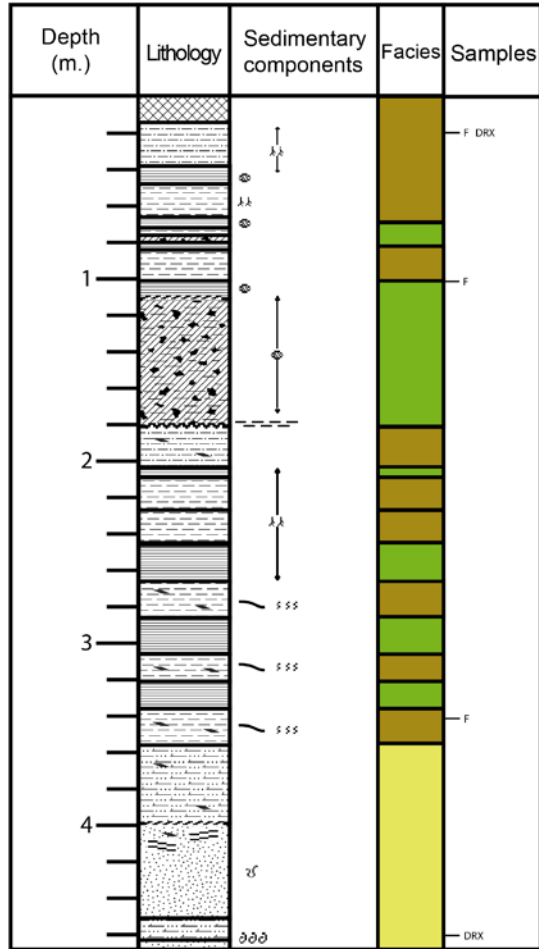
Cores from Bierne and Les Attaques sites. Location in Chapter 3 - Figure 3.2.

BIERNE 7



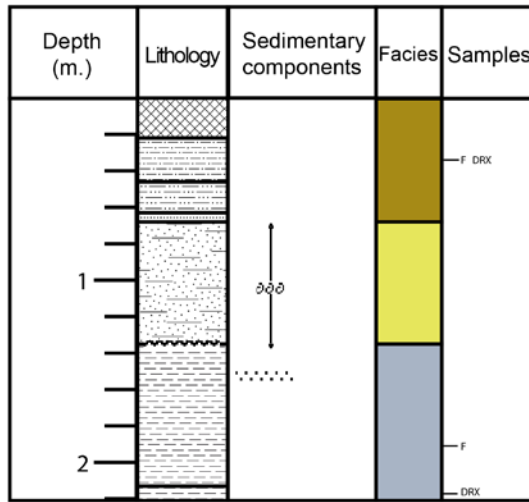
Legend:				
clayey silt	Agricultural ground	Organic-rich facies	Cross-lamination	Peat Fragments
Interbedded sand - mud		Mud facies	Shell Fragments	Shell
fine sand		Heterolithic facies	Organic laminae	Unoriented bioturbation
Organic-rich mud		Sand facies	Wood fragments	Roots traces
Peat		Pleistocene	Plant debris	Horizontal bioturbation
			medium sand layer	Transitional contact
			Organic layer	Irregular contact

BIERNE 2

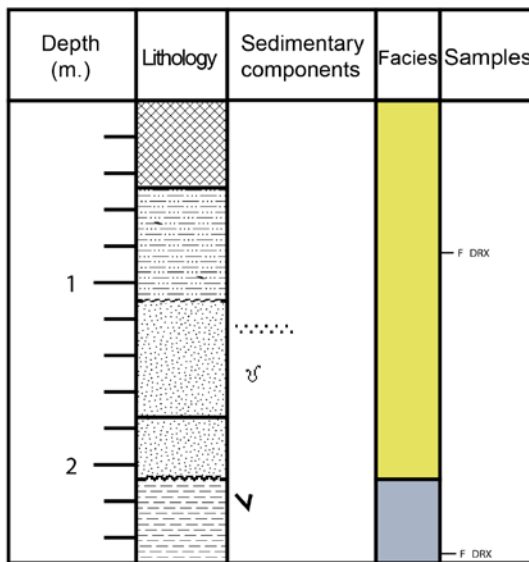


Legend:				
clayey silt	Agricultural ground	Organic-rich facies	Cross-lamination	Peat Fragments
Interbedded sand - mud		Mud facies	Shell Fragments	Shell
fine sand		Heterolithic facies	Organic laminae	Unoriented bioturbation
Organic-rich mud		Sand facies	Wood fragments	Roots traces
Peat		Pleistocene	Plant debris	Horizontal bioturbation
			medium sand layer	Transitional contact
			Organic layer	Irregular contact

BIERNE 3

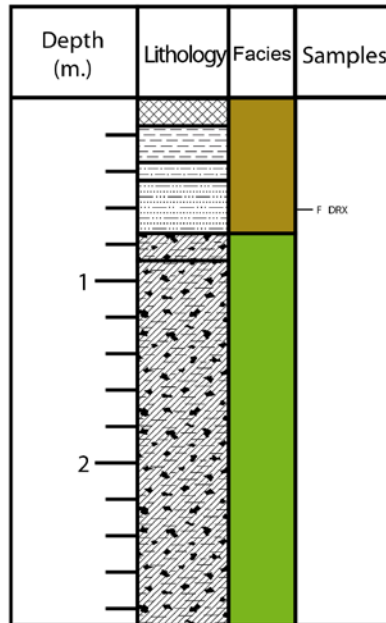


BIERNE 4

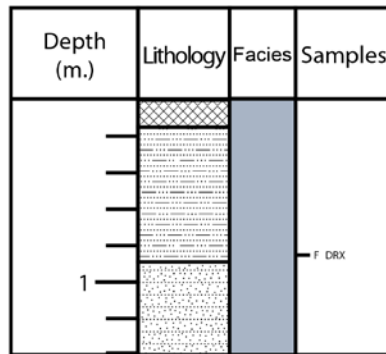


Legend:				

BIERNE 5



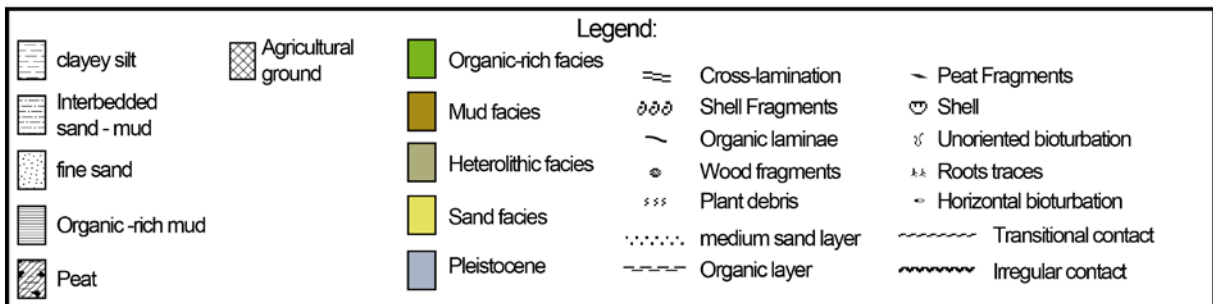
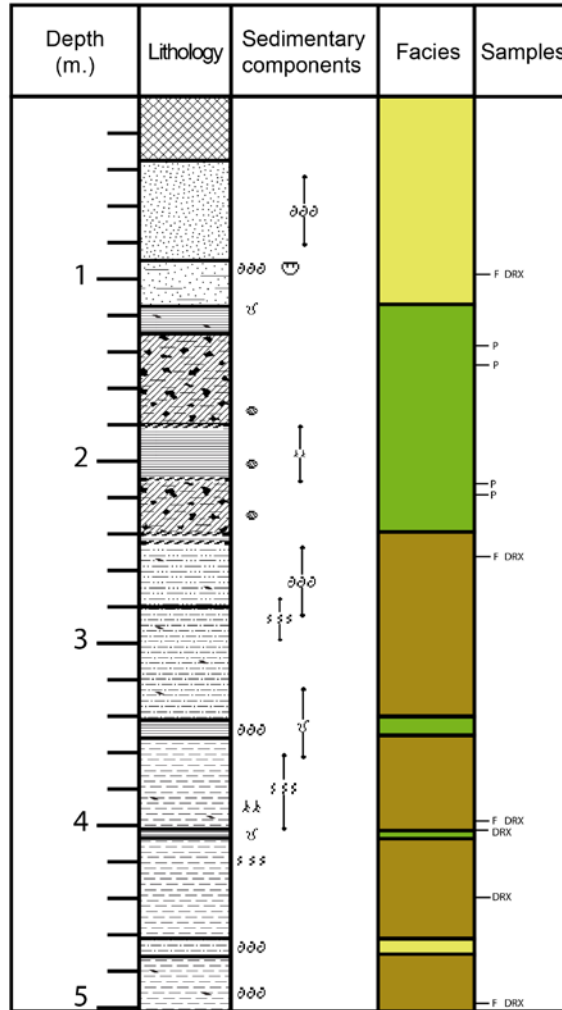
BIERNE 8



Legend:			
	clayey silt		Agricultural ground
	Interbedded sand - mud		Organic-rich facies
	fine sand		Mud facies
	Organic-rich mud		Heterolithic facies
	Peat		Sand facies
			Pleistocene
			Cross-lamination
			Shell Fragments
			Organic laminae
			Wood fragments
			Plant debris
			medium sand layer
			Organic layer
			Peat Fragments
			Shell
			Unoriented bioturbation
			Roots traces
			Horizontal bioturbation
			Transitional contact
			Irregular contact



Les Attaques 2



Les Attaques 3

